

Untersuchung TRPC-modulierender Gestagene und Proteine

Dissertation
zur Erlangung des Doktorgrades
der Naturwissenschaften

vorgelegt beim Fachbereich für Biochemie, Chemie und Pharmazie
der Johann Wolfgang Goethe-Universität
in Frankfurt am Main

von
Susanne Mieke
aus Rochlitz

Frankfurt am Main 2008
(D30)

vom Fachbereich für Biochemie, Chemie und Pharmazie
der Johann Wolfgang Goethe-Universität als Dissertation angenommen.

Dekan: Prof. Dr. Harald Schwalbe
1. Gutachter: Prof. Dr. Dieter Steinhilber
2. Gutachter: Prof. Dr. Andreas Busch
Datum der Disputation: 04. Juli 2008

Investigation of TRPC channel-modulating progestins and proteins

Dissertation
for the Achievement of the Doctor's Degree
of Natural Sciences

submitted to the Faculty of Biochemistry, Chemistry and Pharmacy
of the Johann Wolfgang Goethe-University
Frankfurt am Main

by
Susanne Mieke
from Rochlitz

Frankfurt am Main 2008
(D30)

Table of contents

1	Introduction.....	1
1.1	<i>Calcium signalling.....</i>	1
1.1.1	Store- and receptor-operated Ca ²⁺ influx.....	2
1.1.2	Activation of store-operated channels	4
1.2	<i>The TRP channel superfamily</i>	6
1.3	<i>The TRPC family</i>	9
1.3.1	Structural features of TRPCs.....	9
1.3.2	TRPC-interacting proteins	11
1.3.3	Activation mechanisms	12
1.3.4	TRPC subfamilies	14
1.4	<i>Aims.....</i>	20
2	Materials and methods.....	22
2.1	<i>Materials</i>	22
2.1.1	Chemicals, enzymes, consumables	22
2.1.2	Kits.....	24
2.1.3	Antibodies	25
2.1.4	Bacterial strains	25
2.1.5	Yeast strains	25
2.1.6	Cell lines and primary cells.....	25
2.1.7	Primers	26
2.1.8	siRNA.....	27
2.1.9	Genetic constructs.....	27
2.1.10	Apparatus	28
2.1.11	Buffers, media and solutions	29
2.2	<i>Molecular biological methods</i>	32
2.2.1	Determination of nucleic acid concentrations and cell density	32
2.2.2	Primer construction.....	32
2.2.3	Polymerase chain reaction (PCR)	32
2.2.4	DNA restriction digest.....	32
2.2.5	Dephosphorylation of linearized vectors.....	33
2.2.6	DNA gel electrophoresis.....	33
2.2.7	Ligation	33
2.2.8	TOPO cloning	33
2.2.9	Gateway cloning	34
2.2.10	Transformation of chemically competent bacteria	34
2.2.11	Electroporation of bacteria.....	34
2.2.12	Plasmid amplification and purification.....	34
2.2.13	DNA sequencing.....	35
2.2.14	Analysis of nucleotide and protein sequences.....	35
2.2.15	Expression and purification of GST fusion proteins.....	35
2.3	<i>Yeast two-hybrid (Y2H) system</i>	36
2.3.1	cDNA library titering and amplification.....	37
2.3.2	Transformation of yeast.....	38
2.3.3	β-galactosidase assay.....	39
2.3.4	Plasmid preparation from yeast.....	39
2.4	<i>Culture of mammalian cells</i>	40
2.4.1	Transfection of mammalian cells	42
2.4.2	Generation of a HM1 cell line stably expressing mTRPC5-YFP.....	42

Table of contents

2.5	<i>Protein biochemical methods</i>	42
2.5.1	Preparation of cell lysates.....	42
2.5.2	Determination of protein content.....	43
2.5.3	SDS-PAGE	43
2.5.4	Western blot.....	43
2.5.5	GST pulldown assay.....	44
2.5.6	Co-immunoprecipitation.....	44
2.5.7	Surface expression analysis	44
2.5.8	Peptidyl-prolyl <i>cis-trans</i> isomerization assay	45
2.5.9	Phospholipid overlay assay	46
2.5.10	Cova-PIP specificity plate assay.....	46
2.5.11	Immunofluorescence	46
2.6	<i>Fluorometric [Ca²⁺]_i measurements</i>	47
2.7	<i>Patch clamp recordings</i>	49
2.8	<i>In vitro vascular function</i>	50
2.9	<i>Statistics</i>	51
3	Results	52
3.1	<i>Differential inhibition of TRPC channels by norgestimate</i>	52
3.1.1	FLIPR measurements.....	52
3.1.2	Patch clamp recordings	58
3.1.3	Isometric tension recording of aortic rings	61
3.2	<i>Physical interaction of SESTD1 and TRPC channels</i>	63
3.2.1	Y2H results	63
3.2.2	Mapping of the TRPC4-SESTD1 interaction site.....	64
3.2.3	Biochemical verification of SESTD1-TRPC4/5 binding by GST pulldown	66
3.2.4	Co-immunoprecipitation.....	67
3.2.5	Interaction of SESTD1 and TRPC subfamilies	70
3.3	<i>Functional interaction of SESTD1 and TRPC5</i>	71
3.3.1	Characterization of a HM1 clone stably expressing mTRPC5-YFP	71
3.3.2	Overexpression of SESTD1 in HM1-C5Y cells.....	73
3.3.3	siRNA knock-down of SESTD1	75
3.4	<i>SESTD1</i>	79
3.4.1	Expression	79
3.4.2	Subcellular localization	80
3.4.3	<i>Cis-trans</i> isomerase signature	83
3.4.4	<i>In vitro</i> phospholipid binding	83
3.4.5	SESTD1 siRNA knock-down in HM1 cells changes β -catenin distribution	86
4	Discussion	88
4.1	<i>Norgestimate is a selective inhibitor of the TRPC3/6/7 subfamily</i>	88
4.2	<i>Identification of SESTD1 – a novel TRPC-interacting protein</i>	93
4.2.1	SESTD1 interacts with TRPC4 via the channel's CIRB domain.....	95
4.2.2	Functional effects of SESTD1 knock-down on TRPC5.....	98
4.3	<i>Cell biology of SESTD1</i>	99
4.3.1	Tissue expression and subcellular localization.....	99
4.3.2	Enzymatic function of SESTD1.....	101
4.3.3	Regulation of β -catenin.....	104
5	Summary	106

Table of contents

6	Zusammenfassung	108
7	References	113
8	Appendix	135
8.1	<i>Vectors</i>	135
8.2	<i>Constructs for expression in yeast</i>	135
8.3	<i>Constructs for expression in bacteria</i>	136
8.4	<i>Constructs for expression in mammalian cells</i>	136
8.5	<i>Abbreviations</i>	137
9	Danksagung	141
10	Curriculum vitae	142
11	Eidesstattliche Erklärung	143

1 Introduction

1.1 Calcium signalling

Since the first description of “animal electricity” by Luigi Galvani in the second half of the 18th century, electrical phenomena have been recognized as a basic principle of life. All cells establish charge gradients to generate and store energy, to transduce information and to maintain their structural integrity.

Underlying these electrical processes at the molecular level is an uneven distribution of ions across the lipid-water interface of cellular membranes. To allow for the movement of charges through the *per se* impermeable lipid bilayer, biological membranes contain specific proteins, ion channels, which are essential for the generation and maintenance of the cell’s electrical circuitry.

Classical studies of ion channel physiology have focused on neurons and muscle cells as their functions, e.g. action potential generation, synaptic transmission, or contraction, are largely dependent on ion channel activity. It has been gradually recognized, however, that by regulating ion fluxes and membrane potentials, ion channels are involved in almost all aspects of cellular physiology. In addition to the “fast and furious” electrical responses in excitable cells there are many actions of ion channels that are more subtle, occur on a longer time scale and ultimately control adaptive processes like proliferation, differentiation and cell survival.

Calcium, a small ion, has emerged as a key messenger that accompanies development of an organism from fertilization (acrosomal reaction) until death (apoptosis, necrosis). It translates membrane potential changes and ion channel activity into diverse enzymatic processes (Berridge, 1993). Calcium regulation is achieved by the Ca^{2+} -dependent function of numerous proteins ranging from kinases, proteases and transcription factors to synaptic and contractile proteins. These either interact directly with the ion or they are indirectly modulated by specific Ca^{2+} -binding proteins, such as calmodulin (CaM). In accordance with its pivotal role in signal transduction, the free intracellular cytosolic Ca^{2+} concentration, $[\text{Ca}^{2+}]_i$, temporally and spatially is tightly regulated by ion channels, transporters, adenosine triphosphate (ATP)-driven pumps, and Ca^{2+} -binding proteins. In quiescent cells, $[\text{Ca}^{2+}]_i$ is much lower (around 50-100 nM) compared to the Ca^{2+} concentration of internal stores (1 μM – 3 mM; Meldolesi & Pozzan, 1998) and the extracellular fluid (~2 mM; Clapham *et al.*, 2001). Sustained elevation of $[\text{Ca}^{2+}]_i$ as observed under many pathophysiological conditions, e.g. in cardiac hypertrophy, heart failure, and ischemia, can induce maladaptive remodelling processes (Berridge, 2006; Dietrich *et al.*, 2007) and will eventually lead to cell death (Clapham, 1995; Bano & Nicotera, 2007).

In line with the requirement for a tight control of $[Ca^{2+}]_i$, cells possess numerous Ca^{2+} -influx channels with diverse structures, biophysical properties, and regulation mechanisms. In excitable cells a main determinant of Ca^{2+} influx is the membrane potential. These cells express voltage-dependent Ca^{2+} channels that allow a large, action potential-driven Ca^{2+} entry. Another important class of Ca^{2+} permeable channels, mainly found in neuronal and muscle cells, are ligand-gated cation channels which are directly activated by hormones and neurotransmitters, thereby providing the basis for fast signal transduction at chemical synapses.

Whereas the main Ca^{2+} channels in excitable cells are well characterized, the importance and molecular identity of Ca^{2+} entry channels in non-excitable cells, such as immune cells, endothelial and epithelial cells or hepatocytes, has long remained controversial. In general, these cells do not express voltage-dependent Ca^{2+} channels and Ca^{2+} influx is much smaller than in neurons or muscle cells, making it difficult to functionally isolate and characterize the proteins involved. Work pioneered by Putney, Berridge and others established that store- and receptor-operated cation channels (SOCs and ROCs; reviewed by Parekh, 2006) represent the predominant routes of Ca^{2+} entry into non-excitable cells. Despite great progress in this field, many aspects of SOC/ROC function and their regulation still remain poorly understood and continue to provide challenging topics for basic research as well as drug discovery.

1.1.1 Store- and receptor-operated Ca^{2+} influx

SOCs initiate diverse cellular processes, e.g. enzyme activation (Fagan *et al.*, 2000), gene transcription (Lewis, 2001), and replenishment of intracellular Ca^{2+} stores, mainly the endoplasmic reticulum (ER; Putney, Jr. & Bird, 1993). The latter process, also referred to as capacitative Ca^{2+} entry (CCE; Putney, Jr., 1986), is vital and ubiquitously present (Ambudkar & Ong, 2007). Store repletion after release is important to maintain the many physiological ER functions, e.g. protein folding, posttranslational modification and trafficking, stress response and initiation of cell death (Burdakov *et al.*, 2005). Contrary, ROCs mainly mediate the integration of multiple extracellular stimuli, their amplification and translation into distinct signalling cascades and finally specific physiological responses.

Receptor- and store-operated Ca^{2+} entry is triggered by the activation of receptor tyrosine kinases (RTK) or $G_{q/11}$ protein-coupled receptors (GPCR) which subsequently stimulate phospholipase C (PLC). PLC cleaves phosphatidylinositol 4,5-bisphosphate (PIP_2) into soluble inositol 1,4,5-trisphosphate (IP_3) and membrane-bound 1,2-diacylglycerol (DAG). DAG is an important second messenger with diverse downstream effects such as activation of protein kinase C (PKC; reviewed by Bell & Burns, 1991). This enzyme in turn can phosphorylate channel proteins, thereby regulating their activity (Venkatachalam *et al.*,

2003). IP_3 diffusion to the IP_3 -gated Ca^{2+} -channel (IP_3R) in the ER membrane causes opening of the IP_3R and release of Ca^{2+} from the ER to the cytosol. These signalling events are commonly termed the phosphatidylinositol (PI) response. The IP_3 -evoked depletion of intracellular Ca^{2+} stores subsequently activates SOCs (Fig. 1; reviewed by Berridge, 1993).

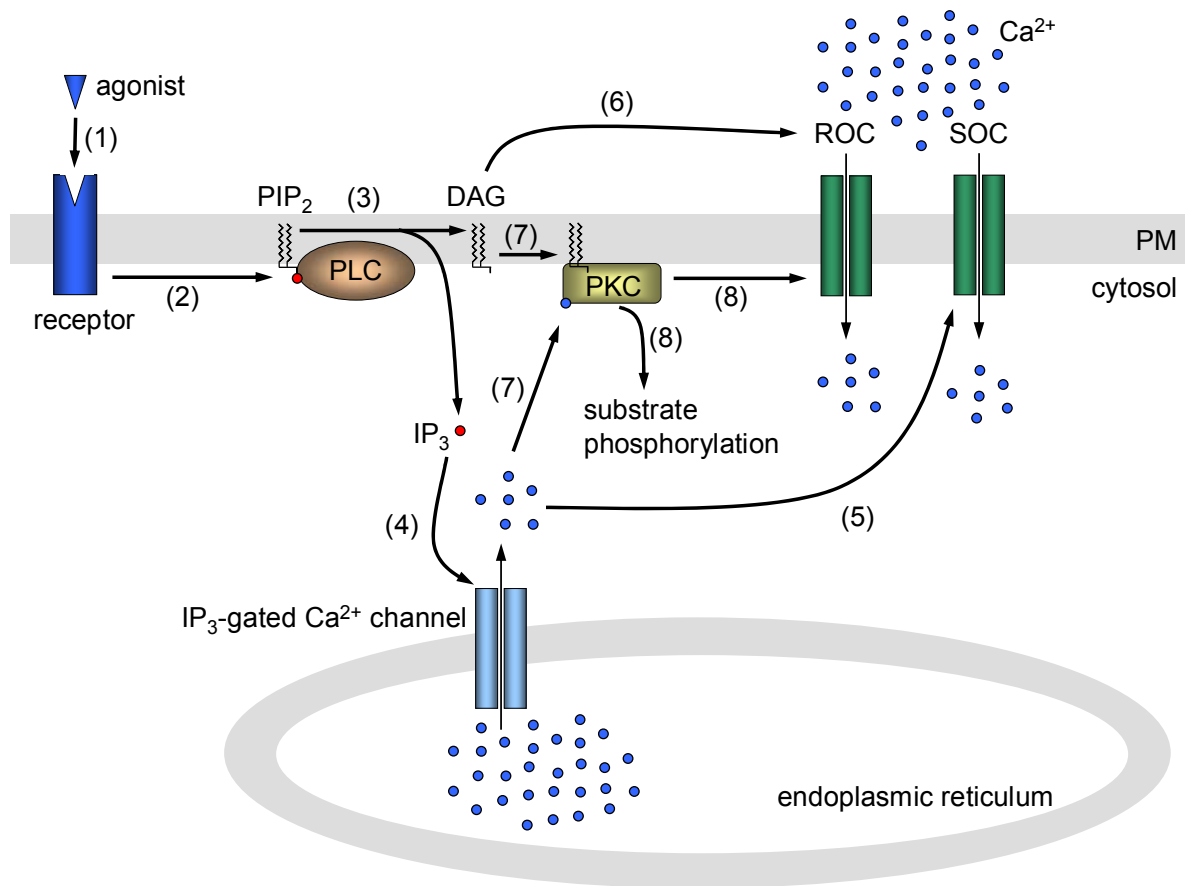


Figure 1: Receptor- and store-operated Ca^{2+} influx. Agonist stimulation of a receptor tyrosine kinase or a $\text{G}_{q/11}$ protein-coupled receptor (1) leads to activation of phospholipase C (PLC) (2). The enzyme cleaves phosphatidylinositol 4,5-bisphosphate (PIP_2) into membrane-bound diacylglycerol (DAG) and soluble inositol 1,4,5-trisphosphate (IP_3) (3). IP_3 diffusion to the IP_3 -gated Ca^{2+} -channel in the ER membrane evokes depletion of intracellular Ca^{2+} stores (4). In parallel, store depletion activates SOCs (5). DAG may directly activate certain ROCs (6) and also, cooperatively with Ca^{2+} , PKC (7). PKC phosphorylates diverse substrates like channel proteins (8).

For a channel to be classified as store-operated, its direct activation by experimental store-depletion has to be demonstrated (Bolotina & Csutora, 2005). Pharmacological agents like cyclopiazonic acid and thapsigargin inhibit the sarcoplasmic/endoplasmic reticulum Ca^{2+} pumps (SERCA; Favre *et al.*, 1996) that normally transport Ca^{2+} against its electrochemical gradient into the ER. Inhibition of this active, ATP-consuming process results in passive Ca^{2+} leakage. Ultimately, Ca^{2+} influx from the extracellular surrounding is mediated by SOCs, even in the absence of receptor stimulation or generation of IP_3 .

ROCs are activated through the same signalling cascade but in contrast to SOCs they do not require store depletion. The phospholipase-derived second messenger DAG has been shown to directly activate ROCs (Hofmann *et al.*, 1999). Furthermore, it is assumed that so

far unknown messengers and PLC-dependent mechanisms are also involved in ROC channel stimulation (Clapham *et al.*, 2001).

Hence, ROCs and SOCs can be activated simultaneously following stimulation of one receptor. But the underlying signalling cascades are definitely distinct.

1.1.2 Activation of store-operated channels

The elevation in $[Ca^{2+}]_i$ caused by store-depletion, the PI response, is not sufficient to initiate store-operated Ca^{2+} entry (Parekh, 2006). How does a store-operated channel in the plasma membrane then sense depletion of intracellular Ca^{2+} stores? At least three general models were proposed (schematically depicted in Fig. 2) that strive to answer this question:

1. **Conformational coupling model:** The IP_3R (located in the ER membrane) is in close vicinity to the SOC (inserted in the plasma membrane) allowing direct protein-protein interaction. IP_3R activation results in “conformational-coupled” stimulation of the channel (Irvine, 1990; Berridge, 1995). Since this model conflicts with the slow channel activation kinetics after store-depletion, it was revised to the “**secretion-like coupling**” hypothesis (Patterson *et al.*, 1999). It is based on the assumption that SOCs and the IP_3R of quiescent cells are physically separated, but the ER can move towards the channel following store depletion. Therefore, a temporal physical interaction between the SOC and the IP_3R is possible but requires some time to build up. It depends on the peripheral cytoskeleton and stabilizing reagents might obstruct the coupling whereas disaggregation could facilitate it (Rosado *et al.*, 2000; Venkatachalam *et al.*, 2002). The participation of the IP_3R at all stages of SOC activation in this model conflicts with the definition of store-operation (see above; Bolotina & Csutora, 2005; Parekh, 2006), but alternatively another ER component might interact with SOCs. An interesting candidate is the stromal interaction molecule 1 (STIM1) that will be introduced in greater detail below.
2. **Calcium influx factor model:** Store depletion is thought to release a so far unknown “diffusible messenger”, termed calcium influx factor (CIF), from the ER. Alternatively, its *de novo* synthesis could be initiated by store depletion. CIF might directly (Takemura *et al.*, 1989; Randriamampita & Tsien, 1993) and also indirectly activate SOCs. It is proposed to stimulate membrane-bound Ca^{2+} -independent phospholipase A_2 (iPLA₂) by releasing it from binding to the inhibitory protein calmodulin. Subsequently, lysophospholipids generated by iPLA₂ could activate the SOC directly (Smani *et al.*, 2003; Bolotina & Csutora, 2005). Besides CIF, other diffusible messengers have been suggested, e.g. 5,6-epoxyeicosatrienoic acid, nitric oxide, and sphingosine-1-

phosphate (Parekh & Putney, Jr., 2005) and are controversially discussed (Bolotina & Csutora, 2005).

- 3. Vesicle-fusion model:** Functional SOCs are stored in cytoplasmic vesicles and recruited to and rapidly inserted into the plasma membrane following stimulation (Yao *et al.*, 1999; Alderton *et al.*, 2000). Exocytotic channel insertion was also observed after receptor stimulation (Cayouette *et al.*, 2004; Bezzerides *et al.*, 2004; Singh *et al.*, 2004; Odell *et al.*, 2005) thus demonstrating that the mechanism might not be exclusive for activation of SOCs but is important for TRP-mediated Ca^{2+} influx in general.

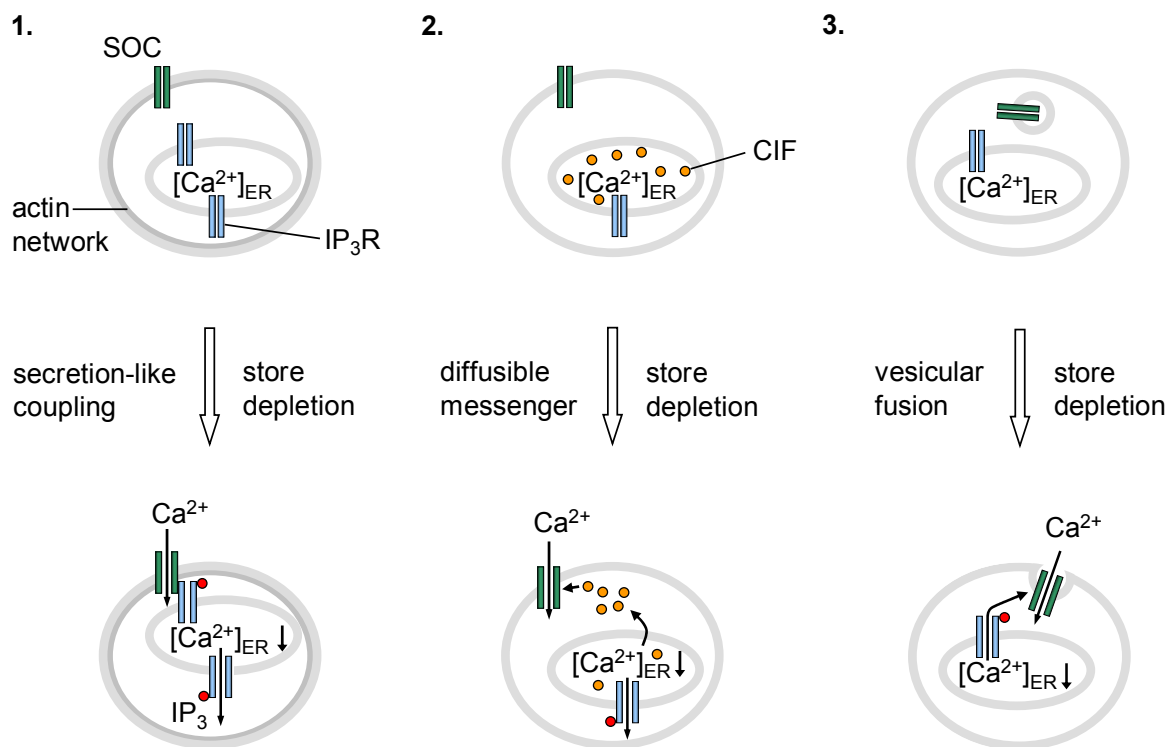


Figure 2: Proposed activation models for store-operated channels (adapted from Parekh, 2006). See text for detailed information.

Over the past two decades, the coupling mechanisms between the ER and store-operated Ca^{2+} -influx channels and also the molecular identity of these channel proteins remained elusive and were intensely investigated. SOCs do not form a uniform group but have diverse biophysical properties. The best studied store-depletion responsive current is the calcium-release-activated calcium (CRAC) current termed I_{CRAC} . First identified in mast cells (Hoth & Penner, 1992), it is found in many cell types, and several genes have been proposed to code for the CRAC channel-constituting proteins.

Most recently, crucial progress was made with the identification of two proteins that function together in sensing store-depletion and subsequently mediating I_{CRAC} . Stromal interaction molecule 1 (**STIM1**) was discovered in two independent RNA interference (RNAi) screens

performed to elucidate the underlying signalling cascades of store-operated Ca^{2+} influx (Liou *et al.*, 2005; Roos *et al.*, 2005). It has a single transmembrane domain and is found inserted in the PM and the ER membrane (Soboloff *et al.*, 2006). Originally identified as tumor suppressor (Sabbioni *et al.*, 1997), it is now also thought to control the ER Ca^{2+} filling state with its luminal Ca^{2+} -binding EF hand motif and to transduce the depletion signal to **Orai1** proteins (Liou *et al.*, 2005; Zhang *et al.*, 2005). These were named after Greek mythological characters (the gate keepers of heaven) by one group (Feske *et al.*, 2006), whereas the term CRAC modulator 1 (**CRACM1**) was coined by another (Vig *et al.*, 2006b). They are predicted to have four membrane-spanning domains and to constitute the ion channel pore subunit (Vig *et al.*, 2006a; Prakriya *et al.*, 2006; Yeromin *et al.*, 2006). A single amino acid substitution (R91W) suppresses I_{CRAC} necessary for T- and B-lymphocyte activation thus causing a rare hereditary form of severe combined immunodeficiency (SCID; Feske *et al.*, 2005; Feske *et al.*, 2006).

While the interaction of STIM1 and Orai1 is generally accepted to be necessary and sufficient to mediate store-operated Ca^{2+} entry, the question of how they communicate has not been unequivocally answered. Physical interactions have been demonstrated by co-immunoprecipitation studies (Yeromin *et al.*, 2006; Vig *et al.*, 2006a; Ong *et al.*, 2007), but neither study resolves whether these are direct or indirect and whether they occur between proteins both inserted in the PM or Orai1 and STIM1 in the ER (Hewavitharana *et al.*, 2007). Three adapted “secretion-like coupling” models are currently discussed as Orai1 activation by one of the other proposed SOC activation mechanisms is less likely. Due to the physical interaction between STIM1 and Orai1, the existence of a diffusible messenger is at least not indispensable (Vig & Kinet, 2007). Moreover, Orai1 is constitutively expressed in the PM and activation does not seem to require exocytosis (Prakriya *et al.*, 2006; Vig *et al.*, 2006b). Nevertheless, exocytotic transport may be involved in STIM1 translocation to the PM (Vig & Kinet, 2007), and also an increased STIM1 pulldown after store depletion in biotinylation experiments has been reported (Zhang *et al.*, 2005). Modulation of CRAC channel function by phosphorylation is discussed as well (Vig & Kinet, 2007). Further studies are required to ascertain which of the proposed mechanisms finally activates the CRAC channel.

1.2 The TRP channel superfamily

As mentioned above, the CRAC channel is the most prominent but not the only SOC (reviewed by Montell, 1997; Vazquez, *et al.*, 2004b; Parekh, 2006). The involvement of store-operated Ca^{2+} entry in so many and diverse physiological processes like exocytosis, contraction, enzyme control, gene regulation, apoptosis, cell proliferation and migration (Parekh & Penner, 1997), motivated many investigators to search for the molecular correlates of these currents. In 1995, these efforts led to the discovery of a novel class of Ca^{2+} -permeable cation channels in mammals, the TRP superfamily (Zhu *et al.*, 1995; Wes *et*

al., 1995). It was named after a spontaneous *Drosophila melanogaster* mutant that has been isolated almost two decades earlier.

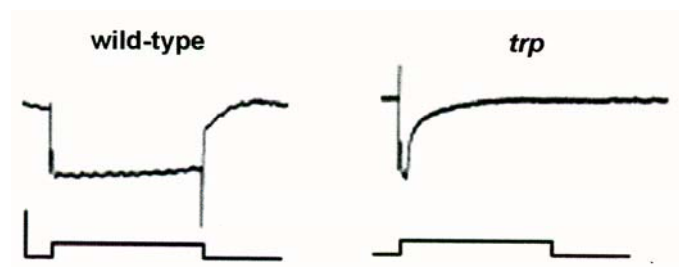


Figure 3: Electrophysiological recordings of *trp* *D. melanogaster* mutants. Dark-adapted flies were exposed to a five seconds pulse of white light (indicated by the event marker). The vertical line of the event marker represents 5 mV (Montell, 2004).

Fruitfly mutants had been screened for defects in their electroretinogram (ERG) recordings in order to elucidate the visual transduction pathways (Cosens & Manning, 1969). Unlike in vertebrates, phototransduction in the fruitfly is coupled to PLC. Light-induced PLC activation results in Na^+ and Ca^{2+} influx, thus depolarizing the photoreceptor cells (Montell, 1999; Hardie & Raghu, 2001). This Ca^{2+} entry is defective in the above mentioned mutants, they abnormally respond with a transient rather than sustained depolarization to prolonged light exposure (Fig. 3) and were therefore named *transient receptor potential (trp)* (Minke *et al.*, 1975).

After the *trp* gene had been cloned (Montell & Rubin, 1989), further studies confirmed that it codes for a novel light-activated, Ca^{2+} -permeable cation channel (Hardie & Minke, 1992; Phillips *et al.*, 1992; Niemeyer *et al.*, 1996). Its Ca^{2+} permeability and coupling to PLC sparked interest in TRPs beyond invertebrate phototransduction exploration as the channel was speculated to be a SOC (reviewed by Montell, 1997). Later on, TRP became evident to be the founding member of a novel channel superfamily. Two more TRP-related channels, TRPL and TRP γ , were found in *Drosophila* (Phillips *et al.*, 1992; Tsunoda & Zuker, 1999; Xu *et al.*, 2000) and up to date 29 mammalian orthologs of the *Drosophila trp* gene have been identified. Some of them are also candidates to form SOCs (Montell *et al.*, 2002b; Montell, 2005; Okuhara *et al.*, 2007), whereas others constitute ROCs, tonically active or stretch-activated channels (Dietrich *et al.*, 2006).

By sequence homology TRPs can be divided into seven families, named after their first recognized members (Pedersen *et al.*, 2005; Ramsey *et al.*, 2006): TRPC (classical), TRPV (vanilloid), TRPM (melastatin), TRPA (ankyrin), TRPP (polycystin) and TRPML (mucolipin). TRP-related channels are found in every metazoan organism genetically studied so far (Montell *et al.*, 2002a) with the seventh existing TRPN (no mechanoreceptor potential C) family containing members in *Drosophila melanogaster*, *Caenorhabditis elegans* and *Danio rerio* (Montell, 2001; Okuhara *et al.*, 2007), but not in mammals (Fig. 4).

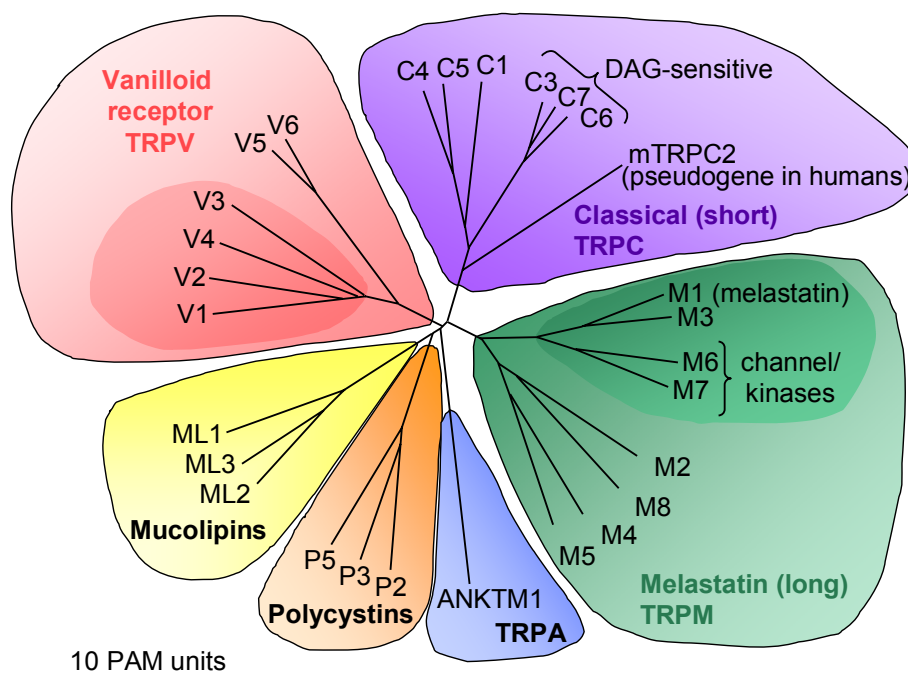


Figure 4: The mammalian TRP family tree (adapted from Clapham, 2003). The branch length symbolizes the evolutionary distance and is graded in point accepted mutations units (PAM, mean number of mutations per 100 residues).

At the time of its cloning, TRP showed no significant homology to known proteins (Montell, 2004). Difficulties in crystallizing these integral membrane proteins so far prevented structure determination by X-ray analysis. A topology analysis of its primary sequence predicted seven hydrophobic, putatively membrane-spanning segments. By virtue of mutagenesis studies, determination of glycosylation sites and in analogy to known voltage-gated and second-messenger-gated ion channels, it is now assumed that TRP channels (with the exception of TRPP1; Okuhara *et al.*, 2007) have six transmembrane domains with cytosolic amino and carboxy termini (Montell & Rubin, 1989; Vannier *et al.*, 1998). Functional channels are thought to be composed of homo- or heterotetramers (Kedei *et al.*, 2001; Hoenderop *et al.*, 2003; Amiri *et al.*, 2003), in which the pore is formed by the fifth and sixth membrane-spanning domains and intervening segments (Fig. 5). They lack the complete voltage sensor formed by positively charged amino acids in the fourth transmembrane domain of many voltage-gated channels (Montell, 2001) and therefore, are only weakly voltage-sensitive. Whereas channels within a family share high amino acid sequence similarity, the families by themselves are quite different, but at least their transmembrane segments are significantly homologous to TRP (Montell, 2001).

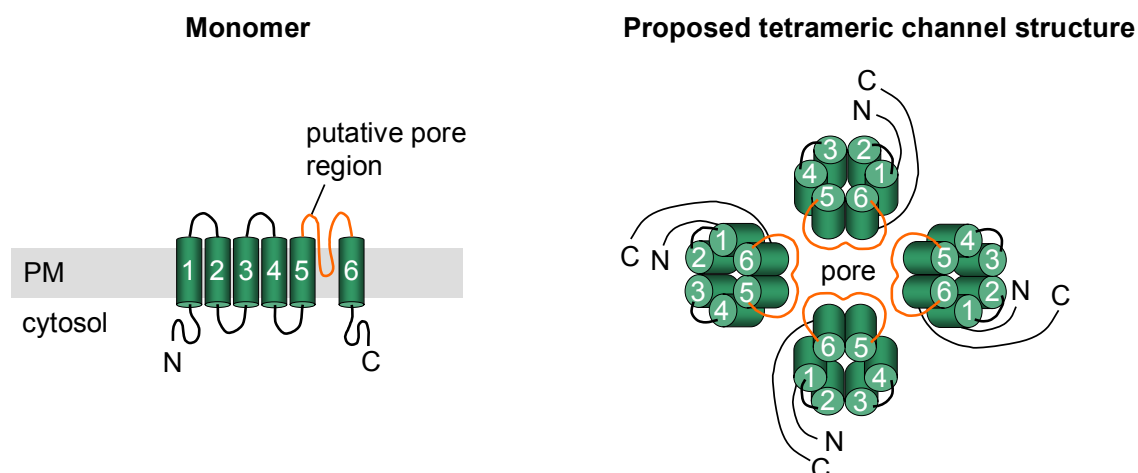


Figure 5: Proposed TRP channel topology (adapted from Li *et al.*, 2002). See text for explanations (abbreviations: C, carboxy terminus; N, amino terminus; 1-6, membrane-spanning segments).

The tissue distribution of TRP channels in mammals is commonly widespread, ranging from non-excitable cells to the nervous system. Activation mechanisms, ion selectivities and putative physiological and pathophysiological roles are strikingly versatile and diverse. Apart from two monovalent-selective exceptions (TRPM4 and -M5), TRP channels are Ca^{2+} -permeable but rather non-selective to cations. They modulate $[\text{Ca}^{2+}]_i$ and regulate membrane potential (Kwan *et al.*, 2007). TRPV5 and -V6 are more Ca^{2+} -selective but not as much as voltage-gated Ca^{2+} -channels (Clapham *et al.*, 2001).

Currently, TRP channels are attracting growing attention due to their possible involvement in human physiology and disease. The ancestral *Drosophila* TRP channel is crucial for visual transduction and several mammalian relatives (especially of the TRPV family) are also important for sensory perception, e.g. of mechanical stimuli, osmolarity, pain, pheromones, taste and temperature. Others are involved in such distinct physiological processes as fertilization and vasorelaxation. TRP channels abnormally activated or dysfunctional due to pathologic mutations cause several channelopathies (for a recent review see Nilius, 2007). For instance, TRPs have been connected to polycystic kidney disease (Mochizuki *et al.*, 1996) and hereditary focal segmental glomerulosclerosis (FSGS; Winn *et al.*, 2005), to the lysosomal storage disorder mucopolisidosis IV (Bassi *et al.*, 2000), to hypomagnesemia with secondary hypocalcaemia (HSH, Schlingmann *et al.*, 2002) and to Guamanian amyotrophic lateral sclerosis and parkinsonism dementia (Hermosura *et al.*, 2005; Hermosura & Garruto, 2007).

1.3 The TRPC family

1.3.1 Structural features of TRPCs

TRPCs were the first TRP proteins discovered in mammals (Wes *et al.*, 1995; Zhu *et al.*, 1995). Seven proteins, referred to as TRPC1 – 7, constitute the canonical (or classical) TRP family that is the closest related to the *Drosophila* TRP protein (30-40% identity; Okuhara *et*

al., 2007). They are thought to share the topology described in Chapter 1.2. The structure of a TRPC channel monomer is schematically depicted in Figure 6 and some known TRPC-interacting proteins are also shown next to their interaction sites within the channel.

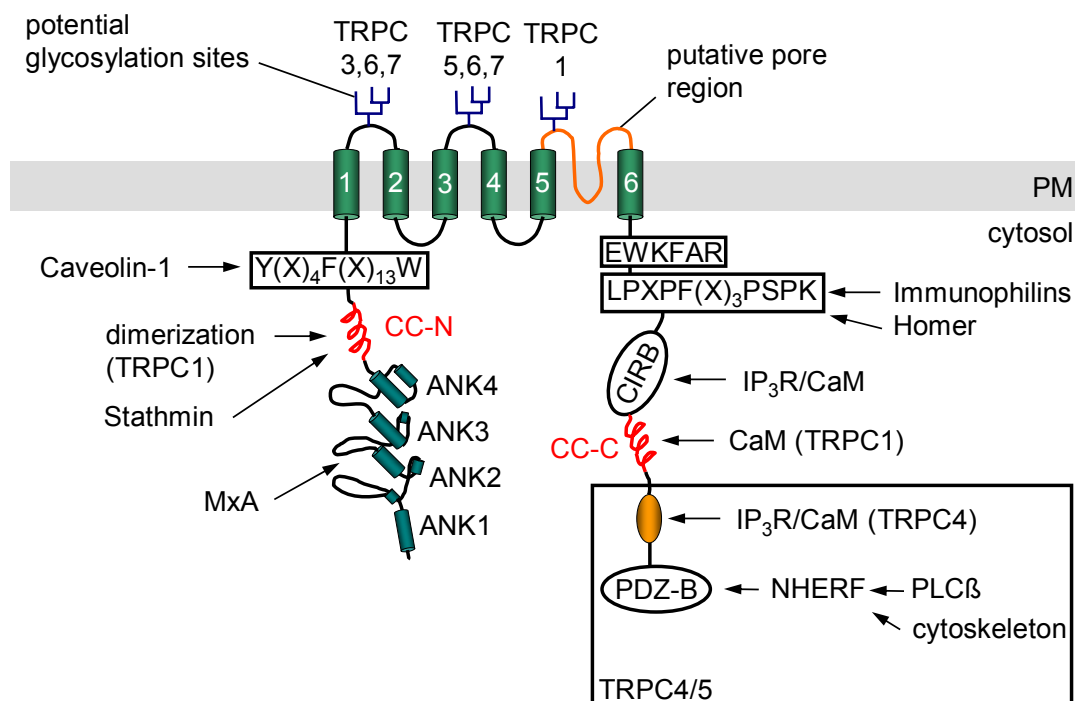


Figure 6: Structure of TRPC monomers (adapted from Vazquez *et al.*, 2004b). The box depicts the extended carboxy terminus that is unique to TRPC4 and -5 proteins. See text for description. The acronyms are: ANK, ankyrin-like repeats; CaM, calmodulin; CC-N, CC-C, coiled-coil domain (N- and C-terminal); CIRB, calmodulin/IP₃ receptor binding region; IP₃R, IP₃ receptor; NHERF, Na⁺/H⁺ exchanger regulatory factor; PDZ-B, PDZ binding domain; PLCβ, phospholipase C β; PM, plasma membrane.

The cytosolic amino termini of TRPC channels contain three to four ankyrin repeats, a coiled-coil domain and a putative caveolin 1-binding domain. A peptide sequence called TRP box (amino acids EWKFAR) is found C-terminal to the sixth transmembrane-spanning domain. This sequence is invariant in TRPC but less conserved in TRPV and TRPM (Clapham, 2003) and its function is not yet understood (Woodard *et al.*, 2007). Moreover, the cytosolic carboxy termini contain a highly conserved proline-rich domain, the calmodulin/IP₃ receptor binding (CIRB) domain and another coiled-coil domain.

Unique to TRPC4 and TRPC5 are extended C-termini with additional binding sites for the IP₃R and CaM. They also contain a PDZ-binding motif that controls TRPC4 channel surface expression (Mery *et al.*, 2002). It interacts with several PDZ domain containing proteins, e.g. the Na⁺/H⁺ exchanger regulatory factor (NHERF; Tang *et al.*, 2000) which links the channel to PLCβ and the cytoskeleton (Tang *et al.*, 2000).

All domains mentioned above function in protein-protein interaction. Ankyrin repeats are common protein-binding motifs that participate in the assembly with cytoskeletal and regulatory proteins (Mosavi *et al.*, 2004). They mediate TRPC channel interaction with MxA,

a member of the dynamin superfamily of GTPases (Lussier *et al.*, 2005), and, as demonstrated for TRPC3 and -6, are required for correct trafficking to the PM (Hofmann *et al.*, 2002; Wedel *et al.*, 2003). The first ankyrin-like repeat was additionally identified as key structure for functional homo- and heteromerization of TRPC4 and -5 channels (Schindl *et al.*, 2007). Coiled-coil domains have been reported to be involved in TRPC1 channel homomerization (Engelke *et al.*, 2002; Lepage *et al.*, 2006) and linkage with other proteins (Greka *et al.*, 2003). An additional site of protein-protein interaction is the C-terminal proline-rich region that was found to interact with FK506 binding proteins (FKBP; Sinkins *et al.*, 2004) and Homer (Yuan *et al.*, 2003).

Mutations within the highly conserved pore-region result in dominant-negative monomers that suppress the function of homo- and heteromeric channels (Hofmann *et al.*, 2002). Furthermore, it was demonstrated that the N-glycosylation pattern can determine the channel's constitutive activity. TRPC3 is a highly constitutive active channel and monoglycosylated in the first extracellular loop. By conversion into the TRPC6-like dually glycosylated form it becomes as tightly regulated by PLC-coupled receptors as TRPC6 and *vice versa* (Dietrich *et al.*, 2003).

1.3.2 TRPC-interacting proteins

Drosophila TRP and other components of the fruitfly phototransduction cascade are clustered in a transducisome (reviewed by Montell, 2004), a macromolecular complex assembled by the scaffolding protein INAD (inactivation no afterpotential D; Shieh & Zhu, 1996). Analogously, TRPCs are suggested to be organized within specific Ca²⁺ signalling complexes that facilitate their physical and/or functional coupling with accessory proteins participating in Ca²⁺ signalling and also with proteins involved in vesicle trafficking, cytoskeletal interaction, and scaffolding (Ambudkar & Ong, 2007). For instance, some TRPCs have been shown to be associated with caveolae (Lockwich *et al.*, 2000; Lockwich *et al.*, 2001; Torihashi *et al.*, 2002). These are detergent-insoluble, glycosphingolipid- and cholesterol-enriched membrane domains (so-called lipid rafts) that are assembled by the cholesterol-binding protein caveolin (Brazier *et al.*, 2003). Several TRPC-associated proteins have been identified which might be involved in regulating channel function, stability, and cellular localization (Ambudkar & Ong, 2007). According to their proposed function as structural or regulatory proteins they are summarized in Table 1.

Table 1: TRPC-interacting proteins.

TRPC1	TRPC2	TRPC3	TRPC4	TRPC5	TRPC6	TRPC7
CaM	CaM	CaM	CaM	CaM	CaM	CaM
TrkR		TrkR			TrkR	
G $\alpha_{q/11}$		G $\alpha_{q/11}$			G $\alpha_{q/11}$	
IP ₃ R	IP ₃ R	IP ₃ R	IP ₃ R	IP ₃ R	IP ₃ R	IP ₃ R
PLC β	PLC β	PLC β	PLC β	PLC β	PLC β	PLC β
PMCA		PMCA	PMCA	PMCA	PMCA	
SERCA		SERCA			SERCA	
STIM1	STIM1		STIM1	STIM1 ¹		
Caveolin		Caveolin	Caveolin	Caveolin		
Enkurin	Enkurin			Enkurin		
FKBP52 ²		FKBP12 ²	FKBP52 ²	FKBP52 ²	FKBP12 ²	FKBP12 ²
Homer1/2/3	Homer 1	Homer 1	Homer 3 ³	Homer 1/3 ³		
MxA	MxA	MxA	MxA	MxA	MxA	MxA
			NHERF	NHERF		
		Orai1 ⁴			Orai1 ⁴	
	PLC γ	PLC γ		PLC γ	PLC γ	
RhoA				RhoA	RhoA	
SNARES		SNARES		SNARES		
			ZO-1	ZO-1		

Only proteins common to at least two TRPCs are listed. Those involved in Ca²⁺ signalling are shown in the top half and those participating in scaffolding and trafficking in the bottom half of the table (adapted from Ambudkar & Ong, 2007; see also references therein). ¹ Yuan *et al.*, 2007; ² Sinkins *et al.*, 2004; ³ Yuan *et al.*, 2003; ⁴ Liao *et al.*, 2007.

1.3.3 Activation mechanisms

All TRPCs can be activated by receptor stimulation and subsequent PLC activation (Ambudkar *et al.*, 2007; Yuan *et al.*, 2007), but available data is controversial whether and under which conditions they act as SOCs. None of the TRPCs shows the high selectivity for Ca²⁺ over Na⁺, low single-channel conductance and pharmacological enhancement by 1-5 μ M 2-APB typical for the long sought after and most prominent store-operated CRAC channel (Clapham, 2003). While SOCs are ubiquitously expressed and have diverse characteristics in different cell types (Ambudkar *et al.*, 2007), it is unlikely that they are formed by a single channel, thus some might indeed be constituted by TRPCs. Many studies investigating the activation mode of TRPC channels were therefore performed, resulting in an abundance of conflicting reports. For instance, TRPC3 has been reported to be solely receptor-operated by some groups (Zhu *et al.*, 1998; Ma *et al.*, 2000; McKay *et al.*, 2000) but also to be store-operated in other laboratories (Boulay *et al.*, 1999; Kiselyov *et al.*, 2000). Similarly, different activation mechanisms have also been reported for TRPC4. Native TRPC4 proteins have been suggested to mediate store-operated Ca²⁺ influx (Freichel *et al.*, 2001; Torihashi *et al.*, 2002) and Philipp *et al.*, 2000, observed that overexpressed TRPC4 channels responded to store depletion. But later work could not confirm these data and showed receptor-dependent activation of heterologously expressed TRPC4 channels (Schaefer *et al.*, 2000; Schaefer *et al.*, 2002). Despite intensive work, the final channel stimulating step following G-protein activation has not been elucidated. It might be a so far

unknown PLC-dependent mechanism or a combination of messengers (Clapham *et al.*, 2001). Finally, basal activity of TRPC4 without stimulation has also been reported (McKay *et al.*, 2000).

Such discrepancies (Trebak *et al.*, 2002) could stem from the different expression systems that might lack certain regulatory or auxiliary proteins necessary for complex formation and specific gating of ectopically expressed TRPCs. Observations could be further confounded by endogenous SOCs (Ambudkar *et al.*, 2007), channel heteromultimerization (Poteser *et al.*, 2006), different channel expression levels (Vazquez *et al.*, 2003), and species-dependent differences in the regulation of channel orthologs (Okada *et al.*, 1999; Riccio *et al.*, 2002).

Despite intensive effort, a general mechanism of TRPC channel activation by store depletion has not been unravelled. Recently, several suggestions were made taking into account the identification of STIM1 and Orai1 as the I_{CRAC} -mediating proteins (see Chapter 1.1.2). A new molecular definition of “store operation” was suggested in which SOCs are plasma membrane channels that are regulated by rearrangement of the ER Ca^{2+} -content sensor STIM1 (Yuan *et al.*, 2007). By these criteria, TRPC1, -4, and -5 function as SOCs as they are directly activated by **STIM1**. TRPC3 and -6 can also function as SOCs due to STIM1-dependent heteromultimerization of TRPC3 with TRPC1 and TRPC6 with TRPC4 (Huang *et al.*, 2006; Yuan *et al.*, 2007). The underlying mechanism of STIM1-dependent TRPC gating still remains to be elucidated. Another group has demonstrated that overexpressed TRPC3 and -6 become store-sensitive by coexpression of any of the three existing **Orai** isoforms (Orai1-3). A novel activation model was deduced from this observation wherein SOCs are composed of TRPC pore-forming subunits and Orai regulatory β -subunits. Orai would relay the store depletion signal from STIM1 to TRPC (Liao *et al.*, 2007). A third candidate that was reported to be involved in TRPC store-dependent activation is the scaffolding protein **Homer**. It mediates the physical interaction of TRPC1 with the IP_3R in HEK293 cells when the stores are replete. Depletion disrupts this association and the released channel mediates Ca^{2+} influx to refill the stores (Yuan *et al.*, 2003). This regulation mechanism could be restricted to certain cell types since contrary observations were reported for endothelial cells and platelets. In these cells, TRPC1-dependent store-operated Ca^{2+} influx required channel association with the IP_3R (Mehta *et al.*, 2003; Rosado *et al.*, 2005). Besides its involvement in TRPC1 gating by the IP_3R , Homer 1 also seems to participate in receptor-mediated TRPC3 translocation to the PM and subsequent channel retrieval upon termination of the stimulation (Kim *et al.*, 2006a; Worley *et al.*, 2007).

It is conceivable that all the proposed activation mechanisms exist *in vivo* and they might even be integrated in the same cell type. Further studies are required to determine their relation to each other.

1.3.4 TRPC subfamilies

Based on amino acid sequence homology and functional similarities, TRPCs can be subclassified into four groups (Clapham *et al.*, 2001; Montell, 2001). Being quite unique within the TRPC family, TRPC1 and TRPC2 each constitute a subfamily by themselves while TRPC4 and -5 are merged just as TRPC3, -6, and -7 (Fig. 7).

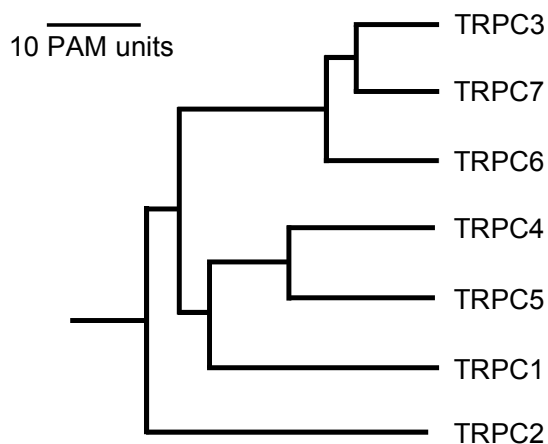


Figure 7: Phylogenetic tree of the TRPC subfamily (adapted from Clapham *et al.*, 2001)
The branch length symbolizes the evolutionary distance and is graded in point accepted mutation units (PAM, mean number of mutations per 100 residues).

Heteromeric interactions within these subfamilies have been shown as well as coassembly of TRPC1 with either TRPC4/5- or TRPC3/6/7-subfamily members (Strubing *et al.*, 2001; Hofmann *et al.*, 2002). It was long thought that cross-association can not occur between the TRPC4/5 and TRPC3/6/7 subgroups, but recently an endogenous redox-sensitive TRPC3/4 heteromer has been found in porcine aortic endothelial cells (Poteser *et al.*, 2006) and STIM1-dependent TRPC4/6 heteromerization has been reported in an overexpression system (Yuan *et al.*, 2007). Heteromers can have distinct biophysical properties compared to the respective monomeric channels (Lintschinger *et al.*, 2000; Strubing *et al.*, 2001; Liu *et al.*, 2005). This fact together with the expression of different TRPCs in a single cell type complicates the characterization of TRPC *in vivo* functions (Pedersen *et al.*, 2005). Nevertheless, several patho- and physiological functions have been suggested for the seven TRPCs (summarized below) but definite proof of concept is lacking in most cases. Given their broad expression and multiplicity of activation mechanisms, the involvement of TRPC channels in essential physiological processes and therefore pathophysiology is most likely. Hence, they are attracting growing attention as potential drug targets (Li *et al.*, 2003; Inoue *et al.*, 2006; Hsu *et al.*, 2007; Nilius, 2007; Okuhara *et al.*, 2007; Kwan *et al.*, 2007; Mukerji *et al.*, 2007; Dietrich *et al.*, 2007a).

TRPC1 subfamily

Functional investigation of the broadly expressed (Beech *et al.*, 2003 and references therein) homomeric TRPC1 has been hampered by absent plasma membrane targeting of the ectopic protein in cell lines. Depending on the overexpression system used, reports range

from lack of robust TRPC1 signals (Strubing *et al.*, 2001) due to retention in intracellular membranes (Wang *et al.*, 1999) to detailed description of channel properties in *Spodoptera frugiperda* sf9 cells (Sinkins *et al.*, 1998). Possible explanations are the absence of auxiliary subunits or interacting proteins in some overexpression systems as plasma membrane expression of the TRPC1 protein has been shown to depend on interaction with other proteins, e.g. TRPCs (Hofmann *et al.*, 2002), caveolin-1 (Brazer *et al.*, 2003), and RhoA (Mehta *et al.*, 2003). Also it is not certain whether homo- or heteromeric expressed or even native channels, which could be stimulated by TRPC1, are measured in sf9 cells (Beech *et al.*, 2003). TRPC1 might not be a pore-forming subunit at all, it could as well function as regulator of other pore-forming channels (Dietrich *et al.*, 2007b) and the existence of a native TRPC1 homomer has not been unequivocally proven so far (Ambudkar *et al.*, 2007).

Whereas several reports have described TRPC1 to be a store-, receptor-, IP₃R-, and/or stretch-activated channel (Ramsey *et al.*, 2006), recent findings in vascular smooth muscle cells of TRPC1^{-/-} mice imply that the channel is not an essential component of store- and stretch-operated channels in these cells (Dietrich *et al.*, 2007b). However, this study does not exclude TRPC1 contribution to such channels in other tissues.

The native protein could be involved in neuronal plasticity, since it is required for the excitatory postsynaptic conductance in Purkinje cells (Kim *et al.*, 2003). TRPC1 also interacts with TRPP2 (Tsiokas *et al.*, 1999), a distantly related TRP protein involved in development of polycystic kidney disease. Moreover, the channel is up-regulated in neointimal hyperplasia (Bergdahl *et al.*, 2004; Kumar *et al.*, 2006) and cardiac hypertrophy (Ohba *et al.*, 2007), interacts with a transcription factor important for myocyte development (Ma *et al.*, 2003) and was proposed to play a role in Duchenne muscular dystrophy (Vandebrouck *et al.*, 2007). In conclusion, TRPC1 may serve as developmental regulator of smooth muscle cells (SMC) and some of its functional roles might not be easily compensated by related TRPCs. It could be engaged in further patho- and physiological processes but its unique physiological functions are not known yet (Dietrich *et al.*, 2007b).

TRPC2 subfamily

TRPC2 is a pseudogene in humans, old world monkeys and apes (Wes *et al.*, 1995; Vannier *et al.*, 1999; Liman & Innan, 2003), but functionally expressed in other mammalian species and essential for pheromone sensation in rodents. Male mice lacking this channel do not show typical male-male aggressive behaviour and court both females and males (Stowers *et al.*, 2002). Antibodies directed to an extracellular domain of TRPC2 inhibit the acrosomal reaction pointing towards its importance in fertilization (Jungnickel *et al.*, 2001). However, TRPC2^{-/-} mice show no defects in reproduction (Stowers *et al.*, 2002). TRPC2 is activated by DAG (Lucas *et al.*, 2003) and does not seem to heteromultimerize with other TRPC channels (Montell, 2005).

TRPC3/6/7 subfamily

These channels share 70–80% amino acid identity and they can be directly activated by the PLC product DAG (Hofmann *et al.*, 1999; Okada *et al.*, 1999; Trebak *et al.*, 2003). TRPC3 and -6 activities are regulated by N-glycosylation (Dietrich *et al.*, 2003) and phosphorylation through the non-receptor tyrosine kinases Src and Fyn (Hisatsune *et al.*, 2004; Vazquez *et al.*, 2004a).

TRPC3 is highly expressed in human brain, smooth and cardiac muscle cells (Dietrich *et al.*, 2006 and references therein). It seems to be involved in axon growth guidance (Li *et al.*, 2005), synaptic plasticity around the time of birth (Li *et al.*, 1999) and cardiac Ca^{2+} homeostasis. In cardiomyocytes, abnormal accumulation of intracellular Na^+ levels due to TRPC3 has been shown to reverse the $\text{Na}^+/\text{Ca}^{2+}$ exchanger (NCX1) transport mode (Eder *et al.*, 2007). This reverse mode transports Ca^{2+} into the cell and might be involved in pathophysiological processes, e.g. heart failure and ischemia (Okuhara *et al.*, 2007). As mentioned above, TRPC3 was also found to coassemble with TRPC4 into a redox-sensitive channel (Poteser *et al.*, 2006). These heteromers could be activated by oxidative stress under pathological conditions. TRPC3 antagonists might be cytoprotective by preventing the uncontrolled Ca^{2+} influx and subsequent cell damage (Montell, 2001; Okuhara *et al.*, 2007). Furthermore, phosphorylation by protein kinase G (PKG) has been reported to inactivate TRPC3. This might provide an endogenous negative feedback regulation mediated by the nitric oxide/cyclic guanosine monophosphate/PKG pathway to protect vascular endothelial cells from excessive Ca^{2+} influx (Kwan *et al.*, 2004).

TRPC6 is present in brain, platelets, vascular and airway SMCs (Inoue *et al.*, 2001; Yu *et al.*, 2003; Pedersen *et al.*, 2005; Dietrich *et al.*, 2006 and references therein). This channel was shown to be an essential part of the α_1 -adrenoceptor-stimulated cation channel in rabbit portal vein myocytes (Inoue *et al.*, 2001). TRPC6 stimulation by agonists or increasing intravascular pressure (Welsh *et al.*, 2002) is postulated to depolarize the membrane, thereby activating L-type voltage-gated Ca^{2+} channels that finally mediate smooth muscle contraction (Large, 2002; Soboloff *et al.*, 2005; Estacion *et al.*, 2006) and reflex vasoconstriction (Bayliss effect; Welsh *et al.*, 2002). On the contrary, agonist-induced bronchoconstriction mainly depends on Ca^{2+} influx mediated by voltage-independent channels (such as TRPC6), hence, L-type Ca^{2+} channel blockers are not effective, e.g. in asthma and chronic obstructive pulmonary disease (COPD; Gudermann *et al.*, 2004). Furthermore, TRPC6 is found in leukocytes probably mediating inflammatory responses in asthma and COPD (Li *et al.*, 2004). Idiopathic pulmonary arterial hypertension (IPAH) is a progressive disease that can be life-shortening by resulting in right heart failure (Dietrich *et al.*, 2006). A major cause for the elevated pulmonary vascular resistance in these patients is

excessive proliferation of pulmonary artery SMCs (PASMCs; Dietrich *et al.*, 2005a). TRPC3 and -6 expression is significantly increased in these cells (Yu *et al.*, 2004), and treatment with TRPC6 small-interfering RNA (siRNA) markedly reduced hyperproliferation (Kunichika *et al.*, 2004). In summary, TRPC6 inhibition seems to be an interesting therapeutic strategy for the treatment of IPAH and other chronic respiratory diseases. But TRPC6 also has physiological functions in airway SMCs that should rather not be blocked. It is essential for acute hypoxic pulmonary vasoconstriction (HPV), thus maintaining proper gas exchange under acute hypoxic conditions by directing blood flow from poorly to well ventilated areas (Weissmann *et al.*, 2006). Disturbances in HPV as occurring in the adult respiratory distress syndrome, pneumonia, and liver failure, can cause life-threatening arterial hypoxemia (Dietrich *et al.*, 2006 and references therein).

Contrary to the proposed physiological functions of the channel described above, TRPC6 deficient mice have an unexpected and surprising phenotype. These animals showed airway smooth muscle hyperreactivity in response to bronchoconstrictors, an elevated mean arterial blood pressure, and exaggerated reflex vasoconstriction. Also the basal and agonist-induced cation entry in SMC of TRPC6^{-/-} mice is higher (Freichel *et al.*, 2005 and references therein; Dietrich *et al.*, 2005b). Partly, this can be explained by an increased expression of the closely related TRPC3 channel (Dietrich *et al.*, 2005b). It has a higher basal activity, is less tightly regulated by vasoconstrictors and has consequently overcompensated TRPC6 knock-out, demonstrating that both channels are not functionally redundant.

The opposite approach revealed a role for TRPC6 in the pathogenesis of cardiac hypertrophy. Cardiac-specific TRPC6 overexpression in transgenic mice leads to an increased Ca²⁺ influx that couples via calcineurin to the stimulation of NFAT (nuclear factor of activated T cells). Pathological heart remodelling is accelerated and these mice have a shortened life expectancy (Kawahara *et al.*, 2006). Whereas *in vivo* TRPC6 upregulation in cardiomyocytes participates in hypertrophy, it seems to have protective antifibrotic functions in cardiac fibroblasts *in vitro* (Nishida *et al.*, 2007). Further *in vivo* studies are needed to estimate the therapeutic value of TRPC6 modulation and the involvement of TRPC3 (Nakayama *et al.*, 2006) and TRPC3/6 heteromers (Dietrich *et al.*, 2007) in the pathogenesis of heart failure.

Finally, convincing evidence for TRPC6 involvement in hereditary FSGS, a significant cause of end-stage renal disease, has been presented. Kidneys ultrafiltrate the plasma with their glomeruli and the glomerular filter is composed of a fenestrated capillary endothelium, the basement membrane and podocytes connected by the slit diaphragm (Gudermann, 2005). Structural damage of the glomerular filter results in proteinuria. TRPC6 gain-of-function mutants found in FSGS patients lead to increased Ca²⁺ and Na⁺ influx into podocyte foot processes (Winn *et al.*, 2005; Reiser *et al.*, 2005), but it is not known whether and how this is disease-causing. Recently, it was also demonstrated that TRPC6 expression is up-regulated

in complement-treated podocytes *in vitro* leading to actin cytoskeleton rearrangement, whereas channel overexpression *in vivo* leads to proteinuria in mice (Moller *et al.*, 2007).

TRPC7 is expressed in heart, lung and eyes and lower transcript levels are found in brain, spleen and testis (Dietrich *et al.*, 2006 and references therein). The channel is constitutively active although it has two predicted glycosylation sites like TRPC6 (Okada *et al.*, 1999). Its physiological function remains obscure (Okuhara *et al.*, 2007).

TRPC4/5 subfamily

These channels share 64% identity and are most closely related to TRPC1 (persuading some groups to classify TRPC1 within this subfamily; Ramsey *et al.*, 2006). A unique feature of this subfamily is the potentiation by micromolar concentrations of the lanthanide cations gadolinium (Gd^{3+}) and lanthanum (La^{3+}) after $G_{q/11}$ -coupled receptor mediated activation (Schaefer *et al.*, 2000; Strubing *et al.*, 2001). In contrast to TRPC2 and the TRPC3/6/7 subgroup, TRPC4 and -5 are not directly activated by the subsequently formed PIP_2 hydrolysis product DAG (Venkatachalam *et al.*, 2003).

Recently, lysophosphatidylcholine (LPC; Flemming *et al.*, 2006) and sphingosine 1-phosphate (S1P; Xu *et al.*, 2006) were identified as endogenous TRPC5 activators. S-nitrosylation, e.g. by nitric oxide (NO), has been shown to activate both TRPC4 and TRPC5 (Yoshida *et al.*, 2006).

TRPC4 is widely expressed and also found in endothelial and smooth muscle cells (Freichel *et al.*, 2001; Beech *et al.*, 2004). The channel was the first TRP gene to be knocked out in mice and these animals provided insight into its biological roles. TRPC4^{-/-} mice are viable and reach maturation (Montell, 2001), but SOC-mediated Ca^{2+} entry into endothelial cells (EC) is markedly reduced resulting in decreased endothelium-dependent vasorelaxation (Freichel *et al.*, 2001). Further studies were performed with thrombin, an important inflammation mediator that is involved in the pathogenesis of vascular injury. In lungs, thrombin increases vascular permeability and thus tissue water content. Lung EC of TRPC4^{-/-} mice lack thrombin-induced actin stress fiber formation, cell retraction is impaired, and lung microvascular permeability subsequently reduced by about 50% (Tiruppathi *et al.*, 2002). TRPC4 is furthermore expressed in different cells within the central nervous system and seems to be involved in neurotransmitter signalling. Release of γ -aminobutyric acid (GABA) following application of 5-hydroxytryptamine (5-HT, serotonin) is drastically reduced in thalamic interneurons from TRPC4^{-/-} mice, whereas GABA release upon stimulation of metabotropic glutamate receptors is not changed (Munsch *et al.*, 2003). The thalamus regulates sleep and wakefulness and TRPC4 could participate in processing of visual information depending on the sleep/wake cycle (Pape *et al.*, 2004). TRPC4 is also found in

pancreatic β -islets and was suggested to be involved in insulin secretion (Qian *et al.*, 2002). However, glucose-tolerance test results were similar in wild-type and TRPC4-deficient mice (Freichel *et al.*, 2004). Finally, the channel could be involved in regulating the motility of the gastrointestinal tract by modulating the pacemaker activity of interstitial cells of Cajal (ICC), (Torihashi *et al.*, 2002).

TRPC5 is highly enriched in brain but also found peripheral, e.g. in SMC (Xu *et al.*, 2005; reviewed in Dietrich *et al.*, 2006). Interestingly, the gene is located on a region of the human X chromosome associated with non-syndromic mental retardation (Sossey-Alaoui *et al.*, 1999), and regulation of neurite outgrowth and growth cone morphology by TRPC5 homomers has been demonstrated in rat hippocampal neurons. Functional channel suppression by transfection of a dominant-negative mutant led to abnormally prolonged neurites, and overexpression resulted in neurite outgrowth inhibition (Greka *et al.*, 2003). Phosphatidylinositol 4-phosphate 5-kinase (PIP(5)K α)-dependent channel insertion from vesicles into the plasma membrane was further reported to be crucial for neurite length regulation by TRPC5 (Bezzarides *et al.*, 2004).

TRPC5 may have multiple functions within the cardiovascular system. For example, SMC motility is crucial in physiological adaptive processes like wound healing but also involved in inflammatory occlusive diseases like atherosclerosis (Inoue *et al.*, 2006). Cell motility of vascular SMC was evoked by the TRPC5 activator S1P and inhibited by a dominant-negative TRPC5 mutant or an anti-TRPC5 antibody (Xu *et al.*, 2006). Furthermore, in failing hearts from patients with end-stage idiopathic dilated cardiomyopathy TRPC5 was found to be selectively upregulated, whereas the expression levels of TRPC1, -4 and -6 were unchanged and TRPC3 was not detectable (Bush *et al.*, 2006). As Ca²⁺-ATPase SERCA2 is downregulated in cardiac hypertrophy, and siRNA-mediated SERCA2 downregulation in neonatal rat cardiac myocytes led to a compensatory upregulation of TRPC5, TRPC4 and NCX expression (Seth *et al.*, 2004), an involvement of TRPC5 (and TRPC4) in cardiac hypertrophy is conceivable (Inoue *et al.*, 2006). Increased TRPC5 expression and channel-mediated Ca²⁺ influx in monocytes of hypertensive patients was reported as well (Liu *et al.*, 2006).

1.4 Aims

The first aim of the present work was to identify new pharmacological tools that may be used to gain a better understanding of TRPC channel function in cells and beyond. There are many open questions regarding the native composition and activation mechanisms, physiological functions, and roles in pathophysiology and disease of TRPC proteins. *In situ* identification of native TRPC channels is complicated by their wide and partially overlapping distribution, potential heteromultimerization, similar electrophysiological properties and a paucity of tool compounds to unequivocally trace these channels (Moran *et al.*, 2004). Compensatory effects have been observed in studies with transgenic mice (Dietrich *et al.*, 2005b), dominant negative channel subunits or when genes were silenced with small interfering RNA, but they are not expected to be seen when channels are instantaneously blocked with a selective tool compound (Beech *et al.*, 2003). The fact that known organic inhibitors and inorganic blockers are not potent and specific enough herefore (Li *et al.*, 2004), motivated us to search for further TRPC blockers. In preliminary in-house experiments the steroidal norgestimate had been identified as novel TRPC6 channel inhibitor. Therefore, the present study was designed to test its applicability as selective TRPC channel blocker by evaluating its sensitivity and selectivity towards the TRPC4/5 and TRPC3/6/7 subfamilies in heterologous expression systems. As norgestimate is a synthetic progestin and the precursor of levonorgestrel, it should be further tested whether levonorgestrel itself and the natural hormone progesterone are as well active on TRPC channels. Moreover the effects of norgestimate should be validated in either cell lines or primary cells expressing endogenous TRPC6-containing channel complexes. Finally, we envisaged to use norgestimate for the study of native TRPC channel function in tissue preparations such as isolated aortic or tracheal rings.

The second part of this study was directed towards the identification of novel regulators of native TRPC4 channel complexes. Dysregulation of endothelial calcium signaling is involved in many cardiovascular pathologies, such as atherosclerosis, coronary syndrome, heart and renal failure, hypertension and thrombosis (Kwan *et al.*, 2007). Evidence from TRPC4-deficient mice suggests its necessity for agonist-induced endothelium-dependent vascular relaxation and involvement in regulating endothelial barrier function (Freichel *et al.*, 2001). Therefore, pharmacological modulation of TRPC4 may be a promising approach to treat the aforementioned pathophysiological conditions. Unfortunately, drug discovery for TRPC4 is hampered by difficulties to faithfully reconstitute native currents in heterologous expression systems. The reported gaps and discrepancies (Freichel *et al.*, 2001; Schaefer *et al.*, 2002) could originate from different channel heteromultimerization *in vivo* and *in vitro*, coupling to diverse cell type-specific signalling cascades or channel interaction with unknown accessory proteins. To search for such novel TRPC4-binding proteins that might modify channel

biophysics, activation and function, we wanted to perform a yeast two-hybrid (Y2H) screen of a human aorta cDNA library with the mTRPC4 α -C-terminus as a bait. The physical interaction of identified preys should be biochemically validated with GST pulldown and co-immunoprecipitation studies. Furthermore, the specificity of this interaction should be tested with regard to related channel proteins. If a specific interaction is detected, we wanted to investigate the functional consequences of this coupling on channel properties, activation, and if possible on *in vivo* function using different approaches including protein overexpression and knock-down experiments.

2 Materials and methods

2.1 Materials

2.1.1 Chemicals, enzymes, consumables

Product	Supplier
Acetic acid	Riedel-de H�en, Seelze, Germany
Acetylcholine chloride	Sigma, Munich, Germany
Adenine	Q-BIOgene, Carlsbad, USA
Agarose	BioRad, Munich, Germany
Aluminium chloride (AlCl ₃)	Sigma, Munich, Germany
2-Aminoethoxydiphenyl borate	Sigma, Munich, Germany
Ampicilline sodium salt	Sigma, Munich, Germany
[Arg ⁸]-vasopressin acetate	Sigma, Munich, Germany
Bacto agar	BD Biosciences, Heidelberg, Germany
Bacto tryptone	BD Biosciences, Heidelberg, Germany
Bacto yeast extract	BD Biosciences, Heidelberg, Germany
BioTrace NT	Pall, Dreieich, Germany
Blasticidine S HCl	Invitrogen, Karlsruhe, Germany
Borosilicate glass capillaries	Hilgenberg, Malsfeld, Germany
Bovine serum albumine (BSA), essentially fatty acid-free	Sigma, Munich, Germany
Calcium chloride	Sigma, Munich, Germany
Calf intestine alkaline phosphatase (CIAP)	GIBCO BRL, Gaithersburg, USA
Carbachol	Sigma, Munich, Germany
Caesium hydroxide (CsOH)	Sigma, Munich, Germany
Cell scraper	Greiner, Frickenhausen, Germany
Complete (protease inhibitor mix)	Roche, Mannheim, Germany
Complete supplement mixture (CSM)	Q-BIOgene, Carlsbad, USA
Coomassie brilliant blue R-250	BioRad, Munich, Germany
Cova-PIP specificity plates	Echelon, Salt Lake City, USA
Cryogenic vials	Nalgene, Rochester, USA
Cs ₄ -BAPTA	Invitrogen, Karlsruhe, Germany
CSM -Trp, -Leu, -Trp/Leu/His, -Trp/Leu/His/Ade	Q-BIOgene, Carlsbad, USA
Deoxyribonucleic acid (from salmon sperm)	Sigma, Munich, Germany
Difco yeast nitrogen base w/o amino acids	BD Biosciences, Heidelberg, Germany
Dimethylformamide (DMF)	Sigma, Munich, Germany
Dimethyl sulphoxide (DMSO)	Sigma, Munich, Germany
Dithiotreitol (DTT)	Sigma, Munich, Germany
Deoxynucleotide (dNTP) mix	Sigma, Munich, Germany
Doxycycline	BD Biosciences, Heidelberg, Germany
Dulbecco's modified eagle medium (DMEM)	Invitrogen, Karlsruhe, Germany
DMEM/Nutrient F12 (with glutaMAX I)	Invitrogen, Karlsruhe, Germany
Dulbeccos's phosphate buffered saline w/o Ca ²⁺ , Mg ²⁺ (D-PBS)	Invitrogen, Karlsruhe, Germany
EDTA	Merck, Darmstadt, Germany
EGTA	Sigma, Munich, Germany

Electroporation cuvettes	BioRad, Munich, Germany
Enhancer solution (for DELFIA)	Perkin Elmer, Waltham, USA
Ethanol	Merck, Darmstadt, Germany
EZ-link sulfo NHS-LC biotin	Pierce, Rockford, USA
EZ load molecular ruler (100 bp, 500 bp, 1 kb)	BioRad, Munich, Germany
Falcon tubes (15/50 mL)	BD, Heidelberg, Germany
Fetal bovine serum (FBS)	PAA, Pasching, Austria
Fetal bovine serum (FBS)	Biochrom, Berlin, Germany
Fluo-4, acetoxymethyl ester (AM)	Invitrogen, Karlsruhe, Germany
Fura-2, acetoxymethyl ester (AM)	Invitrogen, Karlsruhe, Germany
Gateway LR clonase enzyme mix	Invitrogen, Karlsruhe, Germany
Geneticine	Invitrogen, Karlsruhe, Germany
Glass cover slips	Menzel, Braunschweig, Germany
Glucose	Sigma, Munich, Germany
Glutamine (100 mM)	Invitrogen, Karlsruhe, Germany
Glutathione sepharose 4 fast flow	Amersham, Munich, Germany
Glycerol	Sigma, Munich, Germany
Glycine	BioRad, Munich, Germany
H-Abz-Cys-Ala-Pro-Ala-Cys-Ntr-NH ₂	JPT Peptide Technologies, Berlin, Germany
HEPES	Sigma, Munich, Germany
Hydrochloric acid (HCl)	Riedel-de Haen, Seelze, Germany
Hygromycine B	Invitrogen, Karlsruhe, Germany
ISCOVE medium	Biochrom, Berlin, Germany
Isopropyl β -D thiogalactoside (IPTG)	Roche, Mannheim, Germany
Kanamycine	Sigma, Munich, Germany
Lanthanum chloride heptahydrate	Sigma, Munich, Germany
L-Glutathione, reduced	Sigma, Munich, Germany
Lipofectamine 2000	Invitrogen, Karlsruhe, Germany
LL5- α (Multi PIP Grip)	Echelon, Salt Lake City, USA
L-NAME	Sigma, Munich, Germany
Lumi-LightPLUS Western blotting substrate	Roche, Mannheim, Germany
Lysozyme	Sigma, Munich, Germany
Magnesium chloride (MgCl ₂)	Merck, Darmstadt, Germany
Magnesium sulphate (MgSO ₄)	Merck, Darmstadt, Germany
β -Mercaptoethanol (β -ME)	Sigma, Munich, Germany
Methanol	Merck, Darmstadt, Germany
Minimal essential medium (MEM) sodium pyruvate	Invitrogen, Karlsruhe, Germany
MOPS SDS running buffer (20x)	Invitrogen, Karlsruhe, Germany
Norgestimate	ChemPacific Corporation, Baltimore, USA
Nucleic acid sample loading buffer (5x)	BioRad, Munich, Germany
NuPAGE LDS sample buffer (4x)	Invitrogen, Karlsruhe, Germany
NuPAGE Novex 4-12% Bis-Tris gels	Invitrogen, Karlsruhe, Germany
NuPAGE transfer buffer (20x)	Invitrogen, Karlsruhe, Germany
Odyssey blocking buffer	LiCor, Lincoln, USA
Odyssey protein molecular weight marker	LiCor, Lincoln, USA
Opti-MEM	Invitrogen, Karlsruhe, Germany
Paraformaldehyde	Sigma, Munich, Germany
PCR strips	Eppendorf, Hamburg, Germany
Permafluor mounting medium	Invitrogen, Karlsruhe, Germany

<i>Pfu</i> and reaction buffer	Stratagene, La Jolla, USA
Phenol/chloroform/isoamylalcohol (25:24:1)	Roth, Karlsruhe, Germany
Phenylephrine hydrochloride	Sigma, Munich, Germany
PIP strips	Echelon, Salt Lake City, USA
Pipette tips	Eppendorf, Hamburg, Germany
Pipette tips, aerosol-resistant (ART)	M&P, San Diego, USA
Poly-L-lysine (0.01%)	Sigma, Munich, Germany
Ponceau S solution	Sigma, Munich, Germany
Potassium chloride (KCl), dihydrogen phosphate (KH ₂ PO ₄)	Sigma, Munich, Germany
Progesterone	Sigma, Munich, Germany
Protein A sepharose, Protein G sepharose	Amersham, Munich, Germany
Reaction vials (0.5/1.5/2 mL)	Eppendorf, Hamburg, Germany
Reagent packs	Cambrex, East Rutherford, USA
S.O.C. medium	Invitrogen, Karlsruhe, Germany
Select peptone 140	Invitrogen, Karlsruhe, Germany
Sensoplates	Greiner, Frickenhausen, Germany
Sodium chloride (NaCl), dodecyl sulphate (SDS), fluoride (NaF), bicarbonate (NaHCO ₃)	Sigma, Munich, Germany
Streptavidin sepharose	Amersham, Munich, Germany
SYBR safe DNA gel stain concentrate	Invitrogen, Karlsruhe, Germany
T4 DNA ligase and buffer	Invitrogen, Karlsruhe, Germany
TAE buffer (50x)	Invitrogen, Karlsruhe, Germany
Tissue culture flasks	Greiner, Frickenhausen, Germany
Tris buffer	GIBCO BRL, Gaithersburg, USA
Triton X-100	Sigma, Munich, Germany
Trypsin	Sigma, Munich, Germany
Trypsin/EDTA (0.05%/0.02%)	Biochrom, Berlin, Germany
Tween 20	Sigma, Munich, Germany
6-, 24-, 96-, 384-Well plates	Greiner, Frickenhausen, Germany
96-Well plates, poly-D-lysine coated	BD Biosciences, Heidelberg, Germany
X-gal	Sigma, Munich, Germany
Zeocin	Invitrogen, Karlsruhe, Germany

2.1.2 Kits

Product	Supplier
ABI BigDye terminator cycle sequencing ready reaction kit	Applied Biosystems, Darmstadt, Germany
BCA protein assay kit	Pierce, Rockford, USA
iBlot transfer stack	Invitrogen, Karlsruhe, Germany
Clonetics EGM-2 BulletKit	Cambrex, East Rutherford, USA
Clonetics EGM-2 MV BulletKit	Cambrex, East Rutherford, USA
Clonetics SmGM-2 BulletKit	Cambrex, East Rutherford, USA
Endofree plasmid maxi kit	Qiagen, Hilden, Germany
Qiafilter plasmid maxi and giga kit	Qiagen, Hilden, Germany
QIAprep spin miniprep kit	Qiagen, Hilden, Germany
QIAquick gel extraction kit	Qiagen, Hilden, Germany
Zero blunt TOPO PCR cloning kit	Invitrogen, Karlsruhe, Germany

2.1.3 Antibodies

Product	Supplier
Alexa Fluor 488 goat anti-rabbit	Invitrogen, Karlsruhe, Germany
Alexa Fluor 546 goat anti-mouse	Invitrogen, Karlsruhe, Germany
Alexa Fluor 546 goat anti-rabbit	Invitrogen, Karlsruhe, Germany
Alexa Fluor 546 goat anti-rat	Invitrogen, Karlsruhe, Germany
Alexa Fluor 680 goat anti-rabbit	Invitrogen, Karlsruhe, Germany
Alexa Fluor 680 goat anti-rat	Invitrogen, Karlsruhe, Germany
Alexa Fluor 680 rabbit anti-mouse	Invitrogen, Karlsruhe, Germany
goat anti-rabbit horseradish peroxidase (HRP)-conjugated	Pierce, Rockford, USA
goat anti-rabbit, Eu-N1 labelled	Perkin Elmer, Waltham, USA
mouse anti-GAPDH	Chemicon, Wiesbaden, Germany
mouse anti-GFP	Roche, Mannheim, Germany
mouse anti-ZO-1	Invitrogen, Karlsruhe, Germany
rabbit anti-FLAG	Rockland, Gilbertsville, USA
rabbit anti-GST	Sigma, Munich, Germany
rabbit anti-GST, Eu-N1 labelled	Perkin Elmer, Waltham, USA
rabbit anti-SESTD1 #147/148, 0.18 mg/mL	Eurogentec, Seraing, Belgium
rabbit anti- β -catenin	Cell Signaling, Danvers, USA
rabbit anti-TRPC4	Alomone, Jerusalem, Israel
rat anti-HA	Roche, Mannheim, Germany

2.1.4 Bacterial strains

Strain	Supplier
One shot BL21 star (DE3) chemically competent <i>E. coli</i>	Invitrogen, Karlsruhe, Germany
One shot TOP10 chemically competent <i>E. coli</i>	Invitrogen, Karlsruhe, Germany
One shot TOP10 electrocompetent <i>E. coli</i>	Invitrogen, Karlsruhe, Germany

2.1.5 Yeast strains

Strain	Supplier
<i>Saccharomyces cerevisiae</i> AH 109	Clontech, Mountain View, USA

2.1.6 Cell lines and primary cells

Cells	Supplier
A7r5	ATCC, Rockville, USA
human AoSMC (primary cells)	Cambrex, East Rutherford, USA
CASMC (primary cells)	Cambrex, East Rutherford, USA
HAEC (primary cells)	Cambrex, East Rutherford, USA
HEK293 (QBI-HEK 293A)	Q-BIOgene, Morgan Irvine, USA
HEK293 Flp-In T-Rex cell line	Invitrogen, Karlsruhe, Germany
HM1	(Peralta <i>et al.</i> , 1988)
HM1-C5Y	HM1 cells stably transfected with mTRPC5-YFP (see Chapter 2.4.2)

HMVEC-d (primary cells) TRPC3/4/5/6 HEK293 FITR	Cambrex, East Rutherford, USA generated in-house (using the parental HEK 293 Flp-In T-Rex cell line)
--	--

2.1.7 Primers

All primers were bought from Operon (Cologne, Germany).

Cloning primers	5'→3' sequence
hTRPC1c_f_NotI	GCGGCCGCTCTGCTGGTGGCAATGCTT
hTRPC1c_r_PstI	CTGCAGTTAATTTCTTGGATAAAACATAGC
hTRPC6c_f1	GCGGCCGCTATGTTAATTGCCATGATCAACAGTTCATTC
hTRPC6c_r1	GTGCACTTGGTTTCTCTTGATTTGGTTCC
mTRP4a1_f_EcoRI	GAATTCATGTTAATTGCTATGATGAATAATTCTTACCAAC
mTRP4a1_r_BamHI	GGATCCTTATGAACTCGCCGCGTTGGCTGA
mTRP4a2_f_EcoRI	GAATTCGCGGACTCCGACGAGAAGAG
mTRP4a2_r_BamHI	GGATCCTCACAACTTGTGGTACATAATCTTC
mTRP4a3_f_EcoRI	GAATTCCTGAGAAGACATCACCAATAC
mTRP4a3_r_BamHI	GGATCCTTAGTTATCAGCAGCACGCCGCCCAA
mTRP4a4_r_BamHI	GGATCCTTATTCGGTTTTTGCCT
mTRP4a5_r_BamHI	GGATCCTTATTGCTTTAGTTTCT
mTRP4longc_f1	GCGGCCGCTATGTTAATTGCTATGATGAATAATTCTTACCAAC
mTRP4longc_r1	CTGCAGTCACAACTTGTGGTACATAATCTTCGTG
mTRP5c_f1	GCGGCCGCTATGCTCATCGCCATGATGAACAACCTCCTAC
mTRP5c_r1	CTGCAGTTAGAGCCGAGTTGTAACCTGTTCTTCCTGTC
SESTD1_f_BamHI	GGATCCATGGAGGCCTCAGTAATATT
SESTD1_f_Sall	GTCGACCATGGAGGCCTCAGTAATATT
SESTD1_f_XhoI	AAAGCTCGAGTCATGGAGGCCTCAGTAATATTACC
SESTD1_f1_BamHI	GGATCCGAATGGAGGCCTCAGTAATATTACCCATT
SESTD1_f2_BamHI	GGATCCGAGAAAGGTCTGTGGATTTAAACT
SESTD1_f3_BamHI	GGATCCGACCAGCTGATGGAGCATCGAT
SESTD1_r_BamHI	CTAAGGATCCAAGCTCTCTGTGGTACCATTTC
SESTD1_r_XhoI	CTCGAGTTAGCTCTCTGTGGTACCAT
SESTD1_r1_XhoI	CTCGAGTTATTTCTCTTGCTGATTTCTTTATCA
SESTD1_r2_XhoI	CTCGAGTTATGCTACATCTACGCACAACATCCCT
SESTD1_r3_XhoI	CTCGAGTTAGCTCTCTGTGGTACCATTTCAGGA

Sequencing primers	5'→3' sequence
BGH_rev	TAGAAGGCACAGTCGAGG
GAL4-AD_for	TACCACTACAATGGATG
GAL4-AD_rev	AGATGGTGCACGATGCACAG
GAL4-BD_ISA_for	TCATCGGAAGAGAGTAG
GAL4-BD_rev	TAAGAGTCACTTTAAAATTTGTAT
GAL4-BD_ISA_rev	GTCACITTTAAAATTTGTATAC
M13_for	GTAACGACGGCCAG
M13_rev	CAGGAAACAGCTATGAC
pCMV_HA_for	GATCCGGTACTAGAGGAACTGAAAAAC
pEYFP_f_521	CAAATGGGCGGTAGGCGTG
pGEX-4T-1_for	GGGCTGGCAAGCCACGTTTGGTG
pGEX-4T-1_rev	CCGGGAGCTGCATGTGTCAGAGG

SESTD1_f_471	ACAGAAGATTTTGGTGGGAGT
SESTD1_f_1071	AATGCTGGCGATGAGGAAGA
SESTD1_f_1631	CGATGATGCTCAAGAAACGA
SP6	ATTTAGGTGACACTATAG
T7	TAATACGACTCACTATAGGG
mTRP4l_int_for	CTACAATACAGTCAGCCAACGC
mTRP4l_int_rev	ACCAGGGCGGAACCATTG
mTRP5_int_for	GAAACATCCAAGAAGAAGCCTC
mTRP5_int_rev	CTTGGCACGGTTCTGATGAG

2.1.8 siRNA

siRNA	Supplier	Catalogue no.
siGENOME SMARTpool set of 4, siRNA duplexes, human SESTD1	Dharmacon, Lafayette, USA	D-018379
siGENOME set of 4, human SESTD1, duplex 1	Dharmacon, Lafayette, USA	D-018379-01
siGENOME set of 4, human SESTD1, duplex 2	Dharmacon, Lafayette, USA	D-018379-02
siGENOME set of 4, human SESTD1, duplex 3	Dharmacon, Lafayette, USA	D-018379-03
siGENOME set of 4, human SESTD1, duplex 4	Dharmacon, Lafayette, USA	D-018379-04
siGLO red transfection indicator	Dharmacon, Lafayette, USA	D-001630-02-05
<i>SilencerR</i> negative control #2	Ambion, Austin, USA	4613

2.1.9 Genetic constructs

Standard molecular biological procedures (Sambrook *et al.*, 1989) described in Section 2.2 were applied to insert cDNA in vectors, thus constructing plasmids for heterologous expression in yeast, bacteria and mammalian cells. The deployed vectors contain a multiple cloning site (MCS) with recognition sequences for restriction endonucleases, replication origins (ori) and genes for selection in pro- and eukaryotic cells. The constructs that have been used in this work are listed in the appendix.

The yeast two-hybrid screen bait was constructed by integrating the C-terminus of murine TRPC4 α (NM_016984) into pGBKT7, leading to its fusion with the DNA binding domain of the transcription factor GAL4. Since TRPC channels are thought to consist of tetramers, a mutated GCN4-leucine zipper (Harbury *et al.*, 1993; Zerangue *et al.*, 2001) was inserted between the C-terminus and the GAL4-DNA binding domain (mTRPC4 α (615-974)/leucine zipper/pGBKT7). The amino acid sequence of the zipper (underlined) and flanking sequences was GGGSG SRMKQ IEDKL EEILS KLYHI ENELA RIKKL LGERG GSGSA AA. Other baits for directed yeast two-hybrid screens were constructed in the same way with the C-termini from human TRPC1 (NM_003304), murine TRPC5 (NM_009428), and human TRPC6 (NM_004621). For control experiments, the channels' C-termini were replaced by an

enhanced variant of the jellyfish *Aequorea victoria* green fluorescent protein (EGFP/leucine zipper/pGBKT7). To map the SESTD1 interaction site on TRPC4, monomeric truncation bait constructs were generated (lacking the zipper). This facilitated cloning as the TRPC4 C-terminal fragments could be inserted into pGBKT7 with a double instead of a triple ligation. Constructs for recombinant expression of glutathione S-transferase (GST) fusion proteins in bacteria were prepared by inserting full length human SESTD1 (NM_178123) or cDNA fragments in pGEX vectors leading to their N-terminal fusion with GST: GST-SESTD1 (1-696)/pGEX-4T-1, GST-Sec 14 (1-192)/pGEX-5X-3, GST-Spec 1 (193-406)/pGEX-5X-3, and GST-Spec 2 (407-696)/pGEX-5X-3.

Human SESTD1 was also inserted in the vectors pCMV-HA and pEYFP-N1. When transfected into mammalian cells it was expressed N-terminally fused to the hemagglutinin antigenic epitope of human influenza virus (HA tag: YPYDV PDYA) or C-terminally to a yellow-green EGFP mutant protein (EYFP), respectively (Chalfie *et al.*, 1994). DNA constructs were confirmed by sequencing.

2.1.10 Apparatus

Product	Supplier
ABI 3100 genetic analyzer	Applied Biosystems, Foster City, USA
ALA BPS-8 (8-channel valve perfusion system)	ALA Scientific Instruments, Westbury, USA
Axiovert 200	Zeiss, Göttingen, Germany
Biofuge pico, Biofuge fresco	Heraeus, Hanau, Germany
BioPhotometer	Eppendorf, Hamburg, Germany
iBlot gel transfer device	Invitrogen, Karlsruhe, Germany
Casy counter	Schärfe System, Reutlingen, Germany
Cryo 1°C freezing container	Nalgene, Rochester, USA
Dissecting instruments	WPI, Berlin, Germany
DMZ universal puller	Zeitz-Instruments, Munich, Germany
EPC-10	HEKA, Lambrecht, Germany
FLEX station	Molecular Devices, Munich, Germany
Fluorometric imaging plate reader (FLIPR)	Molecular Devices, Munich, Germany
Gel documentation system	Intas, Göttingen, Germany
Gene pulser	BioRad, Munich, Germany
Hera safe working bench	Heraeus, Hanau, Germany
Imaging system	T.I.L.L. Photonics, Gräfeling, Germany
Leica DM IRE2	Leica, Wetzlar, Germany
Lumi imager	Roche, Mannheim, Germany
Milli-Q water purification system	Millipore, Billerica, USA
Multidrop plate washer	Thermo Scientific, Milford, USA
Novex Xcell 2 blotmodul	Invitrogen, Karlsruhe, Germany
Odyssey infrared imaging system	LiCor, Lincoln, USA
Rotator SB2, Stuart	VWR, Darmstadt, Germany
T3 thermocycler	Biometra, Göttingen, Germany
Tecan safire 2, Tecan ultra	Tecan, Crailsheim, Germany
TI1 UV transilluminator	Biometra, Göttingen, Germany

2.1.11 Buffers, media and solutionsBlocking buffer:

- for Western blots

50%	Odyssey blocking buffer
50%	TBS (with 0.6% Tween 20)
- for PIP strips

90 mL	TBST (pH 8)
10 mL	30% BSA (essentially fatty acid-free)

Coomassie blue solution:

- | | |
|------|--------------------------------|
| 0.1% | Coomassie brilliant blue R-250 |
| 10% | Acetic acid |
| 40% | Ethanol |

Intracellular solution (pH 7.4 with NaOH):

- | | |
|--------|---|
| 120 mM | CsOH |
| 120 mM | Gluconic acid |
| 2 mM | MgCl ₂ |
| 3 mM | CaCl ₂ (200 nM free Ca ²⁺) |
| 5 mM | Cs ₄ -BAPTA |
| 10 mM | HEPES |

Luria Bertani (LB) medium/plates:

- | | |
|------------|------------------------------|
| 1.5% (w/v) | Bacto agar (only for plates) |
| 1% (w/v) | Bacto tryptone |
| 0.5% (w/v) | Bacto yeast extract |
| 1% (w/v) | NaCl |

Medium was autoclaved at 120°C for 20 min. Selective media were prepared by adding 100 µg/mL ampicilline (LB/amp) or 50 µg/mL kanamycine (LB/kana).

Lysis buffer (pH 7.4):

- | | |
|--------|--------------|
| 1 mM | EDTA |
| 150 mM | NaCl |
| 50 mM | Tris-HCl |
| 1% | Triton X-100 |

Physiological phosphate-buffered salt solution (PSS):

- | | |
|--------|---------------------------------|
| 119 mM | NaCl |
| 4.7 mM | KCl |
| 1.2 mM | KH ₂ PO ₄ |
| 1.2 mM | MgSO ₄ |
| 1.6 mM | CaCl ₂ |

25 mM	NaHCO ₃
11 mM	Glucose

Standard extracellular solution (pH 7.35 , ~275 mosm):

135 mM	NaCl
1 mM	MgCl ₂
5.4 mM	KCl
2 mM	CaCl ₂
10 mM	HEPES
10 mM	Glucose

(2 mM CaCl₂ were replaced by 0.5 mM EGTA for calcium-free standard extracellular solution).

TBS (pH 8) for PIP strips:

150 mM	NaCl
10 mM	Tris-HCl

• 2.5 μM free Ca²⁺

150 mM	NaCl
10 mM	Tris-HCl
1 mM	EGTA
1 mM	MgCl ₂
1 mM	CaCl ₂

• 0.06 μM free Ca²⁺

150 mM	NaCl
10 mM	Tris-HCl
1 mM	EGTA
1 mM	MgCl ₂
0.9 mM	CaCl ₂

Free Ca²⁺ concentrations were calculated using CaBuf software (Droogmans, 2007).

TBST (pH 8) for PIP strips:

0.1%	Tween 20 in TBS
------	-----------------

TBS (pH 7.4) for Western blots:

500 mM	NaCl
20 mM	Tris-HCl

TBST (pH 7.4) for Western blots:

0.05%	Tween 20 in TBS
-------	-----------------

<u>Yeast breaking buffer (pH 8):</u>	1 mM	EDTA
	100 mM	NaCl
	1% (w/v)	SDS
	10 mM	Tris-HCl
	2% (w/v)	Triton X-100

<u>Yeast complete supplemented medium:</u>	30 mg	Adenine (final concentration 40 mg/L)
	0.65 g	Complete supplement mixture (CSM)
	6.7 g	Difco yeast nitrogen base w/o amino acids
	2% (w/v)	Glucose
	add 1 L sterile, deionized water, sterile filtrate	

Yeast complete supplemented agar plates:

20 g Bacto agar were dissolved in 500 mL H₂O, autoclaved and mixed (after cooling down) with the same volume of 2x yeast complete supplemented medium.

Yeast dropout media and agar plates: -Trp, -Leu, -Trp/Leu, -Trp/Leu/His, -Trp/Leu/His/Ade:

Same recipe as for complete supplemented medium but CSM was replaced by CSM -Trp etc. (in concentrations as suggested by the manufacturer).

<u>YPAD medium:</u>	1% (w/v)	Bacto yeast extract
	2% (w/v)	Select peptone 140
	2% (w/v)	Glucose
	40 mg/L	Adenine

YPAD agar plates:

20 g Bacto agar were dissolved in 500 mL H₂O, autoclaved and mixed (after cooling down) with the same volume of 2x YPAD medium (sterile filtered).

All buffers, media and solutions were prepared with Milli-Q water.

2.2 Molecular biological methods

2.2.1 Determination of nucleic acid concentrations and cell density

Absorbance at 260 nm (A_{260}) was determined in a photometer to calculate the concentration of nucleic acid solutions based on $A_{260} = 1$ for 50 $\mu\text{g/mL}$ double stranded DNA. Contaminants such as aromatic substances, proteins, and RNA absorb at 280 nm (A_{280}). Thus, A_{280} was determined to estimate plasmid purity and A_{260}/A_{280} ratios of 1.8-2.0 were considered as pure. Turbidity of bacteria and yeast cell suspensions was measured as absorbance at 600 nm (A_{600}).

2.2.2 Primer construction

Specific synthetic oligonucleotide primers for sequencing and polymerase chain reactions were derived from GenBank entries (National Center for Biotechnology Information – NCBI, Bethesda, USA) and vector sequences using Lasergene Primer Select software (DNASTar, Madison, USA).

2.2.3 Polymerase chain reaction (PCR)

Polymerase chain reactions allow primer-mediated enzymatic *in vitro* amplification of specific DNA sequences (Saiki *et al.*, 1985) and were performed to introduce specific restriction sites and/or to truncate DNA sequences. They were carried out in a final volume of 50 μL containing 2 μL dNTPs (10 mM), 1 μL of each primer (10 μM), 100-300 ng template DNA, 2 μL *Pyrococcus furiosus* (*Pfu*) DNA polymerase (2.5 units/ μL), and 5 μL tenfold *Pfu* reaction buffer. Amplification was processed in a thermocycler using the basic programme depicted in Table 2. PCR products were analyzed by gel electrophoresis and purified using the QIAquick gel extraction kit.

Table 2: PCR conditions.

Number of cycles	Reaction step	Duration	Temperature ($^{\circ}\text{C}$)
1	denaturation	3 min	95
25	denaturation	30 sec	95
	annealing	30 sec	50-60 ¹
	elongation	1 min/kb	72
1	termination	10 min	72
1	cooling	indefinite	4

¹Annealing temperatures were adapted to the primer features.

2.2.4 DNA restriction digest

Type II restriction endonucleases are bacterial enzymes that cut double-stranded DNA at short specific sequences that are mostly palindromic. The resulting DNA fragments either end in paired nucleotides (blunt ends) or overhanging, unpaired nucleotides (sticky ends).

For analytical digestions, 10 to 20 U restriction enzyme (New England Biolabs, Frankfurt, Germany) were added to 1 µg DNA in a final volume of 30 µL 1x NEBuffer (New England Biolabs). The DNA amount was increased up to 5 µg in 50 µL 1x NEBuffer for preparative digestions. Buffer, addition of BSA, reaction temperature and time were applied as suggested by the manufacturer depending on the enzyme(s) and the amount of DNA used. The resulting DNA fragments were separated by gel electrophoresis and purified using the QIAquick gel extraction kit.

Restriction maps were generated with Lasergene software (DNASTar, Madison, USA).

2.2.5 Dephosphorylation of linearized vectors

Removal of 5'-phosphate groups prevents self-ligation of linearized vectors. 1 U calf intestine alkaline phosphatase (CIAP) was added to the restriction reaction and incubated at 37°C for 5 min. The vector DNA was subsequently purified by gel electrophoresis and gel extraction.

2.2.6 DNA gel electrophoresis

DNA molecules have a net negative charge due to their phosphate backbone. They can thus be forced to migrate through a gel by an electrical field resulting in their size-dependent separation as shorter fragments migrate faster than longer ones. DNA samples were mixed with 5x nucleic acid sample loading buffer and separated in gels of 1% agarose in TAE buffer (prestained with SYBR safe DNA gel stain concentrate). Fragments were separated at 100-120 V for 30-60 min and analyzed on a UV transilluminator by comparing their size with molecular rulers. Pictures were taken with a digital gel documentation system before fragment band excision and DNA elution with the QIAquick gel extraction kit.

2.2.7 Ligation

To join linearized DNA fragments, a final volume of 20 µL T4 DNA ligase buffer containing 50-100 ng linearized vector, the insert in a 3 molar excess and 1 U T4 ligase was incubated for 16 hr at 16°C. The reaction was terminated by denaturing the enzyme for 10 min at 65°C. 2 µL of the reaction were transformed into electrocompetent *E. coli*.

2.2.8 TOPO cloning

For general subcloning, purified PCR products were inserted into the pCR-Blunt II-TOPO vector using the zero blunt TOPO PCR cloning kit according to the manufacturer's instruction. This technique is based on topoisomerase I from *Vaccinia* virus that acts both as restriction endonuclease and ligase. The vector is provided linearized with topoisomerase I covalently attached to the 3' phosphate residues. This bond can be attacked by the 5' hydroxyl groups of an added PCR product that is consequently ligated into the vector. 1 µL of the reaction was transformed into electrocompetent *E. coli*.

2.2.9 Gateway cloning

The Gateway technology (Invitrogen, Karlsruhe, Germany) was used to generate an N-terminal FLAG-tagged mTRPC4 β construct for expression in mammalian cells (FLAG tag amino acid sequence: DYKDDDDK). This system uses lambda (λ) phage-based site-specific recombination (Landy, 1989) to insert a gene into a vector. mTRPC4 β (U50921), obtained from the internal Genomic Sciences department, was already inserted in the entry vector pDONR221 and thus flanked by λ phage attachment (att) sites. The destination vector pcDNA3.1-nFLAG-DEST contains equivalent att sites. Site specific recombination was initiated by mixing with mTRPC4 β /pDONR221 and the LR clonase enzyme mix and resulted in the expression clone. The LR reaction was performed and terminated by incubation with proteinase K according to the manufacturer's instruction. 2 μ L of the reaction were transformed into electrocompetent *E. coli*.

2.2.10 Transformation of chemically competent bacteria

5–10 ng plasmid were added to a vial of thawed chemically competent *E. coli*, mixed gently and incubated on ice for 10 min. Cell membranes were made permeable by heat shock (30 sec, 42°C) and immediately transferred to ice. After addition of 1 mL S.O.C. medium, cells were incubated for one hr at 37°C and 250 rpm. 5 μ L suspension of transformed bacteria were diluted with 95 μ L S.O.C. medium, spread on a selective LB agar plate and incubated overnight at 37°C.

2.2.11 Electroporation of bacteria

2 μ L ligation reaction were added usually into a vial of thawed electrocompetent *E. coli*, mixed gently and transferred to a chilled 0.2 mm cuvette. The electroporator was charged by 2 kV with a load resistance of 400 Ω and 25 μ FD capacity and bacteria were transformed with a pulse of approximately 8 sec length. This electrical pulse disturbs the cell membrane momentarily thus allowing uptake of exogenous DNA. After addition of 1 mL S.O.C. medium, cells were incubated for one hr at 37°C and 250 rpm. 100 μ L of the bacteria suspension were spread on a selective LB agar plate and incubated overnight at 37°C.

2.2.12 Plasmid amplification and purification

Bacteria, transformed with the corresponding plasmid, were plated on selective LB agar plates and incubated overnight at 37°C. Next day, single colonies were used as inoculum for liquid cultures in selective LB medium. Cells were grown overnight at 37°C and 250 rpm, harvested by centrifugation and treated according to the manufacturer's instruction (QIAprep spin miniprep kit, Qiafilter plasmid maxi kit). Plasmids intended for transfection of mammalian cells were harvested and purified with the endofree plasmid maxi kit. The human aorta cDNA

library used for the yeast two-hybrid screen was amplified on agar plates and prepared with the Qiafilter plasmid giga kit (see Chapter 2.3.1).

2.2.13 DNA sequencing

Sequencing was done in-house by the Genomic Sciences department. DNA cycle sequencing reactions were performed based on the dideoxy terminator method (Sanger *et al.*, 1977) with four differentially fluorescent-labelled dideoxynucleotides (Parker *et al.*, 1996). PCR fragments, generated by using the ABI PRISM BigDye terminator cycle sequencing ready reaction kit, were electrophoretically separated, detected, and analyzed on an ABI PRISM 3100 genetic analyzer.

2.2.14 Analysis of nucleotide and protein sequences

Nucleotide and protein sequences were imported from GenBank (NCBI, Bethesda, USA) and analyzed and compared with Lasergene software (DNASTAR, Madison, USA). The NCBI Basic Local Alignment Search Tool (BLAST) was used to identify unknown sequences. Conserved protein domains and motifs were searched with NCBI CD (Marchler-Bauer & Bryant, 2004) and PROSITE (Swiss Institute of Bioinformatics, Basel, Switzerland).

2.2.15 Expression and purification of GST fusion proteins

Glutathione S-transferase (GST) fusion proteins were constructed by inserting a gene or gene fragment in-frame into the MCS of a pGEX vector in which protein expression is under control of the *tac* promoter and inducible by the lactose analogue isopropyl β -D thiogalactoside (IPTG). The resulting plasmid was transformed into protease-deficient and chemically competent BL21 star (DE3) *E. coli*. Bacteria were plated on selective LB agar plates and incubated overnight at 37°C. Next day, single colonies were used as inoculum for a liquid overnight culture in selective LB medium (containing 0.2% (m/v) glucose to repress protein expression). This starter culture was diluted in 100 mL selective LB medium (with 0.2% (m/v) glucose) resulting in $A_{600} = 0.1$. The culture was grown at room temperature (RT) and agitated at 250 rpm. Protein expression was induced at $A_{600} = 0.6$ – 0.8 by adding 10 mM (GST) or 20 mM (GST-SESTD1, GST-SESTD1-fragments) IPTG and incubation was continued for 6 hr. The bacteria suspension was pelleted in 5 mL portions by centrifugation (1 min, 16,000 x *g*, RT), pellets were washed once with 2 mL D-PBS (w/o Ca^{2+} , Mg^{2+}) and stored at -80°C or lysed immediately. Each pellet was resuspended in 250 μ L lysis buffer (containing 1 mg/mL lysozyme) and incubated on ice for 20 min. After sonication (1x 5 sec) the lysate was centrifuged 30 min at 16,000 x *g* and 4°C and the supernatant was transferred to a fresh vial. 50 μ L glutathione sepharose were washed three times with 500 μ L lysis buffer using a 27 gauge (G27) needle before the supernatant was added and filled up to 1 mL with lysis buffer. After incubation on a rotator (1 hr, RT) the beads were washed three times with

500 μ L lysis buffer. GST fusion proteins bound to glutathione sepharose were used for the GST pulldown assay (see Chapter 2.5.5) or eluted with 100 μ L elution buffer (20 mM glutathione, 50 mM Tris-HCl, pH 8). Sepharose was vortexed and centrifuged for 1 min at 380 x g and 4°C. The supernatant was carefully transferred to a slide-a-lyzer MWCO 10,000 unit (Pierce, Rockford, USA) and dialyzed overnight against 50 mM Tris-HCl buffer (pH 8). The protein concentration was subsequently determined using the BCA protein assay kit.

2.3 Yeast two-hybrid (Y2H) system

The MATCHMAKER two-hybrid system 3 (Clontech, Mountain View, USA) was used as a transcriptional assay to screen for novel proteins that interact with the cytosolic C-terminus of mTRPC4 α (aa 615-974) in yeast strain AH109. The system is based on binding of the transcription factor GAL4 upstream of four reporter genes (ADE2, HIS3, lacZ, MEL1) activating their translation and protein expression. GAL4-DNA binding and activation are mediated by two different protein domains which can be physically separated (Fields & Song, 1989).

The bait mTRPC4 α (aa 615-974) was cloned into yeast expression vector pGBKT7 leading to its nuclear expression as a fusion protein with the GAL4 DNA-binding domain (DNA-BD). A mutated GCN4-leucine zipper (Harbury *et al.*, 1993; Zerangue *et al.*, 2001) was also inserted between the C-terminus and the GAL4-DNA binding domain (mTRPC4 α (615-974)/leucine zipper/pGBKT7) to mimick the proposed tetrameric TRPC4 topology. A human aorta cDNA library cloned into yeast expression vector pACT2 was screened with this bait. The library proteins are expressed as fusion proteins with the GAL4 activation domain (GAL4-AD) and also contain a nuclear localization sequence. When library and bait were cotransfected into the auxotroph yeast strain AH109, the TRP1 gene of pGBKT7 and the LEU2 gene of pACT2 served as selection markers allowing survival of cotransformants on medium lacking the otherwise essential amino acids tryptophane (Trp) and leucine (Leu). But only physical interaction of the bait with a library protein brought DNA-BD and GAL4-AD into sufficient spatial proximity reconstituting the functional GAL4 and thus leading to the expression of the reporter genes. These allowed survival on selective media additionally lacking adenine (Ade) and histidine (His) and conversion of X-gal into a blue stain (β -galactosidase assay, lacZ-test). Prey plasmids were isolated from clones surviving on -Trp/-Leu/-His/-Ade agar plates and positive reacting in the β -galactosidase assay. First they were analytically digested with the restriction endonucleases EcoRI/XhoI that cut the cDNA inserts out of the vector MCS. The resulting fragments were separated by gel electrophoresis whereby fragments of identical size pointed towards identical preys. Subsequently, the preys were tested for intrinsic DNA-binding and/or transcriptional activity. Yeast was cotransformed with the prey plasmid and a plasmid coding for the unrelated enhanced green fluorescent protein (EGFP) from *Aequorea victoria* that was also tetramerized and fused to the DNA-BD

(EGFP/leucine zipper/pGBKT7). Only yeast cells cotransformed with preys that did interact unspecifically with EGFP did survive on -Trp/-Leu/-Ade/-His plates. In parallel, prey plasmids had been cotransformed with the bait and were retested for growth on -Trp/-Leu/-His/-Ade agar plates. Prey plasmids from clones surviving on these plates, that also showed no intrinsic DNA-binding and/or transcriptional activity, were finally sequenced. The sequences were compared with Genbank data by using BLAST software. The Y2H screening process is schematically depicted in Figure 8 and described in more detail in the following chapters (2.3.2-2.3.4).

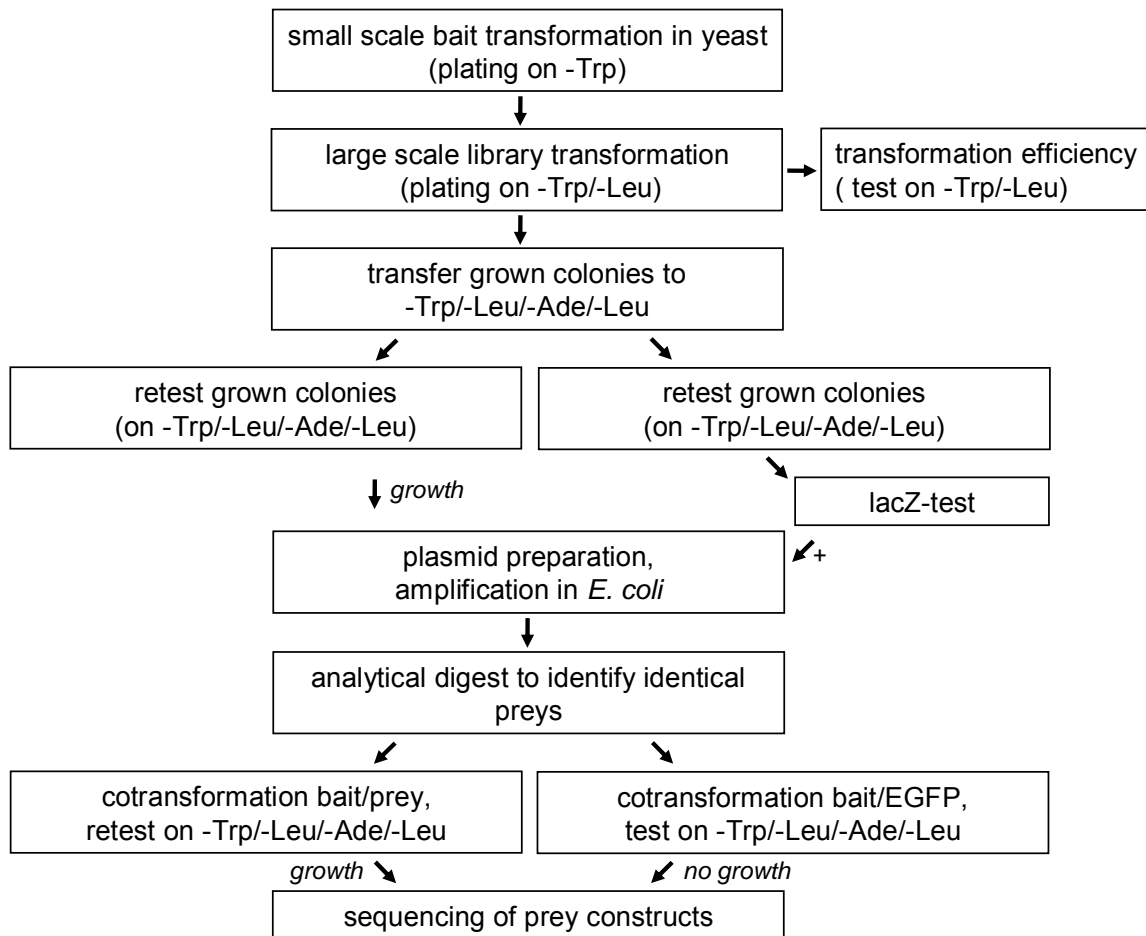


Figure 8: Schematic depiction of the Y2H screening process.

2.3.1 cDNA library titering and amplification

A human aorta MATCHMAKER cDNA library (Clontech, Mountain View, USA) was transformed into *E. coli* BNN132 and amplified to gain enough plasmid for screening in yeast. First its titer was determined by plating dilutions of 1×10^{-6} , 1×10^{-7} , and 2×10^{-7} on LB/amp agar plates. After incubation for 2 days (30°C), the number of grown colonies was counted and resulted in 1.8×10^8 colony forming units (cfu) per mL. The 2.1-fold amount of independent clones present in the library before amplification (which was 3.5×10^6 as provided by the manufacturer) was amplified by spreading 45,000 cfu/150-mm plate on

160 LB/amp agar plates. After 36 hr incubation at 30°C, cells were scraped into liquid LB/amp (final volume ~2.1 L), pooled, partitioned into 4 aliquots, and pelleted by centrifugation. Bacteria were lysed and plasmids purified using the QIAfilter plasmid giga kit. The plasmid preparation protocol was adapted accordingly to the high cell density, starting with the resuspension of each pellet in 400 mL buffer P1. Lysis and neutralization were carried out by adding 400 mL buffer P2 and P3, respectively. An additional filtration step was performed to preclear the lysates before loading onto two equilibrated QIAGEN-tips. Bound DNA was washed, eluted and precipitated with isopropanol. The resulting DNA pellet was washed with ethanol, dried in a vacuum centrifuge and resuspended in TE buffer.

2.3.2 Transformation of yeast

The DNA-BD/bait and the library were sequentially transformed into *Saccharomyces cerevisiae* using the polyethylene-glycol/lithium acetate (PEG/LiAc) method (Ito *et al.*, 1983). Through a small-scale transformation, the DNA-BD/bait was introduced into yeast and plated on selective -Trp agar plates. Single transformants were used as inoculates for the following large-scale transformation with the AD fusion library. It was verified that the bait is not intrinsic DNA-binding and/or transcriptionally active by cotransformation with the negative control vector pGADT7. pGADT7 is an empty vector leading to sole expression of the GAL4-AD in yeast. Since this plasmid does not express a TRPC4-interacting protein, cotransformation with the bait is not sufficient to reconstitute GAL4, thus yeast did not survive on -Trp/-Leu/-Ade/-His plates.

Small-scale transformation

An overnight culture of *Saccharomyces cerevisiae* AH109 grown at 30°C in 2 mL liquid YPAD medium was transferred to 10 mL YPAD medium resulting in an $A_{600} = 0.1$. The cell suspension was grown at 30°C until reaching the logarithmic growth phase ($A_{600} = 0.5$), pelleted by centrifugation (5 min, 2,000 x g, RT), washed with sterile deionized water and resuspended in 200 μ L lithium acetate buffer (100 mM LiAc, 10 mM Tris-HCl, 1 mM EDTA). 18 μ L carrier DNA from salmon sperm (10 mg/mL) were prepared by boiling for 40 sec, and immediately transferred to ice. 1.5 μ g DNA-BD/bait (3 μ g plasmids for coexpressions) were first mixed with the heat-denatured carrier DNA and then added to 200 μ L of the yeast suspension. 1.2 mL PEG/LiAc-solution (40% PEG, 100 mM LiAc, 10 mM Tris-HCl, 1 mM EDTA) were subsequently added and the cell suspension was incubated for 30 min at 30°C. Cells were heat-shocked at 42°C for 15 min, centrifuged, resuspended in 100 μ L TE-Buffer (10 mM Tris-HCl, 1 mM EDTA, pH 8), spread on selective media, and incubated at 30°C for at least 2 days. Yeast transformed with the DNA-BD/bait grew on -Trp medium, cotransformants with a prey on -Trp/-Leu medium.

Large-scale transformation

Three overnight cultures of single yeast colonies transformed with the DNA-BD/bait were transferred to 150 mL -Trp medium, subdivided onto twelve 50 mL-tubes and incubated overnight at 30°C. Next day these starter cultures were pooled, pelleted by centrifugation (3 min, 2,000 x *g*, RT) and resuspended in 10 mL -Trp medium. This suspension was added to 900 mL -Trp medium ($A_{600} = 0.15-0.25$) and cells grew until the logarithmic growth phase was reached ($A_{600} = 0.45-0.75$). The suspension was subdivided onto several 50 mL-tubes, pelleted by centrifugation (5 min, 2,000 x *g*, RT), washed with 300 mL sterile deionized water and pooled in 10 mL water. After washing with 50 mL lithium acetate buffer (100 mM LiAc, 10 mM Tris-HCl, 1 mM EDTA), cells were resuspended in 4 mL lithium acetate buffer.

In triplicates, 40 µg cDNA of the library were mixed with 145 µL heat denaturated carrier DNA (from salmon sperm), 1.2 mL cell suspension and 8.6 mL PEG/LiAc-solution (40% PEG, 100 mM LiAc, 10 mM Tris-HCl, 1 mM EDTA) and incubated for 30 min at 250 rpm and 30°C. After addition of 1 mL dimethyl sulphoxide (DMSO) per tube, cells were heat shocked (15 min, 42°C), cooled down on ice and pelleted by centrifugation (5 min, 2,000 x *g*, RT). Each pellet was resuspended in 25 mL -Trp/-Leu medium before they were pooled and incubated for one hr at 250 rpm and 30°C. After centrifugation (5 min, 2,000 x *g*, RT), cells were resuspended in 12 mL -Trp/-Leu medium, plated in 300 µL aliquots on -Trp/-Leu/-His agar plates (150 mm diameter), and incubated for 2 to 5 days at 30°C. Grown colonies were transferred to -Trp/-Leu/-His/-Ade agar plates and incubated for 2 to 3 more days. Surviving colonies were tested with the β-galactosidase assay and plasmids of positive reacting clones were isolated.

To test the transformation efficiency, dilutions of 10^{-3} to 10^{-6} were plated on -Trp/-His agar plates in parallel and the number of cfus was counted after incubating the plates for 2 days at 30°C. The library was considered to be screened completely, when the 4-fold number of independent clones had been plated in total.

2.3.3 β-galactosidase assay

Clones grown on -Trp/-Leu/-His/-Ade agar plates were top-layered with X-gal agar (0.5% agarose, 500 mM NaPO₄ buffer (pH 7), 1% SDS, 2% X-gal in dimethylformamide (DMF)). The agar was prepared by cooling down melted agarose to 50°C, addition of prewarmed SDS and DMF, and immediate application to the yeast colonies. The yeast colonies were incubated at 30°C up to 12 hr and generation of a blue stain was regularly checked.

2.3.4 Plasmid preparation from yeast

Clones surviving on -Trp/-Leu/-His/-Ade agar plates and positive reacting in the β-galactosidase assay were resuspended in 2 mL -Leu medium and grown overnight at 250 rpm and 30°C. They were pelleted by centrifugation, and resuspended in 200 µL lysis

buffer (2% Triton X-100, 1% SDS, 100 mM NaCl, 10 mM Tris-HCl (pH 8), 1 mM EDTA). 200 μ L phenol/chloroform/isoamylalcohol (25:24:1) and 100 μ L acid-treated glass beads were added and the cell walls were broken by vortexing this mixture. After centrifugation (5 min, 10,000 \times g, RT) 135 μ L of the aqueous phase were transferred to a new tube, mixed with 15 μ L sodium acetate solution (10%) and 375 μ L ethanol, and DNA was subsequently precipitated by centrifugation (30 min, 10,000 \times g, RT). The DNA pellet was washed with ethanol (75%), dried at 37°C for 30 min, and resuspended in 10 μ L Tris-HCl (10 mM, pH 8.5). 2 μ L DNA were transformed by electroporation into *E.coli* and transformed bacteria were grown on selective LB/kana agar plates. Next day, single colonies were grown in liquid overnight cultures and the plasmids were purified using the QIAprep spin miniprep kit.

2.4 Culture of mammalian cells

To avoid contamination, all critical steps were carried out in a working bench under laminar air flow. Cells were stored in liquid nitrogen until usage. A cryogenic vial containing 1.8 mL cell suspension was thawed in a water bath (37°C). Cells were immediately and carefully transferred to 10 mL prewarmed medium and pelleted by centrifugation (3 min, 300 \times g, RT) to remove DMSO. The cell pellet was resuspended in 15 mL fresh medium and cells were grown in plastic tissue flasks of appropriate size at 37°C in a humidified atmosphere (5 or 7% CO₂). Media was replaced one day after thawing and then routinely twice a week. They were split at 90% confluency by washing them once with D-PBS (w/o Ca²⁺, Mg²⁺) and adding 0.05% trypsin/0.02% EDTA for approx. 1 min. The protease solution was removed and cells were detached by gently tapping the flask and rinsing the cells with medium. After counting the cell number with a Casy cell counter, the desired density was adjusted with medium before cells were seeded. For some applications (e.g. Ca²⁺ imaging) glass cover slips had to be coated before cells were seeded. The cover slips were incubated 5 min with poly-L-lysine (0.01% stock solution diluted 1:5 in sterile deionized water), washed twice with water and air-dried overnight. When cells were frozen for long term storage, cryogenic vials and media were kept on ice. Cell pellets were resuspended in cold medium, the resulting cell suspension was diluted with an equivalent volume of DMSO:FBS (1:5) freezing medium and transferred to cryogenic vials. After cooling down in a Cryo 1°C freezing container (with -1°C/min) that was placed in a -80°C freezer, they were transferred to liquid nitrogen on the next day.

Primary cells (human AoSMC, CASMC, HAEC, HMVEC-d) were cultivated according to the provider's instruction.

Some stable cell lines (TRPC3/4/5/6 HEK293 FITR) were used that express recombinant TRPC channels in a tetracycline-inducible manner from a specific genomic location. They were generated in-house by using the Flp-In T-Rex system (Invitrogen, Karlsruhe, Germany)

and thus named FITR. This system is based on Flp recombinase that mediates site specific recombination. The parental HEK293 Flp-In T-Rex cell line contains a Flp recombination target (FRT) site and constitutively expresses the Tet repressor (TetR) controlled by the human cytomegalie virus (CMV) promoter. This cell line is transfected with two plasmids. The first contains the respective TRPC channel gene (flanked by a FRT site) whose protein expression is controlled by a tetracycline-regulated hybrid CMV/*tet* operator 2 (TetO₂) promoter. A cotransfected plasmid constitutively expresses Flp that mediates homologous recombination between the FRT sites leading to integration of the TRPC gene into the cell's genome. TetR binds with high affinity to TetO₂ and represses TRPC channel expression. When tetracycline (or its derivative doxycycline) is added, it binds to TetR leading to a conformational change that prevents binding to TetO₂. Therefore, the promoter that controls TRPC expression is derepressed.

18 to 24 hr prior to the experiments, protein expression was induced in these cell lines by adding 1 µg/mL doxycycline to the medium.

The following media were used for the indicated cell types:

- **A7r5 cells** (smooth muscle cells derived from embryonic rat thoracic aorta): DMEM (with glutaMAX I, 4.5 g/L glucose and 110 mg/mL sodium pyruvate) supplemented with 10% (v/v) FBS (from PAA).
- **HAEC**: Clonetics EGM-2 BulletKit
- **Human AoSMC, CASMC**: Clonetics SmGM-2 BulletKit
- **HEK293 cells**: ISCOVE medium supplemented with 10% (v/v) FBS (Biochrom) and 2 mM glutamine.
- **HM1 cells** (HEK293 cells stably expressing the human muscarinic receptor type 1): DMEM/Nutrient F12 (with glutaMAX I) supplemented with 10% (v/v) FBS (PAA), 1 mM glutamine and 400 µg/mL geneticine. 50 µg/mL zeocin were added for selection and culture of clones stably expressing mTRPC5-YFP (**HM1-C5Y cells**).
- **HMVEC-d**: Clonetics EGM-2 MV BulletKit
- **TRPC3/4/5/6 HEK293 FITR cells** (HEK293 FITR cells expressing hTRPC3 (NM_003305)/mTRPC4β (AAC05178)/mTRPC5 (NM_009428)/hTRPC6 (AF080394) under the control of an inducible promoter as described above): DMEM (with glutaMAX I, 4.5 g/L glucose and 110 mg/mL sodium pyruvate) supplemented with 10% (v/v) FBS (Biochrom), 1 mM glutamine, 1 mM MEM sodium pyruvate, 40 µg/mL hygromycine (50 µg/mL for mTRPC5 FITR cells), and 15 µg/mL blasticidine S HCl.

2.4.1 Transfection of mammalian cells

Since FBS had no significant effect on transfection efficiency, cells were transfected in full medium using Lipofectamine 2000. Only the liposomes were formed and loaded in transfection medium (Opti-MEM). For co-immunoprecipitation experiments 3×10^6 HM1 cells (in 10 mL) were seeded in dishes of 9.4 cm diameter and grown to 80-90% confluency until the next day. 4 μ g of each plasmid were mixed in 1 mL transfection medium and incubated for 20 min (RT) with 20 μ L Lipofectamine 2000 (also diluted in 1 mL Opti-MEM). The mixture was applied to the cells. For siRNA and plasmid cotransfections, 3×10^5 HM1 cells/2 mL/well were seeded in a 6-well plate, growing to 30-50% confluency next day. 4 μ g plasmid were mixed with 2.5 μ L 20 μ M siRNA stock solution in 250 μ L transfection medium and incubated for 20 min (RT) with 5 μ L Lipofectamine 2000 (also diluted in 250 μ L Opti-MEM). The mixture was applied to the cells leading to a final siRNA concentration of 20 nmol/L. These protocols are exemplary and were adapted to the individual experimental conditions.

Success and efficiency of transfection were determined either by Western blot or by additionally transfecting cells with the same amount of plasmid or siRNA and a small amount (0.4 μ g/well in a 6-well plate) of plasmid coding for GFP. 18 to 24 hr post transfection GFP fluorescence was excited with an UV lamp and the number of transfected cells was estimated. Transfection rates of 80% and more were defined as mandatory for functional experiments with cell populations.

2.4.2 Generation of a HM1 cell line stably expressing mTRPC5-YFP

HM1 cells seeded in a 6-well plate and grown to approximately 80% confluency were transfected with 4 μ g of the mTRPC5-YFP construct using Lipofectamine 2000 as described. The construct was generated by inserting an XbaI/NotI fragment of mTRPC5-GFP (Strubing *et al.*, 2003) into pcDNA3.1(-)zeo. The YFP fusion was obtained by joining a NotI/EcoRI cut YFP-PCR fragment to the channel C-terminus. 24 hr post transfection clonal selection started by cultivating the cells in complete medium supplemented with 50 μ g/mL zeocin. Cells were trypsinized and transferred to a new dish (94 mm diameter). Several days later single clones were isolated by manual picking from grown colonies. During expansion, expression of the construct was visually checked by exciting its YFP fluorescence at 515 nm. Clones were functionally characterized in FLIPR assays and patch clamp experiments. One clone was selected for further studies.

2.5 Protein biochemical methods

2.5.1 Preparation of cell lysates

Cells grown in tissue culture flasks were placed on ice (10 min) and washed twice with ice-cold D-PBS (w/o Ca^{2+} , Mg^{2+}) before detaching them with a cell scraper in lysis buffer. They

were placed 1 hr on ice before centrifugation (15 min, 16,000 x g, 4°C). The supernatant was frozen at -20°C (for GST-pulldown assays stabilized with 1 mM dithiothreitol and 10% glycerol) or mixed with NuPAGE LDS sample buffer (4x) and 5% β -mercaptoethanol (β -ME), heat-denatured (95°C, 3 min) and centrifuged (16,000 x g, 2 min) before they were stored at 4°C.

2.5.2 Determination of protein content

The amount of total protein was colorimetrically detected and quantified with the bicinchoninic acid (BCA) protein assay that is based on a biuret reaction. The absorbance of the purple-coloured reaction product was measured at 562 nm with a Tecan safire 2 plate reader and the protein concentration was determined based on a bovine serum albumin (BSA) standard curve. The reaction was set up in a flat-bottom, transparent 96-well plate by mixing

- 5 μ L of each standard dilution (unknown samples were diluted 1:5 in lysis buffer)
- 150 μ L of working reagent (prepared by mixing BCA reagent A with BCA reagent B (50:1))

and incubating the plate at 37°C for 30 min before measuring the absorbance.

2.5.3 SDS-PAGE

This technique, called sodium dodecyl sulphate polyacrylamide gel electrophoresis (SDS PAGE), allows separation of proteins. In samples treated as described in 2.5.1, proteins are denatured and negatively charged by SDS in proportion to their mass. When loaded on Bis-Tris-HCl gradient gels (4-12%), they can thus be electrophoretically separated according to their molecular weight. Electrophoresis was carried out in NuPAGE MOPS SDS running buffer for 75 min at 150 V. Gels were blotted (see Section 2.5.4) or stained for 15 min with Coomassie blue solution. Excess dye was removed by washing with a solution containing 10% acetic acid and 40% ethanol.

2.5.4 Western blot

After proteins have been separated by size with SDS PAGE they were transferred to a nitrocellulose membrane (Bio TraceNT) using NuPAGE Transfer Buffer and a Novex Xcell 2 blotmodul or the iBlot gel transfer system according to the manufacturer's instruction. To verify transfer, the blotted proteins were stained with 0.1% Ponceau S Solution for 1 min and excessive dye was removed by washing with water. The membrane was blocked with blocking buffer (1 hr, RT) before incubating it with the primary antibody (1 hr, RT). After washing it four times with TBST, it was incubated with the fluorescent-labelled or HRP-conjugated secondary antibody (45 min, RT) and washed again four times with TBST. Membranes were analyzed using the Odyssey infrared imaging system or the Lumi imager.

2.5.5 GST pulldown assay

HEK293 cells transiently transfected with the mTRPC4 α -C-terminus or full length mTRPC4 α , mTRPC4 β or mTRPC5 channel were lysed and protein concentration determined using the BCA protein assay kit. An equivalent of 50 μ g total protein was added to GST or the GST fusion proteins bound to glutathione sepharose (see 2.2.15), filled up to 1 mL with lysis buffer and incubated on a rotator (2 hr, RT). Sepharose was washed three times with 500 μ L lysis buffer and a G27 needle before 20 μ L 1x LDS sample buffer (containing 5% β -ME) were added. Samples were denaturated (95°C, 3 min), centrifuged and analyzed by Western blot.

2.5.6 Co-immunoprecipitation

24 hr after transfection, cells were harvested by placing on ice for 10 min before washing twice with 10 mL ice-cold D-PBS (w/o Ca²⁺, Mg²⁺).

Cell membranes were isolated by scraping cells from one dish into 600 μ L homogenization buffer (320 mM sucrose, 5 mM HEPES, pH 7.4, supplemented with Complete protease inhibitor). The cell suspensions from four dishes per transfection condition were pooled, sonicated (1x 5 sec), centrifuged (100 x *g*, 10 min) and the resulting supernatant was partitioned onto three vials and further centrifuged (100,000 x *g*, 30 min). Membrane proteins were lysed from the resulting pellet with 600 μ L lysis buffer (supplemented with Complete protease inhibitor) per pellet, incubated on ice for 1 hr and centrifuged (15 min, 16,000 x *g*, 4°C). The supernatants were transferred to a fresh vial and pooled. An aliquot was kept as input control and the rest of the lysate was divided onto two vials. 4 μ g of the primary antibody were added to each sample and they were incubated overnight at 4°C on a rotator.

Cell lysates were gained by directly scraping cells from one dish into 600 μ L lysis buffer (supplemented with Complete protease inhibitor), incubation on ice for 1 hr and centrifugation (15 min, 16,000 x *g*, 4°C). The supernatant was transferred to a fresh vial, pooled with the lysates of the 3 remaining dishes that were equally transfected, and treated as described above.

The next day, 30 μ L protein A-sepharose or protein G-sepharose suspension, respectively, were washed and added to the samples. Samples were incubated for 2 hr at 4°C. Sepharose was washed three times with a G27 needle and 500 μ L lysis buffer before 20 μ L 2x LDS sample buffer (containing 10% β -ME) were added. Samples were denaturated (95°C, 3 min), centrifuged and analyzed by Western blot.

2.5.7 Surface expression analysis

1.2x 10⁶ HM1 cells stably transfected with mTRPC5-YFP were plated in dishes with 94 mm diameter. The next day, they were transfected with 40 nM siRNA or treated with liposomes only. 48 hr post transfection, cells were washed with D-PBS. Surface proteins were biotinylated by incubation with a membrane-impermeable form of biotin (1 mg/mL EZ-link

sulfo NHS-LC biotin in D-PBS) for 30 min. Excess biotin was quenched by washing twice with 100 mM glycine. Cells were scraped into 100 μ L lysis buffer (supplemented with Complete protease inhibitor), incubated on ice for 1 hr and centrifuged (15 min, 16,000 \times g , 4°C). A BCA test was performed with the supernatant. An aliquot was kept to test SESTD1 siRNA knock-down. 50 μ L streptavidin sepharose per sample were washed and equal protein amounts were added. After overnight incubation on a rotator (4°C), the sepharose was washed before 15 μ L 2x LDS sample buffer (containing 10% β -ME) were added. Samples were denaturated (95°C, 3 min), centrifuged and analyzed by Western blot.

2.5.8 Peptidyl-prolyl *cis-trans* isomerization assay

Peptidyl-prolyl *cis-trans* isomerase (PPIase) activity is measured classically in a coupled assay, where chymotrypsin hydrolyses the anillide bond of the *trans* (but not *cis*) isomer of succinyl-Ala-Ala-Pro-Phe-4-nitroanilide. The absorbance of the subsequently formed 4-nitroanillide is monitored (Harding *et al.*, 1989). We also tested whether SESTD1 acts as PPIase but employed a simplified, fluorescence-based assay whose principle is schematically depicted in Figure 9. The amino acid proline (part of cys-bridged H-Abz-Cys-Ala-Pro-Ala-Cys-Ntr-NH₂) spontaneously isomerizes from *cis* to *trans* (approx. 65% of the cys-bridged peptides are *trans* already). As long as the two cysteines are bridged by a disulfide bond, the conversion of the remaining 35% is inhibited. Reducing agents such as dithiotreitol (DTT) break the bond. This leaves proline in a flexible state from which it isomerizes resulting in formation of fluorescent H-Abz-Cys-Ala-Pro_{trans}-Ala-Cys-Ntr-NH₂ that can be measured in a plate reader (Tecan safire 2). This spontaneous isomerization is accelerated in presence of a PPIase, characterized by a steepening of the slope of the fluorescence curve.

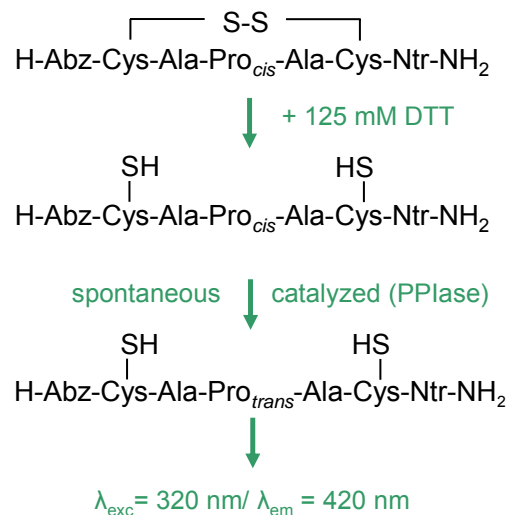


Figure 9: Scheme of the *cis-trans* isomerization assay.

The assay was performed in a 384-well plate. Equal volumes (10 μ L each) of 50 μ M substrate (cys-bridged H-Abz-Cys-Ala-Pro-Ala-Cys-Ntr-NH₂), 125 mM DTT and 1 μ M FKBP12.6 or 4.76 μ M GST-SESTD1, respectively, were mixed manually on ice before fluorescence measurement was started. All solutions were prepared in 50 mM HEPES (pH 7.2), except GST-SESTD1 that was dialyzed against 50 mM Tris (pH 8).

2.5.9 Phospholipid overlay assay

PIP strips are commercially available nitrocellulose membranes containing 100 pmol samples of 15 different phospholipids and a blank sample. They were blocked with blocking buffer for PIP strips (1hr, RT) and incubated with blocking buffer containing 500 ng/mL purified GST or GST-SESTD1 (4 hr, RT). After washing (3 times with blocking buffer), they were incubated at 4°C overnight with the primary antibody anti-GST (1:2,000 in blocking buffer). Three wash steps with TBST (pH 8) were followed by 45 min incubation with the secondary HRP-conjugated anti-rabbit antibody (1:20,000 in blocking buffer). The membranes were washed again three times with TBST (pH 8), incubated with 1 mL Lumi-LightPLUS Western blotting substrate (5 min) and the chemiluminescent signals were analyzed with a Lumi imager.

2.5.10 Cova-PIP specificity plate assay

The GST-tagged PH-domain of LL5- α , GST alone or GST-SESTD1 were diluted in blocking buffer for PIP strips. Cova-PIP specificity plates loaded with 10 or 100 pmol PIP_n per well were incubated with 100 μ L protein solution/well (3 hr, gentle agitation, RT). Plates were washed manually 3 times with blocking buffer for PIP strips before incubation with 100 μ L anti-GST (1:1,000 in blocking buffer) for 1hr (gentle agitation, RT). Plates were washed 4 times with TBST for PIP strips using an automatic plate washer. For dissociation-enhanced lanthanide fluorescence immunoassays (DELFIAs), 100 μ L secondary Eu-N1-labelled anti-rabbit antibody (500 ng/mL in blocking buffer) were added per well and incubated 1 hr (gentle agitation, RT). Plates were washed 4 times with TBST and an automatic plate washer before 100 μ L enhancer solution were added per well. After 20 min incubation, fluorescence of the lanthanide was excited (λ_{exc} = 340 nm) and read (λ_{em} = 620 nm) in a Tecan ultra plate reader.

2.5.11 Immunofluorescence

Five coverslips/well were placed in a 6-well plate and coated with poly-L-lysine (see Chapter 2.4.1). 5×10^5 cells were plated per well in a volume of 2 mL. Next day they were transfected with siRNA (see Chapter 2.4.1). 24 hr post transfection, the coverslips were transferred into a 24-well plate, washed twice with PBS (137 mM NaCl, 2.7 mM KCl, 10.1 mM Na₂HPO₄, 1.4 mM KH₂PO₄) and fixed 15 min with 4% paraformaldehyde (in PBS). After washing with PBS, cells were permeabilized with 0.1% Triton X-100 (in PBS) for 15 min and washed

again. They were blocked 1 hr with LiCor blocking buffer and thereafter incubated with the primary antibody (diluted in LiCor blocking buffer:PBS = 1:1) for 1 hr. After washing, they were incubated with the secondary fluorescent-labelled antibody (diluted in LiCor blocking buffer:PBS = 1:1) for another hour. Four wash steps were followed by incubation with Hoechst 33258 (1:10,000 in PBS) for 1 min and two additional wash steps. The coverslips were mounted in Permafluor mounting medium and air-dried overnight. Probes were analyzed with an inverted microscope (DM IRE2, Leica) and Leica Confocal Software (Leica, Solms, Germany).

2.6 Fluorometric $[Ca^{2+}]_i$ measurements

Changes in cytosolic calcium $[Ca^{2+}]_i$ were measured using the Ca^{2+} -sensitive fluorescent dyes fluo-4 AM and fura-2 AM. The latter is a widely used indicator, whose fluorescence excitation maximum shifts towards shorter wavelengths upon Ca^{2+} binding, while the fluorescence emission maximum is relatively unchanged. Typically, the fluorescence intensities excited at 340 nm (F_{340}) and 380 nm (F_{380}) are measured and the F_{340}/F_{380} ratio is calculated. While F_{340} increases upon binding of Ca^{2+} , F_{380} decreases and an increase in $[Ca^{2+}]_i$ consequently results in a rising F_{340}/F_{380} ratio. Factors that influence fluorescence intensity, such as cell thickness, camera sensitivity, dye concentration and loss by leakage and photobleaching, should affect measurements at both excitation wavelengths to the same extent (Grynkiewicz *et al.*, 1985). Thus, ratiometric measurements are less disturbed by these effects. They were performed with single cells (Ca^{2+} imaging) as well as cell populations (FLEX experiments).

Ca²⁺ imaging

Cells grown on poly-L-lysine-coated 24-mm glass coverslips were loaded in cultivation medium supplemented with 2 μ M fura-2, acetoxymethyl ester (AM; 30 min, 37°C) and subsequently allowed to de-esterify (through intracellular esterases cleaving off the acetate residue) in standard extracellular solution (15 min, 37°C). Changes in $[Ca^{2+}]_i$ were measured using an imaging system that consists of a xenon arc lamp, a monochromator, an inverted microscope (Axiovert 200) and a charge-coupled device (CCD) camera. Fluorescence was excited alternating at 340 nm and 380 nm, long-pass filtered at 440 nm and captured at 2 sec intervals. The 340/380 nm excitation ratio of selected cell areas was calculated with T.I.L.L. vision 4.0 software (T.I.L.L. Photonics, Gräfelfing, Germany) after correction for background fluorescence. All experiments were performed in a recording chamber with approximately 1 mL volume.

FLEX experiments

20,000-40,000 cells/well were seeded in black poly-L-lysine-coated glass bottom 96-well plates (Sensoplates) and grown overnight to an almost confluent monolayer. They were loaded in 100 μ L standard extracellular solution supplemented with 2 μ M fura-2 AM (30 min, 37°C) and allowed to de-esterify (15 min, 37°C). Intracellular calcium signals were ratiometrically measured in a benchtop scanning fluorometer (FLEX). Fluorescence was excited alternating at 340 nm and 380 nm, long-pass filtered at 495 nm and captured at 4 sec intervals. The F_{340}/F_{380} ratio was calculated using SoftMax Pro software (Molecular Devices, Munich, Germany). Baseline fluorescence was detected for 30 sec, before an agonist was applied with the FLEX pipettor. Since the FLEX station has an 8-channel pipettor, it takes more time for reading a 96-well plate than a fluorometric imaging plate reader (FLIPR) with a 96-channel pipettor. Therefore, a FLIPR was used for standard inhibition assays in well characterized FITR cell lines.

In HM1-C5Y cells, Ca^{2+} release was calculated as area under the curve in Ca^{2+} free standard extracellular solution. TRPC5-mediated Ca^{2+} influx was calculated by subtracting Ca^{2+} release from the area under the curve in standard extracellular solution.

FLIPR measurements

Cells grown to an almost confluent monolayer on black poly-D-lysine coated 96-well plates were washed once with standard extracellular solution (E) and incubated (30 min, RT) with dye solution (2 μ M fluo-4 AM, 0.02% Pluronic F127, 0.1% BSA in E). After washing three times with E, induced and non-induced HEK293 FITR cells were either incubated with buffer only or with different concentrations of steroid (10 min). Fluo-4 fluorescence was excited at 488 nm with an argon laser, measured and imaged in the FLIPR and activators were applied by the FLIPR pipettor. Signals were analyzed with the software provided by the manufacturer.

The half maximal inhibitory concentrations (IC_{50}) of norgestimate, progesterone and levonorgestrel on TRPC3 and TRPC6 HEK293 FITR cells were calculated based on area under the curves. Ca^{2+} influx following activation into induced cells that were not incubated with steroid was defined as 0% inhibited. Ca^{2+} influx into induced cells that were neither incubated with steroid nor activated with OAG was set to 100% inhibition.

The IC_{50} values on TRPC4 and TRPC5 HEK293 FITR cells were calculated at $t = 62$ sec, the time point of the channel signal maximum. The raw TRPC4 and TRPC5 channel signals were calculated by subtracting the curve of non-induced, stimulated cells from induced, stimulated cells. Ca^{2+} influx following activation into induced cells not treated with steroid was

defined as 0% inhibited. Ca^{2+} influx into non-induced, stimulated cells was set to 100% inhibition.

All fluorometric $[\text{Ca}^{2+}]_i$ measurements were performed at room temperature.

2.7 Patch clamp recordings

Whole-cell currents of endogenous or recombinant channel proteins were measured with the patch clamp technique (Neher & Sakmann, 1976). A heat-polished patch pipette with resistances of 2–4 M Ω was pulled from a borosilicate glass capillary with filament by using a DMZ-Universal puller. It was filled with standard intracellular solution and pressed against the surface of a single cell that had no contact to its neighbours. The cell-attached configuration was obtained by applying a negative pressure that sealed the cell membrane tightly to the glass wall of the pipette (seal resistance above 1 G Ω) thus electrically isolating it from its surroundings. When more suction was applied, it destructed the membrane patch under the pipette while the high resistance seal between cell membrane and patch pipette remained intact. Electrical access to the cell's interior was gained via a silver/silver chloride electrode coupled to the electrical circuit depicted in Figure 10. This so called whole-cell configuration allowed measuring the current flow through all ion channels in the cell membrane of a single cell that are opened under defined conditions.

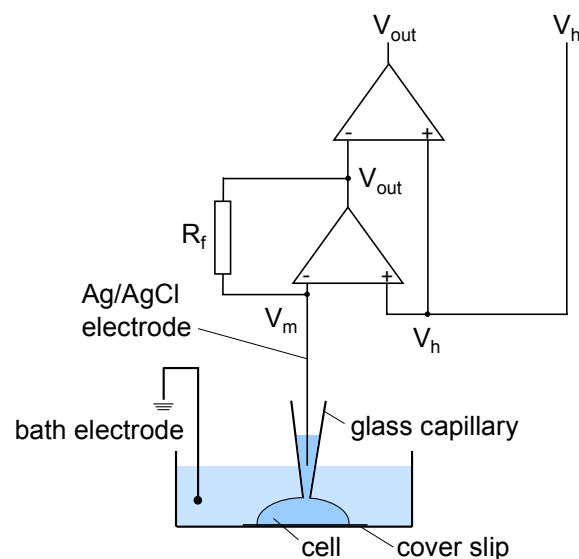


Figure 10: Schematic patch clamp circuit in the whole-cell configuration (adapted from Numberger & Draguhn, 1996). The Ag/AgCl electrode is connected to the inverting (-) input of an operational amplifier that measures the cell membrane potential (V_m). The non-inverting (+) input of the amplifier is connected to the signal generator that determines the holding potential (V_h). By subtracting the membrane from the holding potential ($V_h - V_m = V_{out}$) the operational amplifier detects when ionic currents pass the cell membrane as the cell thus deviates from the holding potential. To readjust the cell to V_h ("voltage clamp"), V_{out} is directed to a feedback resistor (R_f) generating a current that is opposite and equal to the ionic current and injected into the cell (resulting in $V_m = V_h$). The current through the patch is not measured directly but can be calculated as R_f is known and V_{out} measured by a differential amplifier.

24 hr prior to experiments, coverslips were placed in a 24-well plate, coated with poly-L-lysine (see Chapter 2.4) and 10-20,000 cells/well were plated in a volume of 0.5-1 mL. 1 µg/mL doxycycline was added to FITR cells to induce TRPC channel protein expression (see Chapter 2.4). Next day, coverslips were transferred to a recording chamber and cells were continuously superfused with standard extracellular solution and low pressure (approx. 10 kPa, 8-channel valve perfusion system). For A7r5 cells a modified extracellular solution with 200 µM Ca^{2+} was used. Whole-cell recordings were performed with an EPC-10 amplifier and Pulse software (HEKA, Lambrecht, Germany). Cells were held at a potential of -70 mV, and current-voltage (*I-V*) relationships were routinely measured every 3 sec from voltage ramps (-100 mV to +80 mV) lasting 200 msec.

Data was acquired at 6.67 kHz and filtered with 2.22 kHz. The series resistance was compensated. In some experiments channels were activated by intracellular application of AlF_4^- . For its infusion, 2 µL 3 mM AlCl_3 were mixed with 4 µL 0.5 M NaF and diluted in 200 µL standard intracellular solution. All experiments were performed at room temperature. Currents were leak-corrected by subtracting completely blocked currents from currents of activated cells. As TRPC mediated currents decay over time they were interpolated before and after application of a modulator. Current data obtained with the modulator were subsequently normalized to the interpolated values. Mean current densities were calculated by normalizing current amplitudes to the cell capacitance.

2.8 *In vitro* vascular function

Adult male Wistar-Unilever rats (8–11 weeks old; Harlan Winkelmann, Borcheln, Germany) were sacrificed by decapitation. Thoracic aortas were excised quickly, transferred to cold physiological salt solution (PSS) and rinsed. After connective tissue and perivascular fat had been carefully removed, aortas were dissected in 5 mm rings and hung on special hooks (Hugo Sachs, March-Hugstetten, Germany) by inserting two parallel wires into the lumen. The upper hook was connected to a force transducer and the lower hook fixed the aortic rings to the bottom of an organ bath thus allowing isometric tension recording. The aortic rings were equilibrated in PSS (37°C, 15 min) and bath solutions were continuously gassed with carbogen (95% O_2 and 5% CO_2) to provide oxygenation and pH of 7.4. To mimick the physiological state, the rings were set at 1000 mg passive tension (in 200 mg steps). Vessels strongly contracting after application of 60 mM KCl were defined as intact. They were washed out and further used to measure cumulative dose-response curves for norgestimate. Relaxation was expressed as a percentage of the steady-state tension produced by preceding phenylephrine application.

2.9 Statistics

Averaged data is expressed as means \pm SEM and number of experiments is indicated as “*n*”. For statistical analysis, Wilcoxon test was performed with SAS 9 software. P values less than 0.05 were considered as statistically significant and depicted as: P < 0.05: *; P < 0.01: **; P < 0.001: ***.

The half maximal inhibitory concentration (IC_{50}) was calculated with SigmaPlot (Systat software, San Jose, USA) and the sigmoidal Hill-model: $f = ax^b/(c^b+x^b)$. The half maximal effective concentration (EC_{50}) was calculated analogously with $f = y_0+ax^b/(c^b+x^b)$.

3 Results

3.1 Differential inhibition of TRPC channels by norgestimate

According to the World Health Organization (WHO), 30% of all deaths worldwide were caused by various cardiovascular (CV) diseases in 2005 (WHO, 2007). TRPC channels are considered important pharmacological targets for the development of novel medicines for several CV pathologies including cardiomyopathy, vascular remodelling, hypertension and high endothelial permeability (Dietrich *et al.*, 2007a). So far, characterization of native TRPC channels in cardiovascular tissues is hindered by the lack of specific tool compounds that discriminate well between and within the TRPC subfamilies. Cloned channels were at first investigated in heterologous overexpression systems generating controversial data in terms of channel properties and regulation. Valuable insight into native channel properties was gained by their down-regulation in primary cells as well as studying gene-deficient mouse models. Nevertheless, specific pharmacological TRPC inhibitors would be very useful to further elucidate the channels' roles under physiological as well as pathophysiological conditions. Preliminary tests of ion channel-modulating compounds had identified norgestimate as a putative inhibitor of TRPC-mediated Ca^{2+} -influx.

The following studies were performed to evaluate in detail the potential of this compound as a specific pharmacological TRPC6 modulator.

3.1.1 FLIPR measurements

Differential inhibition of TRPC channels by norgestimate

Our initial experiments were aimed to determine the activity of norgestimate towards different members of the TRPC family. HEK293 cell lines heterologously expressing homomeric channels under the control of an inducible promoter (Flp-In T-Rex system, see Chapter 2.4) were used throughout these studies. TRPC3 and TRPC6, two representative members of the DAG-sensitive TRPC3/6/7 subfamily, were tested as well as the DAG-insensitive TRPC4 and TRPC5. TRPC1 was not tested since its expression does not result in measurable ion currents (Strubing *et al.*, 2001).

Fluorometric measurements of Ca^{2+} entry using FLIPR showed that application of oleoyl-2-acetyl-sn-glycerol (OAG), a membrane permeable diacylglycerol analogue, to induced HEK293 Flp-In T-Rex (FITR) cells expressing TRPC3 or TRPC6 resulted in a robust increase in the intracellular Ca^{2+} concentration (see Fig. 11). This increase was completely absent in non-induced cells indicating that the measured responses were solely due to TRPC3 and TRPC6 activity (data not shown). Ca^{2+} influx following application of 30 μM OAG was strongly reduced in cells preincubated with 30 μM norgestimate (Fig. 11 A, C). The IC_{50}

value of norgestimate on TRPC3 was $2.8 \pm 0.4 \mu\text{M}$ ($n = 2$, Fig. 11 B). Norgestimate was similarly active on TRPC6 with an IC_{50} of $5.2 \pm 0.4 \mu\text{M}$ ($n = 4$, Fig. 11 C).

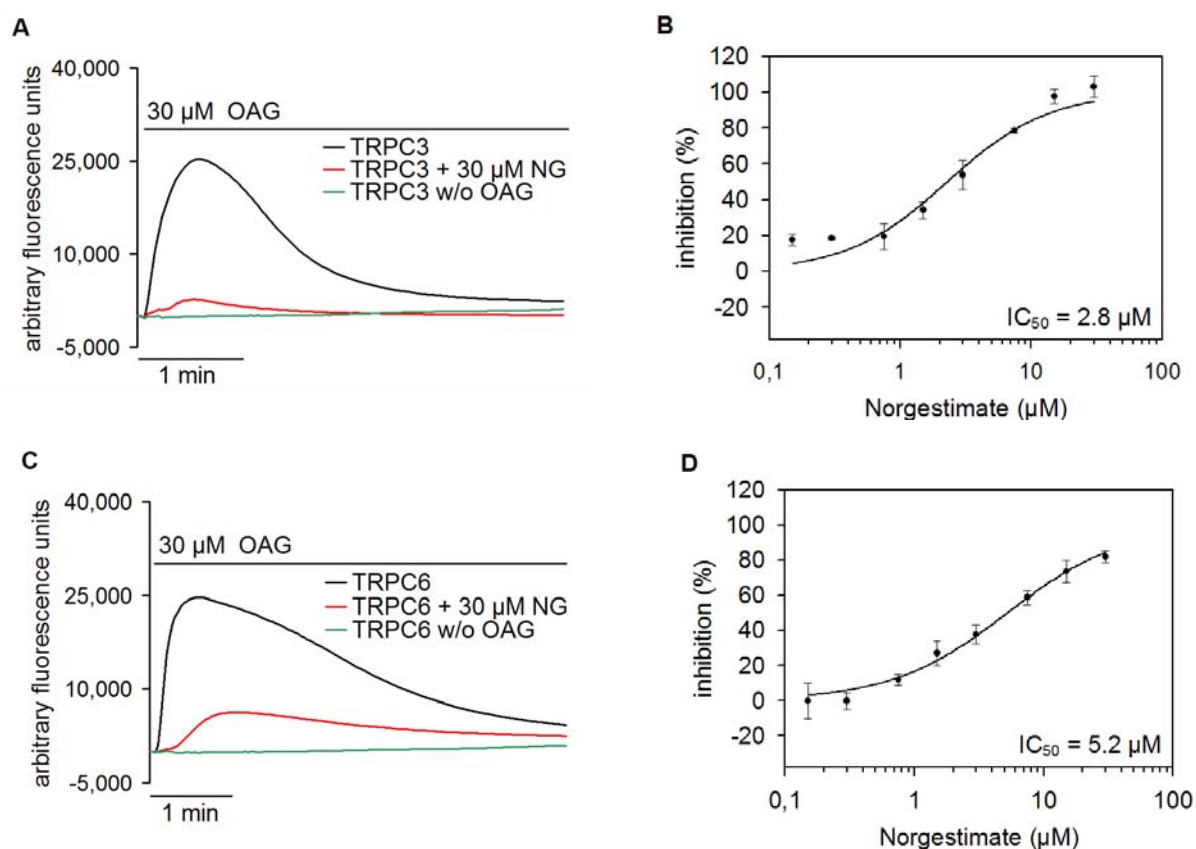


Figure 11: Norgestimate inhibits TRPC3- and TRPC6-mediated Ca^{2+} influx. (A, C) Time-dependent changes of $[\text{Ca}^{2+}]_i$ in fluo-4-loaded induced TRPC3 HEK293 FITR cells (A) and TRPC6 HEK293 FITR cells (C). TRPC-mediated Ca^{2+} influx following application of 30 μM OAG was strongly reduced in cells preincubated with 30 μM norgestimate (NG). Representative traces are shown. Time scale bar 1 min. (B, D) Determination of norgestimate IC_{50} values on TRPC3 (B) and TRPC6 (D). Data is shown as means of 2 wells (B) and 4 wells (D) with 45,000 cells per well.

When these experiments were performed, no direct physiological stimuli of TRPC4 and TRPC5 were known. Therefore, both channels had to be stimulated indirectly, e.g. by application of trypsin, a protease-activated receptor (PAR) stimulating protease. Trypsin is able to activate all four known PAR subtypes and the messenger RNA (mRNA) of three of them (PAR₁, PAR₂ and PAR₃) was shown to be endogenously present in HEK293 cells (Kawabata *et al.*, 1999). PAR activation leads to the depletion of calcium stores in the ER. This PI response (see Chapter 1.1.1) is independent of the channel's presence but consequently leads to activation of receptor-operated channels like TRPC4 and TRPC5. Comparison of trypsin-activated Ca^{2+} entry into induced and non-induced TRPC4 and TRPC5 HEK293 FITR cells showed that channel induction significantly increased Ca^{2+} entry. Basic prerequisite to measure the effect of norgestimate on both channels under these conditions is to exclude PAR antagonism of the compound. Hence, calcium release from ER was compared in non-induced TRPC5 HEK293 FITR cells preincubated with 30 μM

norgestimate or buffer only (10 min). Kinetics and quantity of calcium store release in cells treated with 30 μM norgestimate were not changed compared to untreated cells. Therefore, norgestimate is not a PAR antagonist (Fig. 12) and TRPC4 and TRPC5 activation via PAR stimulation is suitable to measure the channel's inhibition by norgestimate.

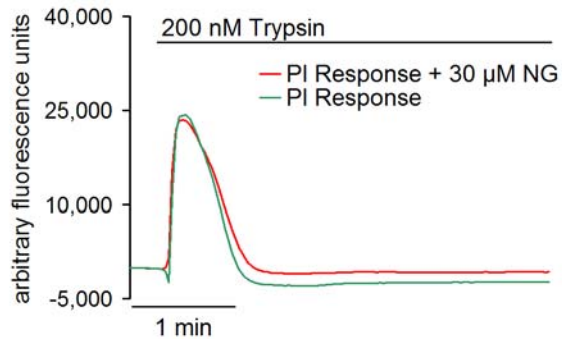


Figure 12: Norgestimate is not a PAR-antagonist. Time-dependent changes in $[\text{Ca}^{2+}]_i$ of fluo-4-loaded TRPC5 HEK293 FITR cells. Rise in $[\text{Ca}^{2+}]_i$ following application of 200 nM trypsin (PI response) in non-induced TRPC5 HEK293 FITR cells was not suppressed in cells preincubated with 30 μM norgestimate (NG). Representative traces are shown. Time scale bar 1 min.

In contrast to TRPC3 and TRPC6, application of norgestimate to TRPC4 or TRPC5 expressing cells only caused a minor decrease of channel-mediated Ca^{2+} entry (Fig. 13 A, C). IC_{50} values of $> 30 \mu\text{M}$ were determined for both TRPC4 ($n = 2$, Fig. 13 B) and TRPC5 ($n = 4$, Fig. 13 D). Channel inhibition by 30 μM norgestimate was amounted to 12.7% and 32.0% for TRPC4 and TRPC5 respectively.

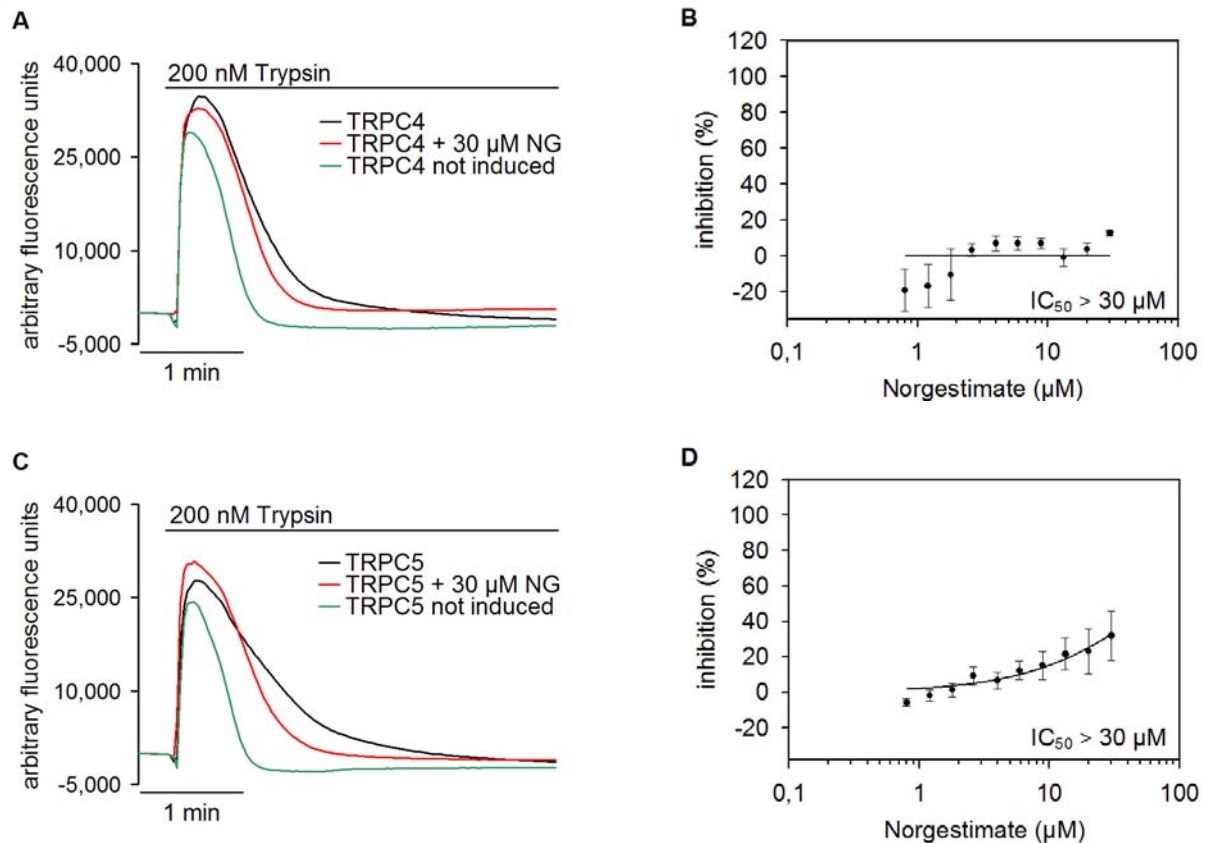


Figure 13: Small effects of norgestimate on TRPC4- and TRPC5-mediated Ca^{2+} influx. (A, C) Time-dependent changes in $[\text{Ca}^{2+}]_i$ of fluo-4-loaded induced TRPC4 (A) and TRPC5 HEK293 FITR cells (C). TRPC-mediated Ca^{2+} influx following application of 200 nM trypsin was only slightly reduced in cells preincubated with 30 μM norgestimate (NG). Representative traces are shown. Time scale bar 1 min. (B, D) Determination of norgestimate IC_{50} values on TRPC4 (B) and TRPC5 (D). Data is shown as means of 2 wells (B) and 4 wells (D) with 47,000 cells per well.

Inhibition of TRPC channels by progesterone

Norgestimate is a gestagen (a synthetic form of the naturally occurring female sex hormone progesterone). Therefore, it was tested whether progesterone itself inhibits TRPC channels. After PAR antagonism of progesterone was excluded (Fig. 14), experiments were performed similarly to the norgestimate measurements.

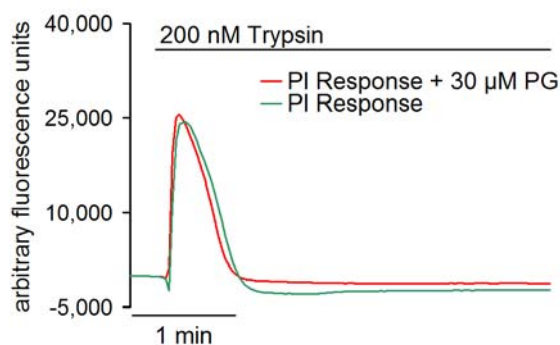


Figure 14: Progesterone is not a PAR-antagonist. Time-dependent changes in $[\text{Ca}^{2+}]_i$ of fluo-4-loaded TRPC5 HEK293 FITR cells. Rise in $[\text{Ca}^{2+}]_i$ following application of 200 nM trypsin (PI response) in non-induced TRPC5 HEK293 FITR cells was not suppressed in cells preincubated with 30 μM progesterone (PG). Representative traces are shown. Time scale bar 1 min.

Progesterone inhibited all three channels tested. While it was much more potent than norgestimate on TRPC4 (IC_{50} of $6.9 \pm 0.5 \mu\text{M}$, $n = 2$; Fig. 15 B) and TRPC5 (IC_{50} of $11.1 \pm 0.4 \mu\text{M}$, $n = 4$, Fig. 15 D), TRPC6 was less potently inhibited by progesterone (IC_{50} of $18 \pm 3 \mu\text{M}$, $n = 4$, Fig. 15 F) than by norgestimate.

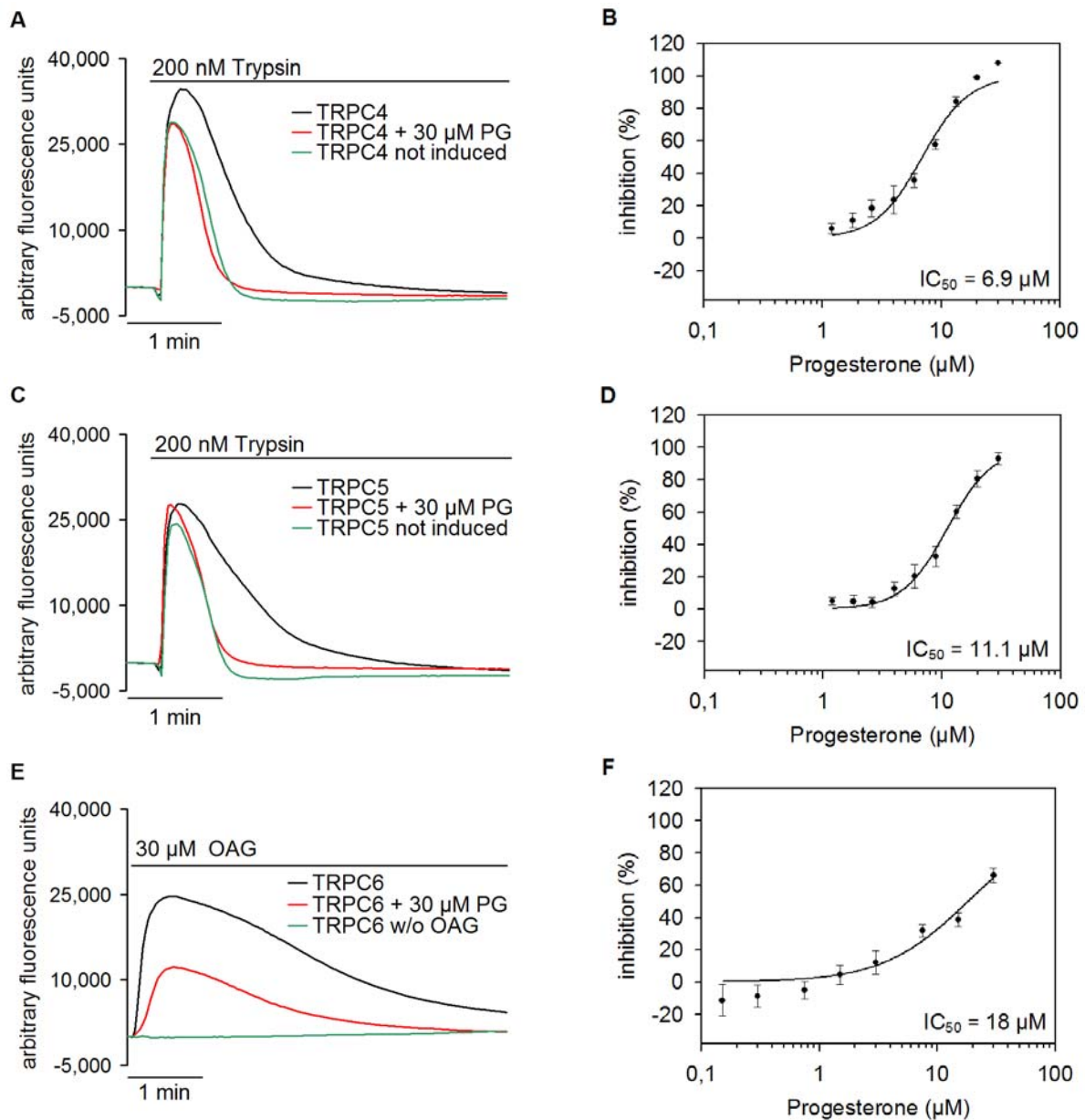


Figure 15: Progesterone inhibits TRPC-mediated Ca^{2+} influx. (A, C, E) Time-dependent changes in $[Ca^{2+}]_i$ of fluo-4-loaded induced TRPC4 (A) and TRPC5 (C) and TRPC6 (E) HEK293 FITR cells. TRPC-mediated Ca^{2+} influx following application of 200 nM trypsin or 30 μM OAG was reduced in cells preincubated with 30 μM progesterone (PG). Representative traces are shown. Time scale bar 1 min. (B, D, F) Determination of progesterone IC_{50} values on TRPC4 (B), TRPC5 (D) and TRPC6 (F). Data is shown as means of 2 wells (B) and 4 wells (D, F) with 45,000-47,000 cells per well.

Effect of progesterone, norgestimate and levonorgestrel on TRPC6

Whether or not norgestimate itself is active *in vivo* or merely serves as levonorgestrel prodrug is controversially discussed (Stanczyk, 1997). Therefore, the effect of levonorgestrel was also exemplarily tested on TRPC6-mediated Ca^{2+} -influx.

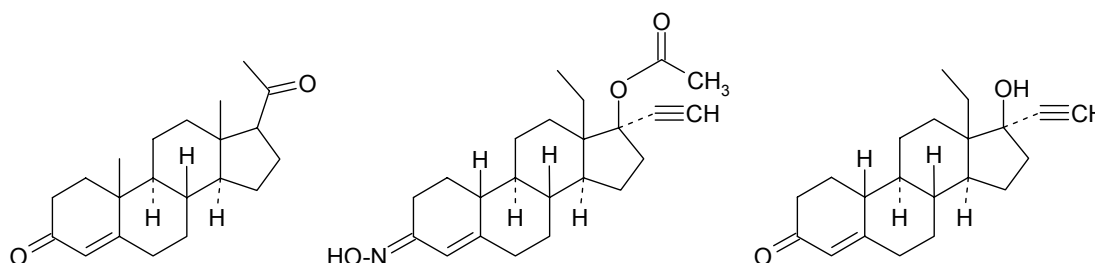


Figure 16: Chemical structures of progesterone (left), norgestimate (middle) and levonorgestrel (right).

In contrast to norgestimate (Fig. 13 B, D) and progesterone (Fig. 15 E, F) that both inhibited TRPC6, levonorgestrel was not active on the channel (Fig. 17 B). Even at 30 μM , the highest levonorgestrel concentration tested, TRPC6 channels were not inhibited (Fig. 17 A).

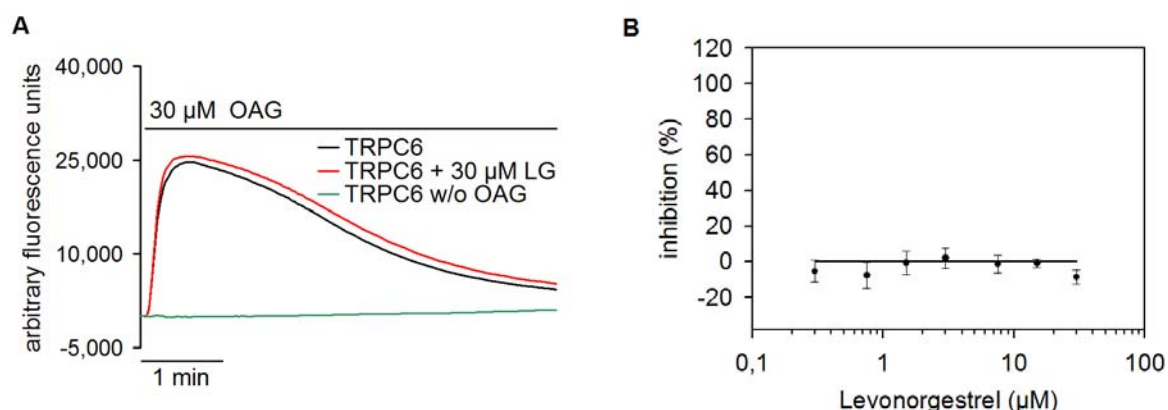


Figure 17: TRPC6 is not inhibited by levonorgestrel. (A) Time-dependent changes in $[\text{Ca}^{2+}]_i$ of fluo-4-loaded induced TRPC6 HEK293 FTR cells. TRPC-mediated Ca^{2+} influx following application of 30 μM OAG was not reduced in cells preincubated with 30 μM levonorgestrel (LG). Representative traces are shown. Time scale bar 1 min. **(B)** Determination of levonorgestrel's IC_{50} value on TRPC6. Data is means of 4 wells with 45,000 cells per well.

In summary, these FLIPR measurements showed that certain gestagens (norgestimate and progesterone) inhibit channels of the TRPC3/6/7 subfamily as well as of the TRPC4/5 subfamily when applied at micromolar concentrations. However, this is not a general effect of gestagens since the norgestimate metabolite levonorgestrel was completely inactive on TRPC6.

Norgestimate was more active on the TRPC3/6/7 than on the TRPC4/5 subfamily, whereas progesterone showed similar effects on the two subfamilies.

3.1.2 Patch clamp recordings

Differential effect of norgestimate on recombinant homomeric TRPC5 and TRPC6 channels

The inhibition of TRPC6- and TRPC5-mediated Ca^{2+} -influx by norgestimate, which has been monitored in cell populations with fluorometric experiments, was then validated by whole-cell patch clamp recordings of single cells. Channels were indirectly excited with aluminium tetrafluoride (AlF_4^-) that was applied intracellularly via the patch pipette. The same stimulus was used to activate both channels for better comparability of the norgestimate effect. AlF_4^- activates G proteins by mimicking guanosine triphosphate (GTP; Sternweis & Gilman, 1982; Bigay *et al.*, 1985). Activated $\text{G}_{q/11}$ proteins stimulate PLC activity and in turn opening of TRPC channels (Fig. 18 A, B). When 10 μM norgestimate were applied to activated TRPC6 channels, the current measured at resting membrane potential was reduced to $10.1 \pm 3.1\%$ ($n = 15$, Fig. 18 C). This inhibition was reversible as the current amplitude increased again after norgestimate wash out. The subsequent block by 10 μM lanthanum (La^{3+}) was complete and reversible (Fig. 18 A) and thus used for background (leak) calculation. By contrast, application of 10 μM norgestimate to stimulated TRPC5 channels only had a minor effect with a current reduction to $74.1 \pm 5.7\%$ ($n = 20$, Fig. 18 C). Since these channels are potentiated by micromolar La^{3+} concentrations (Jung *et al.*, 2003), 2-aminoethoxydiphenyl borate (2-APB), a known TRPC5 blocker (Xu *et al.*, 2005) that completely and reversibly blocked the channel at 10 μM , was used for leak correction (Fig. 18 B).

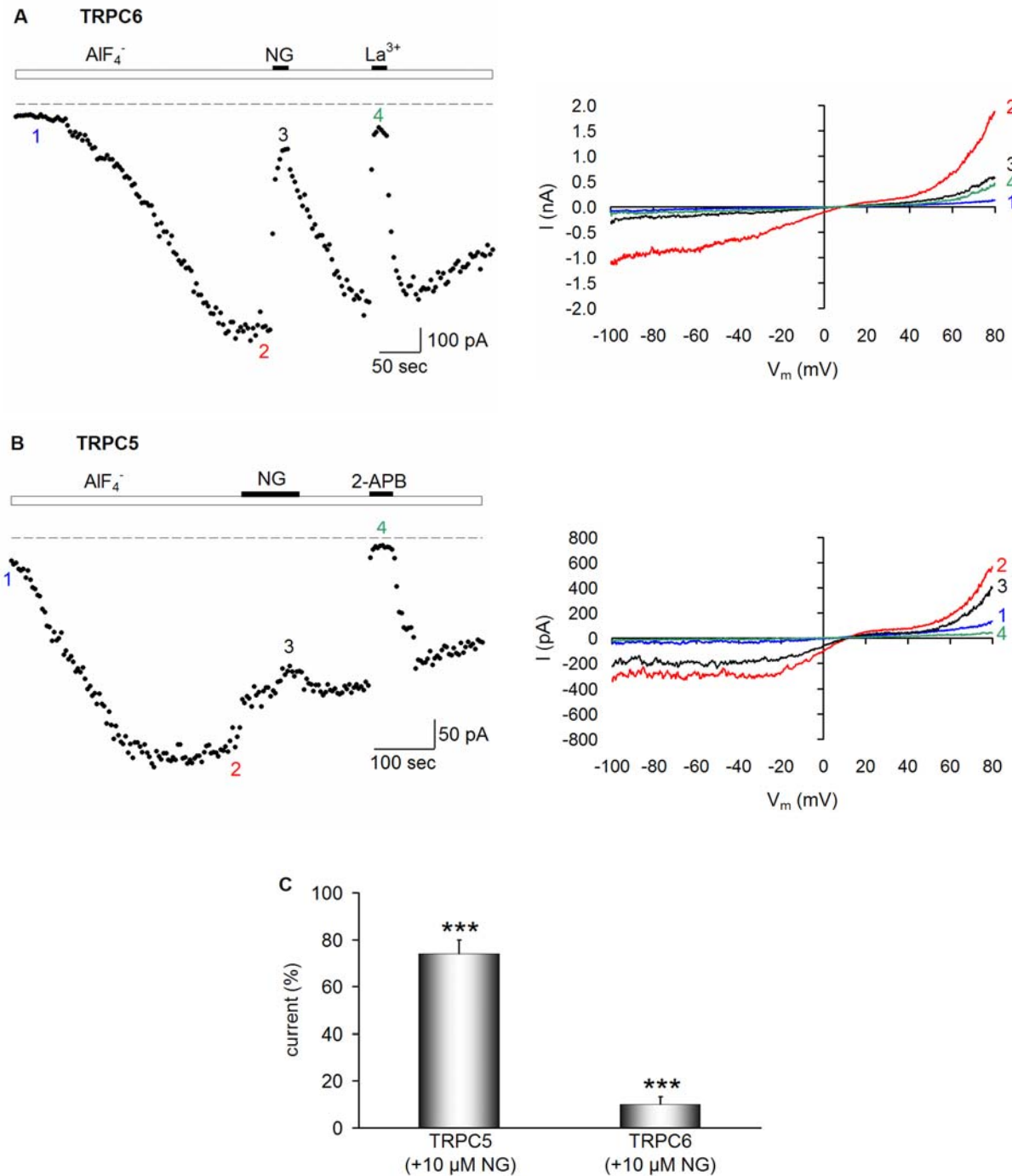


Figure 18: Norgestimate selectively blocks TRPC6 and TRPC5-mediated currents. Effect of 10 μM norgestimate (NG) on whole-cell currents evoked by AIF_4^- infusion into induced TRPC6 (**A**) and TRPC5 (**B**) HEK293 FITR cells. Whole cell currents recorded at -70 mV (left panels) and the corresponding current-voltage (*I-V*) relationships are shown (right panels). For background correction channels were completely blocked with 10 μM La^{3+} (A) or 10 μM 2-APB (B). The curves were obtained during voltage ramps from -100 to +80 mV. (**C**) Statistical analysis of the norgestimate effects. TRPC5-mediated currents were reduced to $74.1 \pm 5.7\%$ ($n = 20$) and TRPC6-mediated currents were reduced to $10.1 \pm 3.1\%$ ($n = 15$) by 10 μM norgestimate ($P < 0.001$, Wilcoxon test, two-sided).

Norgestimate blocks native heteromeric TRPC6/7 channels

So far norgestimate was tested on homomeric channels heterologously expressed in HEK293 cells. It is well known that TRPC channels can heteromultimerize *in vivo* (reviewed by Schaefer, 2005), whereas the exact composition of native channel complexes is still elusive. Therefore, it was interesting to see whether norgestimate also inhibits endogenous TRPC channels.

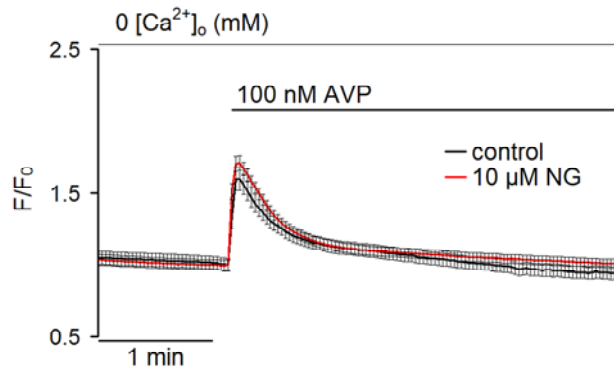


Figure 19: Norgestimate is not a V_1 receptor antagonist. Time-dependent changes in $[Ca^{2+}]_i$ of fura-2-loaded A7r5 cells. Cells were preincubated with or without (control) 10 μ M norgestimate (NG) in calcium-free standard extracellular solution (1 mM EGTA) for 5 min before stimulating the V_1 receptor by application of 100 nM $[Arg^8]$ -vasopressin (AVP). Data is shown as means of 33 cells (control) and 36 cells (10 μ M NG). Time scale bar 1 min.

The A7r5 cell line (derived from rat thoracic aorta SMCs) is a model system expressing native TRPC6-containing channel complexes (Jung *et al.*, 2002; Soboloff *et al.*, 2005). These channels were indirectly stimulated by $[Arg^8]$ -vasopressin (AVP), a vasoconstricting peptide that activates the endogenous vasopressin V_{1A} receptor in these cells (Thibonnier *et al.*, 1991). Before whole-cell patch clamp recordings were performed, it was shown first in calcium imaging experiments that norgestimate does not generally suppress V_{1A} receptors (Fig. 19). Subsequently, A7r5 cells were superfused with 100 nM AVP stimulating non-selective cationic currents that displayed the biophysical properties of TRPC6 channels (Fig. 20).

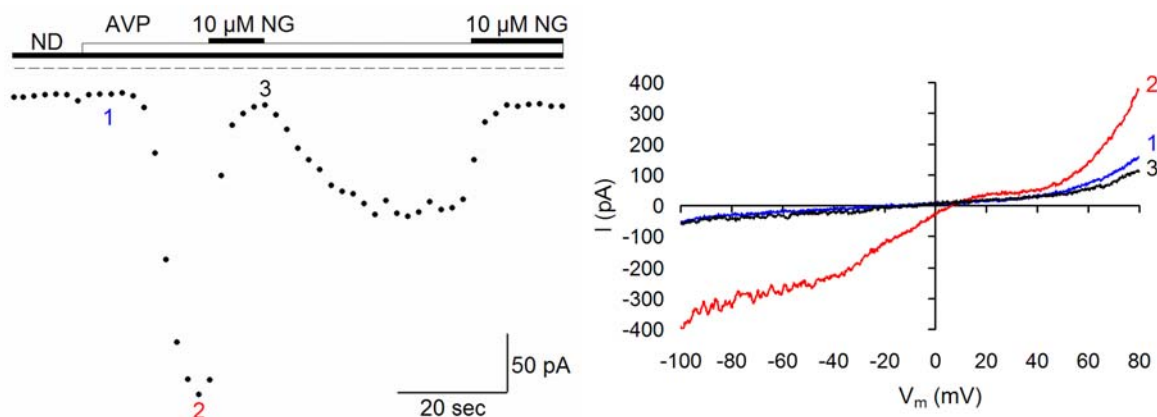


Figure 20: Norgestimate blocks AVP-activated non-selective cation currents in A7r5 cells. Effect of 10 μ M norgestimate (NG) on whole-cell currents evoked by 100 nM AVP in A7r5 cells. Currents were recorded at -60 mV (left panels) and the corresponding I - V relationships are shown (right panels). The curves were obtained during voltage ramps from -100 to +80 mV. L-type voltage-gated Ca^{2+} channels were blocked by 5 μ M nimodipine (ND) during the whole experiment.

The doubly rectifying *I-V* relationship was similar to that of heterologously expressed TRPC6 homomers (Fig. 18 A). When 10 μM norgestimate were applied to AVP-stimulated A7r5 cells, the native current measured at resting membrane potential was reversibly reduced to $13.5 \pm 6.0\%$ ($n = 8$, Fig. 20), which is in good agreement with its effect on recombinant TRPC6 channels (Fig. 18 A, C).

3.1.3 Isometric tension recording of aortic rings

It was postulated that TRPC6 activation leads to depolarization of smooth muscle cell membranes (Soboloff *et al.*, 2005). Consequently, L-type voltage-gated Ca^{2+} channels are activated and finally mediate muscle contraction. Hence, inhibition of TRPC6 by norgestimate in vessels should lead to relaxation. We tested the endothelium-independent effect of norgestimate on the vascular reactivity of male rat thoracic aorta by isometric tension recording in an organ bath. Endothelial nitric oxide synthases (eNOS, iNOS) were inhibited by application of 300 μM N-nitro-L-arginine methyl ester (L-NAME; Moncada *et al.*, 1991). Effective suppression of the endothelium was demonstrated by absent relaxation of vessel rings precontracted with 100 nM phenylephrine in response to 10 μM acetylcholine (Fig. 21). Application of increasing concentrations of norgestimate to precontracted aortic rings led to their relaxation. The half maximal effective dose (EC_{50}) value for norgestimate relaxation averaged 15.1 μM ($n = 6$). The solvent for norgestimate used in this study was DMSO which by itself had no significant effect on tension, the maximal DMSO concentration of 0.33% resulted in $3.7\% \pm 8.3\%$ ($n = 3$) relaxation of phenylephrine-induced contraction (data not shown).

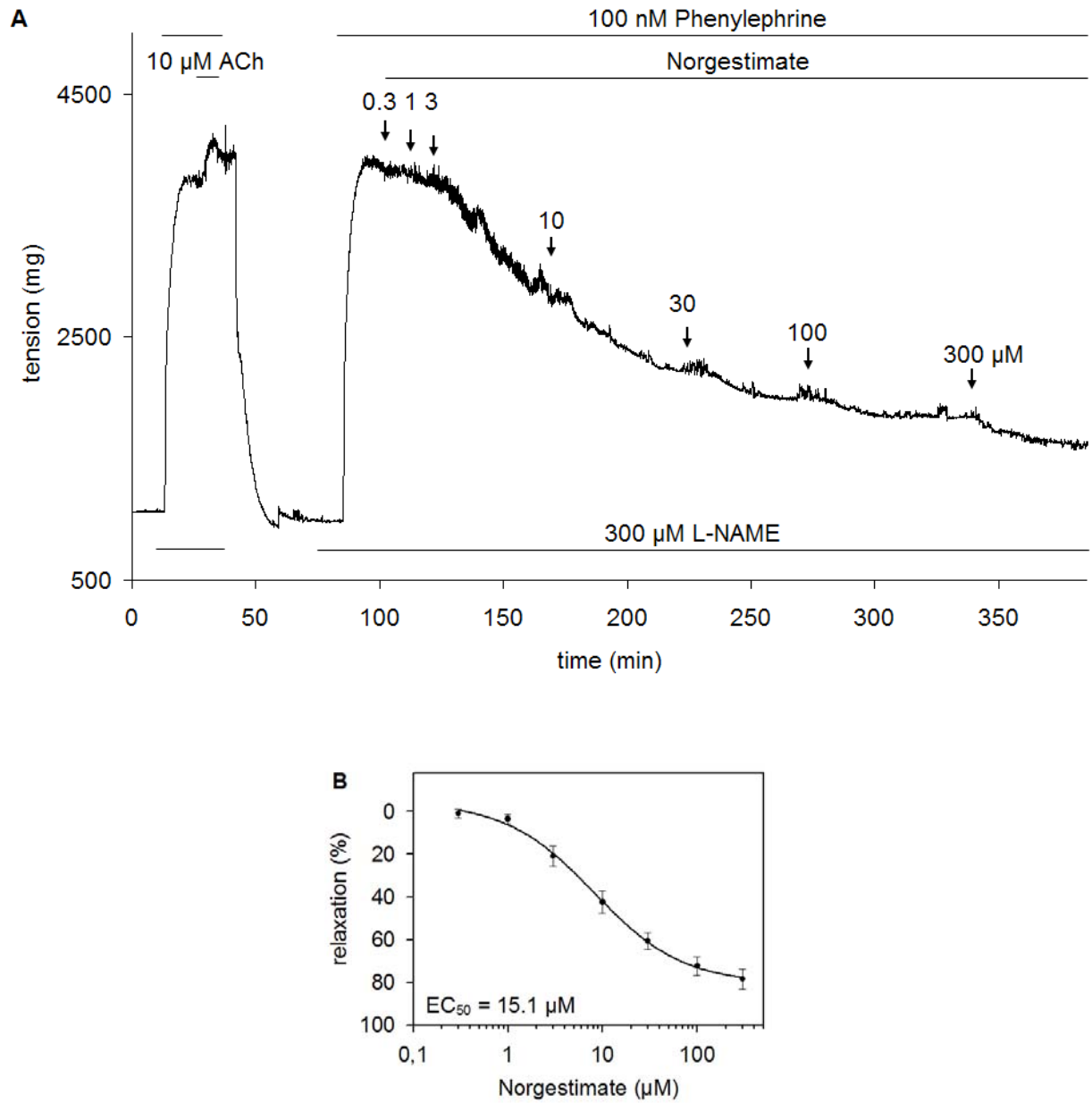


Figure 21: Endothelium-independent relaxation of precontracted rat aortic rings by norgestimate. (A) Application of norgestimate induced significant relaxation of L-NAME treated aortic rings precontracted with phenylephrine. **(B)** Concentration-relaxation curve of norgestimate ($n = 6$).

3.2 Physical interaction of SESTD1 and TRPC channels

3.2.1 Y2H results

The second part of the present work was designed to identify novel TRPC4-interacting proteins. Endothelial dysfunction is believed to be a major cause of various cardiovascular diseases (Kwan *et al.*, 2007) and evidence indicates that TRPC4 plays a critical role in endothelial function. It is associated with regulation of endothelium-dependent vascular relaxation (Freichel *et al.*, 2001), may contribute to oxidative-stress induced endothelial damage (Balzer *et al.*, 1999; Poteser *et al.*, 2006) and is necessary for endothelial barrier function (Tiruppathi *et al.*, 2002). TRPC4 expression in aortic endothelial cells has been reported by several groups (Chang *et al.*, 1997; Garcia & Schilling, 1997; Poteser *et al.*, 2006; Antoniotti *et al.*, 2006). In search of novel proteins that interact with the cytosolic C-terminus of mTRPC4 α (aa 615-974), a human aorta cDNA library was screened with a modified yeast two-hybrid system (Fields & Song, 1989). So far, no X-ray structures of TRPC channels exist but due to similarity with voltage-gated K⁺ channels (Clapham *et al.*, 2001), they are expected also to form tetramers. Although our TRPC4 bait contained a putative TRPC tetramerization domain (Lepage *et al.*, 2006), we wanted to assure the protein assembly in the physiological multimeric state. Therefore, the C-terminus of TRPC4 was fused to a leucine zipper domain that has been shown previously to direct protein tetramerization. Eleven proteins (listed in Table 3) were found to physically interact with the mTRPC4 α -C-terminus in this transcriptional assay.

Table 3: Y2H preys.

Definition	Gene name	Gene Bank accession no.
Ankyrin repeat domain 35	ANKRD35	NM_144698
Apolipoprotein A-I binding protein	APOA1BP	NM_144772
Bromodomain adjacent to zinc finger domain	BAZ1B	AB032253
High-mobility group protein 2-like1 isoform b	HMG2L1	CR456504
Makorin RING finger protein 1	MKRN1	NM_013446
Pre-B-cell leukemia homeobox interacting protein 1	PBXIP1	NM_020524
Sarcoma antigen NY-SAR-48		NM_033417
SEC14 and spectrin domains 1	SESTD1	NM_178123
Spectrin, alpha, non-erythrocytic 1	SPTAN1	U83867
Structural maintenance of chromosomes 3	SMC3	AF067163
Talin 2	TLN2	NM_015059

None of these proteins has been described before to interact with the TRPC4 channel. SESTD1 seemed to be the most interesting potential interaction partner because a domain search (Marchler-Bauer & Bryant, 2004) revealed the presence of an N-terminal Sec14p-like lipid-binding domain (Fig. 22) in SESTD1. The conserved Sec14-motif is known to bind and transport cellular phospholipids (Saito *et al.*, 2007). Several reports have shown regulation of

TRP channels by phospholipids, in particular PIP₂ (Rohacs, 2007). Thus, it was tempting to speculate that SESTD1 is involved in the regulation of TRPC4. In addition to the Sec14p-like lipid-binding domain, two helical structures called spectrin repeats were found in SESTD1. These domains are known to mediate protein-protein interactions (Djinovic-Carugo *et al.*, 2002) and are found in several cytoskeletal proteins. The full length SESTD1 clone was isolated from the human aorta cDNA library and its deduced amino acid sequence is identical to GenBank accession no. NP_835224 except for one exchange (H508Q). It is based on a single point mutation at nucleotide 1571 (NM_178123) that can also be found in the genomic sequence. Another point mutation found at nucleotide 1748 is silent.



Figure 22: Topology of SESTD1. The full length protein consists of 696 amino acids (expected molecular weight 79 kDa) and is composed of three structural domains. *Sec 14* (aa 8-147): *Sec14p-like lipid-binding domain*; *Spec 1* (aa 233-381), *Spec 2* (aa 430-605): *spectrin repeats*

3.2.2 Mapping of the TRPC4-SESTD1 interaction site

In order to verify the results of our initial screen and to define the interaction site of TRPC4 with SESTD1 in more detail a directed yeast two-hybrid analyses was performed. Yeast was cotransformed with SESTD1 as prey and various C-terminal mTRPC4 α protein fragments as baits and plated on selective media. By iterative shortening of the TRPC4-C-terminus we identified that a small stretch of 29 amino acids (aa 700-728) was sufficient to mediate the interaction with full length SESTD1 (Fig. 23). Interestingly, the identified SESTD1 binding site in TRPC4 is highly conserved in TRPC5 and overlaps with the previously described CaM/IP₃R binding (CIRB) site (Tang *et al.*, 2001), indicating that SESTD1 might also interact with TRPC5. Analogous to our above approach we next tried to define the TRPC4 binding site on SESTD1. Three SESTD1 constructs, SESTD1-Sec 14 (aa 1-192), SESTD1-Spec 1 (aa 193-406) and SESTD1-Spec 2 (aa 407-696) as depicted in Figure 24 were constructed by inserting the respective SESTD1 gene fragments into the yeast expression vector pACT2 leading to their expression as a fusion to the GAL4 activation domain (GAL4-AD). These constructs were co-transformed in yeast with the C-terminus of mTRPC4 α as bait and survival of yeast colonies was assayed. To test the hypothesis that TRPC5 might also interact with SESTD1 the same experiments were performed with the C-terminus of mTRPC5 (aa 619-975).

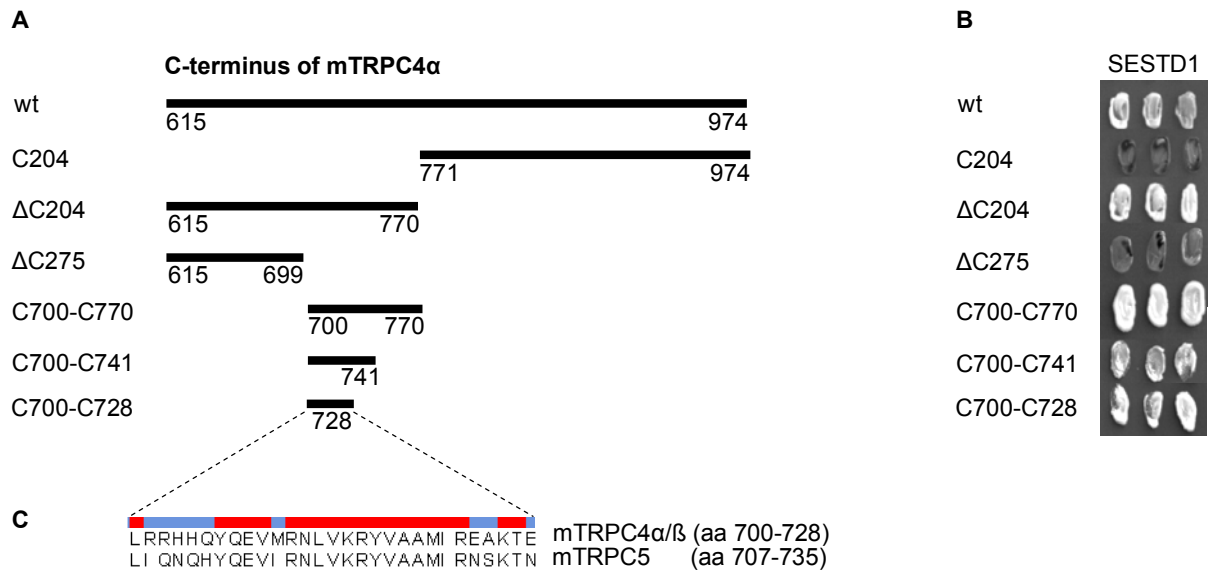


Figure 23: Mapping of the SESTD1-binding site on the mTRPC4 α -C-terminus. (A) Truncation of mTRPC4 α -C-terminus. (B) Yeast colonies cotransformed with truncation mutants of mTRPC4 α -C-terminus (bait) and full length hSESTD1 (prey) were plated on selective -Trp/-Leu/-Ade/-His agar plates. Growth indicates protein-protein interaction. (C) The identified SESTD1 binding site is identical in both mTRPC4 α and mTRPC4 β and highly conserved in TRPC5.

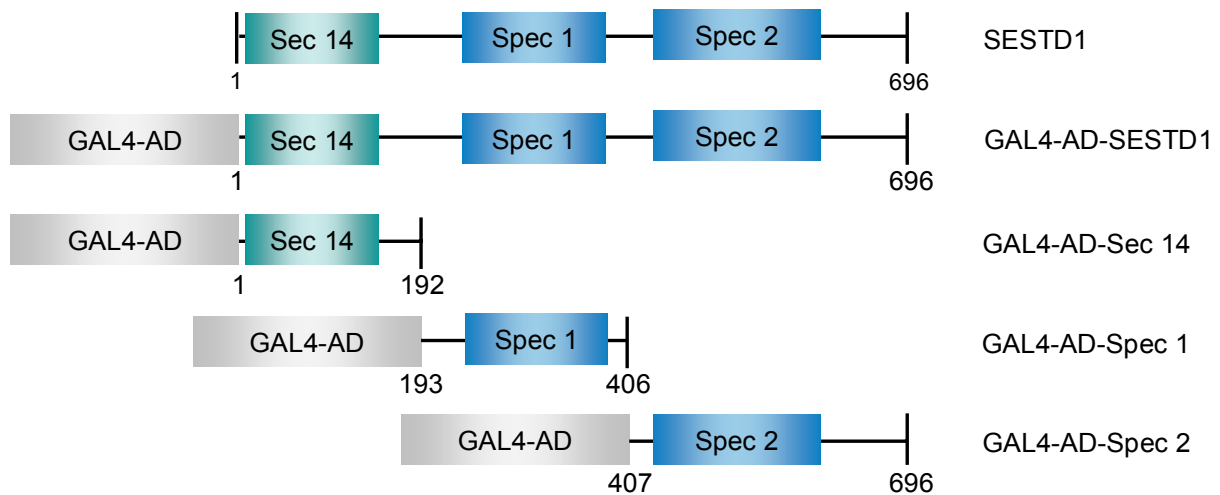


Figure 24: GAL4-AD-SESTD1 constructs. Schematic description of GAL4-AD fusion constructs containing different portions of SESTD1 that were used in directed Y2H assays to detect interaction with TRPC4 and TRPC5 in yeast.

The experimental results depicted in Figure 25 confirmed that TRPC5 also interacts with SESTD1. Both TRPC4 and TRPC5 bind to the first spectrin domain of SESTD1 but not to the Sec14p-like lipid-binding domain. Moreover, the mTRPC5-C-terminus independently interacts with the Spec 2 domain in this directed Y2H assay.

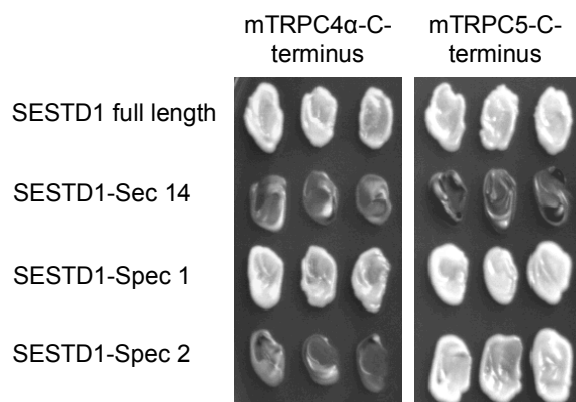


Figure 25: Identification of Spec 1 as interaction site in SESTD1. Yeast colonies cotransformed with the mTRPC4 α -C-terminus (positive control) or mTRPC5-C-terminus and full length SESTD1 or the SESTD1-Sec 14, -Spec 1, or -Spec 2 domains plated on -Trp/-Leu/-His/-Ade agar plates. Growth indicates protein-protein interaction.

3.2.3 Biochemical verification of SESTD1-TRPC4/5 binding by GST pulldown

GST pulldown assays were performed to confirm the physical interaction between SESTD1 and mTRPC4 by a more direct method. In *E. coli* expressed and purified recombinant GST-SESTD1 was used to pull down the overexpressed mTRPC4 α -C-terminus (aa 615-974). In accordance with the yeast two-hybrid data, Figure 26 demonstrates that SESTD1 and the mTRPC4 α -C-terminus can physically interact.

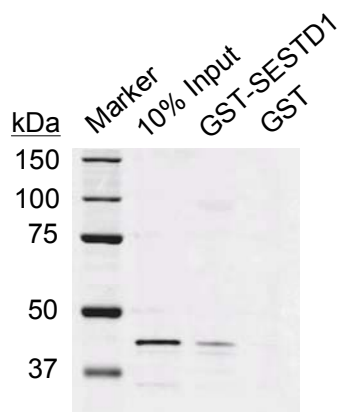


Figure 26: GST-SESTD1 pulldown of mTRPC4 α -C-terminus (aa 615-974). Lysates from HEK293 cells overexpressing mTRPC4 α -C-terminus (aa 615-974) were either incubated with GST-SESTD1 (lane 3) or GST (negative control, lane 4). Lane 2 shows 10% of the lysate input. Samples were separated by SDS-PAGE and blotted onto nitrocellulose. The blot was developed with anti-TRPC4 (1:200) and secondary Alexa Fluor (AF) 680 goat anti-rabbit (1:2,500) antibody.

We also tried to pull-down full length mTRPC4 α protein with GST-SESTD1 fusion protein. However, as both proteins have a similar size, unspecific binding to SESTD1 interfered with the signal detected by anti-TRPC4 antibody. To study the interaction of the full length proteins we, therefore, carried out co-immunoprecipitation experiments (see Chapter 3.2.4).

Having shown that TRPC4 and SESTD1 physically interact in the pulldown assay, this approach was further adapted to investigate the interaction sites between mTRPC4 α , mTRPC5 and SESTD1. We also included the shorter mTRPC4 β splice variant into these experiments. Compared to mTRPC4 α , it is lacking 84 C-terminal amino acids outside the CIRB site (Schaefer *et al.*, 2002). The same three SESTD1 domain constructs as depicted in Figure 24 were used in these studies but they were cloned into pGEX-5X-3 instead of pACT2 and thus expressed as GST fusion proteins in the protease-deficient *E. coli* strain BL21 de3. Under the chosen conditions, it was not possible to purify enough amounts of GST-Sec 14 (aa 1-192) with the Sec14p-like lipid-binding domain from bacteria. Induction of its expression seemed to be toxic as these transformants grew much slower than bacteria transformed with GST-Spec 1 (aa 193-406), GST-Spec 2 (aa 407-696) or full length GST-SESTD1.

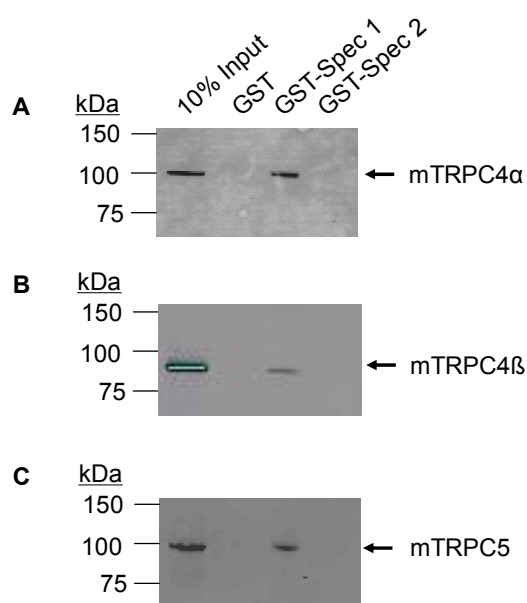


Figure 27: Confirmation of Spec 1 as interaction site in SESTD1. (A, B) Anti-TRPC4 (1:200) immunoblot of samples precipitated with the indicated GST fusion proteins or GST from HEK293 cells overexpressing mTRPC4 α (A) or mTRPC4 β (B). Lane 1 showing 10% of the lysate input (A, B, C) is stained turquoise (B) due to an artefact resulting from camera oversaturation. (C) Anti-TRPC5 (1:200) immunoblot of a similar experiment with HEK 293 cells overexpressing mTRPC5. Blots were developed with secondary AF 680 goat anti-rabbit (1:2,500) antibody.

All three channel proteins strongly interacted with the first spectrin domain (Fig. 27). In some blots, a weak binding to the second domain could also be observed. Thus, the combined results from the directed Y2H analyses (Chapter 3.2.2) and the GST pulldown studies confirmed that the first spectrin domain of SESTD1 is the main site of interaction with TRPC4 α , TRPC4 β , and TRPC5.

3.2.4 Co-immunoprecipitation

Characterization of two polyclonal anti-SESTD1 antibodies

Co-immunoprecipitations allow to investigate protein-protein interactions of native or recombinant proteins *in vivo*. As there were no commercial antibodies available against SESTD1, two polyclonal peptide antibodies were custom-made by Eurogentec. Anti-SESTD1

#147 antibody was directed against a sequence within the first spectrin domain (aa 265-280, CRQRSKRTQLEEIQK) and anti-SESTD1 #148 was directed against the SESTD1-C-terminus (aa 682-696, KRQQLRHPEMVTES). Antibodies were affinity-purified on the respective peptides.

When tested on Western blot, both antibodies detected overexpressed HA-tagged SESTD1 in HM1 cell lysates (expected size 79 kDa). In addition, in non-transfected cells an endogenous protein co-migrating with HA-SESTD1 was recognized by both antibodies. Transfecting HM1 cells with siRNA duplexes directed against SESTD1 (see Chapter 3.3.3) specifically suppressed the band at 79 kDa, strongly supporting the notion that this protein is endogenous SESTD1.

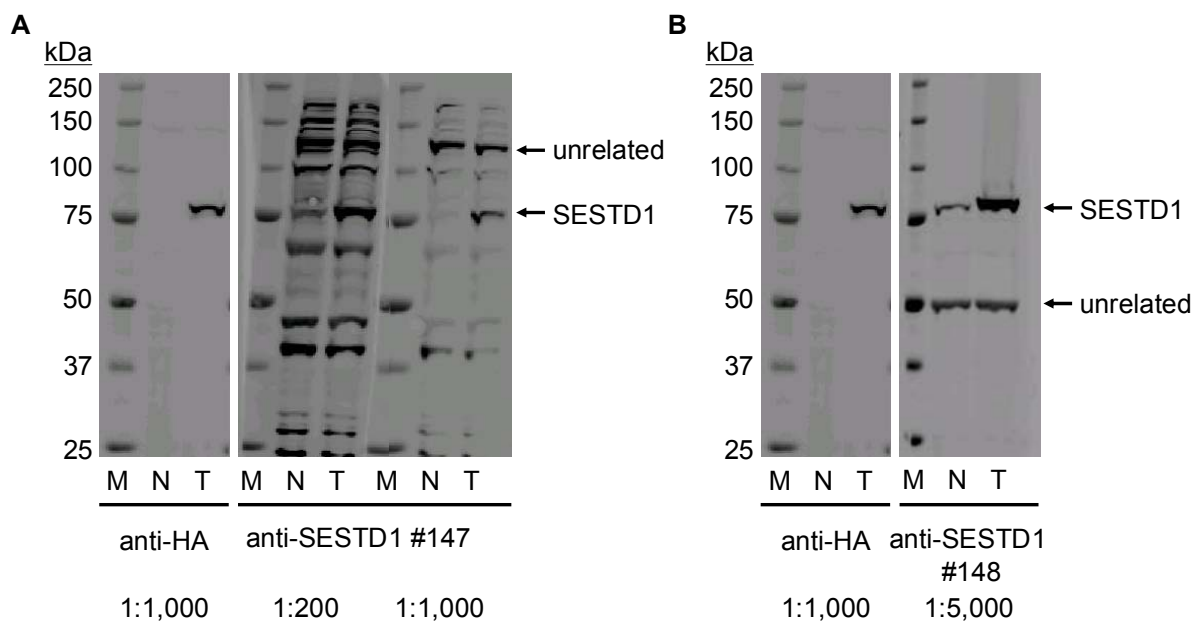


Figure 28: Polyclonal SESTD1 antibodies detect endogenous and overexpressed SESTD1. (A) A Protein marker (M) and lysates from HM1 cells either not transfected (N) or transfected with HA-tagged SESTD1 (T) were probed on Western blots with anti-HA and secondary Alexa Fluor 680 goat anti-rat (1:2,500) or anti-SESTD1 #147 and secondary AF 680 goat anti-rabbit (1:2,500). Anti-SESTD1 #147 detected HA-SESTD1 as well as endogenous SESTD1 (in non-transfected cells) as proteins with an apparent mass around 80 kDa but additionally bound to several unrelated proteins with highest affinity to a protein of ~130 kDa. **(B)** Similar samples as in (A) were probed on Western blots with anti-HA and secondary AF 680 goat anti-rat (1:2,500) or anti-SESTD1 #148 and secondary AF 680 goat anti-rabbit (1:2,500) antibodies. Anti-SESTD1 #148 detected HA-SESTD1 as well as endogenous SESTD1 (in non-transfected cells) but also unspecifically cross-reacted to an unrelated protein of ~50 kDa.

As depicted in Figure 28, anti-SESTD1 #147 recognized several proteins on Western blot independent of the dilution used. In addition to SESTD1, anti-SESTD1 #148 detected another protein with an apparent mass of 50 kDa. This protein was neither suppressed with anti-SESTD1 siRNA (see Chapter 3.3.3) nor detected with anti-SESTD1 #147 (Fig. 28 A), thus the antibody is cross-reacting with an unrelated protein.

Unless stated otherwise the anti-SESTD1 antibody used in the following experiments was anti-SESTD1 #148.

Co-immunoprecipitation of heterologously expressed SESTD1 and mTRPC4 β or mTRPC5

Our GST pulldown experiments (see Chapter 3.2.3) had shown that SESTD1 interacts with mTRPC4 β and mTRPC5. Functional epitope-tagged constructs of these two channels were available and thus used for co-immunoprecipitation experiments. HM1 cells were cotransfected with HA-tagged SESTD1 and FLAG-tagged mTRPC4 β or GFP-tagged mTRPC5, respectively. Cotransfection of the empty vector pcDNA3.1 served as negative control. The ion channels were precipitated from the cells lysates with anti-TRPC4 or anti-GFP antibody (mTRPC5) and precipitates were separated by SDS-PAGE, blotted onto nitrocellulose membranes and then probed with anti-SESTD1 antibody. When mTRPC4 β and mTRPC5 were precipitated from HM1 cell lysates, SESTD1 was found in the precipitated samples (Fig. 29).

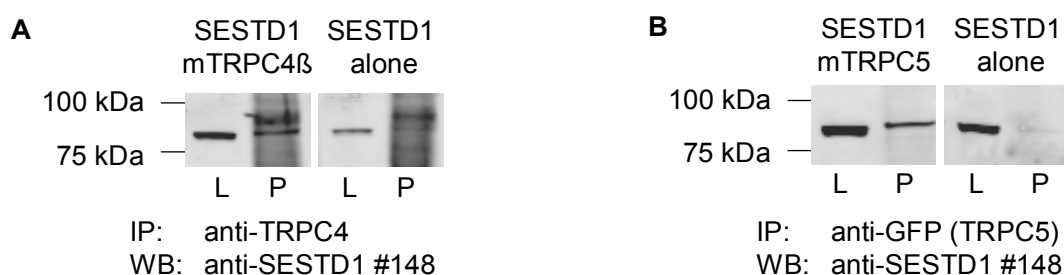


Figure 29: SESTD1 co-immunoprecipitates with mTRPC4 β and mTRPC5. (A) Western blot of anti-TRPC4 immunoprecipitates (P) and the corresponding lysates (L) from membranes of HM1 cells cotransfected with HA-tagged SESTD1 and FLAG-tagged mTRPC4 β or pcDNA3.1. (B) Western blot of anti-GFP immunoprecipitates (P) and the corresponding lysates (L) from HM1 cells cotransfected with HA-tagged SESTD1 and GFP-tagged mTRPC5 or pcDNA3.1. Both blots (A, B) were probed with anti-SESTD1 #148 (1:5,000) and secondary AF 680 goat anti-rabbit (1:2,500) antibodies.

A very small amount of SESTD1 was also precipitated by anti-TRPC4 and anti-GFP antibodies from control HM1 cell lysates that only expressed HA-SESTD1. This unspecific binding was seen under different precipitating conditions. However, it was always much lower than the co-immunoprecipitation with the ion channel proteins.

We also tried to identify naturally occurring channel-SESTD1 complexes. TRPC4 and -5 have been reported to be expressed in rat brain (Strubing *et al.*, 2001) where we also found SESTD1 (see Chapter 3.4.1 below). Unfortunately, using this tissue and commercially available antibodies, we were not able to precipitate these TRPC channels efficiently (data not shown). Therefore, we could not prove yet that TRPC and SESTD1 interact in native cells and tissues.

3.2.5 Interaction of SESTD1 and TRPC subfamilies

The putative SESTD1 binding sequence of mTRPC4 α is conserved in the shorter TRPC4 β isoform as well as TRPC5 but not in other TRPC channels. To verify the specificity of the interaction between SESTD1 and TRPC4/5, yeast was cotransformed with SESTD1 and the individual C-termini of hTRPC1, mTRPC4 β , mTRPC5 or hTRPC6 and plated on selective media.

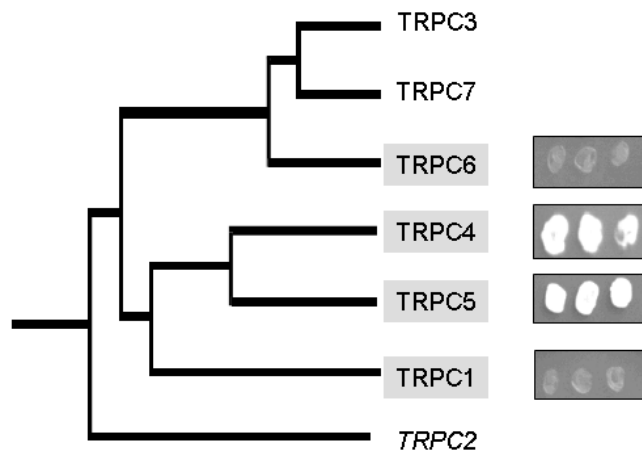


Figure 30: Yeast two-hybrid assay of the interaction between the C-terminus of different TRPCs and SESTD1. Yeast colonies cotransformed with C-termini of the indicated TRPC channels (bait) and full length hSESTD1 (prey) were plated on selective -Trp/-Leu/-Ade/-His agar plates.

Indeed, the results shown in Figure 30 confirm a specific interaction of SESTD1 with TRPC4 and TRPC5.

Whereas Y2H experiments with SESTD1 and the channel C-termini point to a specific interaction of SESTD1 with the TRPC4/5 subfamily, subsequent co-immunoprecipitation studies led to a different result.

HM1 cells were cotransfected with HA-tagged SESTD1 and YFP-tagged versions of hTRPC6, the distantly related TRP channel TRPM8, the unrelated K⁺ channel Kir2.1, or pcDNA3.1 vector as a negative control. The ion channels were first precipitated from cell lysates with anti-GFP antibody and immunoprecipitates were then separated by SDS-PAGE, blotted onto nitrocellulose membranes and probed with anti-SESTD1 antibody for co-precipitation of SESTD1. When hTRPC6 and TRPM8 were precipitated from HM1 cell lysates, SESTD1 was found in the precipitated samples. A very small amount of SESTD1 was also precipitated by the anti-GFP antibody from control HM1 cell lysates that only expressed HA-SESTD1. This unspecific binding was lower than co-immunoprecipitation with hTRPC6 and TRPM8 and also seen in Kir2.1 precipitates (Fig. 31).

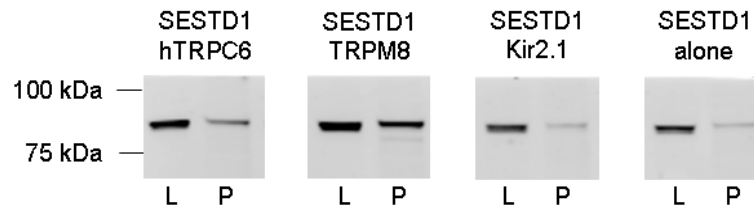


Figure 31: SESTD1 co-immunoprecipitates with hTRPC6 and TRPM8. Western blot of anti-GFP immunoprecipitates (P) and the corresponding lysates (L) of HM1 cells cotransfected with HA-tagged SESTD1 and YFP-tagged hTRPC6, TRPM8 or Kir 2.1. Blot was probed with anti-SESTD1 # 148 (1:5,000) and AF 680 goat anti-rabbit (1:2,500) antibodies.

3.3 Functional interaction of SESTD1 and TRPC5

3.3.1 Characterization of a HM1 clone stably expressing mTRPC5-YFP

Having shown that SESTD1 biochemically binds to TRPC4 and TRPC5, we set out to investigate the functional consequences of this interaction. As there are no established cellular models that allow an easy functional assessment of TRPC4 or TRPC5 channels, we decided to generate a HM1 cell line stably expressing mTRPC5-YFP (HM1-C5Y cells). HM1 cells were chosen because activation of recombinant TRPC channels had previously been described in these cells (Strubing *et al.*, 2003). TRPC5 was used as its overexpression generated much more robust receptor-activated cation currents than TRPC4.

The stable functional expression of TRPC5-YFP in HM1-C5Y cells was verified by fluorometric $[Ca^{2+}]_i$ and electrophysiological measurements. First it was tested, if the parental HM1 cell line showed trypsin- and carbachol-induced Ca^{2+} entry. Cells were either challenged with carbachol, which stimulates muscarinic type 1 receptors (M_1R) present in HM1 cells, or trypsin, that stimulates endogenous protease-activated receptors (PAR). Stimulation of both receptor types in the absence of extracellular Ca^{2+} led to the PI response (see Chapter 1.1.1), a transient rise in intracellular Ca^{2+} due to its release from internal stores (Fig. 32 A, B). In the presence of extracellular Ca^{2+} , both agonists activated a small Ca^{2+} influx that was most likely mediated by endogenous ROCs and/or SOCs. Nevertheless, the Ca^{2+} influx into HM1-C5Y cells evoked by either carbachol or trypsin was significantly larger than in parental HM1 cells demonstrating functionality of the channel (Fig. 32 C, D). To substantiate the results of the fluorometric assays, whole-cell patch clamp recordings of single HM1-C5Y cells were performed. Upon application of carbachol or trypsin both agonists induced currents with double-rectifying $I-V$ relationships characteristic for recombinant TRPC5 channels (Fig. 32 E, F) that could be inhibited by 10 μM 2-APB and stimulated by 100 μM lanthanum in accordance with reported TRPC5 pharmacology (data not shown). The current densities at -70 mV amounted to 15.9 ± 5.5 pA/pF ($n = 10$, carbachol) and 127.8 ± 57.6 pA/pF ($n = 6$, trypsin), whereas no obvious currents were induced by carbachol or trypsin in parental HM1 cells (data not shown).

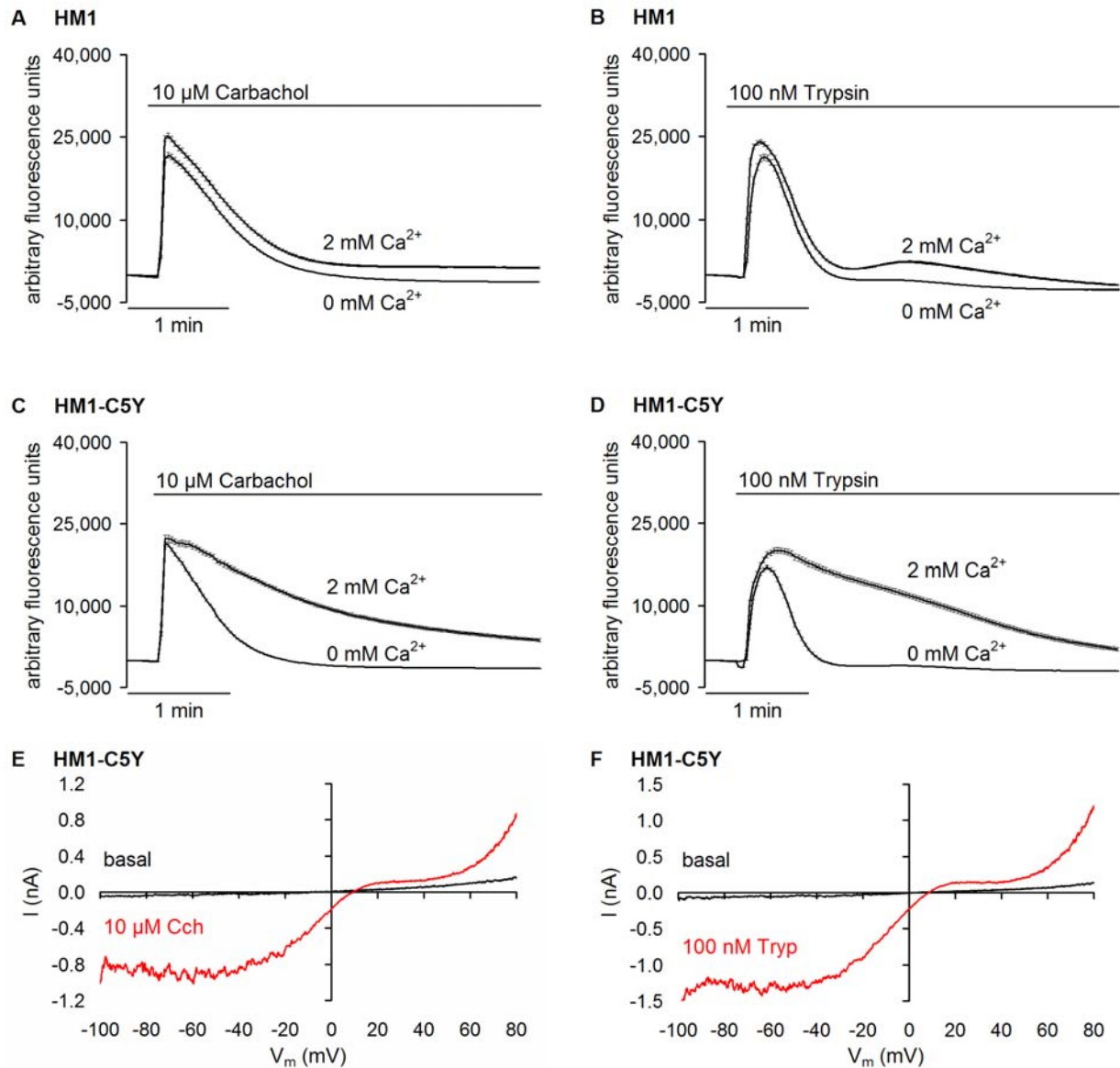


Figure 32: Functional characterization of a mTRPC5-YFP-HM1 cell line. (A, B) Time-dependent changes in $[\text{Ca}^{2+}]_i$ of fluo-4-loaded HM1 cells. Ca^{2+} influx (2 mM extracellular Ca^{2+}) or release from internal stores (0 mM extracellular Ca^{2+}) was evoked by application of 10 μM carbachol (A) or 100 nM trypsin (B). Data is means of 40-48 wells (20,000-25,000 cells per well). Time scale bar 1 min. (C, D) Time-dependent changes in $[\text{Ca}^{2+}]_i$ of fluo-4-loaded HM1 cells stably-transfected with mTRPC5-YFP (HM1-C5Y cells). Ca^{2+} influx (2 mM extracellular Ca^{2+}) or release from internal stores (0 mM extracellular Ca^{2+}) was evoked by application of 10 μM carbachol (A) or 100 nM trypsin (C). Data is means of 8 wells (20,000 cells per well). Time scale bar 1 min. (E, F) Whole-cell patch clamp recordings of HM1-C5Y cells. The agonists carbachol (10 μM , E) and trypsin (100 nM, F) induce currents with characteristic doubly rectifying I - V relationships.

3.3.2 Overexpression of SESTD1 in HM1-C5Y cells

In a first attempt to modulate the interaction between TRPC5 and SESTD1, we transiently overexpressed HA-tagged SESTD1 in HM1-C5Y cells. Since no information was available about the cellular function of SESTD1, experimental readouts were restricted to measuring TRPC5 function at elevated (or decreased, see Chapter 3.3.3) levels of SESTD1. TRPC5-mediated Ca^{2+} influx following application of carbachol or trypsin (Fig. 33 A, C) in HM1-C5Y cells coexpressing HA-SESTD1 did not differ significantly from control cells cotransfected with an unrelated protein (β -galactosidase, bGAL). Ca^{2+} releases from internal stores were also not significantly changed in the presence or absence of HA-tagged SESTD1 (Fig. 33 B, D).

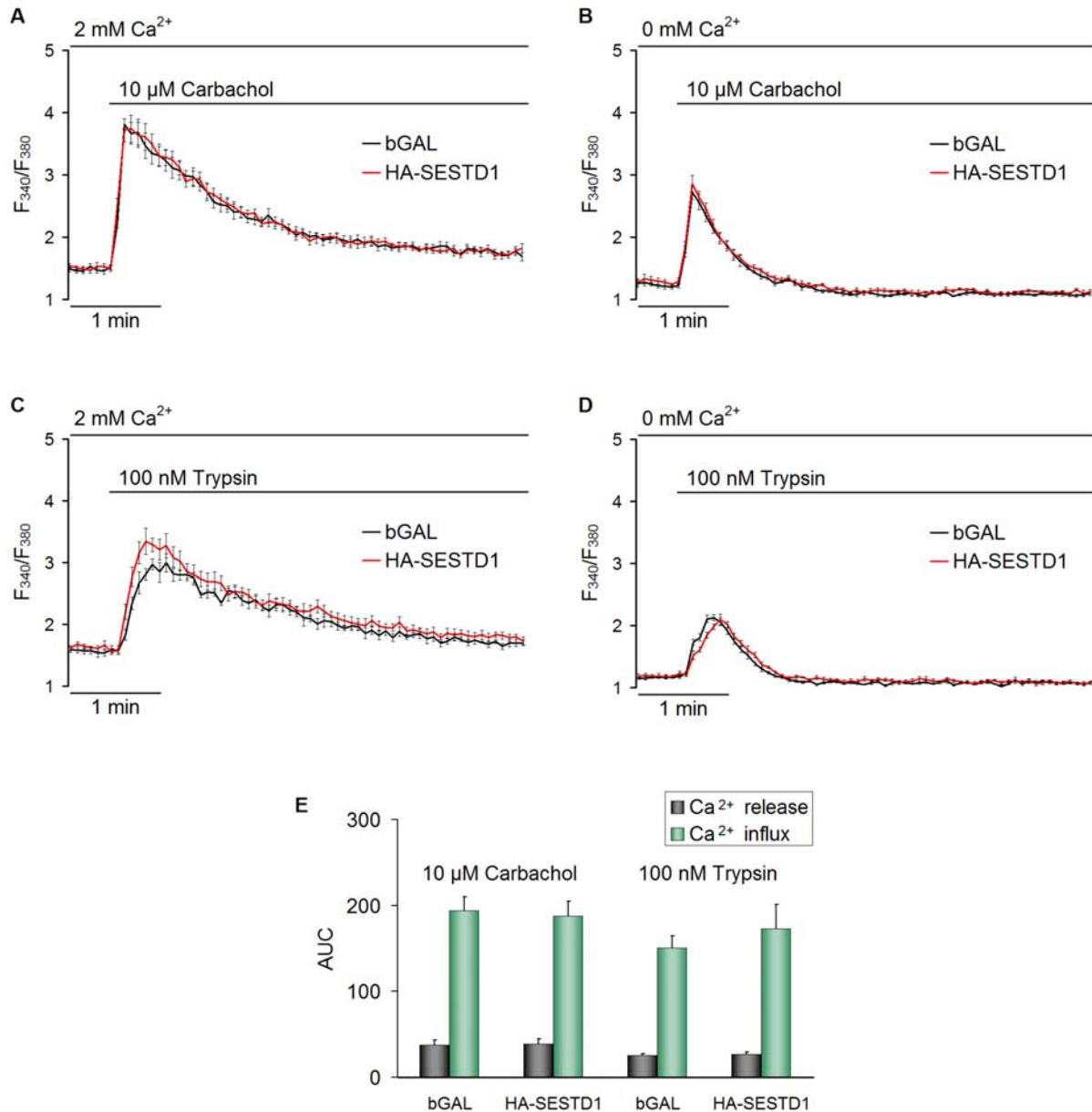


Figure 33: TRPC5-mediated Ca^{2+} -entry is unaltered in HM1-C5Y cells overexpressing heterologous HA-SESTD1. (A-D) Time-dependent changes in $[\text{Ca}^{2+}]_i$ of fura-2-loaded HM1-C5Y cells transiently transfected with HA-tagged SESTD1 or an unrelated protein (β -galactosidase, bGAL). TRPC5-mediated Ca^{2+} influx following application of 10 μM carbachol (A) or 100 nM trypsin (C) was the same in presence and absence of HA-tagged SESTD1. Also Ca^{2+} release from internal stores was not significantly changed in the presence or absence of HA-tagged SESTD1 after application of 10 μM carbachol (B) and 100 nM trypsin (D). Data is shown as means of 5-6 wells (40,000 cells per well). Time scale bar 1 min. (E) Statistical analysis of data presented in A-D ($n = 5-6$ wells per data point). Ca^{2+} release was calculated as area under the curve (AUC; B, D) and Ca^{2+} influx was calculated by their subtraction from the AUCs of (A) and (C), respectively.

3.3.3 siRNA knock-down of SESTD1

As shown above, overexpression of exogenous HA-SESTD1 had no effect on TRPC5-mediated Ca^{2+} influx in our cell model. However, since HM1 cells express SESTD1 endogenously (see Fig. 28), it may not be possible to further enhance SESTD1 function in these cells. Therefore, it was tested whether knock-down of SESTD1 protein expression in HM1 cells had an influence on TRPC5 activity.

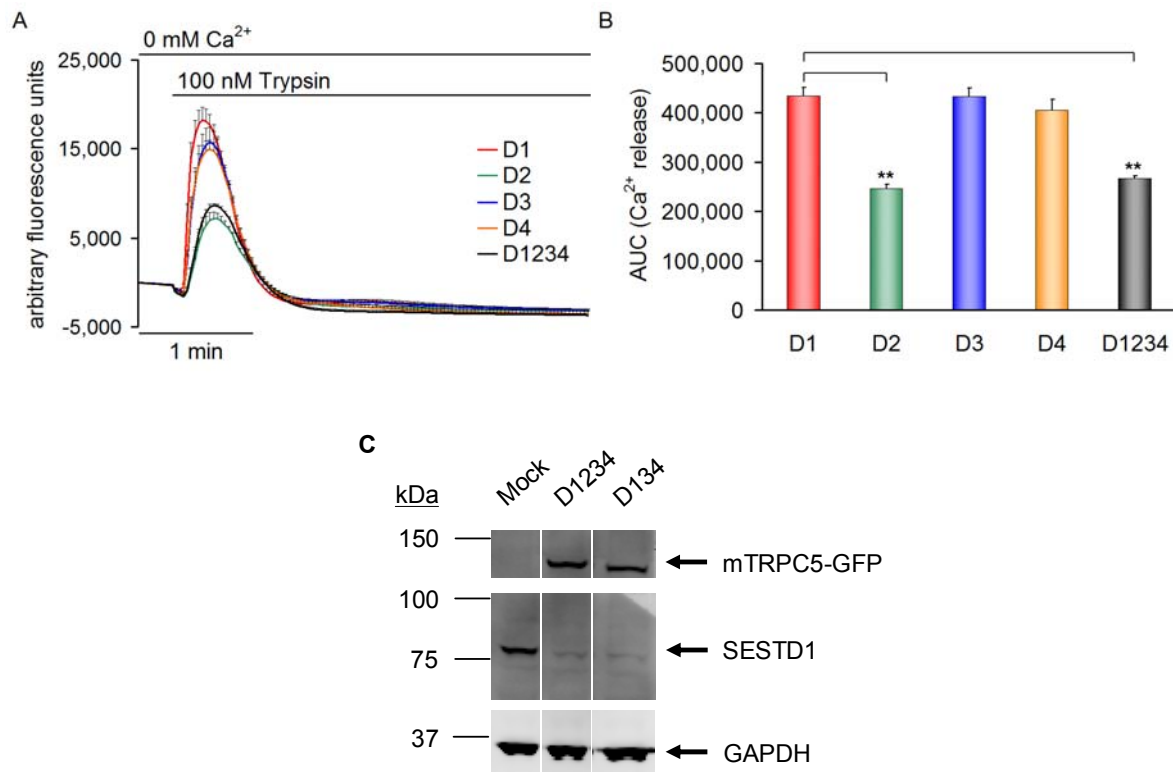


Figure 34: Ca^{2+} release from internal stores is suppressed by SESTD1 siRNA duplex 2. (A) Time-dependent changes in $[\text{Ca}^{2+}]_i$ of fluo-4-loaded HM1 cells transiently transfected with mTRPC5-GFP and 40 nM single (duplex 1 to 4, D1 to D4) or pooled (SMARTpool, D1234) specific siRNA against SESTD1. 48 hr post transfection, Ca^{2+} release from internal stores activated by application of 100 nM trypsin is significantly reduced in cells transfected with D2 or the complete SMARTpool (D1234). Data is shown as means of 6 wells (42,000 cells per well). Time scale bar 1 min. (B) Statistical analysis of data presented in A ($n = 5-6$ wells, $P < 0.01$, Wilcoxon two-sample test). (C) Western blot of HM1 cells transfected with GFP only (mock control) or mTRPC5-GFP plus 40 nM SMARTpool (D1234) or an siRNA pool lacking duplex 2 (D134). Blot was cut and incubated with anti-GFP (1:5,000)/AF 680 rabbit anti-mouse (1:2,500), anti-SESTD1 (1:5,000)/AF 680 goat anti-rabbit (1:2,500) and anti-GAPDH (1:10,000)/AF 680 rabbit anti-mouse (1:2,500) antibodies.

A pool of four siRNA duplexes (D1234, SMARTpool) directed against different sequences of SESTD1 was purchased from Dharmacon and tested for its ability to decrease SESTD1 protein levels. 48 hr post transfection, SESTD1 expression was almost completely knocked down by 40 nM siRNA whereas expression of an unrelated protein (GAPDH) was not altered (Fig. 34 C). HM1 cells cotransfected with 40 nM of either pooled or single siRNA duplexes and mTRPC5-GFP were then functionally analyzed by fluorometric $[\text{Ca}^{2+}]_i$ measurements.

While investigating TRPC5-independent Ca^{2+} release from internal stores that may serve as a control for unspecific siRNA effects, we noted that the SMARTpool and duplex 2 significantly reduced Ca^{2+} release compared to duplex 1, 3 or 4 (Fig. 34 A, B). This observation prompted us to check a new siRNA pool lacking duplex 2 (D134). Indeed, this pool was as efficient as the SMARTpool in silencing SESTD1 expression (Fig. 34 C), but without having an effect on Ca^{2+} release (see Fig. 36 A, B). Thus, it is likely that the suppression of Ca^{2+} release by duplex 2 is an unspecific effect, not related to the SESTD1 protein knock-down. Consequently HM1-C5Y were treated with specific SESTD1 siRNA (new pool of three duplexes, D134), unspecific non-silencing control siRNA or liposomes only (mock). SESTD1 protein expression in suchlike treated cells was reduced by $85.5 \pm 5.5\%$ ($n = 4$, compared to mock-transfected cells) or $82.3 \pm 5.3\%$ ($n = 4$, compared to cells treated with unspecific, non-silencing siRNA; Fig. 35).

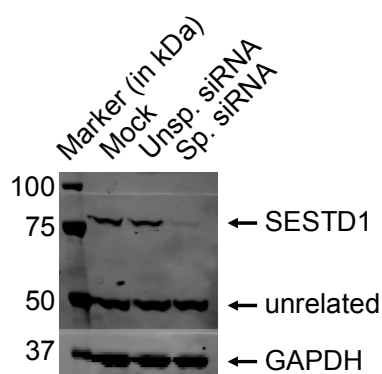


Figure 35: SESTD1 is efficiently knocked-down by 20 nM specific SESTD1 siRNA. Western blot of HM1-C5Y cells transfected with liposomes only (mock control), 20 nM unspecific control siRNA or 20 nM pooled specific SESTD1 siRNA (duplex 1, 3 and 4). Blot was cut and incubated with anti-SESTD1 (1:5,000)/AF 680 goat anti-rabbit (1:2,500) and anti-GAPDH (1:10,000)/AF 680 rabbit anti-mouse (1:2,500) antibodies.

M1 receptor- or PAR-induced Ca^{2+} release from internal stores was not different between the three groups (Fig. 36 A, B). In contrast, TRPC5-mediated Ca^{2+} influx following application of carbachol or trypsin (Fig. 36 C, D) was significantly reduced in cells treated with specific SESTD1 siRNA. TRPC5-mediated Ca^{2+} influx following carbachol stimulation was reduced to $45.4 \pm 2.8\%$ (compared to mock transfected cells) or $49.6 \pm 3.1\%$ (compared to cells transfected with control siRNA, Fig. 36 E). When cells were activated with 100 nM trypsin, TRPC5-mediated Ca^{2+} influx was reduced to $51.4 \pm 3.7\%$ (compared to mock transfected cells) or $58.0 \pm 4.2\%$ (compared to cells transfected with control siRNA, Fig. 36 F).

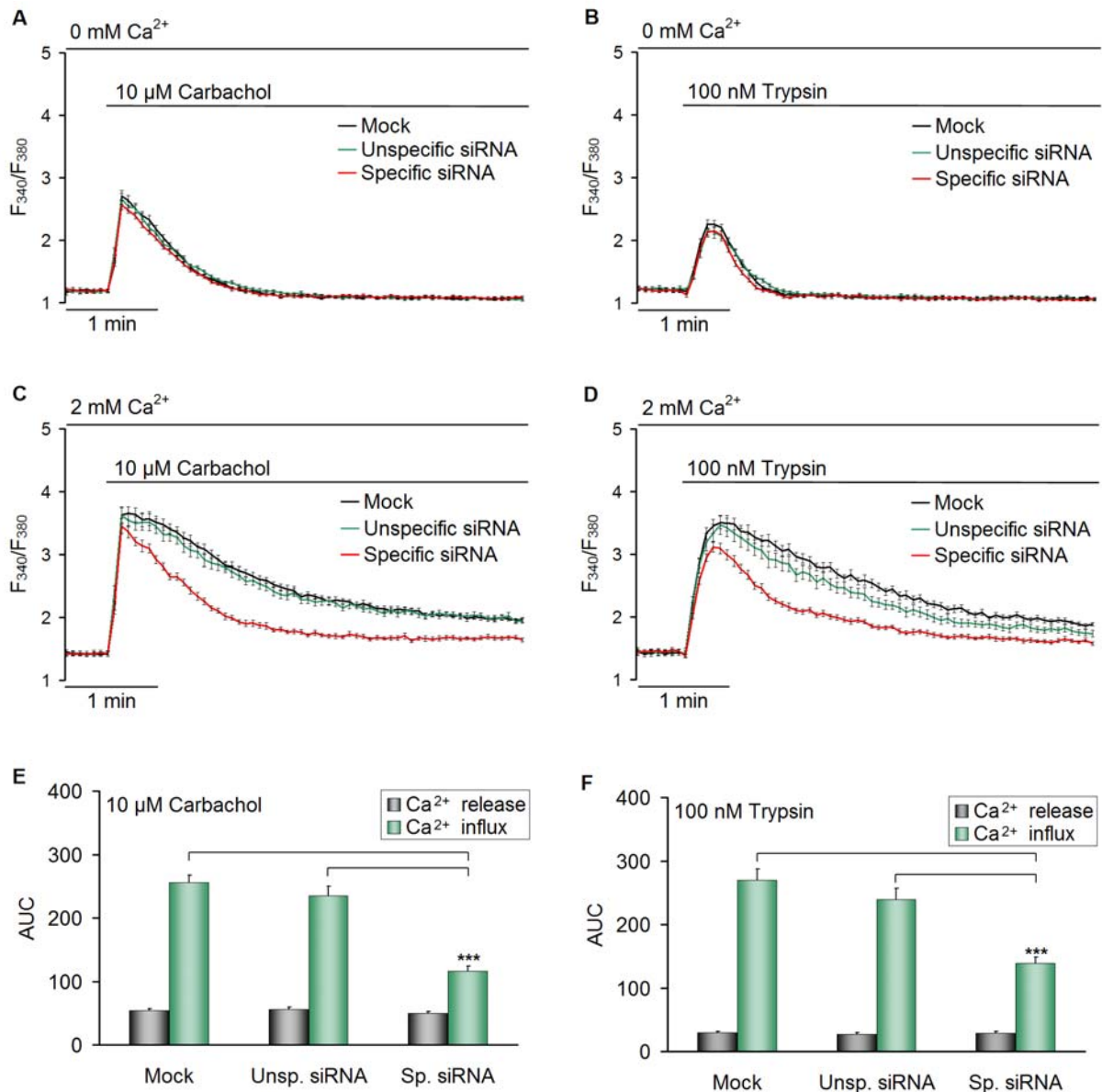


Figure 36: TRPC5 activity is reduced in HM1-C5Y cells transfected with specific SESTD1 siRNA. Time-dependent changes in $[\text{Ca}^{2+}]_i$ of fura-2-loaded HM1-C5Y cells transfected with 20 nM pooled specific SESTD1 siRNA (duplex 1, 3 and 4), unspecific control siRNA or liposomes only (mock) (A, B). 48 hr post transfection, Ca^{2+} release from internal stores activated by application of 10 μM carbachol (A) or 100 nM trypsin (B) is not different under the tested conditions. In contrast, TRPC5-mediated Ca^{2+} influx following application of 10 μM carbachol (C) or 100 nM trypsin (D) was significantly reduced in cells transfected with specific SESTD1 siRNA. Shown are means \pm SEM of three independent experiments (each performed with $n = 5-6$ wells per experimental condition). Time scale bar 1 min.

(E) Statistical analysis of data presented in A and C ($P < 0.001$, Wilcoxon test, two-sided). (F) Statistical analysis of data presented in B and D ($P < 0.001$, Wilcoxon test, two-sided).

The mechanisms by which SESTD1 modulates TRPC5 activity are unknown. Besides direct effects on channel gating, SESTD1 may act as a molecular chaperone that regulates channel biosynthesis or cellular targeting. In the latter case, the reduced TRPC5-mediated Ca^{2+} influx in cells treated with specific SESTD1 siRNA could be due to diminished levels of channel protein at the plasma membrane. To test this hypothesis, membrane expression of TRPC5-YFP in HM1-C5Y cells was investigated by a surface biotinylation assay. Comparable amounts of TRPC5 protein were detected at the plasma membrane of mock, control and SESTD1 siRNA transfected cells (Fig. 37) suggesting that SESTD1 does not modify TRPC5 processing.

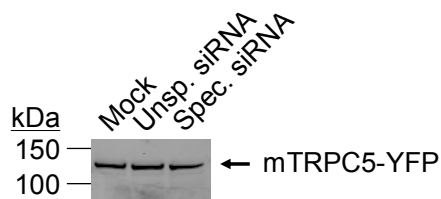


Figure 37: TRPC5 membrane expression is not changed in SESTD1 siRNA-treated cells. Surface proteins of HM1-C5Y cells stably expressing mTRPC5-YFP were biotinylated 48 hr post transfection with liposomes only (Mock), 20 nM unspecific control siRNA or 20 nM specific SESTD1 siRNA. Streptavidin-sepharose precipitates were analyzed by Western blotting with anti-GFP (1: 1,000) and AF 680 rabbit anti-mouse (1:2,500) antibodies.

3.4 SESTD1

3.4.1 Expression

Beyond the described interaction with TRPC4 and TRPC5, there was no data available on the function of SESTD1. In order to gain first insights into possible physiological roles of SESTD1, we studied its expression in tissues and cells. Real-time quantitative PCR (TaqMan; Livak *et al.*, 1995) of different tissues showed that SESTD1 mRNA is ubiquitously expressed in human tissues (Fig. 38).

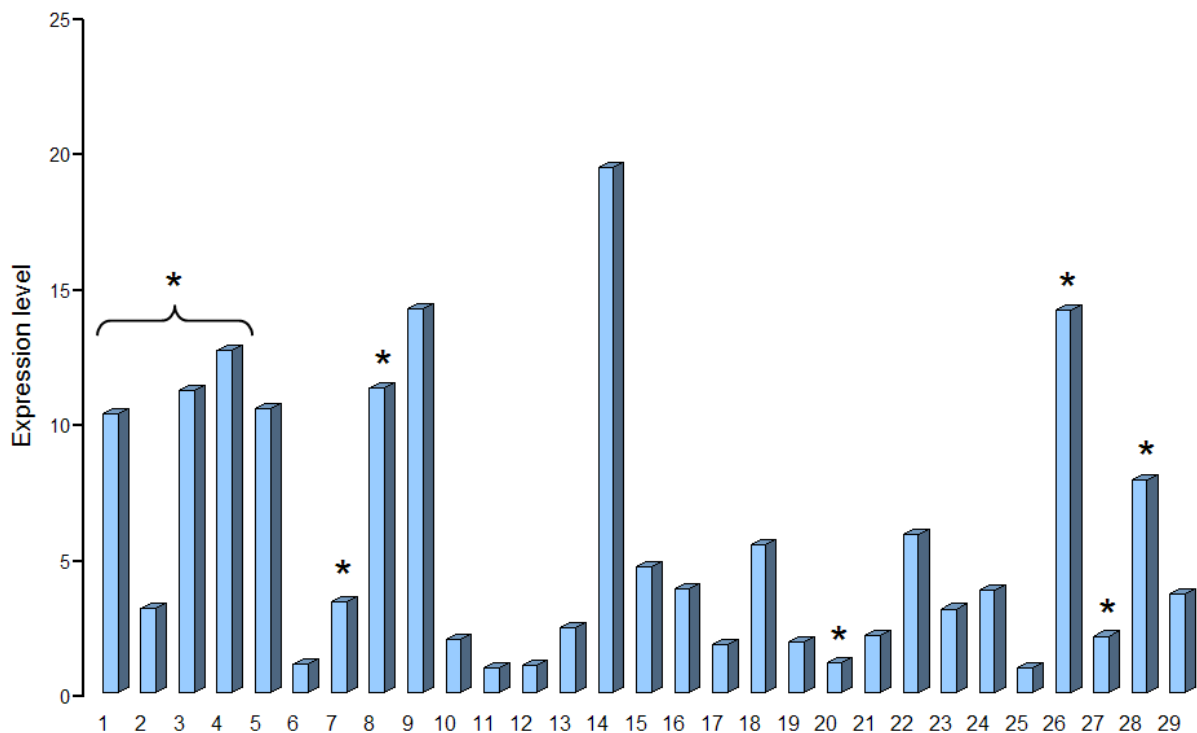


Figure 38: SESTD1 mRNA is ubiquitously expressed in human tissue. SESTD1 mRNA expression was determined in different human tissues with qRT-PCR and normalized to expression of the housekeeping gene RPL37a. Data shown is the mean of duplicates.

1 brain; 2 cerebellum; 3 hippocampus; 4 cortex; 5 spinal cord; 6 adrenal gland; 7 heart; 8 aorta; 9 adipose; 10 spleen; 11 bone marrow; 12 skeletal muscle; 13 skin; 14 trachea; 15 lung; 16 stomach; 17 small intestine; 18 colon; 19 liver; 20 pancreas; 21 kidney; 22 breast; 23 ovary; 24 uterus; 25 placenta; 26 testis; 27 prostate; 28 AoSMC; 29 HUVEC. Asterisks denote tissues in which significant expression of TRPC4 or TRPC5 has been reported. Data kindly provided by the Genomic Sciences department.

Since we found SESTD1 in a cDNA library made from human aorta we were interested to see in which vascular cell type the protein is expressed. Hence, lysates of primary human smooth muscle and endothelial cells were analyzed by Western blot for SESTD1 expression. As depicted in Figure 39, SESTD1 was present both in aortic (AoSMC) and coronary (CASMC) smooth muscle cells, and also in aortic (HAEC) and microvascular (HMVEC-d) endothelial cells.

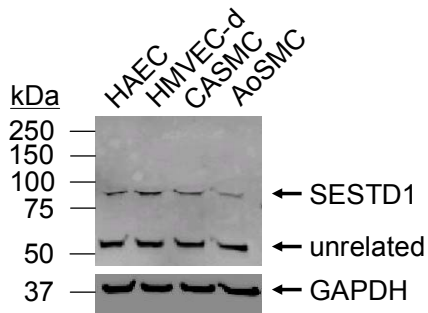


Figure 39: SESTD1 expression in human primary cells. Western blot of the indicated cell samples developed with anti- SESTD1 #148 (1:5,000) and secondary AF 680 goat anti-rabbit antibody (1:2,500). Each lane was loaded with 15 μ g protein (BCA test) and equal loading was visualized by blotting with anti-GAPDH (1:10,000) and secondary AF 680 rabbit anti-mouse antibody (1:2,500).

In addition to human, SESTD1 expression was also tested in rat and mouse tissues. Here, SESTD1 was found in microsomes from rat brain and in the vascular A7r5 cell line. It is also expressed in mice ventricle as well as in HL-5, a cell line derived from murine atrial cardiomyocytes (Fig. 40).

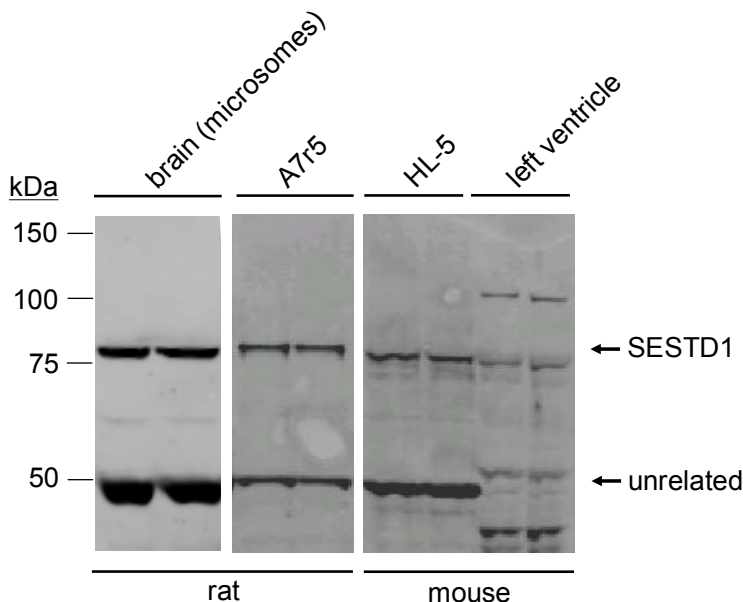


Figure 40: SESTD1 expression in different rodent tissue and cell samples. Varying amounts of rat brain microsomes, A7r5 and HL-5 cells, and mouse left ventricle were separated by SDS PAGE, blotted onto nitrocellulose membranes and stained with anti-SESTD1 #148 (1:5,000) and secondary AF 680 goat anti-rabbit(1:2,500) antibodies. HL-5 and left ventricle lysates were kindly provided by Dr. K. Engel.

3.4.2 Subcellular localization

Identification of SESTD1's subcellular location could give further hints towards its physiological function. Therefore, immunofluorescence experiments were performed with the two antibodies (characterized in Chapter 3.2.4) directed against endogenous SESTD1. Both antibodies detected overexpressed HA-tagged SESTD1 (Fig. 41 A, B) that was found to be evenly distributed within the cells with no apparent preference for a certain subcellular structure. We also investigated C-terminally YFP-tagged SESTD1 (data not shown) to exclude localization artefacts due to the N-terminal HA-tag, but there were no differences detectable. We moved on to determine the localization of endogenous SESTD1 in HM1 cells. Our two antibodies against different SESTD1 epitopes showed very distinct staining patterns. Whereas anti-SESTD1 #148 strongly stained tubular structures that are most likely tubulin (characteristic mitotic cell spindle poles were highlighted, Fig. 41 B), anti-SESTD1 #147

stained vesicular structures (Fig. 41 A). It was already seen in Western blots (Fig. 28) that both antibodies also have high affinities for proteins not related to SESTD1. This might explain our immunocytochemical findings. To further elucidate the location of native SESTD1, better antibodies will be necessary that specifically recognize the protein without unspecific binding to unrelated structures.

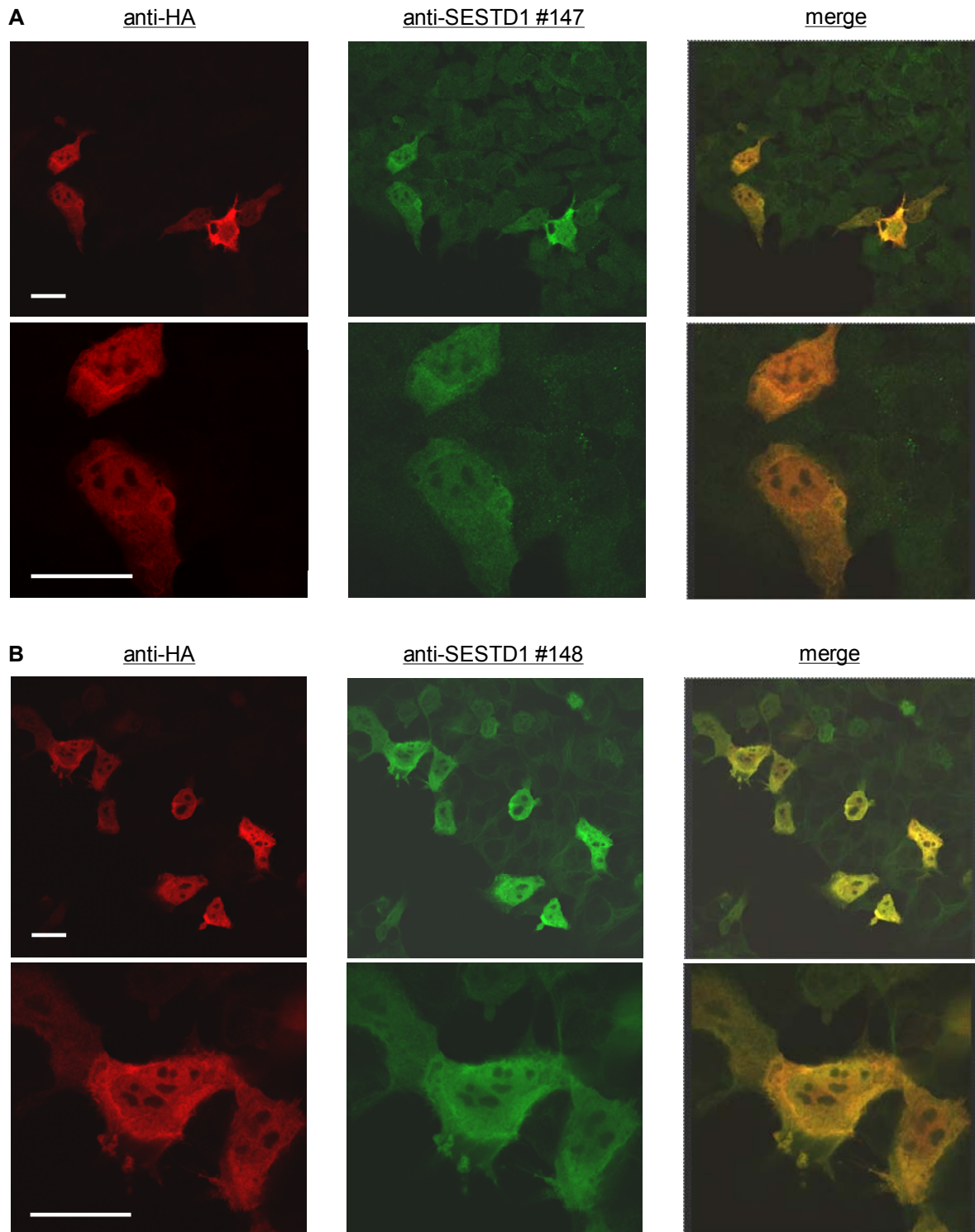


Figure 41: Subcellular localization of overexpressed SESTD1. (A, B) HA-tagged SESTD1 is found evenly distributed within HM1 cells that were stained with anti-HA (1:500) and secondary AF goat 546 anti-rat (1:250) antibody. Cells were stained in parallel with (A) anti-SESTD1 #147 (1:25) and (B) anti-SESTD1 #148 (1:100) and secondary AF 488 goat anti-rabbit (1:250) antibodies in order to additionally visualize endogenous SESTD1. Better antibodies are needed to further elucidate the subcellular localization of native SESTD1 as anti-SESTD1 #147 stained vesicular structures in contrast to anti-SESTD1 #148 that predominantly preliminarily stained tubular structures in untransfected cells. Scale bar is 20 μ m.

3.4.3 *Cis-trans* isomerase signature

A PROSITE motif search of SESTD1 indicated a FKBP-type peptidyl-prolyl *cis-trans* isomerase signature 2 (Pattern-ID PS00454) starting from aa 427 (VDV GLQ GLR EKG QGL LDQ ISN QAS WAY G). Peptidyl-prolyl *cis-trans* isomerases (PPIases) catalyze *cis-trans* isomerization of proline peptide bonds thus accelerating protein folding. A possible PPIase activity of SESTD1 was tested using a fluorescence assay and the cys-bridged peptide H-Abz-Cys-Ala-Pro-Ala-Cys-Ntr-NH₂ as a substrate (see Chapter 2.5.8 for assay principle). The known PPIase activity of FKBP12.6 (Sewell *et al.*, 1994) served as a positive control. Substrate isomerization by FKBP12.6 is a rapid reaction that was completed almost within a minute. It is indicated by a steepening of the slope of the fluorescence curve compared to the spontaneous reaction. In contrast, the slope in presence of GST-SESTD1 did not differ from the spontaneous isomerization (Fig. 42). Hence, in this experiment GST-SESTD1 did not act as PPIase on bridged H-Abz-Cys-Ala-Pro-Ala-Cys-Ntr-NH₂.

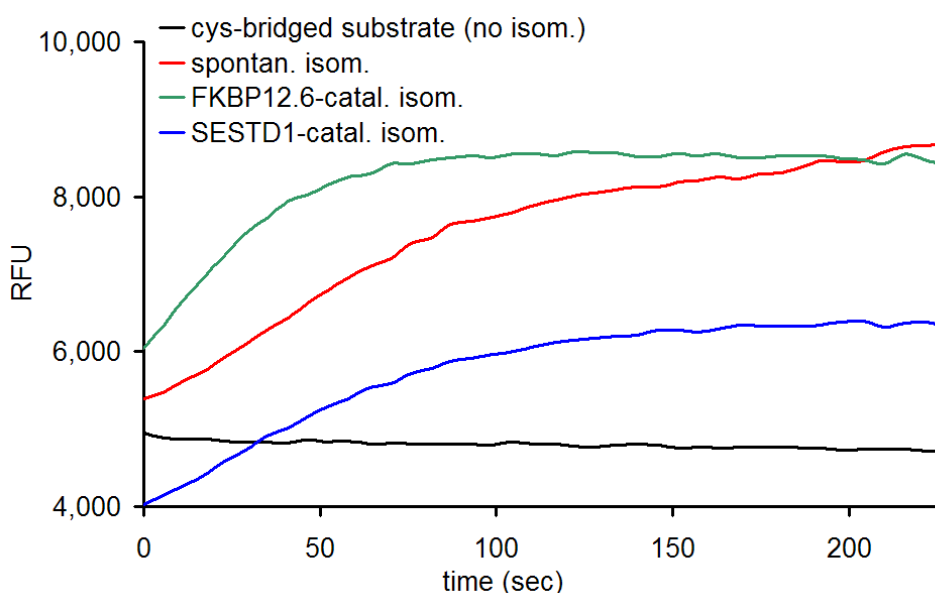


Figure 42: *Cis-trans* isomerization assay of cys-bridged H-Abz-Cys-Ala-Pro-Ala-Cys-Ntr-NH₂. Isomerization results in a fluorescent *trans*-form. When the substrate is not cleaved (no isom.) baseline fluorescence is not changed. Addition of 125 mM DTT cleaves the cys-bridge resulting in spontaneous prolyl *cis-trans* conversion (spontan. isom.). In presence of 1 μ M FKBP12.6 (and 125 mM DTT), isomerization is accelerated (FKBP12.6-catal. isom.). 4.79 μ M GST-SESTD1 (in presence of 125 mM DTT) have no influence on isomerization velocity (SESTD1-catal. isom.). Data is means of 2 wells and was kindly provided by K. Sicka.

3.4.4 *In vitro* phospholipid binding

SESTD1 belongs to the eukaryotic Sec14 protein superfamily that was named after the N-terminal Sec14p-like lipid-binding domain. Due to this domain its members are assumed to specifically bind and transfer different phospholipids (Mousley *et al.*, 2007), but some have also been reported to bind other hydrophobic ligands than phospholipids, e.g. α -tocopherol

and 11-*cis*-retinal (Allen-Baume *et al.*, 2002). In light of the dependence of TRPC channels on phospholipid hydrolysis, it was particularly interesting to test SESTD1's phospholipid binding capability.

PIP strip phospholipid overlay assay

Specific binding of SESTD1 to all physiologically relevant phosphatidylinositol mono- and bisphosphates (PIP and PIP₂) as well as to phosphatidic acid was studied in a phospholipid overlay assay. In the presence of 60 nM Ca²⁺, the approximate physiological concentration in quiescent cells, SESTD1 bound strongly to PIPs and to a lesser degree to phosphatidic acid. Notably, the affinity of SESTD1 to the phospholipid substrates changed depending on the Ca²⁺ concentration. Raising the Ca²⁺ concentration to 2.5 μM led to increased binding of PI(3,5)P₂ and PI(4,5)P₂, phosphatidic acid as well as PI(3,4)P₂, PI(3)P and PI(4)P (Fig. 43).

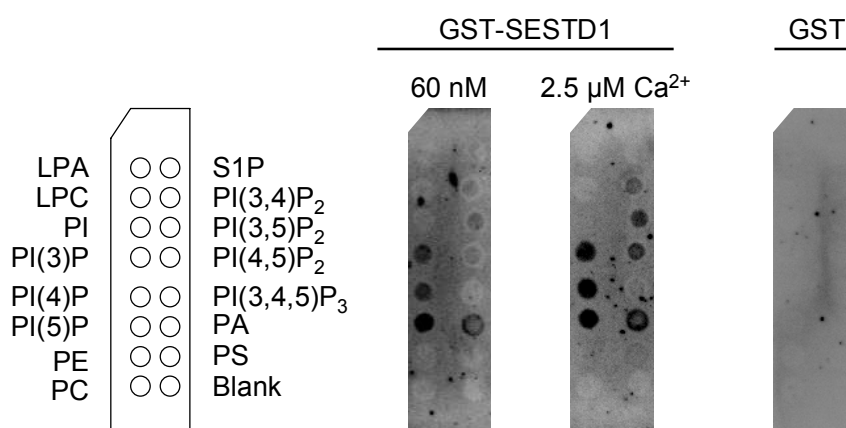


Figure 43: SESTD1 binding of phospholipids is Ca²⁺-dependent. GST-SESTD1 bound PIPs, PIP₂s and PA immobilized on membranes. PIP strips (Echelon) were probed with GST-SESTD1 in blocking buffer containing 60 nM or 2.5 μM free Ca²⁺, or with GST in blocking buffer followed by anti-GST antibodies (1:2,000) and goat anti-rabbit HRP-conjugated antibodies (1:20,000). Signals were detected by enhanced chemiluminescence (ECL).

Cova-PIP plate binding assay

To better quantify the phospholipid binding of SESTD1, it was tested whether SESTD1 binds phospholipids covalently attached to 96-well microtiter plates. These plates (Cova PIP Specificity Plates) coated with 10 pmol substrate/well were provided by Echelon Biosciences. The GST-tagged PH-domain of LL5-α is suggested as a control reagent that recognizes all phosphoinositides (Echelon, 2007). Therefore, a DELFIA binding assay with the LL5-α PH-domain was first established. Our results confirmed that the protein bound to all phosphoinositides but with higher affinity to PI(3,4)P₂ and PI(3,4,5)P₃ (Fig. 44). This preferential binding has also been observed in overlay assays (Echelon, 2007).

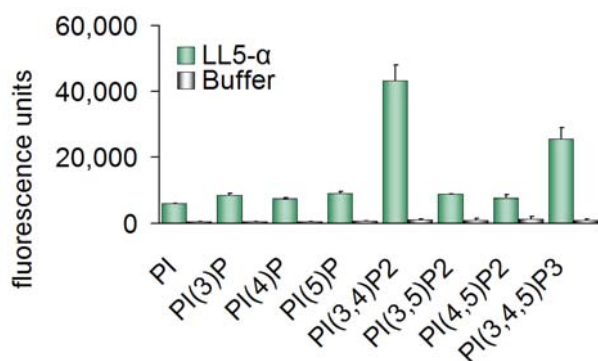


Figure 44: DELFIA of LL5- α binding to Cova-PIP Specificity Plates (Echelon). Polystyrene microtiter wells each loaded with 10 pmol PIP_n were incubated 3 hr with 1 μ g/mL GST-tagged PH-domain of LL5- α or buffer only. Bound protein was detected with Eu-N1-labelled anti-GST (100 ng/well). Lanthanide fluorescence ($\lambda_{\text{exc}} = 340$ nm, $\lambda_{\text{em}} = 620$ nm) was measured.

Binding of varying amounts of SESTD1 was analogously tested. However, no binding could be detected on plates loaded with 10 pmol substrate per well (data not shown). One reason could have been a lower binding affinity of SESTD1 to its substrates. Hence, the experiments were repeated with new plates loaded with 100 pmol substrate per well. Indeed, under these conditions SESTD1 specifically bound to phosphoinositides with highest affinity to PI(4,5)P₂ and PI(3,4)P₂ (Fig. 45).

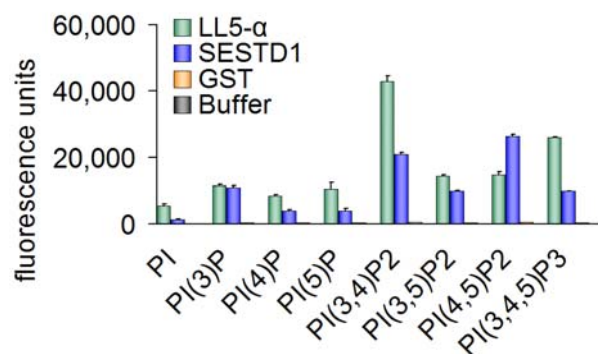


Figure 45: DELFIA of LL5- α and SESTD1 binding to Cova-PIP Specificity Plates (Echelon). Polystyrene microtiter wells each loaded with 100 pmol PIP_n were incubated 3 hr with 1 μ g/mL GST-tagged PH-domain of LL5- α , 100 μ g/mL GST-SESTD1 or GST, respectively, or buffer only. Bound protein was detected with anti-GST (1:1,000) and secondary Eu-N1-labelled anti-rabbit antibody (50 ng/well). Lanthanide fluorescence ($\lambda_{\text{exc}} = 340$ nm, $\lambda_{\text{em}} = 620$ nm) was measured.

Furthermore, we showed that binding of SESTD1 to phospholipids is dose-dependent (Fig. 46) and the apparent binding affinity varies between the different phosphoinositide species. These findings support the assumption that SESTD1, like other SEC14-domain containing proteins (Ile *et al.*, 2006), may regulate cellular signalling by specifically binding and transporting phospholipids.

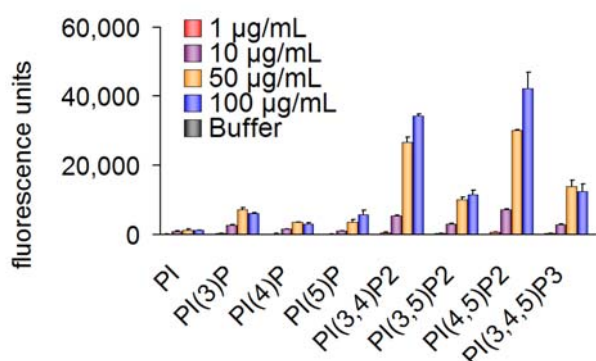


Figure 46: DELFIA of SESTD1 binding to Cova-PIP Specificity Plates (Echelon). Polystyrene microtiter wells each loaded with 100 pmol PIP_n were incubated 3 hr with the given concentrations of GST-SESTD1 or buffer only. Bound protein was detected with anti-GST (1:1,000) and secondary Eu-N1-labelled anti-rabbit antibody (50 ng/well). Lanthanide fluorescence ($\lambda_{\text{exc}} = 340$ nm, $\lambda_{\text{em}} = 620$ nm) was measured.

3.4.5 SESTD1 siRNA knock-down in HM1 cells changes β -catenin distribution

A circumstantial observation prompted us to investigate another possible function of SESTD1. We noted that the morphology of HM1 cells transfected with specific SESTD1 siRNA seemed to differ from cells transfected with unspecific, non-silencing control siRNA or liposomes. They appeared more spindle-shaped. To visualize this subjective impression, protein markers for cellular junctions were tested in immunofluorescence experiments. To evaluate the validity of this cell-based approach, we first determined the siRNA transfection efficiency in this assay. For this purpose, functional siRNA was replaced by siGLO red transfection indicator (Dharmacon), a fluorescent-labelled non-functional control siRNA that localizes to the nucleus. One day post transfection, siRNA intake was reviewed by exciting its fluorescence. Almost all treated cells were successfully transfected (Fig. 47). Thus, analysis of such a homogenous cell population by immunofluorescence microscopy is feasible.

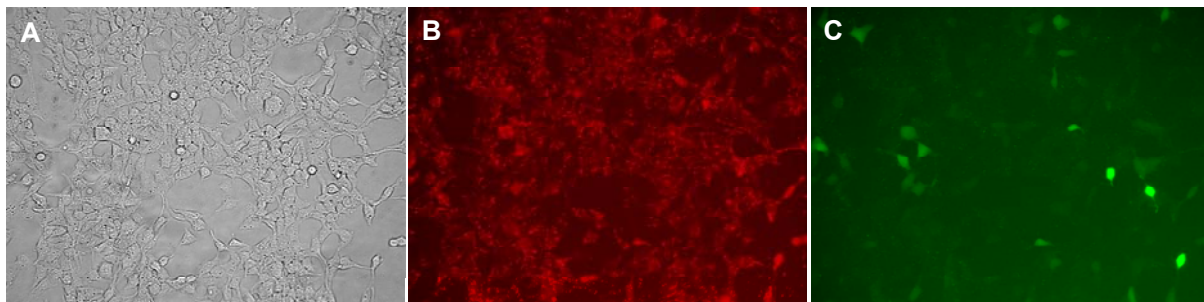


Figure 47: siRNA transfection protocol results in high transfection rate. (A) Transmission of HM1 cells cotransfected with 20 nM siGLO red transfection indicator **(B)** and GFP **(C)**. Pictures were taken 24 hr post transfection with 20x magnification.

Tight junctions were visualized by staining zona occludens 1 (ZO-1), a non-transmembrane protein that is found on the cytoplasmic leaflet of tight junctions. The resulting staining was ambiguous (Fig. 48 A). In some areas there were no obvious differences under all three conditions (as depicted below) but in others (with lower cell density), ZO-1 staining seemed to be weaker in SESTD1 siRNA treated cells. By comparison, localization of β -catenin, a protein associated with E-cadherin in adherens junctions, was clearly changed in cells treated with specific SESTD1 siRNA. Whereas control cells displayed a distinct membrane-associated localization of β -catenin, an increased intracellular accumulation of the protein was observed in cells transfected with the SESTD1-specific D134 siRNA pool (Fig. 48 B). Although, obviously, the regulation of β -catenin distribution by SESTD1 requires further investigation, these results provide a potential novel link between lipid- and cell-cell signalling.

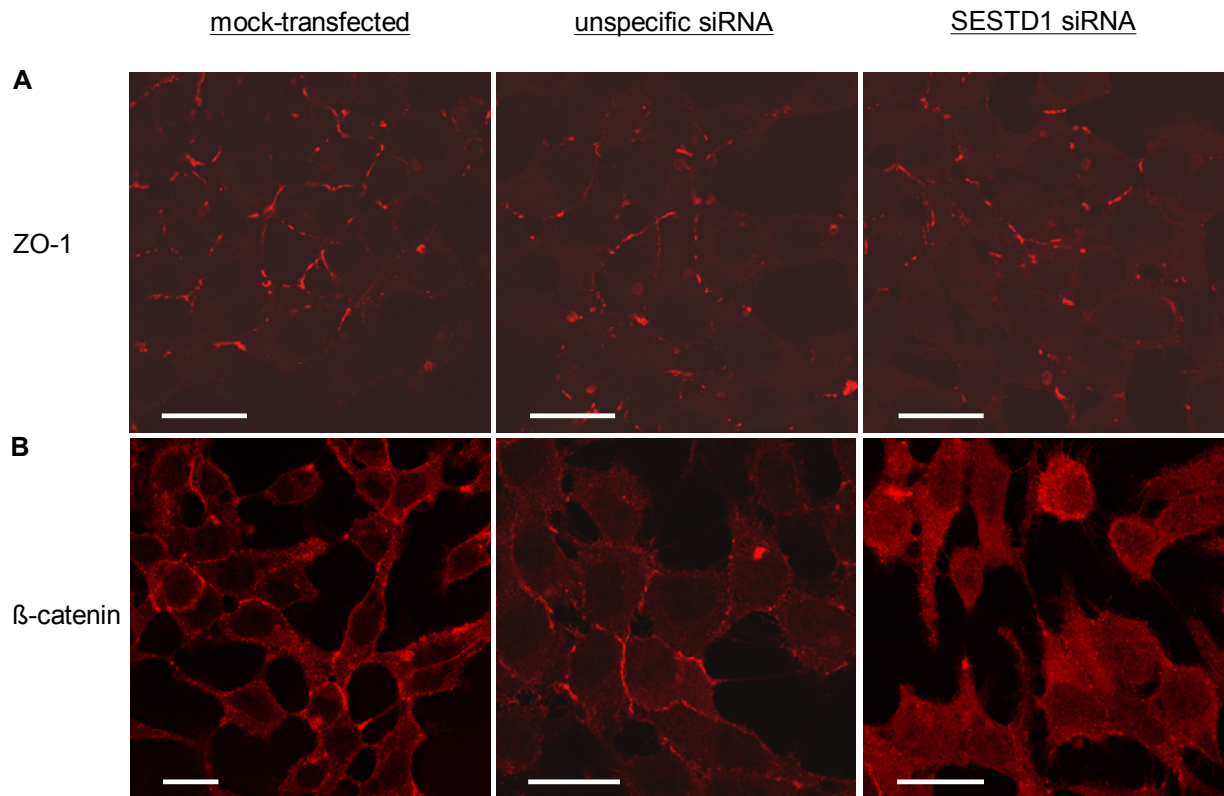


Figure 48: β -catenin distribution is changed in HM1 cells treated with SESTD1 siRNA. 48 hr post transfection, HM1 cells treated with liposomes only (mock-transfected), 20 nM unspecific, non-silencing control siRNA or 20 nM specific SESTD1 siRNA (pool D134) were fixed with paraformaldehyde, permeabilized with Triton X-100, and stained **(A)** with anti-ZO 1 (1:100) and AF 546 goat anti-mouse (1:250) antibodies or with anti- β -catenin (1:250) and AF 546 goat anti-rabbit (1:250) antibodies. Scale bar is 20 μ M.

4 Discussion

4.1 Norgestimate is a selective inhibitor of the TRPC3/6/7 subfamily

In this work, we used complementary pharmacological and molecular biological approaches to gain a better understanding of the physiology of TRPC channels. Our search for new pharmacological tools led to the discovery of two steroids, namely norgestimate and progesterone, which differentially inhibit TRPC channels. While progesterone showed almost equal activity towards all studied TRPC channels with IC_{50} values of $\sim 10\text{-}20\ \mu\text{M}$, norgestimate selectively inhibited the TRPC3/6/7 subfamily with IC_{50} values of $\sim 5\ \mu\text{M}$. This selectivity distinguishes norgestimate from most known TRPC channel modulating compounds.

Based on the calculated inhibition at $10\ \mu\text{M}$, norgestimate was 4 to 5-fold more potent on Ca^{2+} influx mediated by TRPC3 and TRPC6 compared to TRPC5. These results obtained by fluorometric measurements were further validated by patch clamp recordings in the whole-cell configuration. Again, $10\ \mu\text{M}$ norgestimate were 3.5-fold more effective on AlF_4^- -evoked TRPC6-mediated currents compared to TRPC5, thus confirming its selective block of the TRPC3/6/7 subfamily. Norgestimate rapidly inhibited TRPC6 channel function both after direct stimulation by OAG in FLIPR measurements and also after indirect stimulation by AlF_4^- in patch clamp recordings suggesting that it directly blocked the channel. The highest applied norgestimate concentration did not influence calcium store depletion following activation of PAR in HEK293 cells or following stimulation of the V_{1A} receptor in A7r5 cells, therefore excluding IP_3R antagonism or inhibition of the $G_{q/11}/\text{PI}$ signalling cascade as mechanism of channel inhibition. Moreover, genomic effects of steroids that occur on an hours time scale can be excluded as channel inhibition started immediately after norgestimate application and was rapidly and completely reversed upon washout. Taken together, these data suggest that norgestimate inhibits TRPC6 activity by a direct interaction with the channel protein, although single channel recordings, that would provide the most stringent proof, have not been performed.

Compared to known TRPC channel blockers, norgestimate offers the advantage of being reasonably selective for DAG-sensitive TRPCs by inhibiting them at low micromolar concentrations without having an effect on the upstream PI signalling components.

Perhaps the most specific TRPC inhibitor described so far is [1-(5-chloronaphthalene-1-sulphonyl) homopiperazine, HCl] (**ML-9**) which has been shown to block TRPC6 with an IC_{50} value of $7.8\ \mu\text{M}$ but has no effect on isolated, single TRPC5 channels (Shi *et al.*, 2007). Yet, ML-9 is a commonly used blocker of myosin light chain kinase (MLCK; Saitoh *et al.*, 1987) and ML-9-mediated dephosphorylation of myosin light chains modulates the activity of many

membrane proteins, e.g. the Na⁺/H⁺ exchanger NHE3 (Szaszi *et al.*, 2000), and voltage-dependent potassium channels like K_v4.2 and K_v4.3 (Wu *et al.*, 1998). In whole cell patch clamp experiments, TRPC5 was shown to be indirectly modulated by ML-9 (Shimizu *et al.*, 2006; Kim *et al.*, 2006b) as cytoskeletal rearrangements following MLC-dephosphorylation led to internalization and thus apparent inhibition of the channel. These MLCK-dependent actions of ML-9 make the interpretation of its effects on TRPC channels in intact cells and tissues difficult.

Another compound widely used for the pharmacological characterization of TRPC channels is 2-aminoethoxydiphenyl borate (**2-APB**). It was introduced as a IP₃R blocker originally (Maruyama *et al.*, 1997), but later also shown to inhibit the SERCA pump (Missiaen *et al.*, 2001; Bilmen *et al.*, 2002), voltage-gated potassium channels (Wang *et al.*, 2002), volume-regulated anion channels (Lemonnier *et al.*, 2004), and the mitochondrial permeability transition pore (Chinopoulos *et al.*, 2003). Moreover, the compound has been demonstrated to inhibit native SOCs (Bootman *et al.*, 2002; Flemming *et al.*, 2003) and several members of the TRP superfamily, e.g. TRPM8 (Hu *et al.*, 2004). Some groups have shown that 2-APB blocked receptor-dependent activation of TRPC3 (Ma *et al.*, 2000), TRPC5 (Lee *et al.*, 2003b) as well as of TRPC6 (Xu *et al.*, 2005). However, the block of TRPC3 is likely indirect as DAG-stimulated channels were insensitive to 2-APB (Ma *et al.*, 2000). Thus, the mechanism of action of 2-APB on TRPCs is currently unclear and may be more complex than simple binding to the channel proteins.

An old generation blocker of ROCs (Merritt *et al.*, 1990) and SOCs (Demaurex *et al.*, 1992) is the imidazole **SK&F 96365**, which is an optimized derivative of a compound originally synthesized as a thromboxane synthetase inhibitor. Due to its insufficient potency (Li *et al.*, 2004 and references therein) and its side-effects on L-type Ca²⁺ channels (Merritt *et al.*, 1990), K⁺ channels (Schwarz *et al.*, 1994) and Cl⁻ channels (Franzius *et al.*, 1994), the compound is not therapeutically suitable. The poor selectivity of SK&F with reported half maximal inhibitory effects on mast cell I_{CRAC} at 4 μM (Franzius *et al.*, 1994) as well as on TRPC3 (Zhu *et al.*, 1998) and TRPC6 (Estacion *et al.*, 2004) at 5 μM further limits its use in TRPC channel exploration.

Apart from the above mentioned organic blockers, **lanthanides** are used to distinguish the TRPC4/5 from the TRPC3/6/7 subfamily and other non-selective cation channels. TRPC4 and -5 homomers and TRPC1/5 heteromers are potentiated by micromolar concentrations of La³⁺ and Gd³⁺ (Schaefer *et al.*, 2000; Strubing *et al.*, 2001; Jung *et al.*, 2003; Plant & Schaefer, 2003), and human TRPC5 is activated by Gd³⁺ when other stimuli are absent (Zeng *et al.*, 2004). Currents mediated by TRPC1 (Zitt *et al.*, 1996), TRPC3 (Zhu *et al.*, 1996; Kamouchi *et al.*, 1999; Halaszovich *et al.*, 2000), TRPC6 (Inoue *et al.*, 2001; Basora *et al.*, 2003), and TRPC7 (Okada *et al.*, 1999; Riccio *et al.*, 2002) are blocked at these lanthanide

concentrations. But there are also contradictory reports of TRPC5 inhibition by micromolar lanthanide concentrations (Okada *et al.*, 1998; Lee *et al.*, 2003b), and an endothelial store-operated Ca^{2+} current that is absent in TRPC4 knock-out mice is also highly susceptible to inhibition at 1 μM La^{3+} (Freichel *et al.*, 2001). Therefore, the unique feature of TRPC4/5 potentiation by lanthanides might depend on the individual expression system and thus only has limited value for the investigation of native currents. Moreover, due to their toxicity and rather unspecific ion channel blocking activities, the use of lanthanides in many tissue models such as brain slices is not possible.

Norgestimate is a progestin (a synthetic gestagen). Combined with ethinyl estradiol it is a component of oral contraceptives (Cilest[®], Pramino[®]). We examined in fluorometric Ca^{2+} influx tests whether the natural pregnancy-maintaining hormone progesterone, which is structurally related to norgestimate, also inhibits TRPC channels. In fact, progesterone was less active on TRPC6 compared to norgestimate, but TRPC4 and -5 were more effectively inhibited by the hormone. Its overall effect on the TRPC4/5 and the TRPC3/6/7 subfamily was quite comparable. Hence, progesterone does not discriminate between different members of the TRPC family and was therefore not further investigated. Nevertheless, the observed inhibition of TRPC channels may contribute to the reported cardiovascular effects of progesterone. Several studies have shown that progesterone rapidly relaxed vessels, e.g. pig coronary arteries (Crews & Khalil, 1999), rat aorta (Glusa *et al.*, 1997; Mukerji *et al.*, 2000), and also guinea pig airway smooth muscles (Perusquia *et al.*, 1997). This vasorelaxant effect is endothelium-independent and mediated at least partly through inhibition of L-type Ca^{2+} channels (Barbagallo *et al.*, 2001; Zhang *et al.*, 2002). Involvement of SOCs and ROCs (Glusa *et al.*, 1997; Mukerji *et al.*, 2000) and opening of potassium channels (Mukerji *et al.*, 2000 and references therein) has been further proposed. Our study provides first evidence that progesterone is active on TRPC channels which constitute SOCs (Philipp *et al.*, 1996; Philipp *et al.*, 1998; Kiselyov *et al.*, 1998) and ROCs (Zitt *et al.*, 1997; Boulay *et al.*, 1997; Schaefer *et al.*, 2000) in vascular SMC (Dietrich *et al.*, 2006) and EC (Yao & Garland, 2005). Some of them are believed to be involved in vessel constriction, like TRPC6 (Inoue *et al.*, 2001; Estacion *et al.*, 2006). TRPC channel inhibition could thus participate in the progesterone-mediated vasorelaxation observed in these reports.

It remains to be shown whether this hormone also modulates TRPC channels *in vivo*. Even the elevated progesterone plasma levels in pregnant women ($\approx 1 \mu\text{M}$, Barbagallo *et al.*, 2001 and references therein) are still lower than the effective concentrations for TRPC channel inhibition *in vitro* (10-20 μM). However, progestins are highly lipophilic and have a large volume of distribution, therefore resulting in a higher tissue than plasma concentration (Lindenmaier *et al.*, 2005). Hence, it cannot be ruled out that local progesterone

concentrations are high enough to block TRPC channel function. In this regard, reports of TRPC1, -3, -4, and -6 proteins found in term human pregnant myometrium are of interest. They are believed to form SOCs though their exact physiological roles in this tissue are not yet known (Dalrymple *et al.*, 2002; Yang *et al.*, 2002). It is conceivable that TRPC channels would be blocked *in vivo* by the high gestational progesterone concentrations to limit uterine contractibility during pregnancy (Yang *et al.*, 2002; Dalrymple *et al.*, 2007) but further studies are needed to investigate this possibility.

Reports about the metabolic fate of norgestimate are sparse (Stanczyk, 1997). It appears to be a precursor (Alton *et al.*, 1984; Kuhnz *et al.*, 1994) that is rapidly converted to the active metabolite *in vivo*. When we tested the proposed active metabolite, levonorgestrel (Fig. 49), to our surprise even the highest concentration applied (30 μM) had no effect on the Ca^{2+} -influx mediated by TRPC6.

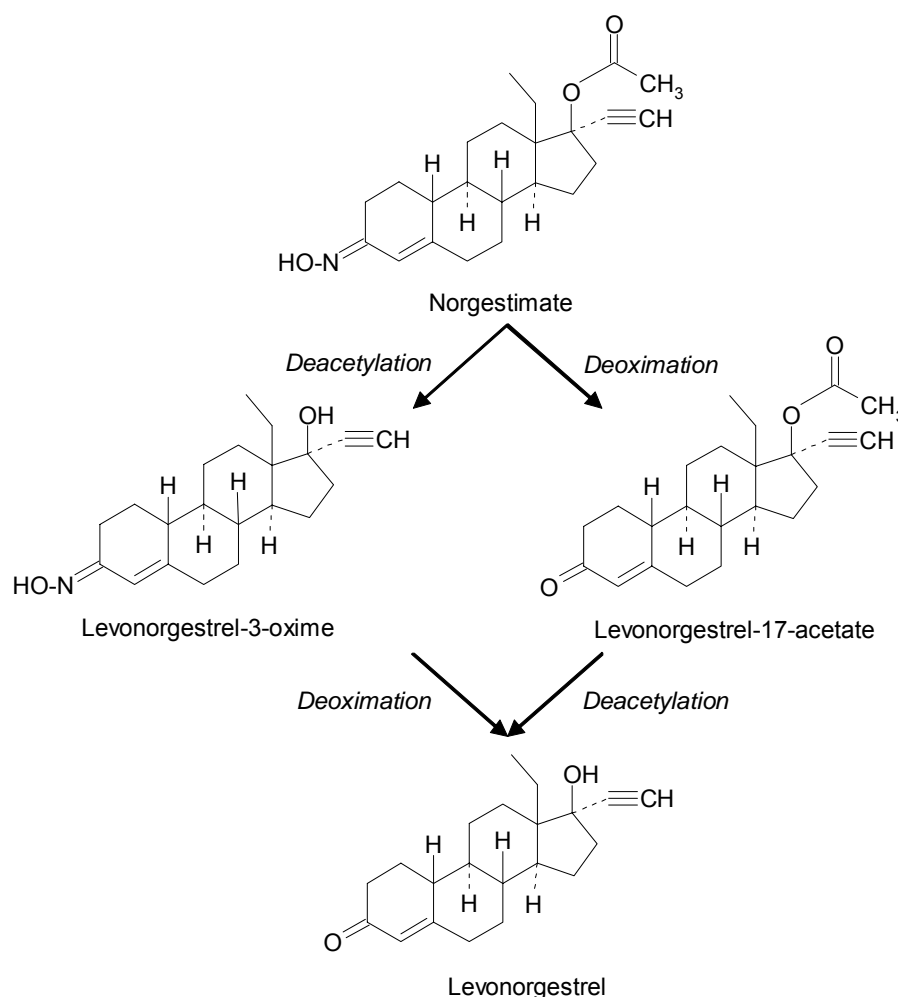


Figure 49: Proposed norgestimate metabolism (Juchem *et al.*, 1993).

This finding could be a promising starting point for the optimization of TRPC6 channel antagonists. Inactive levonorgestrel differs only slightly from active progesterone and norgestimate in its free hydroxyl group at position 17 (steroid numbering according to IUPAC,

1969). In norgestimate this group is less hydrophilic due to esterification and in progesterone it is replaced by a carbonyl function that is attached to position 17 (Fig. 16). Unfortunately, the structural basis for the differential effects of norgestimate, progesterone, and levonorgestrel, on the same molecular target is unknown. However, the insensitivity of TRPC6 to levonorgestrel strongly supports the notion that current inhibition by norgestimate and progesterone is unlikely due to unspecific cellular effects.

Besides recombinant channels we also investigated the modulation of native TRPCs by norgestimate. The A7r5 cell line, which was derived from rat embryonic thoracic aorta SMC, is a validated model system for the study of native TRPC channels (Jung *et al.*, 2002; Soboloff *et al.*, 2005; Maruyama *et al.*, 2006). By means of either siRNA-mediated protein knock-down (Soboloff *et al.*, 2005) or overexpression of dominant negative channel subunits (Maruyama *et al.*, 2006), functional evidence was provided for the contribution of TRPC6 proteins to AVP-induced cationic currents in these cells. The underlying channels are most likely heteromers, and their exact subunit composition seems to depend on the investigated A7r5 strain and cell passage number (Moneer *et al.*, 2005). TRPC channel expression may in addition depend on cultivation conditions (Dietrich *et al.*, 2007) and cell seeding density (own observation). In our hands, more cells responded to AVP when cells were plated at a low density. In the study of Maruyama *et al.*, 2006, clear functional discrepancies between expressed TRPC6 homomers and native channels pointed to TRPC6/7 heteromers underlying the AVP-evoked currents. The endogenous current displayed a similar extracellular Ca^{2+} dependency as heterologously expressed TRPC6/7 heteromers, and native TRPC6/7 complexes were detected by co-immunoprecipitation studies. However, TRPC7 protein was not found in A7r5 cells by another group (Soboloff *et al.*, 2005). We did not investigate the subunit composition of TRPC6-containing channels in our A7r5 cells but confirmed the dependency of AVP-induced currents on extracellular Ca^{2+} described by Maruyama *et al.*, 2006 (data not shown), indicating the presence of TRPC6/7 heteromers. Hence, the comparable norgestimate effect on AVP-stimulated currents in A7r5 cells and on homomeric TRPC6-mediated currents observed in our study may indicate a similar sensitivity of TRPC6 and TRPC7 subunits to norgestimate.

With the demonstration of norgestimate being more potent on the TRPC3/6/7 than on the TRPC4/5 subfamily, we identified a novel pharmacological tool compound that can be added to the list of already known TRP channel blockers. To further prove the potential value of norgestimate, it would be highly interesting to see to which extent norgestimate affects native TRPC4 or TRPC5 channels. Unfortunately, none of the described cellular models expressing TRPC4 or TRPC5 endogenously, e.g. gastric smooth muscle cells (Lee *et al.*, 2005) or

hippocampal growth cones (Greka *et al.*, 2003), is easily accessible and, therefore, a comparative investigation of native TRPC channel inhibition by norgestimate could not be accomplished within the framework of this study.

Nevertheless, we provide further support for the use of norgestimate as a tool compound in vascular tissue. TRPC6 is a non-selective cation channel and permeable both to monovalent, such as Na^+ , and divalent ions like Ca^{2+} . It has been proposed that TRPC6 mainly mediates Na^+ entry in vascular smooth muscle cells, and that the subsequent membrane depolarization results in activation of L-type Ca^{2+} channels that finally mediate vessel constriction (Soboloff *et al.*, 2005). As TRPC6 has been shown to be an essential component of α_1 -AR-activated cation channels in rabbit portal vein smooth muscles (Inoue *et al.*, 2001), and to be present in rat aorta smooth muscle cells (Facemire *et al.*, 2004; Lemos *et al.*, 2007), we tested the effect of norgestimate on isolated vessel rings from rat thoracic aorta precontracted with the α_1 -AR agonist phenylephrine. The vessel rings dose-dependently responded with relaxation to cumulative norgestimate concentrations. Norgestimate had an EC_{50} value of 15.1 μM and the response was endothelium-independent, as both endothelial and inducible nitric oxide synthase were pharmacologically inhibited by L-NAME. Complete vessel relaxation was not achieved even at high micromolar concentrations most likely due to the observed limited solubility of norgestimate in the organ bath solution. Consistent with its suggested role in α_1 -adrenergic vessel constriction (Inoue *et al.*, 2001; Soboloff *et al.*, 2005), this relaxation might be mediated by inhibition of the TRPC6 channel. However, possible additional effects of norgestimate in the vessel preparation need to be evaluated before the exact contribution of TRPC6 to the observed vessel relaxation can be finally determined.

4.2 Identification of SESTD1 – a novel TRPC-interacting protein

More than a decade after the cloning of TRPC4 and its first functional description as capacitative Ca^{2+} entry channel (Philipp *et al.*, 1996), there are still open questions regarding its activation mechanism and the constitution of native TRPC4 channel complexes. For example aortic endothelial cells from TRPC4^{-/-} mice lack an inwardly rectifying, La^{3+} -sensitive current that is activated by store depletion and is highly Ca^{2+} selective ($P_{\text{Ca}}/P_{\text{Na}} = 159.7$; Freichel *et al.*, 2001). In contrast sole TRPC4 expression, for example in HEK293 cells, is not sufficient to reproduce these current properties. Instead, TRPC4 homomers are non-selective ($P_{\text{Ca}}/P_{\text{Na}} = 1.05$), insensitive to store depletion and La^{3+} , and generate currents with a doubly rectifying current-voltage relationship (Schaefer *et al.*, 2002).

These inconsistencies motivated us to search for novel TRPC4-interacting proteins by screening a human aortic cDNA library with a GAL4-based yeast two-hybrid (Y2H) system. The applicability of this transcriptional assay is largely limited to hydrophilic proteins since the monitored interactions take place in the cell nucleus. As the transmembrane-spanning

segments of ion channels are hydrophobic, we could not employ the complete TRPC4 as a bait for our screen but instead used the soluble C-terminus of the longer mTRPC4 α isoform. It was preferred to the N-terminus as all TRPC channels including TRPC4 contain N-terminal ankyrin repeats, which mediate protein-protein interactions and are among the most common structural motifs found in proteins (Mosavi *et al.*, 2004). Therefore, we expected to find a significant number of ankyrin repeat-binding proteins that may not be specific for TRPC4 when using the N-terminal part of TRPC4 as bait. TRP channels are generally assumed to be tetramers, although the molecular determinants of TRPC4 channel oligomerization had not been defined when this study was performed. We therefore wanted to make sure that the mTRPC4 α -C-terminus expressed in our assay mimics its native structure as closely as possible. Hence, the channel fragment was covalently linked with an N-terminal leucine zipper domain, a peptide bearing a coiled-coil structure that mediates tetrameric assembly (Zerangue *et al.*, 2001). We reasoned that this modification favours identification of accessory proteins that require a native, tetrameric TRPC4 channel for their physical interaction.

Six of the eleven found mTRPC4-interacting proteins expressed transcription factors (BAZ1B, HMG2L1) and other nuclear (SMC3, MKRN1) or cytoskeletal (TLN2, SPATN1) proteins. Another identified protein, the pre-B-cell leukemia homeobox interacting protein 1, is believed to regulate the homeodomain protein PBX1 during hematopoiesis and leukemic transformation (Abramovich *et al.*, 2000) and to modulate the estrogen receptor α -dependent rapid estrogen signalling in a microtubule complex (Manavathi *et al.*, 2006). Furthermore, the sarcoma antigen NY-SAR 48 (Lee *et al.*, 2003a) and the apolipoprotein A-I binding protein, which is presumably involved in resorption and degradation of apoA-I (Ritter *et al.*, 2002), were found. None of the above mentioned proteins was further analyzed by us.

Two more proteins, the ANKRD35 and SESTD1 gene products, have not been described so far. Of these two, SESTD1 appeared as promising candidate for further investigation for the following reasons: (1) A domain motif search revealed the presence of an N-terminal Sec14p-like lipid binding domain that has been described to bind phospholipids (Saito *et al.*, 2007). As TRPC channels are activated by phospholipid hydrolysis (Hofmann *et al.*; 1999; Schaefer *et al.*, 2000; Trebak *et al.*, 2003), SESTD1 could potentially be involved in the regulation of TRPC channel function. (2) Two spectrin repeats, that are multivalent binding sites for cytoskeletal and signal transduction proteins (Djinovic-Carugo *et al.*, 2002), were also predicted to be present in SESTD1. Multiprotein complex assembly, a process potentially relevant for localization and anchoring of TRPC4 in caveolae, could be mediated by these domains. The presence of these structural features of SESTD1 finally motivated us to examine its binding to the channel and the functional consequences in more detail.

4.2.1 SESTD1 interacts with TRPC4 via the channel's CIRB domain

The first set of experiments was aimed towards identifying the interaction site between SESTD1 and the mTRPC4 α -C-terminus. For this purpose we conducted binary Y2H tests with SESTD1 as prey and stepwise truncated fragments of the TRPC4-C-terminus as baits. As construction of the leucine zipper-linked baits required a more complex cloning procedure we first tested whether this assay could be done with monomeric instead of tetrameric TRPC4 fragments. Indeed, an interaction between SESTD1 and the complete mTRPC4 α -C-terminus could also be detected when the channel fragment was cloned into the standard Y2H bait vector pGBKT7 (Clontech, Mountain View, USA). Although we cannot exclude the possibility that this C-terminal TRPC4 fragment itself oligomerized in yeast, studies in mammalian cells clearly showed that the C-terminus alone is not sufficient to cause homophilic assembly of TRPC4 channels (Lepage *et al.*, 2006; Schindl *et al.*, 2007). Thus, this result indicates that SESTD1 also is able to bind the C-terminal TRPC4 tail in its monomeric form.

Using the directed Y2H assay, we identified a short peptide sequence of 29 amino acid length (aa 700-728) in the TRPC4-C-terminus that was sufficient to mediate the interaction with full length SESTD1. Most notably, this section overlaps with the CaM/IP₃R binding (CIRB) domain (aa 695-724 of TRPC4) that is conserved in all TRPC channels (Tang *et al.*, 2001). Although the amino acid homology of this region within the TRPC family is only moderate, binding of CaM and the IP₃R to the respective sequences of hTRPC1, mTRPC2, hTRPC3, mTRPC4-7 was demonstrated by GST pulldown (Boulay *et al.*, 1999; Tang *et al.*, 2001). On the functional level, binding of the IP₃R at the CIRB site activates TRPC4 (Tang *et al.*, 2001) and TRPC3 (Zhang *et al.*, 2001). In contrast, competitive, Ca²⁺-dependent binding of CaM exerted an inhibitory effect (Tang *et al.*, 2001; Zhang *et al.*, 2001). More recently, the CIRB site has also been shown to be indispensable for receptor-induced activation of TRPC5 (Ordaz *et al.*, 2005). SESTD1 thus might play a role as an additional competitor at this domain in TRPC channels. However, when tested only TRPC4 and TRPC5, but not TRPC1 and TRPC6, were able to interact with SESTD1 in the Y2H assay, suggesting that, unlike CaM and IP₃R, SESTD1 binds specifically to the TRPC4/5 subfamily. Alignment of all TRPC CIRB domains reveals two non-conservative amino acid substitutions (Glu⁷⁰⁸ and Asn⁷¹² in mTRPC4) in TRPC4/5 compared to the DAG-sensitive TRPCs and TRPC1. These amino acids may be promising starting points for further analysis of the SESTD1-TRPC interaction by site-directed mutagenesis.

Having delineated the SESTD1-binding motif in TRPC4, we further used the Y2H approach to define the binding region in SESTD1. Whereas the Sec14p-like lipid-binding domain of SESTD1 did not interact with either TRPC4 or TRPC5, the Spec 1 domain of SESTD1

promoted growth of yeast colonies on selective -Trp/-Leu/-His/-Ade plates when cotransfected with the mTRPC4 α - or mTRPC5-C-terminus as a bait. Interaction between the second spectrin domain and the mTRPC4 α -C-terminus was not strong enough to allow survival of yeast, but was sufficient after cotransformation with the mTRPC5-C-terminus.

Later GST pulldown experiments confirmed the interaction of TRPC4 and TRPC5 with the Spec 1 domain. Binding of TRPC5 to the Spec 2 domain was only observed in some blots suggesting that this interaction is very weak. Although it can still be picked up by the highly sensitive Y2H assay, the physiological relevance of this interaction is questionable. In summary, the first spectrin repeat of SESTD1 was found with two independent methods to mediate binding to mTRPC4 as well as mTRPC5. Participation of the second spectrin domain in binding is possible but not clearly supported by our protein biochemical studies.

Interestingly, our primary Y2H screen identified the spectrin α -chain as a binding partner of the mTRPC4- α C-terminus, while binding of non-erythrocytic β -spectrin to TRPC5 in rat cerebral cortex was demonstrated by using a proteomics approach (Goel *et al.*, 2005). Although the binding sites on β -spectrin and TRPC5 were not further defined in this study, this interaction could involve the same structural elements as the TRPC4/5-SESTD1 interaction. However, the currently available data does not explain how the spectrin repeats bind to the SESTD1 binding-sequence of TRPC4 and TRPC5. As the identified binding region carries a positive charge at physiological pH, the interaction may involve electrostatic forces. In this regard, it would be informative to study the salt dependency of the SESTD1-channel binding, as high salt conditions weaken electrostatic but strengthen hydrophobic interactions (Cioffi *et al.*, 2005).

Y2H screens are sensitive *in vivo* assays that allow for a relatively fast identification of protein-protein interactions (Auerbach *et al.*, 2002). Nonetheless, they have intrinsic caveats as they are transcriptional assays and the investigated interactions take place in the cell nucleus. It is therefore obligatory to validate the observed physical interactions. For this purpose, we used two protein biochemical methods, namely GST pulldown and co-immunoprecipitation.

Full length SESTD1 N-terminally fused to GST was able to pull down the ectopically expressed mTRPC4 α -C-terminus from HEK293 cell lysates and thus confirmed the protein-protein interaction found in the Y2H assay. We further adapted this assay to confirm the Y2H-based interaction site mapping on SESTD1. The SESTD1 protein was divided into three fragments that were named after the respective included domain: GST-Sec 14 (aa 1-192), GST-Spec 1 (aa 193-406), and GST-Spec 2 (aa 407-696). Unfortunately, GST-Sec 14 could not be purified from *E. coli*. We assume that overexpression of the Sec14p-like lipid binding domain is toxic for bacteria as induction of recombinant protein expression also reduced their

growth noticeably. Similar difficulties were reported by another group (D'Angelo *et al.*, 2006), who was not able to purify the Sec14p-like lipid binding domain of neurofibromatosis type 1 protein. Three full-length channel proteins were tested, mTRPC4 α , mTRPC4 β and mTRPC5, and were significantly bound only by the GST-Spec 1 construct.

The most stringent test for protein-protein interaction *in vivo* is co-immunoprecipitation of the respective binding partners from cells or tissues. Due to the lack of available cell lines expressing native TRPC4 or TRPC5 channels (Greka *et al.*, 2003; Flockerzi *et al.*, 2005) we investigated first whether SESTD1 co-immunoprecipitates with TRPC4 and TRPC5 when overexpressed in HM1 cells. In fact, we detected HA-SESTD1 in precipitates from cells transfected with FLAG-tagged mTRPC4 β as well as GFP-tagged mTRPC5 channels. A small fraction of SESTD1 was unspecifically precipitated by anti-TRPC4 and anti-GFP antibodies from control HM1 cell lysates that only expressed HA-SESTD1 but no channel proteins. This background binding was seen under different precipitating conditions and was always much lower than in the presence of ion channel proteins. We, therefore, concluded that SESTD1 can interact with TRPC4 and TRPC5 *in vivo*.

Our Y2H experiments indicated that SESTD1 specifically interacts with the C-terminal parts of TRPC4 and TRPC5, but not TRPC1 or TRPC6 (see Chapter 3.2.5). When we tested the specificity of the SESTD1-channel interaction using co-immunoprecipitation, we unexpectedly found that SESTD1 and full length TRPC6 precipitated together. Although the fraction of SESTD1 that immunoprecipitated with TRPC6 was smaller compared to TRPC4 or TRPC5, binding was clearly above the unspecific background. Moreover, a distantly related TRP channel, TRPM8, which is lacking the SESTD1 binding domain, also interacted with SESTD1 in this assay. The amount of SESTD1 binding to TRPM8 was comparable to TRPC4/5. It is unlikely that these observations result from unspecific interactions of the used antibodies with overexpressed membrane proteins as overexpressed Kir2.1 channels did not immunoprecipitate with SESTD1. Apparently another SESTD1-binding site must be present in TRPC6 and TRPM8 in addition to the one delineated in this work for TRPC4 and TRPC5, the position of which is currently unknown. Sequence alignment of TRPC6 with TRPM8 does not reveal conserved regions outside the TRP-box, which, at least in the TRPC channels studied, is not interacting with SESTD1. Although the binding mode of SESTD1 to TRPC6 and TRPM8 is unclear, it is noteworthy that TRPC6 as well as TRPM8 are functionally regulated by phosphatidylinositol phosphates (Rohacs *et al.*, 2005; Kwon *et al.*, 2007). Hence, it is conceivable that SESTD1 may control TRPC6- and TRPM8-mediated currents via PIP-binding.

Having demonstrated co-immunoprecipitation of SESTD1 with both TRPC4 and TRPC5 in overexpressing cells, the next important step to verify the physiological relevance of this

interaction would be to verify native channel-SESTD1 complexes. As source of TRPC4 and TRPC5 protein we used rat brain, which was the only tissue for which immunoprecipitation of both channel proteins had been confirmed (Strubing *et al.*, 2001; Bezzerides *et al.*, 2004; Sinkins *et al.*, 2004; Goel *et al.*, 2005) at the time of our study. Unfortunately, using this tissue and commercially available antibodies we were unable to develop a suitable protocol for efficient precipitation of TRPC channels (data not shown). Thus, the final proof of TRPC-SESTD1 complexes in native cells and tissues remains a challenge for future studies.

4.2.2 Functional effects of SESTD1 knock-down on TRPC5

The physical interaction of SESTD1 with TRPC4 and TRPC5 could potentially modulate function of the channel proteins as well as of SESTD1. As the function of SESTD1 was unknown and thus could not be measured, we decided to investigate the effect of SESTD1 on TRPC4- or TRPC5-mediated currents. Because of the above mentioned lack of cells reliably expressing either native TRPC4 or TRPC5, we established a HEK293 cell line stably expressing TRPC5 (HM1-C5Y cells) for this purpose. TRPC5 was chosen since expression of mTRPC4 α or mTRPC4 β generated only variable and relatively small currents (data not shown).

Since SESTD1 co-immunoprecipitated with TRPC5-GFP, we assumed that a C-terminal YFP-tag also should not interfere with interaction of both proteins. Selection of single HM1-C5Y clones was guided by identification of fluorescent TRPC5-expressing cells, and functional channel expression was tested by stimulation of endogenous G_{q/11}-coupled receptors (PAR) or stably overexpressed M₁R in HM1 cells. Patch clamp experiments confirmed that both PAR- and M₁R-agonists activated robust TRPC5-currents in the selected HM1-C5Y clone. As readout for TRPC5 function we used ratiometric measurements of Ca²⁺ influx in HM1-C5Y cells, which allowed a fast and sensitive evaluation of many cells. With this method we also observed endogenous carbachol- and trypsin-sensitive channels in parental HM1 cells, but their contribution to the TRPC5-mediated Ca²⁺ influx signal is negligible (see Figure 32 A–D).

The most straightforward way to test for a SESTD1 effect on TRPC5 function was to overexpress SESTD1 in HM1-C5Y cells. These experiments, however, did not reveal any effect of SESTD1 on agonist-induced Ca²⁺ influx. SESTD1 antibodies detected a protein of expected size suggesting that HM1-C5Y cells also contain native SESTD1 protein. If the endogenous protein is already sufficiently expressed, further expression may not have additional effects on TRPC5.

Hence, we chose an siRNA-based knock-down strategy to investigate the effect of reduced SESTD1 protein levels on TRPC5. The used siRNA-pool decreased the endogenous protein levels by approx. 85% without apparent effects on general gene expression (see Figure 35). SESTD1 knock-down significantly and comparably reduced both carbachol- and trypsin-

activated Ca^{2+} influx by approx. 50% compared to control cells that were only treated with liposomes or unspecific non-targeting siRNA. Since a small portion of the investigated Ca^{2+} influx into HM1-C5Y cells is mediated by the endogenous trypsin- and carbachol-sensitive channels mentioned above, their function might as well be impaired due to reduced SESTD1 protein levels. Nevertheless, we did not further investigate this possibility since they only mediate a small fraction of the Ca^{2+} influx.

Importantly, no differences in Ca^{2+} release from internal stores between the various siRNA- and mock-treated groups were observed indicating that the complex signalling cascade leading from PAR/ M_1R via PLC to IP_3R opening is not affected by SESTD1. In contrast, the function of the TRPC5 channel, which is involved in the same enzymatic signalling cascade, is significantly impaired by SESTD1 protein knock-down pointing to a specific regulation of TRPC5 channels by SESTD1. How this regulation is accomplished remains to be clarified.

Initial patch-clamp analyses also did not reveal substantial changes in the electrophysiological properties of TRPC5-mediated currents in SESTD1-siRNA transfected cells (data not shown). We also tested the idea that SESTD1 is involved in the assembly and/or transport of TRPC5 to the plasma membrane by surface biotinylation experiments. These studies demonstrated similar surface expression of the channel protein independent of the treatment with liposomes, unspecific or specific siRNA. Therefore, interaction is likely to directly modulate the activity of the channel complexes at the plasma membrane. Further insights into the mechanism of SESTD1 regulation may be obtained from mutagenesis of the SESTD1 binding region. In this regard it is notable that mutations in the CIRB domain that overlaps with the SESTD1 binding sequence render TRPC5 insensitive to agonist stimulation (Ordaz *et al.*, 2005). Moreover, the effect of calmodulin and possibly IP_3R binding on the SESTD1-TRPC5 interaction will be of interest. As all three proteins share a common binding domain, competition or allosteric modulation may occur. Clearly, the indicated complex interactions with the CIRB site will make elucidation of the molecular events leading to functional regulation of TRPC5 a formidable task.

4.3 Cell biology of SESTD1

4.3.1 Tissue expression and subcellular localization

Modulation of TRPC channel function by SESTD1 raised the question whether channel activity *vice versa* may also influence SESTD1 function. Apart from the described domain structure and related information, we could not find any published data regarding SESTD1 function. To obtain first hints about its possible physiological roles we investigated SESTD1's expression pattern. Analysis of a human tissue panel revealed that SESTD1 transcripts are ubiquitously expressed and thus also found in tissues which express TRPC4 and/or TRPC5,

e.g. cerebellum, hippocampus, cortex, heart, aorta and AoSMC (Okada *et al.*, 1998; McKay *et al.*, 2000; Schaefer *et al.*, 2002; Facemire *et al.*, 2004; Soboloff *et al.*, 2005; Fowler *et al.*, 2007).

We extended the expression studies to SESTD1 protein, focusing on tissues that may also contain TRPC4 or TRPC5. Western blots confirmed the expression of SESTD1 protein in human endothelial and smooth muscle aortic cells. Because our antibodies were raised against conserved antigenic epitopes, they were predicted to recognize also mouse and rat SESTD1. Indeed, SESTD1 was detected in lysates from murine cardiomyocyte HL-5 cells, rat aortic smooth muscle A7r5 cells, mouse ventricle, and at least a fraction of the native protein is membrane-associated as it was found in the microsomal fraction of rat brain.

Unfortunately, apart from rat brain, we could not demonstrate expression of native TRPC channels in any of the tissues investigated. In brain microsomes we were able to identify TRPC5 (but not TRPC4) only after immunoprecipitation of significant amounts of tissue, but not directly on Western blots indicating a low expression level and/or low affinity to the antibodies used (data not shown). The low detection sensitivity, compared to other studies, may be due to different antibodies employed or differences in the origin and preparation of brain tissue. In light of these technical difficulties we were unable to perform meaningful co-immunoprecipitation studies of TRPC4 or -5 channels with SESTD1. Nevertheless, our preliminary experiments provide a solid basis for further immunocytochemical analysis of putative SESTD1-TRPC protein complexes in brain. The use of new specific antibodies or the isolation of particular brain areas such as hippocampus containing substantial amount of TRPC channels (Strubing *et al.*, 2001; Greka *et al.*, 2003; Fowler *et al.*, 2007) are promising options for improving the sensitivity of the co-immunoprecipitation assay.

To gain more insight into the function of SESTD1 and to investigate whether it colocalizes with TRPC channels, we determined its subcellular localization.

As evidenced by co-staining with anti-HA, our two anti-SESTD1 antibodies recognized overexpressed HA-SESTD1 in HM1 cells. Immunoreactivity was evenly distributed inside the cells. This localization was further confirmed by observation of C-terminally YFP-tagged SESTD1 that showed a similar distribution in HM1 cells (data not shown).

Although anti-SESTD1 #147 and #148 displayed a corresponding staining pattern of overexpressed HA-SESTD1, the two antibodies yielded different results when endogenous SESTD1 was studied by indirect immunofluorescence microscopy. Anti-SESTD1 #147 highlighted a vesicular pattern whereas anti-SESTD1 #148 predominantly visualized a tubular subcellular structure. The latter most likely reflects cross-reactivity with the abundantly expressed cytoskeletal protein tubulin as in some cells mitotic spindle poles were clearly stained. In agreement with this, on Western blots the anti-SESTD1 #148 recognized a

protein with the expected size of tubulin (~50 kDa). Although anti-SESTD1 #147 also unspecifically cross-reacted with an unrelated protein on Western blots, the vesicular pattern stained in immunofluorescence experiments with anti-SESTD1 #147 could indeed visualize the endogenous protein. It might be associated with vesicles due to binding of a specific phospholipid substrate (see 4.3.2 below). The abundance of this substrate in turn could be limiting for the anchoring and localization of SESTD1, thus, leading to the observed cytosolic distribution of heterologously overexpressed protein. In summary, although we could demonstrate that both anti-SESTD1 #147 and anti-SESTD1 #148 recognize overexpressed SESTD1 in immunofluorescence studies, more specific antibodies are needed to definitely elucidate the subcellular localization of endogenous SESTD1 and subsequently perform colocalization studies with TRPC5.

4.3.2 Enzymatic function of SESTD1

We identified two structural motifs in SESTD1 that share homology with known, catalytically active protein domains. The first of these motifs resembles a FKBP-type peptidyl-prolyl *cis-trans* isomerase (PPlase) signature (PROSITE pattern ID PS00454). PPlases accelerate protein folding by catalyzing *cis-trans* isomerization of proline peptide bonds. An additional regulatory role of prolyl isomerization in already folded, functional proteins has been proposed recently (Andreotti, 2006). This mechanism is also based on the isomerization of proline peptide bonds and leads to structural rearrangements, e.g. in the 5-HT₃ receptor, that regulate opening of the neurotransmitter-gated cation channel (Lummis *et al.*, 2005). Immunophilins like FKBP12 and -52 are PPlases (Davies & Sanchez, 2005) and their specific and selective interaction with TRPC3, -6, -7 (FKPB12) and TRPC1, -4, -5 (FKPB52) has been reported (Sinkins *et al.*, 2004). Pharmacological disruption of the FKPB12/TRPC6 interaction by the immunosuppressive drug FK506 attenuated TRPC6 current densities after receptor stimulation. The homology of SESTD1 with the PPlase motif was confined to a short (28 aa) peptide starting from aa 427. When tested for PPlase activity, we were not able to demonstrate this. This finding might be explained by the fact that SESTD1 does not contain the complete (89 aa) PPlase domain (PROSITE pattern ID PS50059) that is present in FKBP12 and -52 (Davies & Sanchez, 2005).

SESTD1 also contains a Sec14p-like lipid binding domain (Smart entry: smart00516), a structural motif named after the prototypic yeast Sec14p protein (Saito *et al.*, 2007). The SEC14 gene was originally identified in a complementation group of temperature-sensitive secretion (*sec*) mutants (Novick *et al.*, 1980) and encodes the major phosphatidylinositol (PI)/phosphatidylcholine (PC) transfer protein in *Saccharomyces cerevisiae* (Bankaitis *et al.*, 1990). It is essential for cell viability and necessary for a certain trafficking pathway from the *trans*-Golgi network to the membrane (Bankaitis *et al.*, 1989). The crystal structure of the

globular Sec14p protein reveals two lobes, the larger constituting a hydrophobic PI-binding pocket (Sha *et al.*, 1998). A homologous domain is found only in eukaryotes and to date more than 500 Sec14-like proteins have been identified (Mousley *et al.*, 2007). In most cases the function of these proteins is unknown. However, in higher eukaryotes Sec14-like proteins are likely to have more specialized functions than just PI transport which is mainly carried out by a structurally unrelated class of proteins, the phosphatidylinositol transfer proteins (PITP; Hsuan & Cockcroft, 2001; Saito *et al.*, 2007).

Although Sec14 domains are quite homologous, two main differences exist: a) some are devoid of the smaller lobe, and b) the amino acids forming the proposed binding pocket for the phospholipid head group are variable. Based on this, the ligands of a certain Sec14 domain are not predictable from protein structure alone (Saito *et al.*, 2007). We therefore tested whether SESTD1 acts as a PI binding protein *in vitro*. Indeed, we demonstrated specific binding of SESTD1 to phosphatidic acid (PA) and all naturally occurring phosphatidylinositol mono- and bisphosphates (Fruman *et al.*, 1998), whereas phosphatidylinositol 3,4,5-trisphosphate was not bound. Most remarkably, binding to phospholipids increased when the Ca^{2+} concentration was raised from resting physiological values (60 nM; Meldolesi & Pozzan, 1998) to a level (2.5 μM) that can be achieved locally by opening of Ca^{2+} influx channels (McCarron *et al.*, 2006). Given the close physical association of SESTD1 with TRPC4 and -5 it can be presumed that the fractional Ca^{2+} -influx mediated by the channels is sufficient to regulate SESTD1 phospholipid binding. The consequences of an increased association of SESTD1 with phosphatidylinositol bisphosphates, however, are unclear.

A recent report demonstrated that TRPC channels can also bind phospholipids directly with a specificity that is strikingly similar to that observed for SESTD1 (Kwon *et al.*, 2007). The PIP binding site was mapped to amino acids 842-873 in hTRPC6, a region overlapping with the CIRB domain (Tang *et al.*, 2001). For TRPC5, PIP binding to the C-terminus was also detected but the binding site was not further mapped and it is also not known whether PIP binding activates or inhibits the channel's activity. Based on this data, it is tempting to speculate about possible mechanisms of TRPC5 regulation by SESTD1. The observation that SESTD1 knock-down inhibits TRPC5 suggests an activating effect of SESTD1 binding to TRPC5. Thus, it is conceivable that competition of SESTD1 with phospholipid-binding to the CIRB site stimulates TRPC4/5. Upon initial activation of the channel, a Ca^{2+} -induced increase in the affinity of SESTD1 for PIPs may displace phospholipids from the channel leading to conformational changes and further channel activation. On the other hand, SESTD1 may not only bind but also transport phospholipids like many of its yeast

homologues (Bankaitis *et al.*, 1990). Ca^{2+} entry could thus facilitate localized delivery of specific PIPs to the channel's C-terminus. This could then enhance channel activity either through direct conformational coupling or by providing a substrate for PLC-mediated activation. Obviously, there are many more possible scenarios for a mechanistic explanation of the SESTD1-TRPC4/5 interaction. The involvement of PIP-binding or -signalling seems to be a sensible key element of such models.

There are some crucial questions that need to be answered in order to refine our current understanding of the putative TRPC-SESTD1-PIP connection. For instance, it would be important to know how TRPC4/5 gating is modulated by PIPs and whether SESTD1 has a PIP-transfer activity.

In order to allow a better quantification of SESTD1 phospholipid binding and to design an assay that may be used to screen for modulators of SESTD1-phospholipid interaction, we tested SESTD1 binding to phospholipid-loaded 96 well polystyrene plates (Cova-PIP Specificity Plates). After modifying the amount of bound PIPs, we found that this assay was suitable to measure SESTD1 binding. The plate assay confirmed the results of the overlay assay by demonstrating selective binding of SESTD1 to PIPs. The highest affinity was observed for $\text{PI}(4,5)\text{P}_2$, the most abundant cellular PIP_2 that is also hydrolyzed by PLC. Thus, one may assume that channel regulation by SESTD1 involves $\text{PI}(4,5)\text{P}_2$.

In contrast to the overlay assay, we also detected binding of SESTD1 to $\text{PI}(3,4,5)\text{P}_3$ in PIP plates. Although this result is interesting in the context of the suggested role of $\text{PI}(3,4,5)\text{P}_3$ in TRP channel regulation (Kwon *et al.*, 2007), it needs to be treated with caution. The phospholipids spotted onto PIP strips and covalently attached to the polystyrene plates (Hy-PIPs) do not differ in terms of their lipids, they possess naturally occurring diC16 acyl chains. Yet, their physiological glycerol backbone is replaced by 1,2,3,4-butanetetraol in Hy-PIPs. This modification introduces an additional hydroxyl group that is further linked to phosphatidylethanolamine and covalently bound to the plate via this amine (information provided by Michael Landward, Echelon Biosciences Inc.). Therefore, the substrates in these two assays are not exactly the same what might explain the different binding observed to $\text{PI}(3,4,5)\text{P}_3$.

Independent of TRPC channel regulation, the lipid binding activity of SESTD1 may hint to other functions of the protein. $\text{PI}(3)\text{P}$ is involved in the membrane trafficking pathway to the lysosome where proteins are degraded. It is present on early endosomes, and it is also a precursor of $\text{PI}(3,5)\text{P}_2$ that is found on later endocytotic compartments. $\text{PI}(4)\text{P}$ is located at the Golgi but also at the PM, where it serves as a substrate for the synthesis of $\text{PI}(4,5)\text{P}_2$. $\text{PI}(5)\text{P}$ was found in the nucleus, the Golgi network and the PM, and is thought to be involved

in bacterial invasion and the control of cell morphology and actin assembly (Behnia & Munro, 2005; Pendaries *et al.*, 2005). PA, that is also bound by SESTD1, serves as a precursor of other phospholipids and triacylglycerol but also as a signalling lipid (Stace & Ktistakis, 2006), e.g. by stimulating cardiac K_{ATP} channels (Fan *et al.*, 2003). The involvement of SESTD1 in any of these processes needs to be established.

Finally, the Sec14p-like domain could regulate SESTD1's spatial distribution as has been demonstrated for some multi-domain proteins with Sec14p-like and spectrin domains like Dbl, Duo and Trio (Ueda *et al.*, 2004; Kostenko *et al.*, 2005; Saito *et al.*, 2007). These proteins contain further functional domains (e.g. RhoGEF and PH domains) and constitute guanine-nucleotide-exchange factors (GEFs) specific for the reactivation of Rho family GTPases. They in turn modulate different downstream effectors that alter actin dynamics and/or localization, cell adhesion, and gene transcription (O'Brien *et al.*, 2000; Bateman & Van Vactor, 2001).

4.3.3 Regulation of β -catenin

HM1 cells, which were depleted of SESTD1 by the use of siRNA, seemed to differ slightly in their morphology compared to control cells treated with unspecific, non-silencing siRNA or liposomes only. Cells appeared more slender and less clustered, but it was difficult to quantify these changes by light microscopy. Therefore, we tried to visualize the morphological changes in siRNA-treated cells by immunostaining of cell adhesion markers. Direct contacts between epithelial cells are formed by tight, gap and anchoring junctions. The latter are subclassified in adherens junctions and desmosomes (Lodish *et al.*, 2003). HM1 cells used for immunofluorescence experiments are of epithelial origin (Peralta *et al.*, 1988; Thomas & Smart, 2005) and express the scaffolding protein zona occludens 1 (ZO-1) that is associated with tight junctions (Stevenson *et al.*, 1986). ZO-1 was shown to colocalize with hTRPC4 in fetal astrocytes, and this interaction was mediated by the PDZ-binding domain at the distal C-terminus of the channel (Song *et al.*, 2005). This motif is unique to TRPC4 and -5 within the TRPC subfamily, but binding of ZO-1 to TRPC5 has not been tested. We compared ZO-1 staining in permeabilized SESTD1 siRNA-treated HM1 cells with control-treated HM1 cells. The results were not unambiguous. Overall ZO-1 distribution was similar in both cell types, but we frequently observed areas with decreased ZO1-staining only in cells with SESTD1 knock-down. Since we did not find conditions under which this effect could be further enhanced, modification of tight junctions by siRNA-mediated SESTD1 protein knock-down remains an open issue.

In contrast to ZO-1, we discerned a clear effect of SESTD1 knock-down on the localization of β -catenin, a protein that connects the adherens junction component E-cadherin to α -catenin.

This cadherin/catenin complex is linked to the actin cytoskeleton by direct binding of α -catenin to actin (Rimm *et al.*, 1995) or to α -actinin (Knudsen *et al.*, 1995). In cells treated with specific siRNA against SESTD1 β -catenin distribution shifted from an almost exclusive plasma membrane-association to a predominantly intracellular localization with some residual staining at cell-cell contacts.

The most plausible explanation for the observed redistribution of β -catenin is that SESTD1 is somehow involved in the formation or maintenance of adherens junctions. If less adherens junctions are formed, less β -catenin in turn is recruited to the PM by binding to E-cadherin. This would also fit to the observed slight changes in cell shape. Direct visualization of E-cadherin could provide further evidence for such a mechanism, but we were unable to detect E-cadherin by immunofluorescence microscopy using commercially available antibodies. Even less clear than the mechanism of β -catenin redistribution itself are the consequences of this process. In addition to being a structural protein, β -catenin serves as intracellular effector of both the integrin-linked kinase (ILK) pathway (Novak *et al.*, 1998) and the Wnt signalling pathway (Miller *et al.*, 1999 and references therein). In the latter, cytosolic β -catenin translocates to the nucleus in a phosphorylation-dependent way, where it acts as cofactor of the lymphoid enhancer factor/T cell factor (LEF/TCF) family of DNA-binding proteins to regulate the transcription of diverse genes (Chesire & Isaacs, 2002 and references therein). The dual role of β -catenin as structural protein and gene transcription-modulating element further complicates the interpretation of our observation.

We have not tested whether SESTD1 knock-down alters expression of other genes. Given the known caveats of siRNA technology a thorough testing of the used siRNAs and the development of appropriate controls are necessary before such experiments can be considered. Undoubtedly, however, such studies hold the potential to reveal many novel aspects of SESTD1 function.

5 Summary

TRPC channels mediate non-selective cation currents and are considered as promising drug targets for the treatment of cardiac, pulmonary and renal diseases. Nevertheless, many questions regarding their native constitution, activation mechanisms, and (patho) physiological roles remain open. Gaining a better understanding of TRPC channel function is complicated by their broad and partially overlapping distribution, possible heteromultimerization and similar electrophysiological properties (Moran *et al.*, 2004). Moreover, available TRPC channel blockers, e.g. 2-APB, SK&F 96365 and lanthanides, are not specific and potent enough to allow an unambiguous pharmacological distinction of TRPC-mediated conductances *in vivo*.

In the first part of this study, we have identified two steroid hormones, the natural hormone progesterone and the synthetic progestin norgestimate, as novel TRPC channel blockers. In fluorometric measurements of TRPC-mediated Ca^{2+} influx both substances blocked the investigated TRPC channels with micromolar activities. TRPC channel inhibition did not seem to be a general steroid effect since another progestin, the norgestimate metabolite levonorgestrel, was not effective. Norgestimate was 4- to 5-fold more active on the TRPC3/6/7 subfamily compared to TRPC4/5, whereas progesterone was similarly potent. This selectivity of norgestimate was confirmed by patch clamp recordings from members of the two TRPC subfamilies. As norgestimate blocked channels directly gated by DAG with a fast kinetic, we assume the compound acts on the channel protein itself. This view is further substantiated by the lack of effects on IP_3R -mediated Ca^{2+} release from the ER which is activated in parallel with TRPCs by $\text{G}_{q/11}$ -coupled receptor stimulation. Norgestimate did not only block ectopically expressed TRPC channels but also native, TRPC-mediated currents in rat A7r5 aortic smooth muscle cells with similar activity. To test the usefulness of norgestimate as a tool compound for the investigation of physiological TRPC functions, we applied it to isolated vessel rings. Consistent with TRPC6 being an essential component of the α_1 -AR-activated cation channel, we demonstrated a direct vasorelaxant, endothelium-independent effect of norgestimate on rat aortic rings precontracted with phenylephrine. Thus, our results provide further experimental support for a role of TRPC6 in α_1 -adrenergic vessel constriction.

In the second part of this study we screened a human aorta cDNA-library for novel TRPC4-interacting proteins with a modified Y2H system in which the TRPC4-C-terminus was expressed as tetrameric bait protein, thereby mimicking the native channel conformation. Eleven interacting proteins were found, none of which has been described before to interact with TRPC4. From these, SESTD1 was chosen for further analyses since it contains a

phospholipid-binding Sec14p-like domain and therefore could be involved in regulation of TRPC channels by phospholipids. First, the found interaction was biochemically validated by GST pulldown and co-immunoprecipitation studies. Employing different parts of SESTD1 in directed Y2H tests, the first spectrin domain was then identified to interact with the CIRB domain of TRPC4. Consistent with this result, SESTD1 co-immunoprecipitated with the closely related TRPC5 protein in which the SESTD1-binding domain is highly conserved. Independent of the CIRB site, co-immunoprecipitation with TRPC6 and the distantly related TRPM8 channel was observed indicating the existence of other sites in these channel proteins that mediate interaction with SESTD1.

Analysis of SESTD1 gene expression in human tissues showed that its transcripts are ubiquitously expressed and tissues with significant coexpression with TRPC4 and -5 were identified. We have generated two polyclonal antisera directed against SESTD1 that consistently detected SESTD1 protein in brain, aorta, heart, and in smooth muscle and endothelial cells.

The functional consequences of the found interaction were investigated by examination of the TRPC5-mediated Ca^{2+} influx in a clonal HM1 cell line stably expressing the channel. Since SESTD1 overexpression had no detectable effects on TRPC5 currents, most likely due to expression of endogenous SESTD1, we knocked-down the native protein with specific siRNA. This procedure reduced TRPC5-mediated Ca^{2+} influx following receptor stimulation by 50%. Parallel biotinylation experiments did not reveal any differences in cell surface expressed TRPC5-protein, suggesting that reduction of TRPC5 activity resulted from a loss of a direct SESTD1 effect on the channel. In addition, we observed that reduced SESTD1 protein levels resulted in a redistribution of the multifunctional protein β -catenin from the plasma membrane to the cytosol. This result may point to an involvement of SESTD1 in formation and maintenance of adherens junctions.

SESTD1 contains a phospholipid-binding Sec14p-like domain and we were the first to demonstrate its Ca^{2+} -dependent binding to phosphatidic acid and all physiological phosphatidylinositol mono- and bisphosphates *in vitro*. The physiological function of this binding activity is not known at present, but might play a role in regulation of associated TRPC channels. TRPC5 channels also directly bind phospholipids although the functional consequences of this binding remain speculative. The TRPC3/6/7 subfamily is directly stimulated by the PIP_2 hydrolysis product DAG and the reduction of the PIP_2 concentration has been proposed to facilitate channel activation in parallel. The presented phospholipid-binding and putative -transferring activity of SESTD1 seems to be involved in this complex channel regulation. The identification of SESTD1 as novel TRPC-interacting protein could thus be an important step forward in the investigation and better comprehension of the molecular mechanisms of TRP channel regulation by lipids.

6 Zusammenfassung

TRPC-Proteine formen Ionenkanäle mit variabler Selektivität für Kationen und erweckten zunächst Interesse als mögliche Vermittler des kapazitiven Ca^{2+} -Einstroms in elektrisch nicht-erregbare Zellen. Aufgrund ihrer Aktivität kontrollieren TRPC-Kanäle viele zelluläre Vorgänge, wie G-Protein vermittelte Rezeptoraktivierung, intrazelluläre Kalziumspeicherung, Phospholipid-Signalweg, Zellwachstum sowie andere wichtige Funktionen. Inzwischen werden sie aber auch als interessante mögliche Angriffsziele zur Behandlung von Herz-, Lungen- und Nierenerkrankungen untersucht.

Über die genaue molekulare Struktur und Wirkungsweise der TRPC-Kanäle ist noch wenig bekannt, was das Verstehen ihrer physiologischen Funktion und ursächlichen Beteiligung an Krankheiten erschwert. Die Gründe hierfür sind, dass die sieben in Säugern vorkommenden TRPC-Proteine eine sehr breite und zum Teil überlappende Gewebsexpression aufweisen, miteinander heteromere Kanalkomplexe bilden können, ähnliche elektrophysiologische Eigenschaften besitzen und bereits bekannte TRPC-Blocker nicht selektiv und spezifisch genug für die Unterscheidung nativer TRPC-Kanäle sind.

Aus diesem Grund haben wir in der vorliegenden Arbeit nach neuen pharmakologischen TRPC-Modulatoren gesucht und zwei Steroide, das natürliche Hormon Progesteron und das synthetische Gestagen Norgestimat, als Inhibitoren identifiziert und näher charakterisiert. Beide Substanzen hemmten die untersuchten TRPC-Kanäle im mikromolaren Konzentrationsbereich. Ein aktiver Metabolit des Norgestimats, das Levonorgestrel, war hingegen nicht wirksam. Diese unterschiedliche Wirkung der strukturell nahe verwandten Substanzen schließt eine unspezifische Hemmung von TRPC-Kanälen durch diese Steroide aus.

In fluorometrischen Messungen des TRPC-vermittelten Ca^{2+} -Einstroms hemmte Norgestimat die Vertreter der TRPC3/6/7-Unterfamilie vier- bis fünfmal stärker als TRPC4 und -5. Im Gegensatz dazu war die Wirkung von Progesteron auf beide Unterfamilien vergleichbar. Die IP_3R -vermittelte Ca^{2+} -Freisetzung aus dem ER, die an der Aktivierung der Kanäle nach Rezeptorstimulation beteiligt ist, war in diesen Experimenten nicht durch die Steroide beeinflusst worden. Dies deutet auf eine direkte Wirkung der Hormone auf die Funktion der Kanäle hin.

Aufgrund seiner selektiven Wirkung wurde Norgestimat hinsichtlich seiner Eignung als potentieller Standardblocker von TRPC-Kanälen näher untersucht. Zunächst konnte seine selektive Wirkung auf die beiden TRPC-Unterfamilien durch Patch Clamp Messungen der entsprechenden Ströme in Zellen bestätigt werden, die stabil mit den Kanälen transfiziert waren. Die Applikation der Substanzen bewirkte eine rasche Hemmung der Kanäle, welche

durch Auswaschen der Blocker ebenso schnell reversibel war. Diese schnelle Kinetik ist ein weiterer Hinweis dafür, dass eine indirekte, für Steroidhormone charakteristische genomische Wirkung als Ursache für die Kanalblockade ausgeschlossen werden kann. Die Steroide hemmten zudem nicht nur die Aktivität der heterolog exprimierten Kanäle, sondern auch native, TRPC-vermittelte Ströme in glatten Gefäßmuskelzellen aus Rattenaorten. Aufgrund dieser Eigenschaften verwendeten wir Norgestimat, um die Beteiligung der TRPC-Kanäle bei der Gefäßrelaxation näher zu untersuchen. Tatsächlich konnte an vorkontrahierten Aortenringen aus der Ratte nach Gabe von Norgestimat eine endothel-unabhängige Relaxation beobachtet werden. In Übereinstimmung mit bekannten Literaturdaten legt auch dieses Ergebnis nahe, dass TRPC6-Kanäle an der Regulation des Gefäßtonus beteiligt sind und damit eine wichtige Rolle bei der Kontrolle des Blutdrucks spielen könnten. Zusammenfassend zeigen die vorgestellten Resultate, dass mit Norgestimat ein geeignetes pharmakologisches Werkzeug gefunden wurde, das die weitere Erforschung der physiologischen Funktionen von TRPC-Proteinen und ihrer Rolle bei humanen Krankheiten erleichtern könnte. Zudem stellt es möglicherweise auch einen ersten Ansatzpunkt für die weitere Entwicklung therapeutisch nützlicher Substanzen dar.

Die Suche nach TRPC-modulierenden Wirkstoffen für die therapeutische Nutzung wird auch dadurch erschwert, dass sich die Eigenschaften von heterolog exprimierten Kanälen von denen der nativen Kanäle unterscheiden können wie es beispielsweise für den TRPC4-Kanal beschrieben wurde. Dies lässt darauf schließen, dass native TRPC4-Kanalkomplexe eine andere molekulare Zusammensetzung aufweisen als heterolog exprimierte TRPC4-Homotetramere und außerdem bislang noch unbekannte Interaktionspartner oder regulatorische Untereinheiten existieren. Ein weiteres Ziel dieser Arbeit war es deshalb, neue Interaktionspartner von TRPC4-Kanälen zu finden und diese anschließend funktionell zu untersuchen. Zu diesem Zweck wurde zunächst eine cDNS-Bibliothek aus menschlichen Aorten mit Hilfe eines modifizierten Hefe Zwei-Hybrid Systems durchmustert. Als Köderprotein diente der C-Terminus des TRPC4-Kanalproteins. Die Besonderheit des verwendeten Hefe Zwei-Hybrid Systems bestand darin, dass das Köderprotein als tetrameres Fusionsprotein, d.h. in seiner nativen Konformation, vorlag.

Nach mehrmaligem Durchmustern der cDNS-Bibliothek wurden insgesamt elf Interaktionspartner des TRPC4-Kanals isoliert, von denen keiner zuvor als Interaktionspartner für TRPC4-Kanäle beschrieben worden ist. Aus diesen wurde das SESTD1-Protein aufgrund seiner Struktur für weitergehende Untersuchungen ausgewählt. Es besitzt eine phospholipidbindende Sec14p-Domäne sowie zwei Spektrindomänen. Da TRPC-Kanäle in ihrer Aktivität durch Phospholipide reguliert werden und Spektrindomänen

an der Bildung von Multiproteinkomplexen beteiligt sind, erschien SESTD1 vielversprechend für eine detailliertere Charakterisierung.

Die in den Hefezellen beobachtete Interaktion von SESTD1 und TRPC4 wurde zunächst durch zwei unabhängige proteinbiochemische Methoden bestätigt. Bakteriell exprimierte und gereinigte GST-SESTD1-Fusionsproteine waren in Pulldown-Experimenten in der Lage, TRPC4-Proteine aus Säugerzellextrakten zu binden. Ebenso wurde die Koimmunopräzipitation beider Proteine aus Lysaten transfizierter Säugerzellen nachgewiesen.

Unter Verwendung von SESTD1-Proteinfragmenten wurde anschließend in direkten Interaktionsstudien in Hefezellen und in GST-Pulldown-Experimenten die erste Spektrindomäne von SESTD1 als notwendig und ausreichend für die Bindung an das TRPC4-Protein identifiziert. Umgekehrt konnte durch den Einsatz von C-terminal verkürzten TRPC4-Köderproteinen die CIRB-Domäne des Kanalproteins als Bindungspartner für die SESTD1-Spektrindomäne bestimmt werden. SESTD1 war auch in der Lage, das nahe verwandte TRPC5-Protein zu binden, da in diesem Kanal die SESTD1-Interaktionssequenz hoch konserviert ist. Die erfolgreiche CIRB-unabhängige Koimmunopräzipitation von SESTD1 mit TRPC6 und dem entfernter verwandten TRPM8-Kanalprotein weisen jedoch darauf hin, dass diese TRP-Kanäle noch weitere SESTD1-Bindungsstellen besitzen müssen.

Nachdem wir die in dem transkriptionellen Hefeassay beobachtete Interaktion zwischen SESTD1 und TRPC4 bzw. -5 mit biochemischen Methoden verifiziert hatten, untersuchten wir die Expression von SESTD1-Transkripten in verschiedenen Geweben. Es stellte sich heraus, dass SESTD1 ubiquitär und damit beispielsweise in Gehirn, Herz und Aorta überlappend mit TRPC4 bzw. -5 exprimiert wird. Für den Nachweis des SESTD1-Proteins wurden zudem polyklonale Antikörper hergestellt. Als Antigene für die Immunisierung von Kaninchen wurden zwei Peptide eingesetzt, deren Aminosäuresequenzen in den SESTD1-Proteinen von Mensch, Maus und Ratte konserviert sind. Beide Antiseren erkannten in Western Blot Analysen von stabil-transfizierten Zelllinien das SESTD1-Protein. Mithilfe dieser Antikörper konnte das Vorkommen von SESTD1 in verschiedenen primären menschlichen Gefäßmuskel- und Endothelzellen nachgewiesen werden. Außerdem wurde SESTD1-Proteinexpression auch im Gehirn von Ratte und im Herz von Maus bestätigt.

Um die subzelluläre Lokalisation des endogenen SESTD1-Proteins und seine mögliche Kolo-kalisation mit dem TRPC5-Kanal zu untersuchen, wurden Immunfluoreszenzstudien an HM1-Zellen durchgeführt. Das Antiserum #148 färbte vorwiegend tubuläre Strukturen an. Dieses Muster beruht sehr wahrscheinlich auf der bereits in der Western Blot Analyse angedeuteten Kreuzreaktivität mit Tubulin. Mit dem Antiserum #147 ergab sich dagegen ein hauptsächlich vesikuläres Verteilungsmuster. Da auch dieses Antiserum im Western Blot ein

weiteres Protein erkannte, kann nicht mit Sicherheit angenommen werden, dass dies die wirkliche subzelluläre Lokalisation von SESTD1 widerspiegelt. Für den eindeutigen Nachweis einer Kolo­kalisierung von SESTD1 mit TRPC5 waren unsere beiden Antiseren aufgrund der zu geringen Spezifität ebenfalls nicht geeignet. Da bisher auch keine weiteren Antiseren beschrieben oder kommerziell erhältlich sind, muss die letztliche Bestimmung der SESTD1 Lokalisation in Zellen zukünftigen Untersuchungen vorbehalten bleiben.

Zur funktionellen Charakterisierung der gefundenen Interaktion wurden mögliche Wirkungen von SESTD1 auf den TRPC5-vermittelten Ca^{2+} -Einstrom exemplarisch untersucht. Dafür wurde eine HM1-C5Y-Zelllinie hergestellt, die zusätzlich zu dem TRPC5-Kanal auch den M_1 -Acetylcholinrezeptor stabil exprimiert, dessen Stimulierung zur TRPC5-Aktivierung genutzt werden kann. Die Überexpression von SESTD1 in dieser Zelllinie hatte jedoch keinen signifikanten Effekt auf den TRPC5-vermittelten Ca^{2+} -Einstrom. Western Blot Studien ergaben allerdings, dass SESTD1 endogen von diesen Zellen exprimiert wird. Wir vermuten deshalb, dass die Menge des endogenen SESTD1-Proteins bereits ausreichend für eine maximale Wirkung auf den TRPC5-vermittelten Ca^{2+} -Einstrom ist. Deshalb wurde in einer weiteren Studie die Menge des endogenen SESTD1-Proteins mittels spezifischer siRNA stark reduziert. Durch die erzielte Hemmung der SESTD1-Expression war der TRPC5-vermittelte Ca^{2+} -Einstrom nach Rezeptorstimulation um etwa die Hälfte verringert. Biotinylierungsstudien zeigten aber, dass die Menge des TRPC5-Proteins an der Plasmamembran nicht verändert war. Diese Ergebnisse legen wiederum einen direkten Einfluss von SESTD1 auf die Kanalaktivität nahe. Immunfluoreszenzstudien zeigten außerdem, dass die siRNA-vermittelte Reduzierung der SESTD1-Proteinexpression zu einer Umverteilung des multifunktionellen β -Catenin-Proteins führte. In Kontrollzellen war es vor allem an der Plasmamembran lokalisiert, wo es an der Vermittlung von Zell-Zell-Kontakten beteiligt ist, während es sich in SESTD1-siRNA-behandelten Zellen vor allem im Zytosol befand. SESTD1 ist also möglicherweise an der Bildung und/oder Aufrechterhaltung von Zell-Zell-Kontakten beteiligt.

Um erste Hinweise auf den molekularen Mechanismus der Interaktion zwischen SESTD1 und TRPC5 zu erhalten, untersuchten wir abschließend, ob SESTD1 Phospholipide binden kann, wie es das Vorhandensein der Sec14p-Domäne andeutet. Wir fanden, dass rekombinantes GST-SESTD1-Fusionsprotein tatsächlich Phospholipide binden konnte, die auf Nitrocellulose-Membranen immobilisiert waren. Neben Phosphatidylsäure wurden auch alle physiologisch vorkommenden Phosphatidylinositolmono- und -diphosphate gebunden. Interessanterweise wurde diese Bindung Ca^{2+} -abhängig moduliert. Diese Calciumsensitivität

eröffnet die faszinierende Möglichkeit einer dualen Regulation sowohl von TRPC4/5 durch SESTD1 als auch von SESTD1 durch TRPC-vermittelten Ca^{2+} -Einstrom.

Für mögliche zukünftige nichtradioaktive SESTD1-Substratbindungsstudien haben wir einen Bindungsassay etabliert, der diese Untersuchungen in 96-Wellplatten und damit die effiziente Identifizierung von SESTD1-Modulatoren ermöglichen könnte.

Phospholipide sind in komplexer Weise an der Regulation von TRPC4 und TRPC5 beteiligt. Sie stellen das Substrat für die zur Kanalaktivierung essentiellen Hydrolysefunktionen von PLC dar und binden darüber hinaus direkt an die Kanalproteine. Die Identifizierung von SESTD1 als TRPC-interagierendes Protein könnte ein wichtiger Schritt zur mechanistischen Aufklärung der Kanal-Lipid-Wechselwirkung sowie ihrer funktionellen Konsequenzen sein.

7 References

- Abramovich C, Shen WF, Pineault N, Imren S, Montpetit B, Largman C, & Humphries RK (2000). Functional cloning and characterization of a novel nonhomeodomain protein that inhibits the binding of PBX1-HOX complexes to DNA. *J Biol Chem* **275**, 26172-26177.
- Alderton JM, Ahmed SA, Smith LA, & Steinhardt RA (2000). Evidence for a vesicle-mediated maintenance of store-operated calcium channels in a human embryonic kidney cell line. *Cell Calcium* **28**, 161-169.
- Allen-Baume V, Segui B, & Cockcroft S (2002). Current thoughts on the phosphatidylinositol transfer protein family. *FEBS Lett* **531**, 74-80.
- Alton KB, Hetyei NS, Shaw C, & Patrick JE (1984). Biotransformation of norgestimate in women. *Contraception* **29**, 19-29.
- Ambudkar IS, Ong HL, Liu X, Bandyopadhyay B, & Cheng KT (2007). TRPC1: The link between functionally distinct store-operated calcium channels. *Cell Calcium* **42**, 213-223.
- Ambudkar IS & Ong HL (2007). Organization and function of TRPC channelosomes. *Pflugers Arch* **455**, 187-200.
- Amiri H, Schultz G, & Schaefer M (2003). FRET-based analysis of TRPC subunit stoichiometry. *Cell Calcium* **33**, 463-470.
- Andreotti AH (2006). Opening the pore hinges on proline. *Nat Chem Biol* **2**, 13-14.
- Antoniotto S, Fiorio PA, Barral S, Scalabrino O, Munaron L, & Lovisolo D (2006). Interaction between TRPC channel subunits in endothelial cells. *J Recept Signal Transduct Res* **26**, 225-240.
- Auerbach D, Galeuchet-Schenk B, Hottiger MO, & Stagljar I (2002). Genetic approaches to the identification of interactions between membrane proteins in yeast. *J Recept Signal Transduct Res* **22**, 471-481.
- Balzer M, Lintschinger B, & Groschner K (1999). Evidence for a role of Trp proteins in the oxidative stress-induced membrane conductances of porcine aortic endothelial cells. *Cardiovasc Res* **42**, 543-549.
- Bankaitis VA, Malehorn DE, Emr SD, & Greene R (1989). The *Saccharomyces cerevisiae* SEC14 gene encodes a cytosolic factor that is required for transport of secretory proteins from the yeast Golgi complex. *J Cell Biol* **108**, 1271-1281.
- Bankaitis VA, Aitken JR, Cleves AE, & Dowhan W (1990). An essential role for a phospholipid transfer protein in yeast Golgi function. *Nature* **347**, 561-562.
- Bano D & Nicotera P (2007). Ca²⁺ signals and neuronal death in brain ischemia. *Stroke* **38**, 674-676.
- Barbagallo M, Dominguez LJ, Licata G, Shan J, Bing L, Karpinski E, Pang PK, & Resnick LM (2001). Vascular Effects of Progesterone: Role of Cellular Calcium Regulation. *Hypertension* **37**, 142-147.
- Basora N, Boulay G, Bilodeau L, Rousseau E, & Payet MD (2003). 20-hydroxyeicosatetraenoic acid (20-HETE) activates mouse TRPC6 channels expressed in HEK293 cells. *J Biol Chem* **278**, 31709-31716.

- Bassi MT, Manzoni M, Monti E, Pizzo MT, Ballabio A, & Borsani G (2000). Cloning of the gene encoding a novel integral membrane protein, mucolipidin and identification of the two major founder mutations causing mucopolidosis type IV. *Am J Hum Genet* **67**, 1110-1120.
- Bateman J & Van VD (2001). The Trio family of guanine-nucleotide-exchange factors: regulators of axon guidance. *J Cell Sci* **114**, 1973-1980.
- Beech DJ, Xu SZ, McHugh D, & Flemming R (2003). TRPC1 store-operated cationic channel subunit. *Cell Calcium* **33**, 433-440.
- Beech DJ, Muraki K, & Flemming R (2004). Non-selective cationic channels of smooth muscle and the mammalian homologues of Drosophila TRP. *J Physiol* **559**, 685-706.
- Behnia R & Munro S (2005). Organelle identity and the signposts for membrane traffic. *Nature* **438**, 597-604.
- Bell RM & Burns DJ (1991). Lipid activation of protein kinase C. *J Biol Chem* **266**, 4661-4664.
- Bergdahl A, Gomez MF, Wihlborg AK, Erlinge D, Eyjolfson A, Xu SZ, Beech DJ, Dreja K, & Hellstrand P (2004). Plasticity of TRPC expression in arterial smooth muscle: correlation with store-operated Ca²⁺ entry. *Am J Physiol Cell Physiol*.
- Berridge MJ (1993). Inositol trisphosphate and calcium signalling. *Nature* **361**, 315-325.
- Berridge MJ (1995). Capacitative calcium entry. *Biochem J* **312** (Pt 1), 1-11.
- Berridge MJ (2006). Remodelling Ca²⁺ signalling systems and cardiac hypertrophy. *Biochem Soc Trans* **34**, 228-231.
- Bezzerrides VJ, Ramsey IS, Kotecha S, Greka A, & Clapham DE (2004). Rapid vesicular translocation and insertion of TRP channels. *Nat Cell Biol* **6**, 709-720.
- Bigay J, Deterre P, Pfister C, & Chabre M (1985). Fluoroaluminates activate transducin-GDP by mimicking the gamma-phosphate of GTP in its binding site. *FEBS Lett* **191**, 181-185.
- Bilmen JG, Wootton LL, Godfrey RE, Smart OS, & Michelangeli F (2002). Inhibition of SERCA Ca²⁺ pumps by 2-aminoethoxydiphenyl borate (2-APB). 2-APB reduces both Ca²⁺ binding and phosphoryl transfer from ATP, by interfering with the pathway leading to the Ca²⁺-binding sites. *Eur J Biochem* **269**, 3678-3687.
- Bolotina VM & Csutora P (2005). CIF and other mysteries of the store-operated Ca²⁺-entry pathway. *Trends Biochem Sci* **30**, 378-387.
- Bootman MD, Collins TJ, Mackenzie L, Roderick HL, Berridge MJ, & Peppiatt CM (2002). 2-aminoethoxydiphenyl borate (2-APB) is a reliable blocker of store-operated Ca²⁺ entry but an inconsistent inhibitor of InsP₃-induced Ca²⁺ release. *FASEB J* **16**, 1145-1150.
- Boulay G, Zhu X, Peyton M, Jiang M, Hurst R, Stefani E, & Birnbaumer L (1997). Cloning and expression of a novel mammalian homolog of Drosophila transient receptor potential (Trp) involved in calcium entry secondary to activation of receptors coupled by the G_q class of G protein. *J Biol Chem* **272**, 29672-29680.
- Boulay G, Brown DM, Qin N, Jiang M, Dietrich A, Zhu MX, Chen Z, Birnbaumer M, Mikoshiba K, & Birnbaumer L (1999). Modulation of Ca(2+) entry by polypeptides of the inositol 1,4,5-trisphosphate receptor (IP₃R) that bind transient receptor potential (TRP): evidence for

- roles of TRP and IP₃R in store depletion-activated Ca²⁺ entry. *Proc Natl Acad Sci U S A* **96**, 14955-14960.
- Brazer SC, Singh BB, Liu X, Swaim W, & Ambudkar IS (2003). Caveolin-1 contributes to assembly of store-operated Ca²⁺ influx channels by regulating plasma membrane localization of TRPC1. *J Biol Chem* **278**, 27208-27215.
- Burdakov D, Petersen OH, & Verkhratsky A (2005). Intraluminal calcium as a primary regulator of endoplasmic reticulum function. *Cell Calcium* **38**, 303-310.
- Bush EW, Hood DB, Papst PJ, Chapo JA, Minobe W, Bristow MR, Olson EN, & McKinsey TA (2006). Canonical transient receptor potential channels promote cardiomyocyte hypertrophy through activation of calcineurin signaling. *J Biol Chem* **281**, 33487-33496.
- Cayouette S, Lussier MP, Mathieu EL, Bousquet SM, & Boulay G (2004). Exocytotic insertion of TRPC6 channel into the plasma membrane upon G_q protein-coupled receptor activation. *J Biol Chem* **279**, 7241-7246.
- Chalfie M, Tu Y, Euskirchen G, Ward WW, & Prasher DC (1994). Green fluorescent protein as a marker for gene expression. *Science* **263**, 802-805.
- Chang AS, Chang SM, Garcia RL, & Schilling WP (1997). Concomitant and hormonally regulated expression of trp genes in bovine aortic endothelial cells. *FEBS Lett* **415**, 335-340.
- Chesire DR & Isaacs WB (2002). Ligand-dependent inhibition of beta-catenin/TCF signaling by androgen receptor. *Oncogene* **21**, 8453-8469.
- Chinopoulos C, Starkov AA, & Fiskum G (2003). Cyclosporin A-insensitive permeability transition in brain mitochondria: inhibition by 2-aminoethoxydiphenyl borate. *J Biol Chem* **278**, 27382-27389.
- Cioffi DL, Wu S, Alexeyev M, Goodman SR, Zhu MX, & Stevens T (2005). Activation of the Endothelial Store-Operated ISOC Ca²⁺ Channel Requires Interaction of Protein 4.1 With TRPC4. *Circ Res* **97**, 1164-1172.
- Clapham DE (1995). Calcium signaling. *Cell* **80**, 259-268.
- Clapham DE, Runnels LW, & Strubing C (2001). The TRP ion channel family. *Nat Rev Neurosci* **2**, 387-396.
- Clapham DE (2003). TRP channels as cellular sensors. *Nature* **426**, 517-524.
- Cosens DJ & Manning A (1969). Abnormal electroretinogram from a *Drosophila* mutant. *Nature* **224**, 285-287.
- Crews JK & Khalil RA (1999). Antagonistic effects of 17 beta-estradiol, progesterone, and testosterone on Ca²⁺ entry mechanisms of coronary vasoconstriction. *Arterioscler Thromb Vasc Biol* **19**, 1034-1040.
- D'Angelo I, Welti S, Bonneau F, & Scheffzek K (2006). A novel bipartite phospholipid-binding module in the neurofibromatosis type 1 protein. *EMBO Rep* **7**, 174-179.
- Dalrymple A, Slater DM, Beech D, Poston L, & Tribe RM (2002). Molecular identification and localization of Trp homologues, putative calcium channels, in pregnant human uterus. *Mol Hum Reprod* **8**, 946-951.

- Dalrymple A, Mahn K, Poston L, Songu-Mize E, & Tribe RM (2007). Mechanical stretch regulates TRPC expression and calcium entry in human myometrial smooth muscle cells. *Mol Hum Reprod* **13**, 171-179.
- Davies TH & Sanchez ER (2005). FKBP52. *Int J Biochem Cell Biol* **37**, 42-47.
- Demaurex N, Lew DP, & Krause KH (1992). Cyclopiazonic acid depletes intracellular Ca²⁺ stores and activates an influx pathway for divalent cations in HL-60 cells. *J Biol Chem* **267**, 2318-2324.
- Dietrich A, Schnitzler M, Emmel J, Kalwa H, Hofmann T, & Gudermann T (2003). N-linked protein glycosylation is a major determinant for basal TRPC3 and TRPC6 channel activity. *J Biol Chem* **278**, 47842-47852.
- Dietrich A, Kalwa H, Rost BR, & Gudermann T (2005a). The diacylglycerol-sensitive TRPC3/6/7 subfamily of cation channels: functional characterization and physiological relevance. *Pflugers Arch* **451**, 72-80.
- Dietrich A, Mederos YS, Gollasch M, Gross V, Storch U, Dubrovskaja G, Obst M, Yildirim E, Salanova B, Kalwa H, Essin K, Pinkenburg O, Luft FC, Gudermann T, & Birnbaumer L (2005b). Increased vascular smooth muscle contractility in TRPC6^{-/-} mice. *Mol Cell Biol* **25**, 6980-6989.
- Dietrich A, Chubanov V, Kalwa H, Rost BR, & Gudermann T (2006). Cation channels of the transient receptor potential superfamily: their role in physiological and pathophysiological processes of smooth muscle cells. *Pharmacol Ther* **112**, 744-760.
- Dietrich A, Kalwa H, Fuchs B, Grimminger F, Weissmann N, & Gudermann T (2007a). In vivo TRPC functions in the cardiopulmonary vasculature. *Cell Calcium* **42**, 233-244.
- Dietrich A, Kalwa H, Storch U, Mederos YS, Salanova B, Pinkenburg O, Dubrovskaja G, Essin K, Gollasch M, Birnbaumer L, & Gudermann T (2007b). Pressure-induced and store-operated cation influx in vascular smooth muscle cells is independent of TRPC1. *Pflugers Arch* **455**, 465-477.
- Djinovic-Carugo K, Gautel M, Ylanne J, & Young P (2002). The spectrin repeat: a structural platform for cytoskeletal protein assemblies. *FEBS Lett* **513**, 119-123.
- Droogmans G (2007). CaBuf Program. <http://www.kuleuven.be/fysio/trp/?q=cabuf>
- Echelon (2007). Technical Data Sheet for MultiPIP Grip (LL5-α). http://www.echelon-inc.com/objects/catalog/product/extras/1211_G-1100.pdf
- Eder P, Probst D, Rosker C, Poteser M, Wolinski H, Kohlwein SD, Romanin C, & Groschner K (2007). Phospholipase C-dependent control of cardiac calcium homeostasis involves a TRPC3-NCX1 signaling complex. *Cardiovasc Res* **73**, 111-119.
- Engelke M, Friedrich O, Budde P, Schafer C, Niemann U, Zitt C, Jungling E, Rocks O, Luckhoff A, & Frey J (2002). Structural domains required for channel function of the mouse transient receptor potential protein homologue TRP1beta. *FEBS Lett* **523**, 193-199.
- Estacion M, Sinkins WG, & Schilling WP (2001). Regulation of Drosophila transient receptor potential-like (TrpL) channels by phospholipase C-dependent mechanisms. *J Physiol* **530**, 1-19.

- Estacion M, Li S, Sinkins WG, Gosling M, Bahra P, Poll C, Westwick J, & Schilling WP (2004). Activation of human TRPC6 channels by receptor stimulation. *J Biol Chem* **279**, 22047-22056.
- Estacion M, Sinkins WG, Jones SW, Applegate MA, & Schilling WP (2006). Human TRPC6 expressed in HEK 293 cells forms non-selective cation channels with limited Ca²⁺ permeability. *J Physiol* **572**, 359-377.
- Facemire CS, Mohler PJ, & Arendshorst WJ (2004). Expression and relative abundance of short transient receptor potential channels in the rat renal microcirculation. *Am J Physiol Renal Physiol* **286**, F546-F551.
- Fagan KA, Smith KE, & Cooper DM (2000). Regulation of the Ca²⁺-inhibitable adenylyl cyclase type VI by capacitative Ca²⁺ entry requires localization in cholesterol-rich domains. *J Biol Chem* **275**, 26530-26537.
- Fan Z, Gao L, & Wang W (2003). Phosphatidic acid stimulates cardiac K_{ATP} channels like phosphatidylinositols, but with novel gating kinetics. *Am J Physiol Cell Physiol* **284**, C94-102.
- Favre CJ, Jerstrom P, Foti M, Stendhal O, Huggler E, Lew DP, & Krause KH (1996). Organization of Ca²⁺ stores in myeloid cells: association of SERCA2b and the type-1 inositol-1,4,5-trisphosphate receptor. *Biochem J* **316** (Pt 1), 137-142.
- Feske S, Prakriya M, Rao A, & Lewis RS (2005). A severe defect in CRAC Ca²⁺ channel activation and altered K⁺ channel gating in T cells from immunodeficient patients. *J Exp Med* **202**, 651-662.
- Feske S, Gwack Y, Prakriya M, Srikanth S, Puppel SH, Tanasa B, Hogan PG, Lewis RS, Daly M, & Rao A (2006). A mutation in Orai1 causes immune deficiency by abrogating CRAC channel function. *Nature* **441**, 179-185.
- Fields S & Song O (1989). A novel genetic system to detect protein-protein interactions. *Nature* **340**, 245-246.
- Flemming R, Xu SZ, & Beech DJ (2003). Pharmacological profile of store-operated channels in cerebral arteriolar smooth muscle cells. *Br J Pharmacol* **139**, 955-965.
- Flemming PK, Dedman AM, Xu SZ, Li J, Zeng F, Naylor J, Benham CD, Bateson AN, Muraki K, & Beech DJ (2005). Sensing of lysophospholipids by TRPC5 calcium channel. *J Biol Chem* **281**, 4977-4982.
- Flockerzi V, Jung C, Aberle T, Meissner M, Freichel M, Philipp SE, Nastainczyk W, Maurer P, & Zimmermann R (2005). Specific detection and semi-quantitative analysis of TRPC4 protein expression by antibodies. *Pflugers Arch* **451**, 81-86.
- Fowler MA, Sidiropoulou K, Ozkan ED, Phillips CW, & Cooper DC (2007). Corticolimbic Expression of TRPC4 and TRPC5 Channels in the Rodent Brain. *PLoS ONE* **2**, e573.
- Franzius D, Hoth M, & Penner R (1994). Non-specific effects of calcium entry antagonists in mast cells. *Pflugers Arch* **428**, 433-438.
- Freichel M, Suh SH, Pfeifer A, Schweig U, Trost C, Weissgerber P, Biel M, Philipp S, Freise D, Droogmans G, Hofmann F, Flockerzi V, & Nilius B (2001). Lack of an endothelial store-operated Ca²⁺ current impairs agonist-dependent vasorelaxation in TRP4^{-/-} mice. *Nat Cell Biol* **3**, 121-127.

- Freichel M, Vennekens R, Olausson J, Stolz S, Philipp S, Weissgerber P, & Flockerzi V (2005). Functional role of TRPC proteins in native systems: implications from knockout and knock-down studies. *J Physiol* **567**(Pt 1), 59-66.
- Fruman DA, Meyers RE, & Cantley LC (1998). Phosphoinositide kinases. *Annu Rev Biochem* **67**, 481-507.
- Garcia RL & Schilling WP (1997). Differential expression of mammalian TRP homologues across tissues and cell lines. *Biochem Biophys Res Commun* **239**, 279-283.
- Glusa E, Graser T, Wagner S, & Oettel M (1997). Mechanisms of relaxation of rat aorta in response to progesterone and synthetic progestins. *Maturitas* **28**, 181-191.
- Goel M, Sinkins W, Keightley A, Kinter M, & Schilling WP (2005). Proteomic analysis of T. *Pflugers Arch* **451**, 87-98.
- Greka A, Navarro B, Oancea E, Duggan A, & Clapham DE (2003). TRPC5 is a regulator of hippocampal neurite length and growth cone morphology. *Nat Neurosci* **6**, 837-845.
- Grynkiewicz G, Poenie M, & Tsien RY (1985). A new generation of Ca²⁺ indicators with greatly improved fluorescence properties. *J Biol Chem* **260**, 3440-3450.
- Gudermann T, Hofmann T, Schnitzler M, & Dietrich A (2004). Activation, subunit composition and physiological relevance of DAG-sensitive TRPC proteins. *Novartis Found Symp* **258**, 103-118.
- Gudermann T (2005). A new TRP to kidney disease. *Nat Genet* **37**, 663-664.
- Halaszovich CR, Zitt C, Jungling E, & Luckhoff A (2000). Inhibition of TRP3 channels by lanthanides. Block from the cytosolic side of the plasma membrane. *J Biol Chem* **275**, 37423-37428.
- Harbury PB, Zhang T, Kim PS, & Alber T (1993). A switch between two-, three-, and four-stranded coiled coils in GCN4 leucine zipper mutants. *Science* **262**, 1401-1407.
- Hardie RC & Minke B (1992). The trp gene is essential for a light-activated Ca²⁺ channel in *Drosophila* photoreceptors. *Neuron* **8**, 643-651.
- Hardie RC & Raghu P (2001). Visual transduction in *Drosophila*. *Nature* **413**, 186-193.
- Hardie RC (2003). Regulation of TRP channels via lipid second messengers. *Annu Rev Physiol* **65**, 735-759.
- Harding MW, Galat A, Uehling DE, & Schreiber SL (1989). A receptor for the immunosuppressant FK506 is a *cis-trans* peptidyl-prolyl isomerase. *Nature* **341**, 758-760.
- Harteneck C, Plant TD, & Schultz G (2000). From worm to man: three subfamilies of TRP channels. *Trends Neurosci* **23**, 159-166.
- Hermosura MC, Nayakanti H, Dorovkov MV, Calderon FR, Ryazanov AG, Haymer DS, & Garruto RM (2005). A TRPM7 variant shows altered sensitivity to magnesium that may contribute to the pathogenesis of two Guamanian neurodegenerative disorders. *Proc Natl Acad Sci U S A* **102**, 11510-11515.
- Hermosura MC & Garruto RM (2007). TRPM7 and TRPM2-Candidate susceptibility genes for Western Pacific ALS and PD? *Biochim Biophys Acta* **1772**, 822-835.

- Hewavitharana T, Deng X, Soboloff J, & Gill DL (2007). Role of STIM and Orai proteins in the store-operated calcium signaling pathway. *Cell Calcium* **42**, 173-182.
- Hisatsune C, Kuroda Y, Nakamura K, Inoue T, Nakamura T, Michikawa T, Mizutani A, & Mikoshiba K (2004). Regulation of TRPC6 channel activity by tyrosine phosphorylation. *J Biol Chem* **279**, 18887-18894.
- Hoenderop JG, Voets T, Hoefs S, Weidema F, Prenen J, Nilius B, & Bindels RJ (2003). Homo- and heterotetrameric architecture of the epithelial Ca²⁺ channels TRPV5 and TRPV6. *EMBO J* **22**, 776-785.
- Hofmann T, Obukhov AG, Schaefer M, Harteneck C, Gudermann T, & Schultz G (1999). Direct activation of human TRPC6 and TRPC3 channels by diacylglycerol. *Nature* **397**, 259-263.
- Hofmann T, Schaefer M, Schultz G, & Gudermann T (2002). Subunit composition of mammalian transient receptor potential channels in living cells. *Proc Natl Acad Sci U S A* **99**, 7461-7466.
- Hoth M & Penner R (1992). Depletion of intracellular calcium stores activates a calcium current in mast cells. *Nature* **355**, 353-356.
- Hsu YJ, Hoenderop JG, & Bindels RJ (2007). TRP channels in kidney disease. *Biochim Biophys Acta* **1772**, 928-936.
- Hsuan J & Cockcroft S (2001). The PITP family of phosphatidylinositol transfer proteins. *Genome Biol* **2**, REVIEWS3011.
- Huang GN, Zeng W, Kim JY, Yuan JP, Han L, Muallem S, & Worley PF (2006). STIM1 carboxyl-terminus activates native SOC, I(crac) and TRPC1 channels. *Nat Cell Biol* **8**, 1003-1010.
- Ile KE, Schaaf G, & Bankaitis VA (2006). Phosphatidylinositol transfer proteins and cellular nanoreactors for lipid signaling. *Nat Chem Biol* **2**, 576-583.
- Inoue R, Okada T, Onoue H, Hara Y, Shimizu S, Naitoh S, Ito Y, & Mori Y (2001). The transient receptor potential protein homologue TRP6 is the essential component of vascular alpha(1)-adrenoceptor-activated Ca(2+)-permeable cation channel. *Circ Res* **88**, 325-332.
- Inoue R, Jensen LJ, Shi J, Morita H, Nishida M, Honda A, & Ito Y (2006). Transient receptor potential channels in cardiovascular function and disease. *Circ Res* **99**, 119-131.
- Irvine RF (1990). 'Quantal' Ca²⁺ release and the control of Ca²⁺ entry by inositol phosphates-a possible mechanism. *FEBS Lett* **263**, 5-9.
- Ito H, Fukuda Y, Murata K, & Kimura A (1983). Transformation of intact yeast cells treated with alkali cations. *J Bacteriol* **153**, 163-168.
- IUPAC Commission on the Nomenclature of Organic Chemistry and IUPAC-IUB Commission on Biochemical Nomenclature (1969). Revised tentative rules for nomenclature of steroids. *Biochem J* **113(1)**, 5-28.
- Juchem M, Pollow K, Elger W, Hoffmann G, & Mobus V (1993). Receptor binding of norgestimate-a new orally active synthetic progestational compound. *Contraception* **47**, 283-294.

- Jung S, Strotmann R, Schultz G, & Plant TD (2002). TRPC6 is a candidate channel involved in receptor-stimulated cation currents in A7r5 smooth muscle cells. *Am J Physiol Cell Physiol* **282**, C347-C359.
- Jung S, Muhle A, Schaefer M, Strotmann R, Schultz G, & Plant TD (2003). Lanthanides potentiate TRPC5 currents by an action at extracellular sites close to the pore mouth. *J Biol Chem* **278**, 3562-3571.
- Jungnickel MK, Marrero H, Birnbaumer L, Lemos JR, & Florman HM (2001). Trp2 regulates entry of Ca²⁺ into mouse sperm triggered by egg ZP3. *Nat Cell Biol* **3**, 499-502.
- Kamouchi M, Philipp S, Flockerzi V, Wissenbach U, Mamin A, Raeymaekers L, Eggermont J, Droogmans G, & Nilius B (1999). Properties of heterologously expressed hTRP3 channels in bovine pulmonary artery endothelial cells. *J Physiol* **518 Pt 2**, 345-358.
- Kawabata A, Saifeddine M, Al-Ani B, Leblond L, & Hollenberg MD (1999). Evaluation of proteinase-activated receptor-1 (PAR1) agonists and antagonists using a cultured cell receptor desensitization assay: activation of PAR2 by PAR1-targeted ligands. *J Pharmacol Exp Ther* **288**, 358-370.
- Kedei N, Szabo T, Lile JD, Treanor JJ, Olah Z, Iadarola MJ, & Blumberg PM (2001). Analysis of the native quaternary structure of vanilloid receptor 1. *J Biol Chem* **276**, 28613-28619.
- Kim JY, Zeng W, Kiselyov K, Yuan JP, Dehoff MH, Mikoshiba K, Worley PF, & Muallem S (2006a). Homer 1 mediates store- and inositol 1,4,5-trisphosphate receptor-dependent translocation and retrieval of TRPC3 to the plasma membrane. *J Biol Chem* **281**, 32540-32549.
- Kim MT, Kim BJ, Lee JH, Kwon SC, Yeon DS, Yang DK, So I, & Kim KW (2006b). Involvement of calmodulin and myosin light chain kinase in activation of mTRPC5 expressed in HEK cells. *Am J Physiol Cell Physiol* **290**, C1031-C1040.
- Kim SJ, Kim YS, Yuan JP, Petralia RS, Worley PF, & Linden DJ (2003). Activation of the TRPC1 cation channel by metabotropic glutamate receptor mGluR1. *Nature* **426**, 285-291.
- Kiselyov K, Xu X, Mozhayeva G, Kuo T, Pessah I, Mignery G, Zhu X, Birnbaumer L, & Muallem S (1998). Functional interaction between InsP3 receptors and store-operated Htrp3 channels. *Nature* **396**, 478-482.
- Kiselyov KI, Shin DM, Wang Y, Pessah IN, Allen PD, & Muallem S (2000). Gating of store-operated channels by conformational coupling to ryanodine receptors. *Mol Cell* **6**, 421-431.
- Knudsen KA, Soler AP, Johnson KR, & Wheelock MJ (1995). Interaction of alpha-actinin with the cadherin/catenin cell-cell adhesion complex via alpha-catenin. *J Cell Biol* **130**, 67-77.
- Kostenko EV, Mahon GM, Cheng L, & Whitehead IP (2005). The Sec14 homology domain regulates the cellular distribution and transforming activity of the Rho-specific guanine nucleotide exchange factor Dbs. *J Biol Chem* **280**, 2807-2817.
- Kuhn W, Blode H, & Mahler M (1994). Systemic availability of levonorgestrel after single oral administration of a norgestimate-containing combination oral contraceptive to 12 young women. *Contraception* **49**, 255-263.
- Kumar B, Dreja K, Shah S, Cheong A, Xu SZ, Sukumar P, Naylor J, Forte A, Cipollaro M, McHugh D, Kingston PA, Heagerty AM, Munsch CM, Bergdahl A, Hultgardh-Nilsson A, Gomez MF, Porter KE, Hellstrand P, & Beech DJ (2006). Upregulated TRPC1 Channel in

- Vascular Injury *In Vivo* and Its Role in Human Neointimal Hyperplasia. *Circ Res* **98**, 557-563.
- Kunichika N, Landsberg JW, Yu Y, Kunichika H, Thistlethwaite PA, Rubin LJ, & Yuan JX (2004). Bosentan inhibits transient receptor potential channel expression in pulmonary vascular myocytes. *Am J Respir Crit Care Med* **170**, 1101-1107.
- Kuwahara K, Wang Y, McAnally J, Richardson JA, Bassel-Duby R, Hill JA, & Olson EN (2006). TRPC6 fulfills a calcineurin signaling circuit during pathologic cardiac remodeling. *J Clin Invest* **116**, 3114-3126.
- Kwan HY, Huang Y, & Yao X (2004). Regulation of canonical transient receptor potential isoform 3 (TRPC3) channel by protein kinase G. *Proc Natl Acad Sci U S A* **101**, 2625-2630.
- Kwan HY, Huang Y, & Yao X (2007). TRP channels in endothelial function and dysfunction. *Biochim Biophys Acta* **1772**, 907-914.
- Kwon Y, Hofmann T, & Montell C (2007). Integration of phosphoinositide- and calmodulin-mediated regulation of TRPC6. *Mol Cell* **25**, 491-503.
- Landy A (1989). Dynamic, structural, and regulatory aspects of lambda site-specific recombination. *Annu Rev Biochem* **58**, 913-949.
- Large WA (2002). Receptor-operated Ca²⁺-permeable nonselective cation channels in vascular smooth muscle: a physiologic perspective. *J Cardiovasc Electrophysiol* **13**, 493-501.
- Lee KP, Jun JY, Chang IY, Suh SH, So I, & Kim KW (2005). TRPC4 is an essential component of the nonselective cation channel activated by muscarinic stimulation in mouse visceral smooth muscle cells. *Mol Cells* **20**, 435-441.
- Lee SY, Obata Y, Yoshida M, Stockert E, Williamson B, Jungbluth AA, Chen YT, Old LJ, & Scanlan MJ (2003a). Immunomic analysis of human sarcoma. *Proc Natl Acad Sci U S A* **100**, 2651-2656.
- Lee YM, Kim BJ, Kim HJ, Yang DK, Zhu MH, Lee KP, So I, & Kim KW (2003b). TRPC5 as a candidate for the nonselective cation channel activated by muscarinic stimulation in murine stomach. *Am J Physiol Gastrointest Liver Physiol* **284**, G604-G616.
- Lemonnier L, Prevarskaya N, Mazurier J, Shuba Y, & Skryma R (2004). 2-APB inhibits volume-regulated anion channels independently from intracellular calcium signaling modulation. *FEBS Lett* **556**, 121-126.
- Lemos VS, Poburko D, Liao CH, Cole WC, & van BC (2007). Na⁺ entry via TRPC6 causes Ca²⁺ entry via NCX reversal in ATP stimulated smooth muscle cells. *Biochem Biophys Res Commun* **352**, 130-134.
- Lepage PK, Lussier MP, Barajas-Martinez H, Bousquet SM, Blanchard AP, Francoeur N, Dumaine R, & Boulay G (2006). Identification of two domains involved in the assembly of transient receptor potential canonical channels. *J Biol Chem* **281**, 30356-30364.
- Lewis RS (2001). Calcium signaling mechanisms in T lymphocytes. *Annu Rev Immunol* **19**, 497-521.
- Li HS, Xu XZ, & Montell C (1999). Activation of a TRPC3-dependent cation current through the neurotrophin BDNF. *Neuron* **24**, 261-273.

- Li SW, Westwick J, & Poll CT (2002). Receptor-operated Ca^{2+} influx channels in leukocytes: a therapeutic target? *Trends Pharmacol Sci* **23**, 63-70.
- Li S, Westwick J, & Poll C (2003). Transient receptor potential (TRP) channels as potential drug targets in respiratory disease. *Cell Calcium* **33**, 551-558.
- Li S, Westwick J, Cox B, & Poll CT (2004). TRP channels as drug targets. *Novartis Found Symp* **258**, 204-213.
- Li Y, Jia YC, Cui K, Li N, Zheng ZY, Wang YZ, & Yuan XB (2005). Essential role of TRPC channels in the guidance of nerve growth cones by brain-derived neurotrophic factor. *Nature* **434**, 894-898.
- Liao Y, Erxleben C, Yildirim E, Abramowitz J, Armstrong DL, & Birnbaumer L (2007). Orai proteins interact with TRPC channels and confer responsiveness to store depletion. *Proc Natl Acad Sci U S A* **104**, 4682-4687.
- Liman ER & Innan H (2003). Relaxed selective pressure on an essential component of pheromone transduction in primate evolution. *Proc Natl Acad Sci U S A* **100**, 3328-3332.
- Lintschinger B, Balzer-Geldsetzer M, Baskaran T, Graier WF, Romanin C, Zhu MX, & Groschner K (2000). Coassembly of Trp1 and Trp3 proteins generates diacylglycerol- and Ca^{2+} -sensitive cation channels. *J Biol Chem* **275**, 27799-27805.
- Liou J, Kim ML, Heo WD, Jones JT, Myers JW, Ferrell JE, Jr., & Meyer T (2005). STIM is a Ca^{2+} sensor essential for Ca^{2+} -store-depletion-triggered Ca^{2+} influx. *Curr Biol* **15**, 1235-1241.
- Liu D, Scholze A, Zhu Z, Krueger K, Thilo F, Burkert A, Streffer K, Holz S, Harteneck C, Zidek W, & Tepel M (2006). Transient receptor potential channels in essential hypertension. *J Hypertens* **24**, 1105-1114.
- Liu X, Bandyopadhyay BC, Singh BB, Groschner K, & Ambudkar IS (2005). Molecular Analysis of a Store-operated and 2-Acetyl-sn-glycerol-sensitive Non-selective Cation Channel: HETEROMERIC ASSEMBLY OF TRPC1-TRPC3. *J Biol Chem* **280**, 21600-21606.
- Livak KJ, Flood SJ, Marmaro J, Giusti W, & Deetz K (1995). Oligonucleotides with fluorescent dyes at opposite ends provide a quenched probe system useful for detecting PCR product and nucleic acid hybridization. *PCR Methods Appl* **4**, 357-362.
- Lockwich TP, Liu X, Singh BB, Jadowiec J, Weiland S, & Ambudkar IS (2000). Assembly of Trp1 in a signaling complex associated with caveolin-scaffolding lipid raft domains. *J Biol Chem* **275**, 11934-11942.
- Lockwich T, Singh BB, Liu X, & Ambudkar IS (2001). Stabilization of cortical actin induces internalization of transient receptor potential 3 (Trp3)-associated caveolar Ca^{2+} signaling complex and loss of Ca^{2+} influx without disruption of Trp3-inositol trisphosphate receptor association. *J Biol Chem* **276**, 42401-42408.
- Lodish HF, Berk A, Matsudeira P, Kaiser CA, Krieger M, Scott MP, Zipursky SL, & Darnell J (2003). *Molecular cell biology*, 5th ed. W.H. Freeman and Company, New York.
- Lucas P, Ukhanov K, Leinders-Zufall T, & Zufall F (2003). A diacylglycerol-gated cation channel in vomeronasal neuron dendrites is impaired in TRPC2 mutant mice: mechanism of pheromone transduction. *Neuron* **40**, 551-561.

- Lummis SC, Beene DL, Lee LW, Lester HA, Broadhurst RW, & Dougherty DA (2005). *Cis-trans* isomerization at a proline opens the pore of a neurotransmitter-gated ion channel. *Nature* **438**, 248-252.
- Ma HT, Patterson RL, van Rossum DB, Birnbaumer L, Mikoshiba K, & Gill DL (2000). Requirement of the inositol trisphosphate receptor for activation of store-operated Ca^{2+} channels. *Science* **287**, 1647-1651.
- Ma R, Rundle D, Jacks J, Koch M, Downs T, & Tsiokas L (2003). Inhibitor of myogenic family, a novel suppressor of store-operated currents through an interaction with TRPC1. *J Biol Chem* **278**, 52763-52772.
- Manavathi B, Acconcia F, Rayala SK, & Kumar R (2006). An inherent role of microtubule network in the action of nuclear receptor. *Proc Natl Acad Sci U S A* **103**, 15981-15986.
- Marchler-Bauer A & Bryant SH (2004). CD-Search: protein domain annotations on the fly. *Nucleic Acids Res* **32**, W327-W331.
- Maruyama T, Kanaji T, Nakade S, Kanno T, & Mikoshiba K (1997). 2APB, 2-aminoethoxydiphenyl borate, a membrane-penetrable modulator of $Ins(1,4,5)P_3$ -induced Ca^{2+} release. *J Biochem (Tokyo)* **122**, 498-505.
- Maruyama Y, Nakanishi Y, Walsh EJ, Wilson DP, Welsh DG, & Cole WC (2006). Heteromultimeric TRPC6-TRPC7 channels contribute to arginine vasopressin-induced cation current of A7r5 vascular smooth muscle cells. *Circ Res* **98**, 1520-1527.
- McCarron JG, Chalmers S, Bradley KN, MacMillan D, & Muir TC (2006). Ca^{2+} microdomains in smooth muscle. *Cell Calcium* **40**, 461-493.
- McKay RR, Szymeczek-Seay CL, Lievreumont JP, Bird GS, Zitt C, Jungling E, Luckhoff A, & Putney JW, Jr. (2000). Cloning and expression of the human transient receptor potential 4 (TRP4) gene: localization and functional expression of human TRP4 and TRP3. *Biochem J* **351 Pt 3**, 735-746.
- Mehta D, Ahmmed GU, Paria BC, Holinstat M, Voyno-Yasenetskaya T, Tiruppathi C, Minshall RD, & Malik AB (2003). RhoA interaction with inositol 1,4,5-trisphosphate receptor and transient receptor potential channel-1 regulates Ca^{2+} entry. Role in signaling increased endothelial permeability. *J Biol Chem* **278**, 33492-33500.
- Meldolesi J & Pozzan T (1998). The endoplasmic reticulum Ca^{2+} store: a view from the lumen. *Trends Biochem Sci* **23**, 10-14.
- Merritt JE, Armstrong WP, Benham CD, Hallam TJ, Jacob R, Jaxa-Chamiec A, Leigh BK, McCarthy SA, Moores KE, & Rink TJ (1990). SK&F 96365, a novel inhibitor of receptor-mediated calcium entry. *Biochem J* **271**, 515-522.
- Mery L, Strauss B, Dufour JF, Krause KH, & Hoth M (2002). The PDZ-interacting domain of TRPC4 controls its localization and surface expression in HEK293 cells. *J Cell Sci* **115**, 3497-3508.
- Mesiano S (2007). Myometrial progesterone responsiveness. *Semin Reprod Med* **25**, 5-13.
- Miller JR, Hocking AM, Brown JD, & Moon RT (1999). Mechanism and function of signal transduction by the Wnt/beta-catenin and Wnt/ Ca^{2+} pathways. *Oncogene* **18**, 7860-7872.
- Minke B, Wu C, & Pak WL (1975). Induction of photoreceptor voltage noise in the dark in *Drosophila* mutant. *Nature* **258**, 84-87.

- Missiaen L, Callewaert G, De SH, & Parys JB (2001). 2-Aminoethoxydiphenyl borate affects the inositol 1,4,5-trisphosphate receptor, the intracellular Ca^{2+} pump and the non-specific Ca^{2+} leak from the non-mitochondrial Ca^{2+} stores in permeabilized A7r5 cells. *Cell Calcium* **29**, 111-116.
- Mochizuki T, Wu G, Hayashi T, Xenophontos SL, Veldhuisen B, Saris JJ, Reynolds DM, Cai Y, Gabow PA, Pierides A, Kimberling WJ, Breuning MH, Deltas CC, Peters DJ, & Somlo S (1996). PKD2, a gene for polycystic kidney disease that encodes an integral membrane protein. *Science* **272**, 1339-1342.
- Moller CC, Wei C, Altintas MM, Li J, Greka A, Ohse T, Pippin JW, Rastaldi MP, Wawersik S, Schiavi S, Henger A, Kretzler M, Shankland SJ, & Reiser J (2007). Induction of TRPC6 channel in acquired forms of proteinuric kidney disease. *J Am Soc Nephrol* **18**, 29-36.
- Moncada S, Palmer RM, & Higgs EA (1991). Nitric oxide: physiology, pathophysiology, and pharmacology. *Pharmacol Rev* **43**, 109-142.
- Montell C & Rubin GM (1989). Molecular characterization of the *Drosophila* trp locus: a putative integral membrane protein required for phototransduction. *Neuron* **2**, 1313-1323.
- Montell C (1997). New light on TRP and TRPL. *Mol Pharmacol* **52**, 755-763.
- Montell C (1999). Visual transduction in *Drosophila*. *Annu Rev Cell Dev Biol* **15**, 231-268.
- Montell C (2001). Physiology, phylogeny, and functions of the TRP superfamily of cation channels. *Sci STKE* **2001**, RE1.
- Montell C, Birnbaumer L, & Flockerzi V (2002a). The TRP channels, a remarkably functional family. *Cell* **108**, 595-598.
- Montell C, Birnbaumer L, Flockerzi V, Bindels RJ, Bruford EA, Caterina MJ, Clapham DE, Harteneck C, Heller S, Julius D, Kojima I, Mori Y, Penner R, Prawitt D, Scharenberg AM, Schultz G, Shimizu N, & Zhu MX (2002b). A unified nomenclature for the superfamily of TRP cation channels. *Mol Cell* **9**, 229-231.
- Montell C (2004). Molecular genetics of *Drosophila* TRP channels. *Novartis Found Symp* **258**, 3-12.
- Montell C (2005). The TRP superfamily of cation channels. *Sci STKE* **2005**, re3.
- Moran MM, Xu H, & Clapham DE (2004). TRP ion channels in the nervous system. *Curr Opin Neurobiol* **14**, 362-369.
- Mosavi LK, Cammett TJ, Desrosiers DC, & Peng ZY (2004). The ankyrin repeat as molecular architecture for protein recognition. *Protein Sci* **13**, 1435-1448.
- Mousley CJ, Tyeryar KR, Vincent-Pope P, & Bankaitis VA (2007). The Sec14-superfamily and the regulatory interface between phospholipid metabolism and membrane trafficking. *Biochim Biophys Acta* **1771**, 727-736.
- Mukerji MS, Leathard HL, & Huddart H (2000). The effect of progesterone on spontaneous and agonist-evoked contractions of the rat aorta and portal vein. *J Pharm Pharmacol* **52**, 843-849.
- Mukerji N, Damodaran TV, & Winn MP (2007). TRPC6 and FSGS: The latest TRP channelopathy. *Biochim Biophys Acta* **1772**, 859-868.

- Munsch T, Freichel M, Flockerzi V, & Pape HC (2003). Contribution of transient receptor potential channels to the control of GABA release from dendrites. *Proc Natl Acad Sci U S A* **100**, 16065-16070.
- Nakayama H, Wilkin BJ, Bodi I, & Molkentin JD (2006). Calcineurin-dependent cardiomyopathy is activated by TRPC in the adult mouse heart. *FASEB J* **20**, 1660-1670.
- Neher E & Sakmann B (1976). Single-channel currents recorded from membrane of denervated frog muscle fibres. *Nature* **260**, 799-802.
- Niemeyer BA, Suzuki E, Scott K, Jalink K, & Zuker CS (1996). The *Drosophila* light-activated conductance is composed of the two channels TRP and TRPL. *Cell* **85**, 651-659.
- Nilius B (2007). TRP channels in disease. *Biochim Biophys Acta* **1772**, 805-812.
- Nishida M, Onohara N, Sato Y, Suda R, Ogushi M, Tanabe S, Inoue R, Mori Y, & Kurose H (2007). Galpha 12/13-mediated upregulation of TRPC6 negatively regulates endothelin-1-induced cardiac myofibroblast formation and collagen synthesis through NFAT activation. *J Biol Chem* **282**, 23117-23128.
- Novak A, Hsu SC, Leung-Hagesteijn C, Radeva G, Papkoff J, Montesano R, Roskelley C, Grosschedl R, & Dedhar S (1998). Cell adhesion and the integrin-linked kinase regulate the LEF-1 and beta-catenin signaling pathways. *Proc Natl Acad Sci U S A* **95**, 4374-4379.
- Novick P, Field C, & Schekman R (1980). Identification of 23 complementation groups required for post-translational events in the yeast secretory pathway. *Cell* **21**, 205-215.
- Numberger M & Draguhn A (1996). *Patch Clamp Technik* Spektrum Akademischer Verlag, Heidelberg.
- O'Brien SP, Seipel K, Medley QG, Bronson R, Segal R, & Streuli M (2000). Skeletal muscle deformity and neuronal disorder in Trio exchange factor-deficient mouse embryos. *Proc Natl Acad Sci U S A* **97**, 12074-12078.
- Odell AF, Scott JL, & Van Helden DF (2005). Epidermal growth factor induces tyrosine phosphorylation, membrane insertion, and activation of transient receptor potential channel 4. *J Biol Chem* **280**, 37974-37987.
- Ohba T, Watanabe H, Murakami M, Takahashi Y, Iino K, Kuromitsu S, Mori Y, Ono K, Iijima T, & Ito H (2007). Upregulation of TRPC1 in the development of cardiac hypertrophy. *J Mol Cell Cardiol* **42**, 498-507.
- Okada T, Shimizu S, Wakamori M, Maeda A, Kurosaki T, Takada N, Imoto K, & Mori Y (1998). Molecular cloning and functional characterization of a novel receptor-activated TRP Ca²⁺ channel from mouse brain. *J Biol Chem* **273**, 10279-10287.
- Okada T, Inoue R, Yamazaki K, Maeda A, Kurosaki T, Yamakuni T, Tanaka I, Shimizu S, Ikenaka K, Imoto K, & Mori Y (1999). Molecular and functional characterization of a novel mouse transient receptor potential protein homologue TRP7. Ca(2+)-permeable cation channel that is constitutively activated and enhanced by stimulation of G protein-coupled receptor. *J Biol Chem* **274**, 27359-27370.
- Okuhara DY, Hsia AY, & Xie M (2007). Transient receptor potential channels as drug targets. *Expert Opin Ther Targets* **11**, 391-401.
- Ong HL, Cheng KT, Liu X, Bandyopadhyay BC, Paria BC, Soboloff J, Pani B, Gwack Y, Srikanth S, Singh BB, Gill D, & Ambudkar IS (2007). Dynamic assembly of TRPC1-STIM1-

- Orai1 ternary complex is involved in store-operated calcium influx. Evidence for similarities in store-operated and calcium release-activated calcium channel components. *J Biol Chem* **282**, 9105-9116.
- Ordaz B, Tang J, Xiao R, Salgado A, Sampieri A, Zhu MX, & Vaca L (2005). Calmodulin and calcium interplay in the modulation of TRPC5 channel activity. Identification of a novel C-terminal domain for calcium/calmodulin-mediated facilitation. *J Biol Chem* **280**, 30788-30796.
- Parekh AB & Penner R (1997). Store depletion and calcium influx. *Physiol Rev* **77**, 901-930.
- Parekh AB & Putney JW, Jr. (2005). Store-operated calcium channels. *Physiol Rev* **85**, 757-810.
- Parekh AB (2006). On the activation mechanism of store-operated calcium channels. *Pflugers Arch* **453**, 303-311.
- Parker LT, Zakeri H, Deng Q, Spurgeon S, Kwok PY, & Nickerson DA (1996). AmpliTaq DNA polymerase, FS dye-terminator sequencing: analysis of peak height patterns. *Biotechniques* **21**, 694-699.
- Patterson RL, van Rossum DB, & Gill DL (1999). Store-operated Ca²⁺ entry: evidence for a secretion-like coupling model. *Cell* **98**, 487-499.
- Pedersen SF, Owsianik G, & Nilius B (2005). TRP channels: An overview. *Cell Calcium* **38**, 233-252.
- Pendaries C, Tronchere H, Racaud-Sultan C, Gaits-Iacovoni F, Coronas S, Manenti S, Gratacap MP, Plantavid M, & Payrastre B (2005). Emerging roles of phosphatidylinositol monophosphates in cellular signaling and trafficking. *Adv Enzyme Regul* **45**, 201-214.
- Peralta EG, Ashkenazi A, Winslow JW, Ramachandran J, & Capon DJ (1988). Differential regulation of PI hydrolysis and adenylyl cyclase by muscarinic receptor subtypes. *Nature* **334**, 434-437.
- Perusquia M, Hernandez R, Montano LM, Villalon CM, & Campos MG (1997). Inhibitory effect of sex steroids on guinea-pig airway smooth muscle contractions. *Comp Biochem Physiol C Pharmacol Toxicol Endocrinol* **118**, 5-10.
- Philipp S, Cavalie A, Freichel M, Wissenbach U, Zimmer S, Trost C, Marquart A, Murakami M, & Flockerzi V (1996). A mammalian capacitative calcium entry channel homologous to *Drosophila* TRP and TRPL. *EMBO J* **15**, 6166-6171.
- Philipp S, Hambrecht J, Braslavski L, Schroth G, Freichel M, Murakami M, Cavalie A, & Flockerzi V (1998). A novel capacitative calcium entry channel expressed in excitable cells. *EMBO J* **17**, 4274-4282.
- Philipp S, Trost C, Warnat J, Rautmann J, Himmerkus N, Schroth G, Kretz O, Nastainczyk W, Cavalie A, Hoth M, & Flockerzi V (2000). TRP4 (CCE1) protein is part of native calcium release-activated Ca²⁺-like channels in adrenal cells. *J Biol Chem* **275**, 23965-23972.
- Phillips AM, Bull A, & Kelly LE (1992). Identification of a *Drosophila* gene encoding a calmodulin-binding protein with homology to the trp phototransduction gene. *Neuron* **8**, 631-642.
- Plant TD & Schaefer M (2003). TRPC4 and TRPC5: receptor-operated Ca²⁺-permeable nonselective cation channels. *Cell Calcium* **33**, 441-450.

- Poteser M, Graziani A, Rosker C, Eder P, Derler I, Kahr H, Zhu MX, Romanin C, & Groschner K (2006). TRPC3 and TRPC4 associate to form a redox-sensitive cation channel. Evidence for expression of native TRPC3-TRPC4 heteromeric channels in endothelial cells. *J Biol Chem* **281**, 13588-13595.
- Prakriya M, Feske S, Gwack Y, Srikanth S, Rao A, & Hogan PG (2006). Orai1 is an essential pore subunit of the CRAC channel. *Nature* **443**, 230-233.
- Putney JW, Jr. (1986). A model for receptor-regulated calcium entry. *Cell Calcium* **7**, 1-12.
- Putney JW, Jr. & Bird GS (1993). The inositol phosphate-calcium signaling system in nonexcitable cells. *Endocr Rev* **14**, 610-631.
- Qian F, Huang P, Ma L, Kuznetsov A, Tamarina N, & Philipson LH (2002). TRP genes: candidates for nonselective cation channels and store-operated channels in insulin-secreting cells. *Diabetes* **51 Suppl 1**, S183-S189.
- Ramsey IS, Delling M, & Clapham DE (2006). An introduction to TRP channels. *Annu Rev Physiol* **68**, 619-647.
- Randriamampita C & Tsien RY (1993). Emptying of intracellular Ca²⁺ stores releases a novel small messenger that stimulates Ca²⁺ influx. *Nature* **364**, 809-814.
- Reiser J, Polu KR, Moller CC, Kenlan P, Altintas MM, Wei C, Faul C, Herbert S, Villegas I, vila-Casado C, McGee M, Sugimoto H, Brown D, Kalluri R, Mundel P, Smith PL, Clapham DE, & Pollak MR (2005). TRPC6 is a glomerular slit diaphragm-associated channel required for normal renal function. *Nat Genet* **37**, 739-744.
- Riccio A, Mattei C, Kelsell RE, Medhurst AD, Calver AR, Randall AD, Davis JB, Benham CD, & Pangalos MN (2002). Cloning and functional expression of human short TRP7, a candidate protein for store-operated Ca²⁺ influx. *J Biol Chem* **277**, 12302-12309.
- Rimm DL, Koslov ER, Kebriaei P, Cianci CD, & Morrow JS (1995). Alpha 1(E)-catenin is an actin-binding and -bundling protein mediating the attachment of F-actin to the membrane adhesion complex. *Proc Natl Acad Sci U S A* **92**, 8813-8817.
- Ritter M, Buechler C, Boettcher A, Barlage S, Schmitz-Madry A, Orso E, Bared SM, Schmiedeknecht G, Baehr CH, Fricker G, & Schmitz G (2002). Cloning and characterization of a novel apolipoprotein A-I binding protein, AI-BP, secreted by cells of the kidney proximal tubules in response to HDL or ApoA-I. *Genomics* **79**, 693-702.
- Rohacs T, Lopes CM, Michailidis I, & Logothetis DE (2005). PI(4,5)P(2) regulates the activation and desensitization of TRPM8 channels through the TRP domain. *Nat Neurosci* **8**, 626-634.
- Rohacs T (2007). Regulation of TRP channels by PIP(2). *Pflugers Arch* **453**, 753-762.
- Roos J, DiGregorio PJ, Yeromin AV, Ohlsen K, Liudyno M, Zhang S, Safrina O, Kozak JA, Wagner SL, Cahalan MD, Velicelebi G, & Stauderman KA (2005). STIM1, an essential and conserved component of store-operated Ca²⁺ channel function. *J Cell Biol* **169**, 435-445.
- Rosado JA, Jenner S, & Sage SO (2000). A role for the actin cytoskeleton in the initiation and maintenance of store-mediated calcium entry in human platelets. Evidence for conformational coupling. *J Biol Chem* **275**, 7527-7533.

- Rosado JA, Redondo PC, Sage SO, Pariente JA, & Salido GM (2005). Store-operated Ca^{2+} entry: vesicle fusion or reversible trafficking and de novo conformational coupling? *J Cell Physiol* **205**, 262-269.
- Sabbioni S, Barbanti-Brodano G, Croce CM, & Negrini M (1997). GOK: a gene at 11p15 involved in rhabdomyosarcoma and rhabdoid tumor development. *Cancer Res* **57**, 4493-4497.
- Saiki RK, Scharf S, Faloona F, Mullis KB, Horn GT, Erlich HA, & Arnheim N (1985). Enzymatic amplification of beta-globin genomic sequences and restriction site analysis for diagnosis of sickle cell anemia. *Science* **230**, 1350-1354.
- Saito K, Tautz L, & Mustelin T (2007). The lipid-binding SEC14 domain. *Biochim Biophys Acta* **1771**, 719-726.
- Saitoh M, Ishikawa T, Matsushima S, Naka M, & Hidaka H (1987). Selective inhibition of catalytic activity of smooth muscle myosin light chain kinase. *J Biol Chem* **262**, 7796-7801.
- Sambrook J, Fritsch E, & Maniatis T (1989). *Molecular cloning. A laboratory manual*, 2nd ed. Cold Spring Harbor, New York.
- Sanger F, Nicklen S, & Coulson AR (1977). DNA sequencing with chain-terminating inhibitors. *Proc Natl Acad Sci U S A* **74**, 5463-5467.
- Schaefer M, Plant TD, Obukhov AG, Hofmann T, Gudermann T, & Schultz G (2000). Receptor-mediated regulation of the nonselective cation channels TRPC4 and TRPC5. *J Biol Chem* **275**, 17517-17526.
- Schaefer M, Plant TD, Stresow N, Albrecht N, & Schultz G (2002). Functional differences between TRPC4 splice variants. *J Biol Chem* **277**, 3752-3759.
- Schaefer M (2005). Homo- and heteromeric assembly of TRP channel subunits. *Pflugers Arch* **451**, 35-42.
- Schindl R, Frischauf I, Kahr H, Fritsch R, Krenn M, Derndl A, Vales E, Muik M, Derler I, Groschner K, & Romanin C (2007). The first ankyrin-like repeat is the minimum indispensable key structure for functional assembly of homo- and heteromeric TRPC4/TRPC5 channels. *Cell Calcium*. (doi:10.1016/j.ceca.2007.05.015).
- Schlingmann KP, Weber S, Peters M, Niemann NL, Vitzthum H, Klingel K, Kratz M, Haddad E, Ristoff E, Dinour D, Syrrou M, Nielsen S, Sassen M, Waldegger S, Seyberth HW, & Konrad M (2002). Hypomagnesemia with secondary hypocalcemia is caused by mutations in TRPM6, a new member of the TRPM gene family. *Nat Genet* **31**, 166-170.
- Schwarz G, Droogmans G, & Nilius B (1994). Multiple effects of SK&F 96365 on ionic currents and intracellular calcium in human endothelial cells. *Cell Calcium* **15**, 45-54.
- Seth M, Sumbilla C, Mullen SP, Lewis D, Klein MG, Hussain A, Soboloff J, Gill DL, & Inesi G (2004). Sarco(endo)plasmic reticulum Ca^{2+} ATPase (SERCA) gene silencing and remodeling of the Ca^{2+} signaling mechanism in cardiac myocytes. *Proc Natl Acad Sci U S A* **101**, 16683-16688.
- Sewell TJ, Lam E, Martin MM, Leszyk J, Weidner J, Calaycay J, Griffin P, Williams H, Hung S, Cryan J, Sigal NH, & Wiederrecht GJ (1994). Inhibition of calcineurin by a novel FK-506-binding protein 2. *J Biol Chem* **269**, 21094-21102.

- Sha B, Phillips SE, Bankaitis VA, & Luo M (1998). Crystal structure of the *Saccharomyces cerevisiae* phosphatidylinositol-transfer protein. *Nature* **391**, 506-510.
- Shi J, Takahashi S, Jin XH, Li YQ, Ito Y, Mori Y, & Inoue R (2007). Myosin light chain kinase-independent inhibition by ML-9 of murine TRPC6 channels expressed in HEK293 cells. *Br J Pharmacol* **152**(1),122-31.
- Shieh BH & Zhu MY (1996). Regulation of the TRP Ca^{2+} channel by INAD in *Drosophila* photoreceptors. *Neuron* **16**, 991-998.
- Shimizu S, Yoshida T, Wakamori M, Ishii M, Okada T, Takahashi M, Seto M, Sakurada K, Kiuchi Y, & Mori Y (2006). Ca^{2+} -calmodulin-dependent myosin light chain kinase is essential for activation of TRPC5 channels expressed in HEK293 cells. *J Physiol* **570**, 219-235.
- Singh BB, Lockwich TP, Bandyopadhyay BC, Liu X, Bollimuntha S, Brazer SC, Combs C, Das S, Leenders AG, Sheng ZH, Knepper MA, Ambudkar SV, & Ambudkar IS (2004). VAMP2-dependent exocytosis regulates plasma membrane insertion of TRPC3 channels and contributes to agonist-stimulated Ca^{2+} influx. *Mol Cell* **15**, 635-646.
- Sinkins WG, Estacion M, & Schilling WP (1998). Functional expression of TrpC1: a human homologue of the *Drosophila* Trp channel. *Biochem J* **331** (Pt 1), 331-339.
- Sinkins WG, Goel M, Estacion M, & Schilling WP (2004). Association of immunophilins with mammalian TRPC channels. *J Biol Chem* **279**, 34521-34529.
- Smani T, Zakharov SI, Leno E, Csutora P, Trepakova ES, & Bolotina VM (2003). Ca^{2+} -independent phospholipase A2 is a novel determinant of store-operated Ca^{2+} entry. *J Biol Chem* **278**, 11909-11915.
- Soboloff J, Spassova M, Xu W, He LP, Cuesta N, & Gill DL (2005). Role of endogenous TRPC6 channels in Ca^{2+} signal generation in A7r5 smooth muscle cells. *J Biol Chem* **280**, 39786-39794.
- Soboloff J, Spassova MA, Hewavitharana T, He LP, Xu W, Johnstone LS, Dziadek MA, & Gill DL (2006). STIM2 is an inhibitor of STIM1-mediated store-operated Ca^{2+} Entry. *Curr Biol* **16**, 1465-1470.
- Song X, Zhao Y, Narcisse L, Duffy H, Kress Y, Lee S, & Brosnan CF (2005). Canonical transient receptor potential channel 4 (TRPC4) co-localizes with the scaffolding protein ZO-1 in human fetal astrocytes in culture. *Glia* **49**, 418-429.
- Sossey-Alaoui K, Lyon JA, Jones L, Abidi FE, Hartung AJ, Hane B, Schwartz CE, Stevenson RE, & Srivastava AK (1999). Molecular cloning and characterization of TRPC5 (HTRP5), the human homologue of a mouse brain receptor-activated capacitative Ca^{2+} entry channel. *Genomics* **60**, 330-340.
- Stace CL & Ktistakis NT (2006). Phosphatidic acid- and phosphatidylserine-binding proteins. *Biochim Biophys Acta* **1761**, 913-926.
- Stanczyk FZ (1997). Pharmacokinetics of the new progestogens and influence of gestodene and desogestrel on ethinylestradiol metabolism. *Contraception* **55**, 273-282.
- Sternweis PC & Gilman AG (1982). Aluminum: a requirement for activation of the regulatory component of adenylate cyclase by fluoride. *Proc Natl Acad Sci U S A* **79**, 4888-4891.

- Stevenson BR, Siliciano JD, Mooseker MS, & Goodenough DA (1986). Identification of ZO-1: a high molecular weight polypeptide associated with the tight junction (zonula occludens) in a variety of epithelia. *J Cell Biol* **103**, 755-766.
- Stowers L, Holy TE, Meister M, Dulac C, & Koentges G (2002). Loss of sex discrimination and male-male aggression in mice deficient for TRP2. *Science* **295**, 1493-1500.
- Strubing C, Krapivinsky G, Krapivinsky L, & Clapham DE (2001). TRPC1 and TRPC5 form a novel cation channel in mammalian brain. *Neuron* **29**, 645-655.
- Strubing C, Krapivinsky G, Krapivinsky L, & Clapham DE (2003). Formation of novel TRPC channels by complex subunit interactions in embryonic brain. *J Biol Chem* **278**, 39014-39019.
- Szaszi K, Kurashima K, Kapus A, Paulsen A, Kaibuchi K, Grinstein S, & Orlowski J (2000). RhoA and rho kinase regulate the epithelial Na⁺/H⁺ exchanger NHE3. Role of myosin light chain phosphorylation. *J Biol Chem* **275**, 28599-28606.
- Takemura H, Hughes AR, Thastrup O, & Putney JW, Jr. (1989). Activation of calcium entry by the tumor promoter thapsigargin in parotid acinar cells. Evidence that an intracellular calcium pool and not an inositol phosphate regulates calcium fluxes at the plasma membrane. *J Biol Chem* **264**, 12266-12271.
- Tang J, Lin Y, Zhang Z, Tikunova S, Birnbaumer L, & Zhu MX (2001). Identification of common binding sites for calmodulin and inositol 1,4,5-trisphosphate receptors on the carboxyl termini of trp channels. *J Biol Chem* **276**, 21303-21310.
- Tang Y, Tang J, Chen Z, Trost C, Flockerzi V, Li M, Ramesh V, & Zhu MX (2000). Association of mammalian trp4 and phospholipase C isozymes with a PDZ domain-containing protein, NHERF. *J Biol Chem* **275**, 37559-37564.
- Thibonnier M, Bayer AL, Simonson MS, & Kester M (1991). Multiple signaling pathways of V1-vascular vasopressin receptors of A7r5 cells. *Endocrinology* **129**, 2845-2856.
- Thomas P & Smart TG (2005). HEK293 cell line: a vehicle for the expression of recombinant proteins. *J Pharmacol Toxicol Methods* **51**, 187-200.
- Tiruppathi C, Freichel M, Vogel SM, Paria BC, Mehta D, Flockerzi V, & Malik AB (2002). Impairment of store-operated Ca²⁺ entry in TRPC4(-/-) mice interferes with increase in lung microvascular permeability. *Circ Res* **91**, 70-76.
- Torihashi S, Fujimoto T, Trost C, & Nakayama S (2002). Calcium oscillation linked to pacemaking of interstitial cells of Cajal: requirement of calcium influx and localization of TRP4 in caveolae. *J Biol Chem* **277**, 19191-19197.
- Trebak M, Bird GS, McKay RR, & Putney JW, Jr. (2002). Comparison of human TRPC3 channels in receptor-activated and store-operated modes. Differential sensitivity to channel blockers suggests fundamental differences in channel composition. *J Biol Chem* **277**, 21617-21623.
- Tsiokas L, Arnould T, Zhu C, Kim E, Walz G, & Sukhatme VP (1999). Specific association of the gene product of PKD2 with the TRPC1 channel. *Proc Natl Acad Sci U S A* **96**, 3934-3939.
- Tsunoda S & Zuker CS (1999). The organization of INAD-signaling complexes by a multivalent PDZ domain protein in Drosophila photoreceptor cells ensures sensitivity and speed of signaling. *Cell Calcium* **26**, 165-171.

- Ueda S, Kataoka T, & Satoh T (2004). Role of the Sec14-like domain of Dbl family exchange factors in the regulation of Rho family GTPases in different subcellular sites. *Cell Signal* **16**, 899-906.
- Vandebrouck A, Sabourin J, Rivet J, Balghi H, Sebillé S, Kitzis A, Raymond G, Cognard C, Bourmeyster N, & Constantin B (2007). Regulation of capacitative calcium entries by alpha1-syntrophin: association of TRPC1 with dystrophin complex and the PDZ domain of alpha1-syntrophin. *FASEB J* **21**, 608-617.
- Vannier B, Zhu X, Brown D, & Birnbaumer L (1998). The membrane topology of human transient receptor potential 3 as inferred from glycosylation-scanning mutagenesis and epitope immunocytochemistry. *J Biol Chem* **273**, 8675-8679.
- Vannier B, Peyton M, Boulay G, Brown D, Qin N, Jiang M, Zhu X, & Birnbaumer L (1999). Mouse trp2, the homologue of the human trpc2 pseudogene, encodes mTrp2, a store depletion-activated capacitative Ca²⁺ entry channel. *Proc Natl Acad Sci U S A* **96**, 2060-2064.
- Vazquez G, Wedel BJ, Trebak M, St JB, & Putney JW, Jr. (2003). Expression level of the canonical transient receptor potential 3 (TRPC3) channel determines its mechanism of activation. *J Biol Chem* **278**, 21649-21654.
- Vazquez G, Wedel BJ, Kawasaki BT, Bird GS, & Putney JW, Jr. (2004a). Obligatory role of Src kinase in the signaling mechanism for TRPC3 cation channels. *J Biol Chem* **279**, 40521-40528.
- Vazquez G, Wedel BJ, Aziz O, Trebak M, & Putney JW, Jr. (2004b). The mammalian TRPC cation channels. *Biochim Biophys Acta* **1742**, 21-36.
- Venkatachalam K, van Rossum DB, Patterson RL, Ma HT, & Gill DL (2002). The cellular and molecular basis of store-operated calcium entry. *Nat Cell Biol* **4**, E263-E272.
- Venkatachalam K, Zheng F, & Gill DL (2003). Regulation of canonical transient receptor potential (TRPC) channel function by diacylglycerol and protein kinase C. *J Biol Chem* **278**, 29031-29040.
- Vig M, Beck A, Billingsley JM, Lis A, Parvez S, Peinelt C, Koomoa DL, Soboloff J, Gill DL, Fleig A, Kinet JP, & Penner R (2006a). CRACM1 multimers form the ion-selective pore of the CRAC channel. *Curr Biol* **16**, 2073-2079.
- Vig M, Peinelt C, Beck A, Koomoa DL, Rabah D, Koblan-Huberson M, Kraft S, Turner H, Fleig A, Penner R, & Kinet JP (2006b). CRACM1 is a plasma membrane protein essential for store-operated Ca²⁺ entry. *Science* **312**, 1220-1223.
- Vig M & Kinet JP (2007). The long and arduous road to CRAC. *Cell Calcium* **42**, 157-162.
- Wang W, O'Connell B, Dykeman R, Sakai T, Delporte C, Swaim W, Zhu X, Birnbaumer L, & Ambudkar IS (1999). Cloning of Trp1beta isoform from rat brain: immunodetection and localization of the endogenous Trp1 protein. *Am J Physiol* **276**, C969-C979.
- Wang Y, Deshpande M, & Payne R (2002). 2-Aminoethoxydiphenyl borate inhibits phototransduction and blocks voltage-gated potassium channels in Limulus ventral photoreceptors. *Cell Calcium* **32**, 209-216.
- Wedel BJ, Vazquez G, McKay RR, St JB, & Putney JW, Jr. (2003). A calmodulin/inositol 1,4,5-trisphosphate (IP₃) receptor-binding region targets TRPC3 to the plasma membrane in a calmodulin/IP₃ receptor-independent process. *J Biol Chem* **278**, 25758-25765.

- Weissmann N, Dietrich A, Fuchs B, Kalwa H, Ay M, Dumitrascu R, Olschewski A, Storch U, Schnitzler M, Ghofrani HA, Schermuly RT, Pinkenburg O, Seeger W, Grimminger F, & Gudermann T (2006). Classical transient receptor potential channel 6 (TRPC6) is essential for hypoxic pulmonary vasoconstriction and alveolar gas exchange. *Proc Natl Acad Sci U S A* **103**, 19093-19098.
- Welsh DG, Morielli AD, Nelson MT, & Brayden JE (2002). Transient receptor potential channels regulate myogenic tone of resistance arteries. *Circ Res* **90**, 248-250.
- Wes PD, Chevesich J, Jeromin A, Rosenberg C, Stetten G, & Montell C (1995). TRPC1, a human homolog of a Drosophila store-operated channel. *Proc Natl Acad Sci U S A* **92**, 9652-9656.
- WHO (2007). Cardiovascular diseases. *Fact Sheet N° 317*
- Winn MP, Conlon PJ, Lynn KL, Farrington MK, Creazzo T, Hawkins AF, Daskalakis N, Kwan SY, Ebersviller S, Burchette JL, Pericak-Vance MA, Howell DN, Vance JM, & Rosenberg PB (2005). A Mutation in the TRPC6 Cation Channel Causes Familial Focal Segmental Glomerulosclerosis. *Science* **308**, 1801-1804.
- Woodard GE, Sage SO, & Rosado JA (2007). Transient receptor potential channels and intracellular signaling. *Int Rev Cytol* **256**, 35-67.
- Worley PF, Zeng W, Huang G, Kim JY, Shin DM, Kim MS, Yuan JP, Kiselyov K, & Muallem S (2007). Homer proteins in Ca(2+) signaling by excitable and non-excitable cells. *Cell Calcium* **42**, 363-371.
- Wu RL, Butler DM, & Barish ME (1998). Potassium current development and its linkage to membrane expansion during growth of cultured embryonic mouse hippocampal neurons: sensitivity to inhibitors of phosphatidylinositol 3-kinase and other protein kinases. *J Neurosci* **18**, 6261-6278.
- Xu XZ, Chien F, Butler A, Salkoff L, & Montell C (2000). TRPgamma, a drosophila TRP-related subunit, forms a regulated cation channel with TRPL. *Neuron* **26**, 647-657.
- Xu SZ, Zeng F, Boulay G, Grimm C, Harteneck C, & Beech DJ (2005). Block of TRPC5 channels by 2-aminoethoxydiphenyl borate: a differential, extracellular and voltage-dependent effect. *Br J Pharmacol* **145**, 405-414.
- Xu SZ, Muraki K, Zeng F, Li J, Sukumar P, Shah S, Dedman AM, Flemming PK, McHugh D, Naylor J, Cheong A, Bateson AN, Munsch CM, Porter KE, & Beech DJ (2006). A sphingosine-1-phosphate-activated calcium channel controlling vascular smooth muscle cell motility. *Circ Res* **98**, 1381-1389.
- Yang M, Gupta A, Shlykov SG, Corrigan R, Tsujimoto S, & Sanborn BM (2002). Multiple Trp isoforms implicated in capacitative calcium entry are expressed in human pregnant myometrium and myometrial cells. *Biol Reprod* **67**, 988-994.
- Yao X & Garland CJ (2005). Recent developments in vascular endothelial cell transient receptor potential channels. *Circ Res* **97**, 853-863.
- Yao Y, Ferrer-Montiel AV, Montal M, & Tsien RY (1999). Activation of store-operated Ca²⁺ current in Xenopus oocytes requires SNAP-25 but not a diffusible messenger. *Cell* **98**, 475-485.

- Yeromin AV, Zhang SL, Jiang W, Yu Y, Safrina O, & Cahalan MD (2006). Molecular identification of the CRAC channel by altered ion selectivity in a mutant of Orai. *Nature* **443**, 226-229.
- Yoshida T, Inoue R, Morii T, Takahashi N, Yamamoto S, Hara Y, Tominaga M, Shimizu S, Sato Y, & Mori Y (2006). Nitric oxide activates TRP channels by cysteine S-nitrosylation. *Nat Chem Biol* **2**, 596-607.
- Yu Y, Sweeney M, Zhang S, Platoshyn O, Landsberg J, Rothman A, & Yuan JX (2003). PDGF stimulates pulmonary vascular smooth muscle cell proliferation by upregulating TRPC6 expression. *Am J Physiol Cell Physiol* **284**, C316-C330.
- Yu Y, Fantozzi I, Remillard CV, Landsberg JW, Kunichika N, Platoshyn O, Tigno DD, Thistlethwaite PA, Rubin LJ, & Yuan JX (2004). Enhanced expression of transient receptor potential channels in idiopathic pulmonary arterial hypertension. *Proc Natl Acad Sci U S A* **101**, 13861-13866.
- Yuan JP, Kiselyov K, Shin DM, Chen J, Shcheynikov N, Kang SH, Dehoff MH, Schwarz MK, Seeburg PH, Muallem S, & Worley PF (2003). Homer binds TRPC family channels and is required for gating of TRPC1 by IP₃ receptors. *Cell* **114**, 777-789.
- Yuan JP, Zeng W, Huang GN, Worley PF, & Muallem S (2007). STIM1 heteromultimerizes TRPC channels to determine their function as store-operated channels. *Nat Cell Biol* **9**, 636-645.
- Zeng F, Xu SZ, Jackson PK, McHugh D, Kumar B, Fountain SJ, & Beech DJ (2004). Human TRPC5 channel activated by a multiplicity of signals in a single cell. *J Physiol* **559**, 739-750.
- Zerangue N, Malan MJ, Fried SR, Dazin PF, Jan YN, Jan LY, & Schwappach B (2001). Analysis of endoplasmic reticulum trafficking signals by combinatorial screening in mammalian cells. *Proc Natl Acad Sci U S A* **98**, 2431-2436.
- Zhang M, Benishin CG, & Pang PK (2002). Rapid inhibition of the contraction of rat tail artery by progesterone is mediated by inhibition of calcium currents. *J Pharm Pharmacol* **54**, 1667-1674.
- Zhang SL, Yu Y, Roos J, Kozak JA, Deerinck TJ, Ellisman MH, Stauderman KA, & Cahalan MD (2005). STIM1 is a Ca²⁺ sensor that activates CRAC channels and migrates from the Ca²⁺ store to the plasma membrane. *Nature* **437**, 902-905.
- Zhang Z, Tang J, Tikunova S, Johnson JD, Chen Z, Qin N, Dietrich A, Stefani E, Birnbaumer L, & Zhu MX (2001). Activation of Trp3 by inositol 1,4,5-trisphosphate receptors through displacement of inhibitory calmodulin from a common binding domain. *Proc Natl Acad Sci U S A* **98**, 3168-3173.
- Zhu X, Chu PB, Peyton M, & Birnbaumer L (1995). Molecular cloning of a widely expressed human homologue for the Drosophila trp gene. *FEBS Lett* **373**, 193-198.
- Zhu X, Jiang M, Peyton M, Boulay G, Hurst R, Stefani E, & Birnbaumer L (1996). trp, a novel mammalian gene family essential for agonist-activated capacitative Ca²⁺ entry. *Cell* **85**, 661-671.
- Zhu X, Jiang M, & Birnbaumer L (1998). Receptor-activated Ca²⁺ influx via human Trp3 stably expressed in human embryonic kidney (HEK)293 cells. Evidence for a non-capacitative Ca²⁺ entry. *J Biol Chem* **273**, 133-142.

Zitt C, Zobel A, Obukhov AG, Harteneck C, Kalkbrenner F, Luckhoff A, & Schultz G (1996). Cloning and functional expression of a human Ca^{2+} -permeable cation channel activated by calcium store depletion. *Neuron* **16**, 1189-1196.

Zitt C, Obukhov AG, Strubing C, Zobel A, Kalkbrenner F, Luckhoff A, & Schultz G (1997). Expression of TRPC3 in Chinese hamster ovary cells results in calcium-activated cation currents not related to store depletion. *J Cell Biol* **138**, 1333-1341.

8 Appendix

8.1 Vectors

Vector	Supplier
pGEX-4T-1	Amersham, Munich, Germany
pGEX-5X-3	Amersham, Munich, Germany
pACT2	Clontech, Mountain View, USA
pcDNA3.1	Invitrogen, Karlsruhe, Germany
pCMVbeta	Invitrogen, Karlsruhe, Germany
pCMV-HA	Invitrogen, Karlsruhe, Germany
pCR-Blunt II-TOPO	Invitrogen, Karlsruhe, Germany
pGADT7	Clontech, Mountain View, USA
pGBKT7	Clontech, Mountain View, USA
pGreen Lantern	GIBCO BRL, Gaithersburg, USA
pEYFP-N1	Clontech, Mountain View, USA

8.2 Constructs for expression in yeast

Construct	Primers	Restriction sites
EGFP/leucine zipper/pGBKT7	kindly provided by PD Dr. B. Schwappach, Rupprecht-Karls Universität Heidelberg, Germany)	
hTRPC1 (640-759)/leucine zipper/pGBKT7	hTRPC1c_f_NotI hTRPC1c_r_PstI	EcoRI/NotI/PstI
hTRPC6 (722-931)/leucine zipper/pGBKT7	hTRPC6c_f1 hTRPC6c_r1	EcoRI/NotI/Sall
mTRPC4 α (615-974)/leucine zipper/pGBKT7	mTRPC4longc_f1 mTRPC4longc_r1	EcoRI/NotI/PstI
wt: mTRPC4 α (615-974)/pGBKT7	mTRPC4 α 1_f_EcoRI mTRPC4 α 2_r_BamHI	EcoRI/BamHI
C204: mTRPC4 α (771-974)/pGBKT7	mTRPC4 α 2_f_EcoRI mTRPC4 α 2_r_BamHI	EcoRI/BamHI
Δ C204: mTRPC4 α (615-770)/pGBKT7	mTRPC4 α 1_f_EcoRI mTRPC4 α 1_r_BamHI	EcoRI/BamHI
Δ C275: mTRPC4 α (615-699)/pGBKT7	mTRPC4 α 1_f_EcoRI mTRPC4 α 3_r_BamHI	EcoRI/BamHI
C700-C770: mTRPC4 α (700-770)/pGBKT7	mTRPC4 α 3_f_EcoRI mTRPC4 α 1_r_BamHI	EcoRI/BamHI
C700-C741: mTRPC4 α (700-741)/pGBKT7	mTRPC4 α 3_f_EcoRI mTRPC4 α 5_r_BamHI	EcoRI/BamHI
C700-C728: mTRPC4 α (700-728)/pGBKT7	mTRPC4 α 3_f_EcoRI mTRPC4 α 4_r_BamHI	EcoRI/BamHI
mTRPC5 (619-975)/leucine zipper/pGBKT7	mTRPC5c_f1 mTRPC5c_r1	EcoRI/NotI/PstI
hSESTD1 (1-696)/pACT2	prey from Y2H screen	
hSESTD1 (1-192)/pACT2	SESTD1_f1_BamHI SESTD1_r1_XhoI	BamHI/XhoI
hSESTD1 (193-406)/pACT2	SESTD1_f2_BamHI SESTD1_r2_XhoI	BamHI/XhoI
hSESTD1 (407-696)/pACT2	SESTD1_f3_BamHI SESTD1_r3_XhoI	BamHI/XhoI

8.3 Constructs for expression in bacteria

Construct	Primers	Restriction sites
GST-SESTD1 (1-696)/pGEX-4T-1	SESTD1_f_BamHI SESTD1_r_XhoI	BamHI/XhoI
GST-Sec 14 (1-192)/pGEX-5X-3	SESTD1_f1_BamHI SESTD1_r1_XhoI	BamHI/XhoI
GST-Spec 1 (193-406)/pGEX-5X-3	SESTD1_f2_BamHI SESTD1_r2_XhoI	BamHI/XhoI
GST-Spec 2 (407-696)/pGEX-5X-3	SESTD1_f3_BamHI SESTD1_r3_XhoI	BamHI/XhoI

8.4 Constructs for expression in mammalian cells

Construct	Primers	Restriction sites
mTRPC4 α (615-974)/pcDNA3.1(+)	cut from Y2H bait	BamHI/NotI
mTRPC4 β /pcDNA3.1-nFLAG-DEST	GATEWAY cloning (see methods)	
hSESTD1/pcDNA3.1(+)	cut from Y2H prey	XhoI/BamHI
hSESTD1/pCMV-HA	SESTD1_f_Sall SESTD1_r_XhoI	Sall/XhoI
hSESTD1/pEYFP-N1	SESTD1_f_XhoI SESTD1_r_BamHI	XhoI/BamHI

Constructs not listed above were kindly provided by Dr. Vladimir Chubanov (Philipps-Universität Marburg, Germany), PD Dr. Niels Decher (Philipps-Universität Marburg, Germany) and Dr. Carsten Strübing (Sanofi-Aventis Deutschland GmbH).

8.5 Abbreviations

A7r5	clonal cell line (derived from rat thoracic aortic smooth muscle cells)
α_1 -AR	α_1 -adrenergic receptor
2-APB	2-aminoethoxydiphenyl borate
Ade	adenine
ANKRD35	ankyrin repeat domain 35
APOA1BP	apolipoprotein A-I binding protein
AoSMC	aortic smooth muscle cells
ATP	adenosine triphosphate
att	attachment
AVP	[Arg ⁸]-vasopressin
BAZ1B	bromodomain adjacent to zinc finger domain
BCA	bicinchoninic acid
BSA	bovine serum albumine
CaM	calmodulin
CASMC	coronary artery smooth muscle cells
CCE	capacitative Ca ²⁺ entry
cDNA	copy DNA
cfu	colony forming units
CIF	Ca ²⁺ influx factor
CIRB domain	CaM/IP ₃ R-binding domain
CMV	cytomegalie virus
COPD	chronic obstructive pulmonary disease
CRAC	calcium-release-activated calcium channel
CRACM1	CRAC modulator 1
CSM	complete supplement mixture
Cs ₄ -BAPTA	1,2-bis(2-aminophenoxy)ethane- <i>N,N,N',N'</i> -tetraacetic acid
C-terminal	carboxy terminal
DAG	diacylglycerol
DELFLIA	dissociation-enhanced lanthanide fluorescence immunoassay
DMEM	Dulbecco's modified eagle medium
DMF	dimethylformamide
DMSO	dimethyl sulphoxide
DNA	deoxynucleic acid
DNA-BD	DNA binding domain of transcription factor GAL4
dNTP	deoxynucleotide
D-PBS	Dulbecco's phosphate buffered saline
DTT	dithiotreitol
<i>E. coli</i>	<i>Escherichia coli</i>
EC	endothelial cells
EC ₅₀	half maximal effective concentration
ECL	enhanced chemiluminescence
EDTA	ethylenediaminetetraacetic acid
EGFP	enhanced green fluorescent protein
EGTA	ethylene glycol-bis(β -aminoethylether)- <i>N,N,N',N'</i> -tetraacetic acid
eNOS	endothelial nitric oxide synthase
ERG	electroretinogram
EYFP	enhanced yellow-green GFP mutant protein

FBS	fetal bovine serum
FITR	<i>Flp-In T-Rex</i> (inducible expression system)
FKBP	F506 binding protein
FLIPR	fluorometric imaging plate reader
FRT site	Flp recombination target site
FSGS	focal segmental glomerulosclerosis
GAL4	transcription factor
GAL4-AD	activation domain of transcription factor GAL4
GAPDH	glyceraldehyde-3-phosphate dehydrogenase
GCN4	general control nondepressible 4 (transcriptional activator protein)
GFP	green fluorescent protein
GST	glutathione S-transferase
GTP	guanosine triphosphate
5-HT	5-hydroxytryptamine (serotonin)
5-HT ₃ receptor	subtype of the 5-hydroxy tryptamine (serotonin) receptor
HA	antigenic epitope of human influenza virus hemagglutinin protein
HAEC	human aortic endothelial cells
HEK293	human embryonal kidney cells
HL-5	a cell line derived from murine atrial cardiomyocytes
HMG2L1	high-mobility group protein 2-like1 isoform b
HMVEC-d	human dermal microvascular endothelial cells
HPV	hypoxic pulmonary vasoconstriction
HRP	horseradish peroxidase
IC ₅₀	half maximal inhibitory concentration
I _{CRAC}	calcium-release-activated calcium current
iNOS	inducible nitric oxide synthase
IP ₃	inositol-1,4,5-trisphosphate
IP ₃ R	IP ₃ receptor
IP ₆	inositol hexaphosphate
IPAH	idiopathic pulmonary arterial hypertension
iPLA ₂	inducible phospholipase 2
IPTG	isopropyl β-D thiogalactoside
<i>I-V</i>	current-voltage
Kir	inwardly rectifying K ⁺ channel
Kv	voltage-dependent K ⁺ channel
LB medium	Luria Bertani medium
LiAc	lithium acetate
L-NAME	N-nitro-L-arginine methyl ester
β-ME	β-mercaptoethanol
M ₁ R	muscarinic type 1 receptor
MAEC	mouse vascular endothelial cells
MCS	multiple cloning site
MEM	minimal essential medium
MKRN1	makorin RING finger protein 1
ML-9	[1-(5-chloronaphthalene-1-sulphonyl) homopiperazine, HCl]
MLCK	myosin light chain kinase
mRNA	messenger RNA
NCBI	National Center for Biotechnology Information
NCX	Na ⁺ /Ca ²⁺ exchanger
NHE	Na ⁺ /H ⁺ exchanger

NHERF	Na ⁺ /H ⁺ exchanger regulatory factor
NO	nitric oxide
N-terminal	amino terminal
OAG	oleoyl-2-acetyl-sn-glycerol
PA	phosphatidic acid
PAGE	polyacrylamide gel electrophoresis
PAR	protease-activated receptor
PBXIP1	pre-B-cell leukemia homeobox interacting protein 1
PCR	polymerase chain reaction
PDZ domain	protein-protein interaction mediating domain
PDZ-B	PDZ-binding motif that interacts with PDZ domains
PEG	polyethylene-glycol
<i>Pfu</i>	<i>Pyrococcus furiosus</i>
pH	negative decadic logarithm of the concentration of hydrogen ions
PH domain	pleckstrin homology domain
PI, PIP, PIP ₂ , PIP ₃	phosphatidylinositol, mono-/bis-/trisphosphate
PKC	protein kinase C
PKG	protein kinase G
PLC	phospholipase C
PM	plasma membrane
PPlase	peptidyl-prolyl <i>cis-trans</i> isomerase
PSS	physiological phosphate-buffered salt solution
RNA	ribonucleic acid
ROC	receptor-operated channel
rpm	rotations per minute
RT	room temperature
S1P	sphingosine 1-phosphate
SCID	severe combined immunodeficiency
SDS	sodium dodecyl sulphate
SDS PAGE	sodium dodecyl sulphate polyacrylamide gel electrophoresis
SEM	standard error of the mean
Sec 14	Sec14p-like lipid-binding domain
SERCA	sarcoplasmic/endoplasmic reticulum Ca ²⁺ pump
SESTD1	SEC14 and spectrin domains
siRNA	small interference RNA
SK&F 96365	1-(β-[3-(4-methoxyphenyl)propoxy]-4-methoxyphenethyl)-1 <i>H</i> -HCl
SMC	smooth muscle cells
SMC3	structural maintenance of chromosomes 3
Spec 1, Spec 2	spectrin repeats
SPTAN1	spectrin, alpha, non-erythrocytic 1
SOC	store-operated channel
STIM1	stromal interaction molecule 1
TetO ₂	<i>tet</i> operator 2
TetR	Tet repressor
TLN2	talin 2
tBHQ	tert-butyl-benzohydroquinone
Tris-HCl	Tris(hydroxymethyl)aminomethane hydrochloride
TRP	transient receptor potential
Tween 20	polyethylene glycol sorbitan monolaurate

U	unit
UV	ultraviolet
v/v	volume per volume
V _{1A}	vasopressin receptor
w/v	weight per volume
wt	wild type
X-gal	5-bromo-4-chloro-3-indolyl β -D-galactopyranoside
Y2H	yeast two-hybrid
YFP	yellow-green GFP mutant protein
ZO-1	zona occludens 1

amino acids:

alanine, Ala, A; arginine, Arg, R; aspartic acid, Asp, D; asparagine, Asn, N; cysteine, Cys, C; glutamic acid, Glu, E; glutamine, Gln, Q; glycine, Gly, G; histidine, His, H; isoleucine, Ile, I; leucine, Leu, L; lysine, Lys, K; methionine, Met, M; phenylalanine, Phe, F; proline, Pro, P; serine, Ser, S; threonine, Thr, T; tryptophane, Trp, W; tyrosine, Tyr, Y; valine, Val, V.

9 Danksagung

Die vorliegende Dissertation wurde als externe Doktorarbeit in der Sektion „Molekulare Pharmakologie“ der Abteilung „Herz-Kreislauf-Erkrankungen“ der Sanofi-Aventis Deutschland GmbH in Frankfurt am Main angefertigt.

Mein herzlicher Dank gilt:

Herrn Dr. Carsten Strübing für die Bereitstellung des Themas sowie für die hervorragende fachliche Betreuung, seine Diskussionsbereitschaft und umfassende Unterstützung, die ganz wesentlich zum Gelingen dieser Arbeit beigetragen haben.

Herrn Prof. Dr. Andreas E. Busch für die Möglichkeit, diese Arbeit in der Sanofi-Aventis Deutschland GmbH durchführen und fertig stellen zu können, und für die wissenschaftliche Begutachtung meiner Dissertation.

Herrn Prof. Dr. Dieter Steinhilber von der J.W. Goethe-Universität in Frankfurt am Main für die wissenschaftliche Begutachtung meiner Doktorarbeit.

Herrn PD Dr. Klaus Steinmeyer für seine Hilfsbereitschaft, den freundschaftlichen Zuspruch, das Interesse an meiner Arbeit und deren kritische Durchsicht.

Frau Andrea Bieberstein für die gute praktische Zusammenarbeit und ihre tatkräftige Unterstützung.

Herrn Dr. Florian Bundis für die Einarbeitung in das Hefe Zwei-Hybrid System und den tieferen Einblick, den er mir in die Molekularbiologie vermittelt hat.

Herrn Dr. Rolf Vajna für das schnelle Korrekturlesen dieser Arbeit.

Den Kolleginnen und Kollegen aus den „Herz-Kreislauf“- und „Genomic Sciences“-Laboren für konstruktiven Gespräche und Anregungen, die gute Zusammenarbeit und nette Arbeitsatmosphäre sowie die erfahrene praktische Unterstützung; insbesondere Beate Preitz, Stefan Müller, Dr. Katrin Engel, Alexandra Endlich, Dr. Petra Arndt, Dr. Thorsten Sadowski, Dr. Manuel Baader, Jennifer Reb, Dr. Aimo Kannt, Florian Werner, Kerstin Sicka, Karolina Daton, Simone Stengelin, Elsa Kern, Elke Deckert, Claire Chenel, Dr. Paulus Wohlfart, Dr. Thomas Wendrich, Ulrike Siebers, Dr. Ingrid Wagner, Matthias Ozog, Dr. Matthias Löhn, Dr. Matthias Schäfer, Andreas Hertler und Dr. Yuri Ivashchenko.

Dr. Vladimir Chubanov, PD Dr. Niels Decher und PD Dr. Blanche Schwappach für die Bereitstellung genetischer Konstrukte.

Natürlich auch meiner Familie und vor allem Thomas.

10 Curriculum vitae

Aus datenschutzrechtlichen Gründen online nicht verfügbar.

11 Eidesstattliche Erklärung

Hiermit erkläre ich, Susanne Miehe, geboren am 21.02.1978 in Rochlitz, dass ich die vorliegende Arbeit mit dem Titel „Untersuchung TRPC-modulierender Gestagene und Proteine“ selbständig angefertigt und keine anderen Quellen oder Hilfsmittel als die hier angegebenen benutzt habe. Ich habe bisher an keiner anderen Universität ein Gesuch um Zulassung zur Promotion eingereicht oder eine andere Arbeit als Dissertation vorgelegt.

Teile dieser Arbeit sind Bestandteile von Patentanmeldungen (Europäische Anmeldungen Nr. 07291300.7 und 07291301.7) der Sanofi-Aventis Deutschland GmbH.